Polarforschung

P O L A R F O R S C H U N G

Contents / *Inhalt*

Mitteilungen /*Notes*

Cover illustration: The German icebreaking research vessel "Polarstern" (left) and the Swedish icebreaker "Oden" (right) moored at a large ice floe at the geographic North Pole. Both research vessels reached this 'magic point' first time for non-nuclear-powered ships in the morning of September 7th 1991 in the course of their mutual research activities. The multidisciplinary International Arctic Ocean Expedition ARCTIC 91 has become a milestone in Arctic Ocean research. It demonstrated that by fully co-operative joint navigation and operation the amount of scientific research could strongly be increased.

Umschlagbild: Das deutsche eisbrechende Forschungsschiff "Polarstern" (links) und der schwedische Eisbrecher "Oden" (rechts), festgemacht an einer riesigen Eisscholle am Geographischen Nordpol. Am Vormittag des 7. September 1991 erreichten die beiden Forschungsschiffe im Rahmen ihrer gemeinsamen Forschungsarbeiten während der "International Arctic Ocean Expedition ARCTIC 91" als erste nicht-nuklear angetriebene Schiffe den Nordpol.

„Wir sind gewiss nicht hinausgezogen, um den mathematischen Punkt, der das nördliche Ende der Erdachse bildet, zu suchen – denn diesen Punkt zu erreichen hat an und für sich nur geringen Wert –, sondern um Untersuchungen in dem großen, unbekannten Teil der Erde, welcher den Pol umgibt, anzustellen und diese Untersuchungen werden nahezu die gleiche große wissenschaftliche Bedeutung haben, ob die Reise nun über den mathematischen Pol selbst führt oder ein Stück davon entfernt bleibt ...
Aber man muss den Pol erreichen, damit die Besessenheit aufhört."   Fridtjof Nansen (um 1900)

Advances of Sea-Ice Observations since ARCTIC 91[*]

by Wolfgang Dierking[1] and Christian Haas[2]

Abstract : One of the first systematic sea ice studies in the central Arctic was carried out in 1991 during the International Arctic Ocean Expedition ARCTIC 91. The work program included in-situ measurements of physical sea-ice properties, and ground-based radar measurements in conjunction with the launch of the European Remote Sensing satellite ERS-1. Based on results and experiences made during this expedition, new measurement techniques were developed in the following years, in particular for the retrieval of sea-ice thickness. They were successfully tested and applied on several expeditions into the pack ice of the Arctic and Antarctic. Satellite instrument technology as well as the methods for analysing space-borne sea-ice observations have made large progress. Now, more than twenty years later, the annual Arctic summer sea-ice minimum extent has decreased dramatically, and the collected knowledge about sea-ice properties and interaction mechanisms between ocean, sea ice, and atmosphere is a key ingredient in explaining recent sea-ice cover variations and their impact on regional and global climate. In this paper, the authors pick up examples how sea-ice observation technology advanced during the past twenty years, thereby focusing on topics, which have largely been initiated during the ARCTIC 91 expedition.

Zusammenfassung: Eine der ersten systematischen Untersuchungen des Meereises in der zentralen Arktis wurde 1991 während der Internationalen Nordpolarmeer-Expedition (ARCTIC 91) durchgeführt. Das Arbeitsprogramm beinhaltete in-situ Messungen von physikalischen Eigenschaften des Meereises sowie bodengebundene Radarmessungen im Zusammenhang mit dem Start des europäischen Fernerkundungssatelliten ERS-1. Auf Grundlage der auf dieser Expedition gewonnenen Ergebnisse und Erfahrungen wurden in den folgenden Jahren neue Messtechniken entwickelt, insbesondere für die Ermittlung der Meereisdicke. Diese Techniken wurden erfolgreich getestet und auf zahlreichen Expeditionen in das Packeis der Arktis und Antarktis angewendet. Auch die Technologie von Satelliteninstrumenten und die Methoden der Satellitendatenauswertung haben große Fortschritte gemacht. Mehr als zwanzig Jahre nach ARCTIC 91 nimmt das Sommerminimum der Meereisausdehnung dramatisch ab, und das gesammelte Wissen über die Eigenschaften des Meereises und die Wechselwirkung zwischen Ozean, Eis, und Atmosphäre ist eine wichtige Voraussetzung zur Erklärung von gegenwärtigen Variationen der Meereisbedeckung und deren Einfluss auf das regionale und globale Klima. In diesem Artikel zeigen die Autoren anhand von Beispielen, wie sich die Technologien zur Beobachtung des Meereises in den letzten 20 Jahren weiterentwickelt haben. Dabei konzentrieren sie sich auf Themenbereiche, die zu einem großen Teil auf der ARCTIC 91-Expedition angestoßen wurden.

INTRODUCTION

The expedition ARCTIC 91 (ARK-VIII/3, 1991) of the German research vessel "Polarstern" and the Swedish icebreaker "Oden" into the pack ice of the central Arctic was in many respects special for the participating sea-ice researchers from Germany, Sweden, and Finland. The joint ship operations facilitated movements in the ice considerably. Fruitful cooperations between scientists on board both vessels were established. The European Remote Sensing (ERS-1) satellite had been launched on 17 July 1991, i.e., only a few days before "Polarstern" headed for the Arctic Ocean on 01 August. And finally, plans about developing and applying new technologies for the measurements of sea-ice thickness took shape in the heads of the participating specialists who until then almost solely had used ice drills. As it turned out, the ARCTIC 91 expedition strongly influenced sea-ice research at the Alfred Wegener Institute (AWI). In this article, a brief overview is given on how different research activities, including field-work on the ice and data acquisitions from helicopters, aircrafts, and satellites over the ice, evolved over the past two decades. The 1991-expedtion is taken as a starting point for the (necessarily) brief (and therefore incomplete) historic journey through the evolution of sea-ice observation technology since then. Unfortunately it is not possible to mention all the numerous interesting and exciting results that were obtained during the last two decades. We focused on topics with a strong link to the sea ice and remote sensing program of the ARCTIC 91 expedition and to the recent changes of sea-ice thickness observed in the Arctic. Only now and then the look will be directed also to the Antarctic and the Baltic Sea. Readers interested in a more comprehensive overview of topics related to physics and observations of sea ice are referred to the textbooks by WADHAMS (2000) and LUBIN & MASSOM (2006) and the studies cited therein.

First, we present an introduction to the atmosphere – sea-ice – ocean system and its current state, followed by fundamentals of remote sensing methods. These two sections provide the reader with some background knowledge. Then we touch upon the situation in Arctic sea-ice research and remote sensing in the early 90s and pick up examples of corresponding results from the ARCTIC 91 expedition. In the subsequent sections we deal with the development of ice thickness measurement technology and the knowledge about variations and trends of sea-ice thickness gained during the past twenty years. This part is followed by a presentation of advances in sea-ice observations by space-borne imaging radar from the early 90s until present. The emphasis is on the increasing technological flexibility of imaging radar systems, the benefit of combining satellite, airborne and ground-based measurements, on ice-type classification, on the retrieval of ice surface characteristics from radar images, and on the changes in the appearance of sea ice in radar images during the melt season. Finally, we take a look into the future of sea-ice research and remote sensing.

THE ATMOSPHERE – SEA ICE – OCEAN SYSTEM AND ITS CURRENT STATE

Large areas of the ocean's surface are covered by ice wherein the ice extent is varying considerably over the seasons. In the Arctic, it increases from 7 to 14 million km^2 from summer to winter, for the Antarctic the corresponding numbers are 4 and

---

[1] Alfred Wegener Institute for Polar and Marine Research, Bussestraße 24, D-27570 Bremerhaven, Germany; <wolfgang.dierking@awi.de>
[2] University of Alberta, Depts. Earth & Atmospheric Sciences and Geophysics, Edmonton, Alberta, T6G 2E3, Canada; <chaas@ualberta.ca>

20 million km^2, respectively. For comparison, the USA cover an area of 9.6 million km^2, Russia's extent is 17.1 million km^2.

Why should one be interested in sea ice? In fact, it induces or influences a number of processes that have direct or indirect impact on Earth's climate. From the ice surface, a much larger fraction of the incoming solar radiation is reflected back into space than from the surface of the open ocean. This mechanism affects the ocean and air temperatures, which would be higher without any ice coverage in the Polar Regions. Sea ice forms a barrier between the atmosphere above and the ocean below, i.e., it reduces or even stops the exchange of heat, moisture and matter. It also changes the transfer of momentum between ocean and atmosphere. The energy transfer from wind to waves is replaced by a near-surface air flow influenced by an irregular mixture of level ice, open water leads, edges of single ice floes, and ice blocks piled up in ridges (Fig. 1).

When sea ice forms, the salt contained in the water accumulates in small liquid-filled pores between the ice crystals. This brine is expelled into the water layer beneath the ice. As the upper water layer gains weight due to the inflow of dense brine, it may eventually become heavier than the water mass below and start to sink down. In many cases, such processes remain local effects, but if the areas of growing ice are large and special conditions are met (e.g., a weak density stratification of the water column below the ice), the brine rejection induces kilometre-scale convection in the ocean, which even affects the global ocean circulation.

Long-term changes of the sea-ice cover state are regarded as an indicator of broader climate change such as global warming. When viewed from space, the ice cover is visible over the entire Arctic Ocean and adjacent ocean basins. Variations of the ice extent can be determined on different temporal scales. A sequence of daily images collected over a whole year
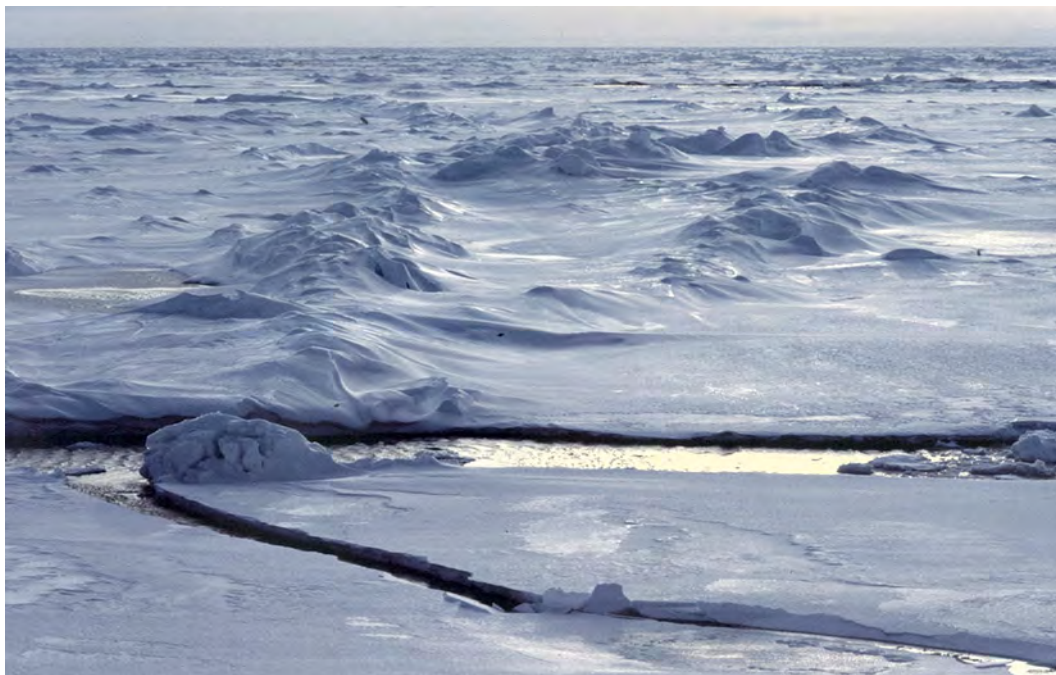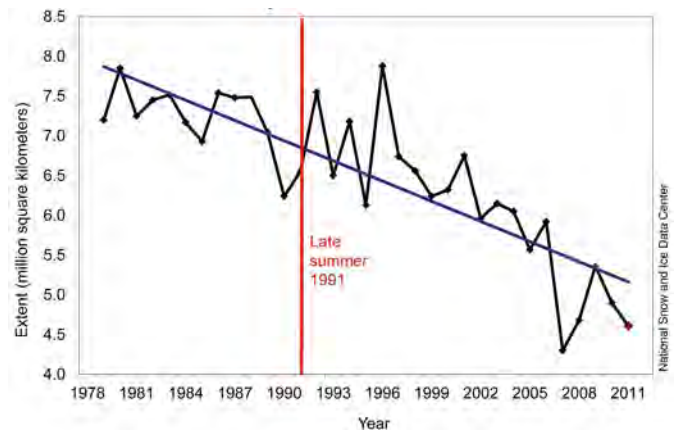
Fig. 2: Average monthly Arctic sea ice extent in September for the years 1979 to 2011 derived from satellite observations. The vertical red line marks the timing of the ARCTIC 91 expedition.

Abb. 2: Monatsmittel der arktischen Meereisausdehnung für September über die Jahre von 1979 bis 2011, abgeleitet aus Satellitendaten. Die senkrechte rote Linie markiert den Zeitpunkt der ARCTIC 91-Expedition.

reflects the increase of ice extent from summer to winter and the succeeding decrease from winter to summer. For climate research, it is more interesting to compare the ice extent measured on a fixed date for a number of years. In Figure 2, a curve resulting from this approach is shown. Here, the date of the minimum extent during summer was taken as the annual reference point. It shows large variations from year to year. But more importantly, it reveals a significant decrease of ice extent over the last decades. This trend was not obvious in 1991, with corresponding data available only for a little more than one decade. The curve represents the total, Arctic-wide sea-ice extent. Since this is an area of 7 million km^2, a closer look at local and regional ice conditions is useful. Figure 3 shows maps of sea-ice concentration gathered at the timing of the summer sea-ice minimum in the years from 2005 to 2010. At some locations, the spatial distribution of the ice cover and of the belts of equal ice concentration differs from year to year. One example is the Beaufort Sea north of Canada. At other locations, ice conditions appear to be more stable, for example north of Greenland. Such image sequences are useful when it comes to explaining the observed decrease of the Arctic sea-ice cover. However, they cannot be employed as isolated information. It is important to collect all relevant data on atmospheric and oceanic conditions. Different hypotheses are then examined with computer

Fig. 1: Sea-ice floes in the Arctic, with ice ridges and open water leads (Photo: W. Dierking).

Abb. 1: Eisrücken-bedeckte Meereisschollen in der Arktis durch Wasserrinnen voneinander getrennt (Foto: W. Dierking).
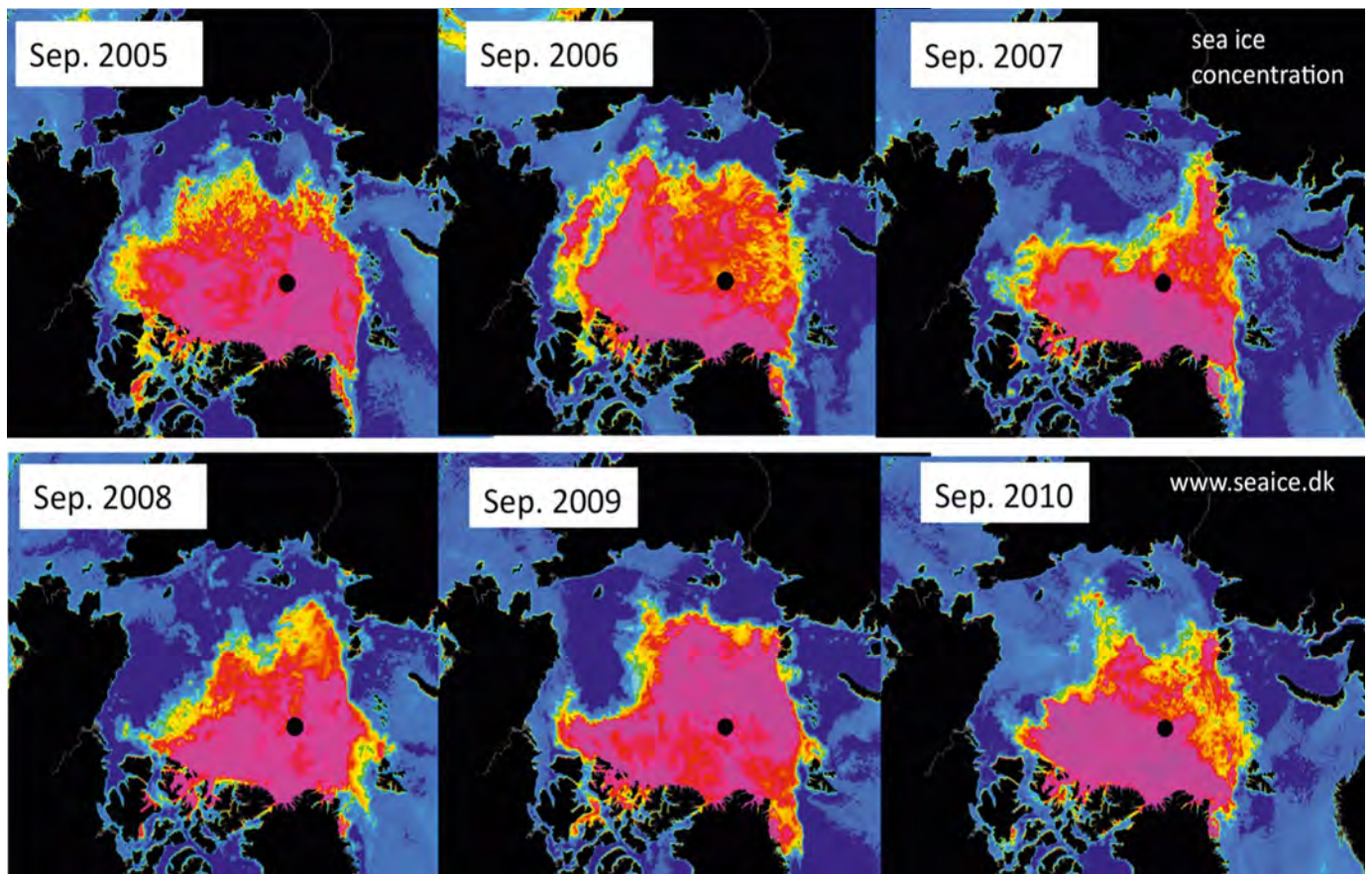
Fig. 3: Arctic sea-ice coverage at the time of the annual summer minimum for different years. The colours indicate the magnitude of sea-ice concentration (i.e. the fraction of a unit area on the ocean surface covered by ice). Blue is open water, green and yellow indicate low to moderate ice concentrations, and red and violet high concentration up to a closed ice cover. Source: http://seaice.dk.

Abb. 3: Meereisbedeckung der Arktis zum Zeitpunkt des jährlichen Sommerminimums für verschiedene Jahre. Die Farben zeigen das Werteintervall der Eiskonzentration (d.h. des vom Eis bedeckten Flächenanteils eines Meeresgebietes). Blau bedeutet offenes Wasser, grün und gelb sind geringe und mittlere Konzentrationen, rot und violett bedeuten hohe Konzentrationen bis zu einer geschlossenen Eisdecke. Quelle: http://seaice.dk.

simulations that are based on physical models. Such models describe the interactions between atmosphere, sea ice, and ocean and use measured meteorological and ocean data as input.

The absolute minimum in Arctic sea-ice extent hitherto was observed in summer 2007. Scientists (e.g., STROEVE & SERREZE 2008) named as key factors:
- ice pack thinning in preceding years,
- an unusual pattern of atmospheric circulation in 2007, during which persistent southerly winds gave rise to higher temperatures and ice transport away from the Siberian coast and Beaufort Sea, and
- predominantly clear skies fostering strong melt.

What can be expected for the future? Any answer to this question is not indisputable. Climate model projections indicate that the Arctic may be ice-free during summers already in the late 2020s (WANG & OVERLAND 2009). It is concluded that an anthropogenic influence on the most extreme negative trends in sea-ice extent is evident, but the effect of the natural variability can be strong on timescales between two and ten years (KAY et al. 2011). The perennial ice fraction in the Arctic reveals large rates of decline, which is in agreement with the observation of a decrease in the average ice thickness (COMISO 2012).

At this point it is interesting to also have a closer look on the Antarctic. Overall, there has been a slight increase in the maximum Antarctic sea-ice extent – but there are significant regional differences. At the western side of the Antarctic Peninsula, in particular in the Bellingshausen Sea, an increase in average winter air temperature, a warming of the ocean surface and a change to more northerly winds have been observed recently, which cause a decline of the sea-ice covered area. In the Weddell and Ross seas, both the sea-ice extent and the length of the sea-ice season increase. In the Ross Sea, for example, this is attributed to changes in regional atmospheric circulation patterns. Sea-ice researchers are hence intensively focusing on the changes in the large-scale circulation patterns around Antarctica and their impact on the sea-ice cover (TURNER et al. 2009).

SEA ICE REMOTE SENSING

If one considers the huge areal extent of the Polar Regions and the logistic difficulties to access this partly hostile environment, it becomes evident why field measurements from those regions are spatially and temporally sparse. Hence, observations from space are extremely useful for polar research. But how can such data be applied in a meaningful way, considering that the measurement devices are flown hundreds of
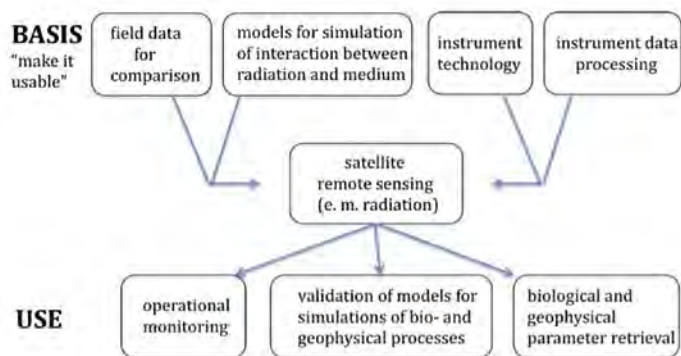
3

Fig. 4: The network of research disciplines around satellite remote sensing.

Abb. 4: Das Netzwerk von Forschungsdisziplinen, in dem die Fernerkundung eingebettet ist.

kilometres above the ice surface? In case of so-called passive instruments they measure the intensity of sunlight reflections or of thermal emission from the Earth surface. Active devices, such as laser or radar, transmit an electromagnetic signal and measure the travel time of this signal on its path between the satellite and the Earth's surface and back, and the signal echo intensity. In special instrument configurations, in which two and more signal channels are available, the phase differences between signals are also recorded. One of the major tasks of specialists working in the field of remote sensing is to develop methods by which a parameter of interest, for example sea-ice extent or concentration, can be retrieved from the directly measured quantities, for example from the brightness temperature. The latter depends on the physical temperature of an object and its emissivity, i.e., its "ability" to emit energy by radiation.

A major problem for remote sensing is that the Polar Regions are shrouded in clouds and darkness over long periods of the year. Hence, sensors measuring sunlight reflections or thermal infrared emission are only of limited use for sea ice and ocean research. A solution to this problem are instruments working with microwaves, i.e., with electromagnetic radiation in the wavelength range from 1 mm to 1 m, corresponding to frequencies between 300 and 0.3 GHz. Microwave sensors can see through clouds and are not affected by light conditions. However, scientist first had to learn how microwave radiation interacts with the medium "sea ice". Questions that had to be addressed were, for example, how one can explain the appearance of sea ice in radar images, or which frequency ranges reveal the largest emissivity contrasts between open water and different types of sea ice?

The successful use of remote sensing technologies for providing the information that is needed by sea-ice specialists and in other research disciplines requires the consideration of various aspects that are important for data interpretation and analysis (Fig. 4). The understanding on how sea-ice properties influence the emission, absorption, and scattering of microwave radiation has been developed on the basis of theoretical models. For such models, the results of field measurements are a mandatory input. How is sea ice structured? What do typical salinity and temperature profiles from the ice surface to the ice – water interface look like? How rough is the ice surface? How many air bubbles are found in the ice, how large are they,

and which shape do they have? These are a few questions to which field measurements give answers. The questions arise from our fundamental knowledge of various processes that occur while an electromagnetic wave is propagating in a medium. For example, the incoming wave is partly reflected at the ice surface according to Snell's Law and partly scattered in all directions, dependent on the surface roughness. Also air bubbles in the ice scatter the electromagnetic waves. Some of the wave energy is absorbed, and the magnitude of absorption depends on ice salinity and temperature. The sea-ice model used for simulating the microwave signal measured by the satellite sensor is often a simplification of the real ice conditions. For example, vertical profiles of continuously changing densities and salinities are replaced by thin layers with constant physical properties, or air bubbles of arbitrary shape are approximated by spheres or ellipsoids. Vertical and lateral variations of physical sea-ice properties occur on different spatial and temporal scales and can in many cases only be quantified inadequately. For practical purposes, the algorithms for simulating different scattering mechanisms often need to be computationally efficient, which means that suitable approximations are employed.

Two other important aspects are to be considered when extracting information from remote sensing data, that is the instrument technology, and closely related to it the processing of the raw instrument data. Obviously, different factors such as spatial resolution, areal coverage, or the noise level of the instrument affect the information extraction. As part of data processing, various signal filters and algorithms can be used. Filters are applied, for example, to suppress inherent instrument artefacts. A large number of algorithms exist for information enhancement, data segmentation, data classification, and other tasks.

Remote sensing data are used mainly for operational services, but also for supporting studies on sea-ice properties, kinematics, and dynamics. Operational sea-ice monitoring has an immediate economical and social impact. Ice services in different countries have to provide local and regional-scale sea-ice charts and forecasting of ice conditions for seasonally or perennially ice-covered waters in support of marine transport and offshore operations. In sea-ice research, various data products derived from satellite measurements are a valuable basis for assessments on how realistically sea-ice conditions and their changes are reproduced by computer simulations of ocean – ice – atmosphere interactions. The closer such models simulate recent ice conditions dependent on various meteorological and oceanic input parameters, the more useful they are assumed to be for predictions of future sea-ice state.

As already mentioned above, one of the central tasks of remote sensing specialists is the development of retrieval algorithms or interpretation strategies, which link the satellite data to the actual ice conditions. In operational sea-ice mapping, for example, trained analysts generate sea-ice charts using optical and radar images from satellite instruments together with observations from airplanes, helicopters and ships. Thereby they may be supported by the results of computer-based analyses of sea-ice conditions such as ice extent, concentration, drift, thickness, degree of deformation, or occurrence of different ice types. The situation is similar in more scientifically motivated studies. In the latter case, spatial and temporal

scales of observations as well as the ice parameters of major interests may be different. Examples are the Arctic- or Antarctic-wide timing of melt-onset and freeze-up and the regional melt pond coverage.

SEA ICE MEASUREMENTS IN THE CENTRAL ARCTIC PRIOR TO 1991

Before ARCTIC 91, only few projects had systematically studied sea-ice properties in the Central Arctic Ocean. Knowledge about sea ice in that region until then was mainly based on:

- Nansen's "Fram" drift 1893-1896 (NANSEN 1897),
- Russian activities related to the "Sever" expeditions of airborne Arctic surveillance when measurements were performed during aircraft landings on ice floes or during the drift of North Pole Research Stations since 1937 (e.g., ROMANOV 1995, FROLOV et al. 2005),
- US and UK military nuclear submarine cruises, which carried upward-looking sonars for the measurement of sea-ice thickness and since 1958 occasionally surfaced at the North Pole (e.g., BOURKE & GARRET 1987).
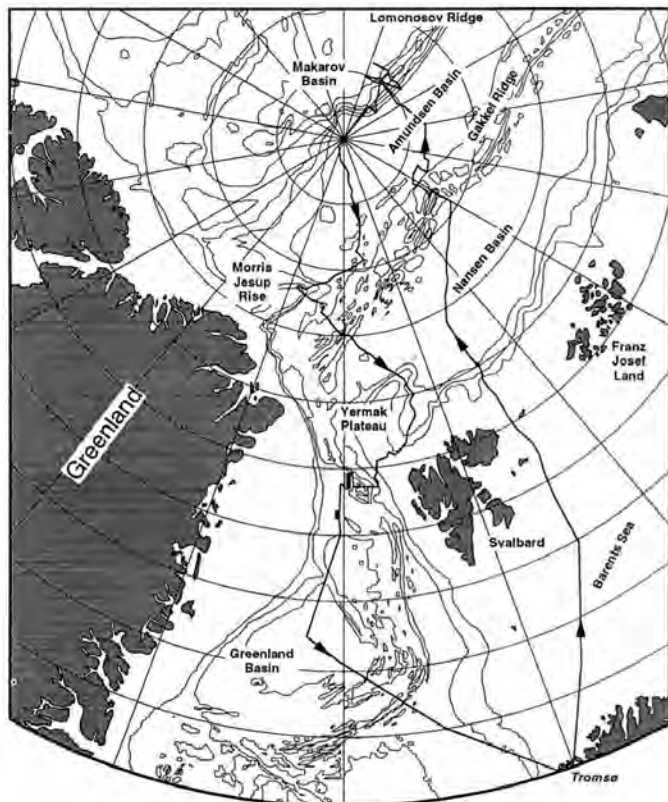
Fig. 6: Melt ponds on the sea ice in the central Arctic (Photo: W. Dierking).

Abb. 6: Mit Schmelztümpeln überdecktes Meereis in der zentralen Arktis (Foto: W. Dierking).

A number of scientific ice observations were made during the British Trans-Arctic Expedition in 1968/69 crossing the North Pole (KOERNER 1973), and significant studies were carried out in the Beaufort Sea during the US-Canadian Arctic Ice Dynamics Joint Experiment in the 1970s (AIDJEX, e.g, UNTERSTEINER et al. 2007). A detailed overview of the studies carried out prior to 1991 and of the results achieved until then are beyond the scope of this paper. At the beginning of the 1990s, comparatively little was known about structure, composition, and properties of Arctic multi-year ice (EICKEN et al. 1995). The knowledge on processes related to the Arctic melt season was in parts only marginal (EICKEN 1994). The potential of using satellite imaging radars for sea-ice observations was recognized in the late 1970s with the SEASAT mission (DIERKING & BUSCHE 2006) and through ice monitoring by Russian radar satellites since the early 1980s. Those research topics strongly influenced the activities of the sea ice and remote sensing teams that participated in the ARCTIC 91 expedition.

SEA-ICE MEASUREMENTS IN 1991

The ARCTIC 91 leg from Tromsø to the North Pole and back, which is addressed here, is shown in Figure 5. Preliminary results of the different measurement programs of the expedition are described in the cruise report (FÜTTERER 1992). In the following section, the sea-ice measurements and results are briefly summarized, as well as the data acquisitions carried out in conjunction with the remote sensing studies.

Fig. 5: Cruise track of RV "Polarstern" during Leg ARK-VIII/3 (ARCTIC 91), August – September 1991. Source: FÜTTERER 1992.

Abb. 5: Route von FS "Polarstern" im Sommer 1991 während des Fahrtabschnitts ARK VIII/3 (ARCTIC 91). Quelle: FÜTTERER 1992.

Actually, the ARCTIC 91 sea-ice sampling program was one of the first systematic sea-ice studies in the central Arctic (EICKEN et al. 1995). It included observations of ice conditions from the bridge of "Polarstern", helicopter observations of melt ponds on the ice surface (Fig. 6), ice-thickness measurements, and coring for physical, chemical, and biological analyses of the ice. The ice concentration along the ship's cruise (Fig. 5) in the pack ice was 91 ±13 %, and floe sizes

Fig. 7: Top: Drilling in a melt pond for ice thickness measurements (Photo: W. Dierking). Bottom: ice thickness measured during the cruise ARK-VIII/3 (ARCTIC 91) The ice thickness was either measured along 50 m long profiles or on different ice floes accessed by helicopter (from FÜTTERER 1992).

Abb. 7: Oben: Bohrung zur Ermittlung der Eisdicke unter einem Schmelzwassertümpel (Foto: W. Dierking). Unten: Während der Expedition ARCTIC 91 gemessene Eisdicken. Die Eisdicke wurde entweder entlang von 50 m langen Profilen oder auf verschiedenen Eisschollen ermittelt, die mit dem Hubschrauber angeflogen wurden (aus FÜTTERER 1992).
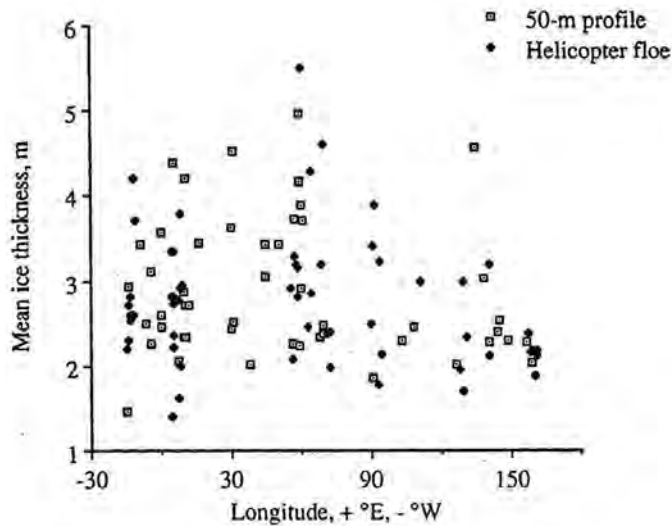
were frozen over by ice. More detailed analyses of these measurements are presented in EICKEN (1994) and EICKEN et al. (1995).

The remote sensing work on "Polarstern" was focused on collecting data for improving retrieval algorithms for sea-ice concentration and drift. To this end, Advanced Very High Resolution Radiometer (AVHRR) images with a horizontal resolution of 1 km were received on board (Fig. 8) (VIEHOFF 1990), and a line-scan camera was flown on the helicopter to obtain images with a horizontal resolution of 1-3 m (dependent on altitude) for comparison. The surface temperature was recorded with a ship-based radiometer and served as ground-truth for the AVHRR data. In addition, the ice surface topography was measured with a ground-based mechanical profilometer for studying the centimetre-scale roughness, and with an airborne laser altimeter mounted on a helicopter for detecting meter-scale undulations and determination of ice ridge statistics. The former was of interest for improving surface scattering models needed for simulating remote sensing data (see above), the latter served also as preparation for measurements in the Weddell Sea one year later (DIERKING 1995).

varied between hundreds of metres to few kilometres. In most cases, ridges and hummocks covered less than 5 % of the ice floe area, but at some locations, the corresponding value was as large as 30 %. Altogether 23 icebergs with a diameter of more than 100 m were sighted during the first half of the cruise. Level ice thickness data were collected in the vicinity of the ship along 50 m long profiles with a spacing of 5 m. In addition, thickness measurements were carried out on randomly chosen ice floes accessed by helicopter several kilometres away from the ship. For the first time ever, the pilots used GPS receivers to find their way back to the ship. The ice-thickness data are shown as a function of longitude in Figure 7. Ice cores were taken for on board analyses of ice texture, density, salinity, distribution and size of pores, and chlorophyll-a concentration. During helicopter flights, the areal fraction of melt ponds was recorded (Fig. 6). At some locations, ponds covered up to 50 % of the ice surface. At the end of August, almost all ponds
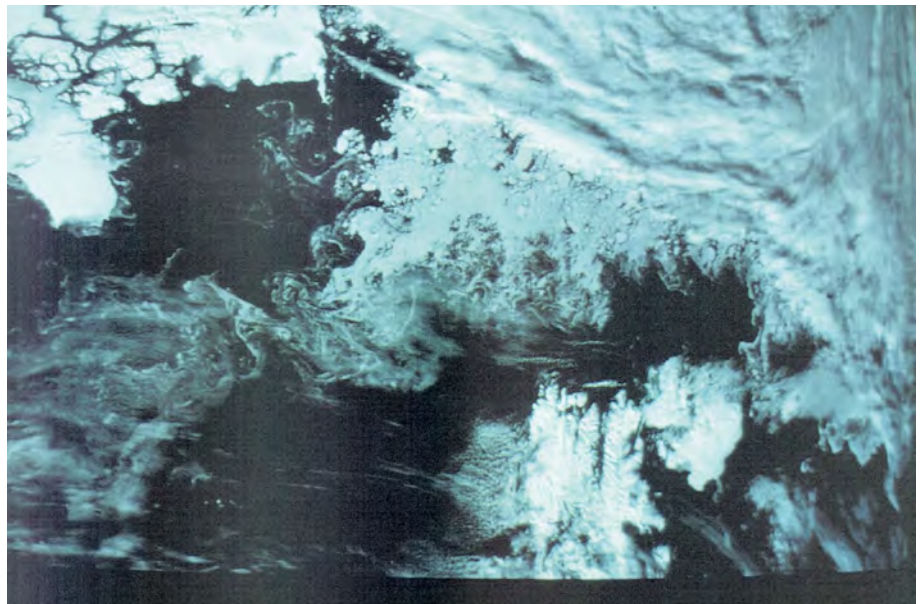
Fig. 8: AVHRR (Advanced Very High Resolution Radiometer) image (optical channel) received on RV "Polarstern". The image shows Fram Strait between the northeast coast of Greenland (upper left) and the northern part of Svalbard (lower right). In the centre of the image, the marginal sea ice zone is visible. To the north (upper right), the ice is hidden under clouds.

Abb. 8: Bild des Satelliteninstruments AVHRR (optischer Kanal), empfangen auf FS "Polarstern". Es zeigt die Framstraße zwischen der Nordostküste Grönlands (oben links) und dem nördlichen Teil Spitzbergens (unten rechts). In der Mitte des Bildes ist die Eisrandzone sichtbar. Im Norden (oben rechts) ist das Eis unter Wolken verborgen.

The data that were gathered by the remote sensing team on board "Oden" contributed significantly to a better understanding of the dominant interaction mechanism between radar waves and thick multi-year sea ice (CARLSTRÖM & ULANDER 1993). The team operated a ship-based radar system at the same frequency as the imaging radar on the ERS-1 satellite.

Concurrent to the radar data acquisitions from the ship, snow and ice properties were surveyed. The data acquisitions included snow depth along horizontal profiles, and snow density and wetness as a function of depth. The centimetre-scale ice surface roughness was measured using a laser profiler (Fig. 9). Ice density, temperature, and salinity were obtained from ice cores. Photographs were taken of the upper low-density ice layer, which were later used for determination of air bubble sizes.
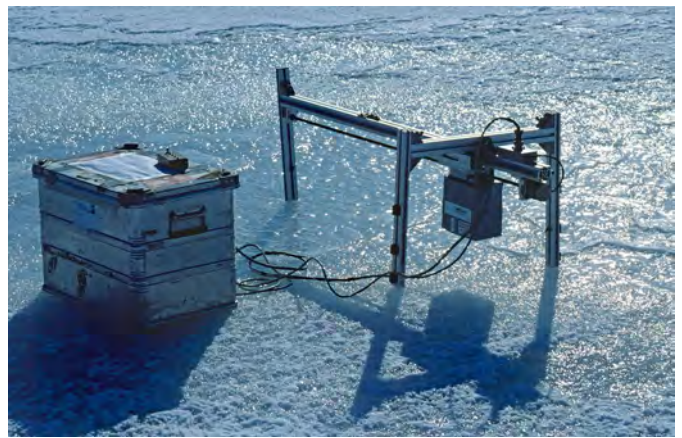
The joint expedition of "Polarstern" and "Oden" emphasized the importance of ship cruises into sea-ice covered regions for detailed in-situ investigation of ice properties. The field program of "Polarstern" during ARCTIC 91 covered studies from biology, geology, and oceanography that all benefitted from the results of the sea-ice measurement program.

Fig. 9: Swedish laser system for measuring centimetre-scale roughness on the ice surface (Photo: W. Dierking).

Abb. 9: Das schwedische Lasersystem zum Messen der Eisrauigkeit im Zentimeterbereich (Foto W. Dierking).

OBSERVATIONS OF SEA-ICE THICKNESS SINCE 1991

Ground-based measurements of sea-ice thickness

The growing experience with ship operations in the central Arctic since 1991 made it possible to visit the region of the North Pole more regularly, offering new opportunities for more systematic work. Subsequently, significant sea-ice studies were performed during follow-up cruises of "Polarstern" in 1996, 1998, 2001, 2007, and 2011 (see below), and during Canadian, US, and Swedish North Pole crossings in 1994 (e.g. TUCKER et al. 1999) and 2005 (e.g. PEROVICH et al. 2009).

Two of the most important sea-ice properties are its thickness and its degree of deformation, as they result from the integrative effects of the various growth and ablation processes and of external and internal forces which the ice experi-

ences during its lifetime. They are indicators of changes of the ocean–ice–atmosphere and climate systems in the Arctic. Their local and regional distributions in turn affect growth, melt, and drift of the ice. In 1991, there were only two means of obtaining accurate ice thickness information: submarine upward-looking sonar (ULS) and drill-hole measurements. Although military submarine ULS provided accurate information over large regions, scientists had little influence on times and regions of data acquisitions, and often data were released only many years later and with blurred geographic information. Extensive drilling was therefore performed during ARCTIC 91 (see Fig. 7). However, although this was a key activity during this dedicated cruise, only 653 measurements could be obtained during 56 ice stations on as many floes (EICKEN et al. 1995).

As it became evident that ice thicknesses would change significantly with impending climate change, and because future "Polarstern" cruises would provide ideal conditions for systematic ice-thickness surveys, AWI-scientists subsequently looked for easier ways of ice-thickness measurement to obtain more
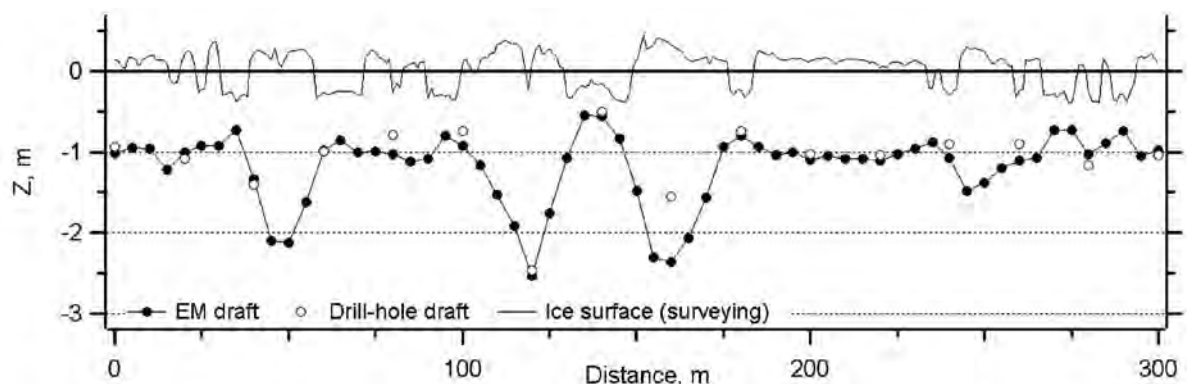
Fig. 10: Typical ice thickness profile of first-year sea ice measured during summer 1995 in the Laptev Sea, showing surface elevation and draft obtained by a combination of surface surveying, melt-pond depth sounding using a ruler stick, EM sounding, and drill-holes for validation (from HAAS & EICKEN 2001). The water level is at Z = 0 m. Negative surface elevation indicates location and depth of melt ponds.

Abb. 10: Typische Variationen der Eisdicke in einem Meereisprofil über einjährigem Meereis, gemessen in der Laptewsee im Sommer 1995. Die Abbildung zeigt das Oberflächenprofil und den Verlauf der Eisunterseite. Die jeweiligen Profile wurden durch die Kombination von Vermessungen der Oberfläche, Messungen der Tiefe von Schmelzwassertümpeln mit einem Messstab, elektromagnetischer Sondierung und Bohrungen zu Überprüfungszwecken gewonnen (aus HAAS & EICKEN 2001). Der Wasserspiegel liegt auf Z = 0 m; negative Werte des Oberflächenprofils zeigen die Positionen und Tiefen von Schmelzwassertümpeln an.

Fig. 11: Ice thickness measurements during ARK XVII/1, using a ground-based EM instrument housed in a kayak (Photo: J. Bareiss).

Abb. 11: Eisdickenmessungen auf der Expedition ARK XVII/1 mit einer in einem Kajak untergebrachten elektromagnetischen Sonde (Foto: J. Bareiss).

extensive surveys than could be obtained by drilling. Therefore, on four "Polarstern" expeditions in the years from 1993 to 1996, extensive studies of the suitability and performance of the geophysical methods of electromagnetic induction (EM) sounding and seismics using flexural waves were carried out. Although seismic measurements held some promise not only to retrieve ice thickness but also ice mechanical properties (HAAS 1997), EM sounding proved to provide most accurate and rapid measurements of level ice thickness in summer and winter, and good relative thickness estimates over deformed ice (HAAS et al. 1997, HAAS & EICKEN 2001). Through the active transmission of an electromagnetic field and induction of eddy currents in the conductive seawater under the resistive ice, this method senses the average electrical conductivity of the underground, which decreases with increasing ice thickness. Because the resistivity of snow and ice are both very high, these two media cannot be distinguished by EM measurements and the measured thickness corresponds to the total, ice plus snow thickness. Those "Polarstern" summer and winter expeditions provided ideal conditions for the validation and operationalizing of the EM method, and extensive comparisons with drill-hole measurements were performed (Fig. 10).

Because the EM method does not require contact with the ground and can be performed while moving, survey progress was improved by deploying EM instruments inside kayaks (Fig. 11), which served as amphibious sledges and allowed surveys across melt ponds. In 2001, average profile lengths of more than 2 km could be achieved during 54 ice stations. The method was subsequently also used from the ship while ice breaking, when an EM instrument was operated in front of "Polarstern" suspended 4 m above the ice with the bow crane (HAAS 1998).

Ice thickness from airborne electromagnetic sounding

Until 2001 ice-thickness measurements were limited to individual ice floes and could only be performed when the ice was thick enough to walk on. Therefore, in 1999 AWI scientists decided to develop an airborne EM sensor, which could be operated by helicopter (Fig. 12), and potentially with one of AWI's fixed-wing aircrafts. The sensor, named EM-Bird, was designed together with Aerodata AG (Braunschweig) and Ferra Dynamics Inc. (Canada). Besides the EM sounding devices for measuring the distance to the underside of the ice, the bird includes a laser altimeter to determine the distance to the ice surface (if the ice is covered by snow, it is the snow surface). The difference of those two measures is the ice (plus snow) thickness. The bird has to be towed 20 to 80 m under the aircraft to facilitate operation close to the ice where the measured EM fields are the strongest, and to avoid noise through induction in the metal of the aircraft. The first AWI EM-Bird was inaugurated during the "Polarstern" Arctic Mid-Ocean Ridge Expedition (AMORE) in 2001. Since then it

Fig. 12: Left: First flights with the EM-bird in the central Arctic Ocean in 2001. The bird is flown by helicopter 15 m above the ice surface (Photo: J. Lieser). Right: Since 2009, airborne EM ice thickness surveys are conducted with AWI's "Polar 5" airplane (Foto: C. Haas).

Abb. 12: Links: Erste Flüge mit der elektromagnetischen Sonde 2001 im zentralen Nordpolarmeer. Während des Hubschrauber-Fluges befindet sich die Sonde in einer Höhe von 15 m über dem Eis.
Rechts: Seit 2009 werden Flüge zur Eisdickenmessung mit elektromagnetischen Sonden auch mit AWI-Flugzeugen (hier "Polar 5") durchgeführt (Foto: C. Haas).

was used extensively not only during all "Polarstern" cruises into the Central Arctic Ocean and during the Ice Station "Polarstern" (ISPOL) and Winter Weddell Outflow Study (WWOS) projects in 2004 and 2006, respectively, but also from land-bases like Longyearbyen (Svalbard), Canadian Forces Station Alert (Canada), Barrow (USA), and even at the Russian North Pole Station Barneo. While surveys from land bases are limited by the range of the helicopters, "Polarstern" provides a mobile operating base and thus supports surveys over much larger regions than possible from land. In 2007, for example, more than 3000 km of profile data were collected.

A combination of electromagnetic sounding and laser altimetry for measurements of sea-ice thickness was also devised by PRINSENBERG et al. (2002). However, they tested the option of hard mounting the sensor on a helicopter instead of using a towed bird. Measurements by the fixed system are either carried out in "spot" mode (the helicopter remains over the same position during measurements, with its skids touching the ground) or in profiling mode (the helicopter is flown at very low altitudes). This way the level of necessary logistics is reduced, and the sensor's footprint on the ice is small. One major disadvantage is that such a system cannot be used on fixed-wing aircrafts.

Since 2009, the EM-Bird has been operated with AWI's "Polar 5" aircraft (Fig. 12), which now allows thickness surveys of more than 1000 km length during individual flights, and which can map most key regions of the Arctic within a few weeks (HAAS et al. 2010). However, the region of the North Pole and Eastern Arctic is still largely inaccessible by the range-limit of the aircraft, and future surveys will continue to rely on repeat visits by "Polarstern". Ship cruises also still offer unique opportunities for careful in-situ validation of the EM measurements by means of drill-hole and underwater ULS data, which require significant extra efforts during aircraft missions and can only be performed with ski-equipped planes.

During all thickness surveys in the 20 years since ARCTIC-91, AWI scientists and national and international collaborators have documented substantial changes, which are important for the understanding of the overall retreat of the sea-ice cover (Fig. 3). These are summarized in Figure 13. Modal (mean) ice thicknesses have decreased from 2.5 (3.11) m in 1991 to 0.9 (1.3) m in 2007 and 2011 (EICKEN et al. 1995, HAAS 2004, HAAS et al. 2008, Hendricks pers. comm.), i.e. by 64 % (mode) and 58 % (mean). The strongest drop occurred between 2004 and 2007. Because of the thinner ice "Polarstern" is now able to operate alone in the waters of the North Pole. Another effect was that the dramatic thinning substantially reduced the efforts required to perform validation and calibration drill-hole measurements. While in 1991 three auger sections of 1 m length had to be connected to drill through the ice, in 2001 the ice could be penetrated mostly with only two auger sections, and in 2007 one section was often enough!

In parallel to the efforts of the AWI-team to improve ice thickness observations in the central Arctic Ocean in the past 20 years, significant advances have been made by other groups with airborne laser altimetry (e.g. HVIDEGAARD & FORSBERG 2002, KWOK et al. 2012) and satellite laser and radar altimetry (e.g. KWOK et al., 2009, LAXON et al. 2003). These methods
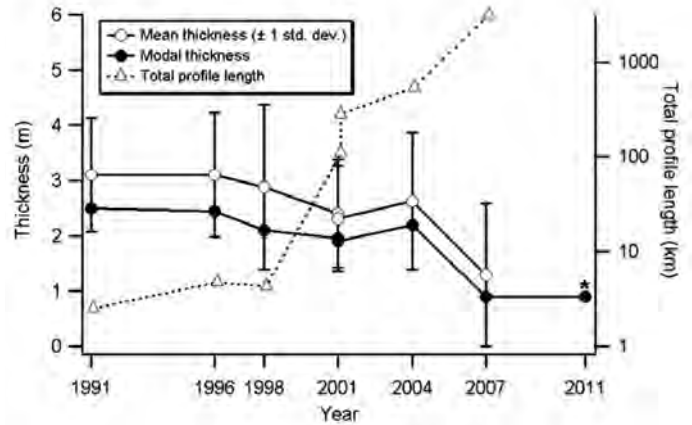
Fig. 13: Ice thickness change observed on "Polarstern" cruises to the central Arctic Ocean during the past 20 years. The increase in total profile length is also shown (dashed curve), and is due to improvements of the observational methods (1991 = drilling, 1996-2001 = ground-based EM-sounding, since 2001 = airborne EM sounding). Data from 2011 marked by an assterisk are courtesy of S. Hendricks (AWI).

Abb. 13: Änderungen der Eisdicke, beobachtet auf "Polarstern"-Expeditionen im zentralen Arktischen Ozean während der letzten 20 Jahre. Die Zunahme der gemessenen Profillängen ist ebenfalls gezeigt (gestrichelte Kurve). Sie ist Folge der technologischen Verbesserungen des Messverfahrens (1991 = einzelne Bohrungen, 1996-2001 = bodengebundene elektromagnetische Sondierung, 2001 und folgend = Sondierungen vom Hubschrauber oder Flugzeug). Die Daten von 2011, gekennzeichnet durch Sternchen, stammen von S. Hendricks (AWI).

obtain estimates of the snow or ice freeboard (i.e. the height of the snow or ice surface above the local water level), from which ice thickness can be calculated based on assumptions of isostatic equilibrium, the thickness of the snow, and the densities of snow and ice. Between 2004 and 2008, the laser altimeter measurements of NASA's ICESat satellite showed similar amounts of thinning as found during the "Polarstern" expeditions, but provided more extensive information because it covered the complete Arctic Ocean twice per year (KWOK et al. 2009). Using the radar altimeter aboard ESA's Envisat, GILES et al. (2009) showed the regional extent of the strong thinning between the winters of 2004–2007 and 2008, which corresponded to the strong thinning observed by the "Polarstern" in the summer of the same time period (HAAS et al. 2008). In 2010, ESA launched the CryoSat satellite, dedicated to observe thickness changes of Arctic and Antarctic sea ice with an improved, synthetic-aperture radar altimeter (WINGHAM et al. 2006).

The strong sea-ice thinning is not only caused by thermodynamic changes, but also by changes in ice drift and dynamics which have led to reductions in the amount of old, thick ice in the Arctic Ocean (e.g. KWOK et al. 2009, MASLANIK et al. 2011). Satellite passive-microwave and scatterometer observations have been instrumental in these observations, which are facilitated by the differences between microwave properties of first- and multi-year ice. In particular, these data show that

- in 2007 the region of the North Pole was covered only by first-year ice for the first time since satellite observations were available in 1979,
- thick multi-year ice has retreated into a narrow band off the coasts of Greenland and Canada, and
- the majority of the Arctic Ocean is now covered by first- and second-year ice only.

This means that today research vessels such as "Polarstern"

can traverse and investigate most regions of the Arctic Ocean with relative ease, and that multi-ship expeditions are no more required for operational reasons alone.

THE USE OF IMAGING RADAR FOR SEA-ICE MONITORING

Sea ice observations with the ERS-1 radar systems

In conjunction with the launch of ERS-1, a number of projects were started that focused intensively on research topics related to radar remote sensing of sea ice. Topics included:
- experimental and theoretical investigations of radar wave scattering from sea ice,
- ground-based and airborne field campaigns for collecting radar signatures typical for different ice types and ice conditions,
- development of image processing algorithms specifically adapted to sea ice observations, and
- the implementation of operational sea ice monitoring strategies.

The ERS-1 satellite carried different radar systems and other instruments on board. The synthetic aperture radar (SAR) was used to collect images along a 100 km wide swath with a horizontal resolution of 30 m. Such a high resolution requires a large antenna that cannot be mounted on a satellite. The notation "synthetic aperture" indicates that a long antenna is "synthesized" when processing the raw data that are measured by the shorter physical antenna. The so-called (radar) scatterometer measures the intensity reflected from the Earth's surface at a much coarser resolution of 48 km. This instrument type has been applied, for example, to derive large-scale ice drift-patterns over the entire Arctic and Antarctic. The third radar instrument on ERS-1 was an altimeter. Its data were applied for retrieving ice thickness (as mentioned above) and for the mapping of sea-ice extent.

Comparing and combing data from different satellite radar systems

In 1995, two more satellites with imaging radars on board were launched: the European ERS-2 (with the same radar instruments as ERS-1), and the Canadian RADARSAT. The latter used radar signals at a polarization different from ERS-1/2. With the SAR system of RADARSAT it became possible to select a number of imaging ("beam") modes that differed in swath width (50-500 km), spatial resolution (8-100 m), and the viewing angle relative to nadir (selectable in the interval 10-59°). This flexibility made it possible to acquire image series with higher temporal resolution than with ERS-1/2. ERS-1 was taken out of operation in 2000, ERS-2 in 2011. In 2002, ESA launched ENVISAT, which – besides other instruments – carried an advanced SAR (ASAR) and a radar altimeter on board, but no scatterometer. Communication with ENVISAT was lost in 2012. Also the ENVISAT ASAR provided options to select different imaging geometry, and in addition different polarizations of the radar signal. All those SAR systems were using the same radar frequency (C-band, wavelength 5.7 cm). The SAR on SEASAT, which was the first satellite designed for monitoring ocean regions, was operated at L-band (wavelength 25 cm). Unfortunately, the mission ended abruptly in 1978 after only four months duration because of a short circuit in the satellite's electrical system. Also the Japanese satellites JERS-1 (1992-1998) and ALOS (2006-2011) were equipped with an L-band SAR. Shorter wavelengths (X-band, wavelength 3.1 cm) are used for the German TerraSAR-X (in space since 2007). Typical for the recent satellite missions is the much larger flexibility in selecting different modes for image acquisitions.

This (incomplete) list of satellites carrying imaging radars is an example for the development of space technology, which has considerably improved the information retrieval of state and variations of the polar sea-ice covers. Sea ice remote sensing does not only benefit from more and more advanced radar sensors but also from progress in the technology of other space-borne, airborne, and ground-based instruments – as the example of sea-ice thickness measurements pictured above demonstrates.

The combination of satellite, airborne, and ground-based data acquisitions

Comparisons of satellite SAR imagery with optical and radar images acquired at a high spatial resolution from airplanes are extremely useful to assess the potential of different radar configurations for ice-type classification. In the high-resolution low-noise images of aircraft instruments, many structural details of the ice cover can be identified. An example of airborne multi-polarization images acquired by an airborne SAR system at C- and L-band is shown in Figure 14. Aerial photography provides the means for the interpretation of the radar data. A problem, however, is that sea ice is often covered by snow which means that no information can be obtained about the ice structure beneath the snow from photos taken in the visible or infrared. This is a great advantage of radar: if the snow is dry, radar can look through it. The strategy of combining optical and radar aircraft and satellite images was used, for example, in a field campaign around Svalbard. The objective was to assess the technical performance of the European Space Agency's Sentinel-1 SAR mission for sea-ice mapping (DIERKING 2010).

For a direct comparison of different radar configurations, ground-based measurements offer the advantage that sea-ice properties affecting the radar waves can be directly measured concurrently – one only has to make sure that the work on the ice does not interfere with the radar measurements from the ship. A comparison of radar systems that operate at different wavelengths was, e.g., carried out by DIERKING et al. (1999) in the Baltic Sea. Their measurement results indicated that a number of different interaction mechanisms between sea ice and radar waves were effective. Both surface and volume scattering mechanisms have to be taken into account, but their relative contributions depend on the radar frequency. DIERKING et al. (1999) found, for example, that the radar intensities at X-band (3 cm wavelength) were mainly influenced by the air bubbles in the subsurface ice layer, at C-band (5.7 cm) by the centimetre-scale surface roughness, and at L-band (25 cm) by the structure of the ice-water interface. The latter result is special for the Baltic Sea where ice does not survive the summer melt (i.e. it is first-year ice) and its salinity is between 0 and 2 psu (practical salinity units). In the Arctic and the Antarctic, the salinity of
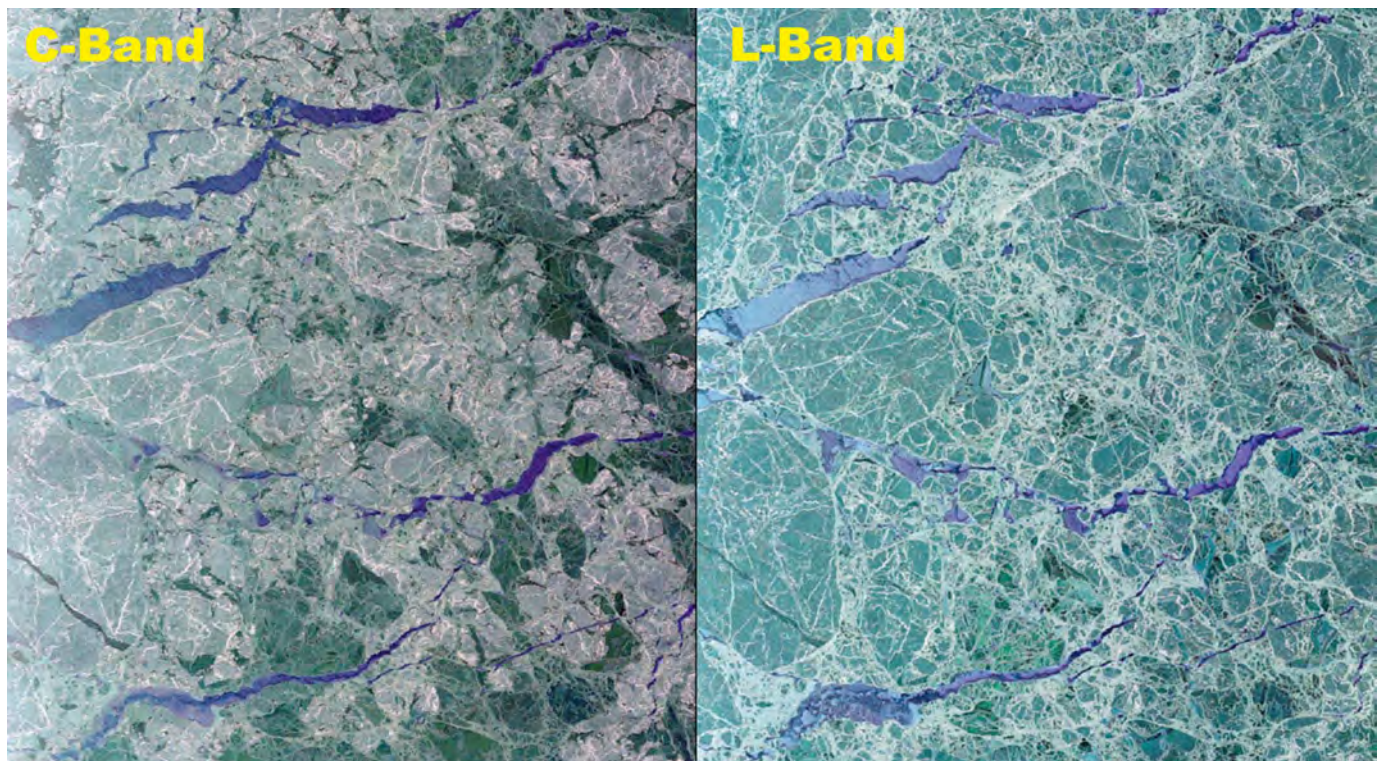
Fig. 14: Airborne radar images of sea ice north of Svalbard, acquired at a frequency of 1.25 GHz (L-band) and at 5.3 GHz (C-Band). The image width corresponds to 12 km. At each frequency data were measured at different polarization combinations (HH, HV+VH, VV, V = vertical, H = horizontal, first letter = transmitted signal, second letter = received signal). The colour images are composed of three layers (red, green, blue: RGB, with R-HV+VH, G-HH, B-VV). Bluish areas are thin ice and open water. Dark green patches at C-band (upper image) indicate young ice, light green patches older ice. Bright lines and patterns in the radar images are ridges and deformation zones, respectively (Courtesy: Technical University of Denmark).

Abb. 14: Luftbilder, aufgenommen mit verschiedenen Radarsystemen über dem Meereis nördlich von Spitzbergen. Die Radarsysteme wurden mit Frequenzen von 1.25 GHz (L-Band) und 5.3 GHz (C-Band) betrieben. Die Breite der Bilder entspricht einer Strecke von 12 km. Die Daten wurden in verschiedenen Polarisations-kombinationen aufgenommen (HH, HV und VH, VV; V = senkrecht, H = waagerecht; erster Buchstabe = abgestrahltes Signal, zweiter Buchstabe = empfangenes Signal). Die Farbbilder sind aus drei Ebenen (RGB, rot-grün-blau) zusammengesetzt, denen die Polarisationskombinationen wie folgt zugeordnet wurden: R-HV+VH, G-HH, B-VV. Blaue Flächen sind dünnes Eis und offenes Wasser. Die dunkelgrünen Flächen im C-Band (oben) stehen für junges Eis, hellgrün bedeutet älteres Eis. Die hellen Linien und Muster sind Eisrücken und zerbrochene und/oder zusammengeschobene Eisflächen (Quelle: Technische Universität Dänemark in Lyngby).

first-year ice varies from 5 to 12 psu, and the influence of the ice-water interface on the measured radar signal, which depends on ice salinity and thickness, is much weaker. At this point one could ask whether the knowl-edge about scattering mechanisms and their relative contributions is necessary in such detail? The answer is definitely yes. This knowledge is the basis for any interpretation of radar signatures observed in satellite images, and, going one step further, it is needed to develop methods for sea-ice type classification and for the extraction of information on geophysical parameters related to the ice conditions, for example the onset of melt (see below).

The disadvantage of ground-based radar measurements is that they are restricted to a few small spots on the ice. With air- and space-borne image acquisitions larger areas with different ice conditions and ice types can be covered within short time intervals. But considering the logistic problems in ice-covered waters, it is often difficult to get the field crew into the view of the satellite or aircraft at a scheduled time. Airborne measurements are more flexible with respect to the flight path, but it depends much on the weather conditions whether they can be carried out. Satellites fly on orbits fixed in space and time.

One important aspect of combining ground, airborne and satellite measurements is the possibility of upscaling or down-

scaling. Related issues are, for example: how does the coarser spatial resolution of a satellite sensor affect the capability to separate different ice types? In which way is the local ice state observed on the ground or from the airplane influenced by regional conditions, which can only be determined from satellite images because of their wider imaging swath? Is it possible to devise algorithms by which geophysical parameters can be retrieved on sub-pixel scale?

Ice type separation in radar images

One central question that arose in particular for operational ice mapping services was how well one can separate different ice types in SAR images. For getting an answer, STEFFEN & HEINRICH (1994) used ERS-1 and optical images of the Landsat Thematic Mapper from the Beaufort Sea. First- and multi-year ice revealed different radar intensity ranges and could be clearly distinguished. If frost flowers (Fig. 15) covered the surface of young ice, the radar intensity was much higher compared to a bare ice surface. Ice-free areas in the pack ice could be reliably detected only under calm wind conditions or at wind speeds >10 m s^{-1}. This can be explained as follows: The wind generates small ripple waves (lengths millimetres to decimetres) on the water surface. The backscattered radar

intensity is the larger the rougher a surface is. Hence, the radar intensity of an open water surface may be very similar to the ice at certain wind speeds. The highly variable radar signatures of open water are in fact one of the challenges in automatic mapping of sea-ice conditions.

FETTERER et al. (1994) investigated the quality of ice type maps from the Arctic that were automatically generated using radar intensity as classifier. They found that first-year ice and multi-year ice could be separated with high accuracy, but the algorithm sometimes failed to correctly classify open water and new ice as well as smooth and rough first-year ice. It is important to note that the radar intensities measured for different ice types and their relative differences are a function of radar frequency, polarization, and incidence angle. In the case of ERS-1, none of those parameters could be varied. Another important point is that the radar intensity of sea ice changes partly drastically with the onset of melt (see below). In the investigations by STEFFEN & HEINRICH (1994) and FETTERER et al. (1994), the images used for the analyses were acquired under freezing conditions.

Ship-based radar measurements combined with ground-based laser-profiling of the ice surface revealed a strong sensitivity of the observed radar intensity to the surface roughness at centimetre- to decimetre-scale (DIERKING et al. 1997), such as shown in Figure 9. Frost flowers (Fig. 15), saline snow, and slush on the ice surface can considerably influence the backscattered radar intensities. This effect was investigated in more detail by ULANDER et al. (1995), who used ERS-1 images and
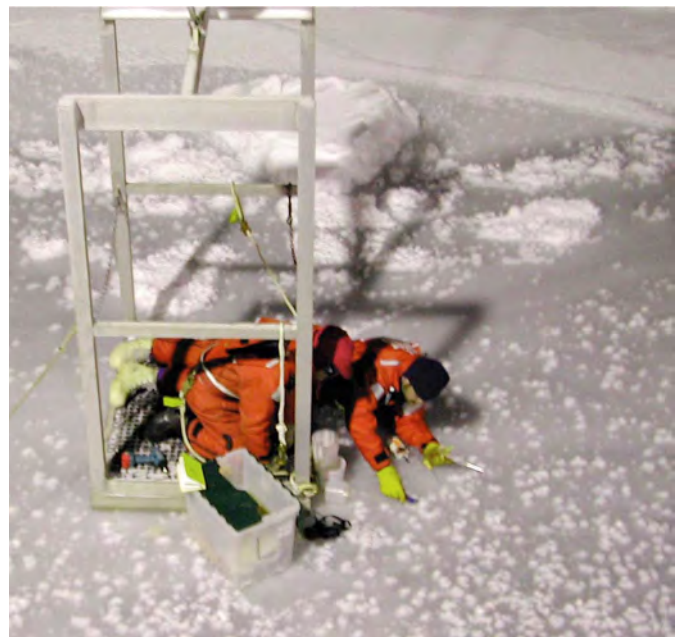

Fig. 15: Sampling of frost flowers on sea ice (Photo: W. Dierking).

Abb. 15: Beprobung von Raureif auf dem Meereis aus einem Personenkorb vom Schiff aus (Foto: W. Dierking).

developed a theoretical scattering model on the basis of in-situ data from the ARCTIC 91 expedition. They found that surface scattering dominated the radar signal and that different surface
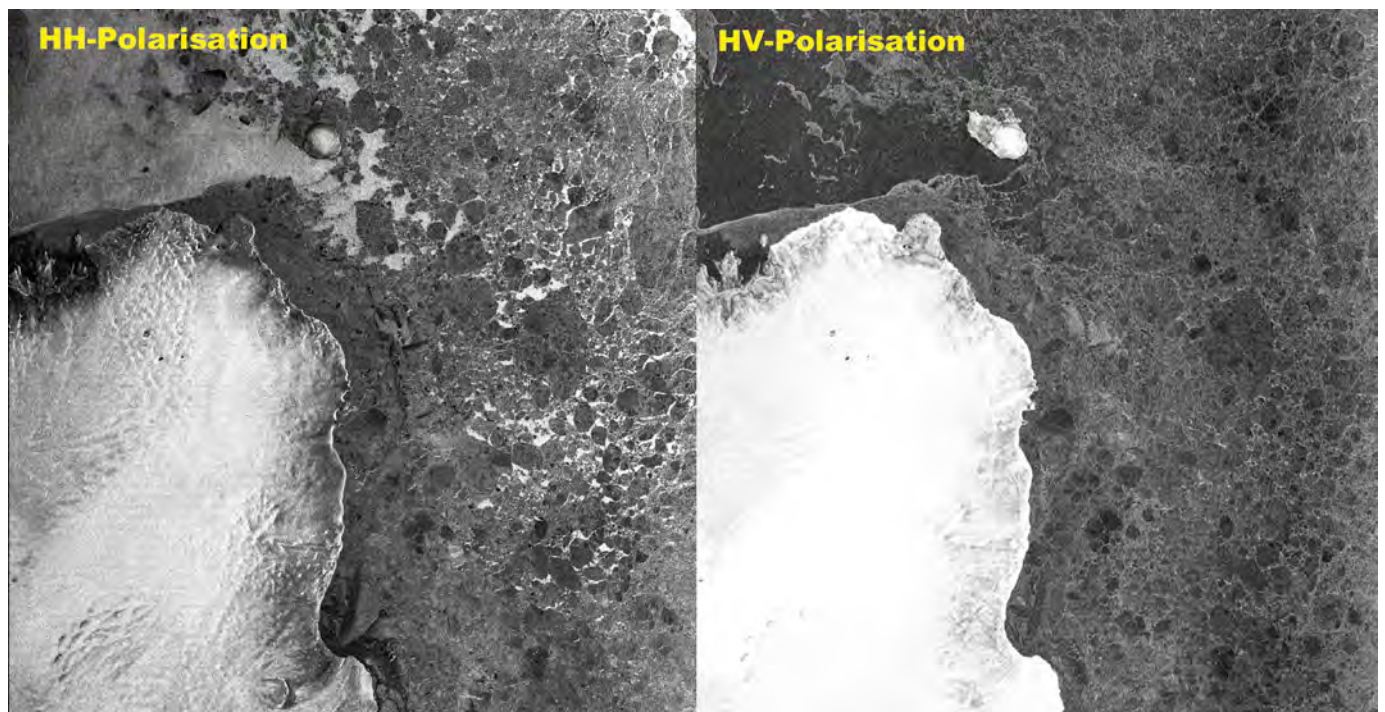
Fig. 16: Envisat ASAR images over sea ice (appearing greyish) and land ice (bright) around the northeast tip of Nordaustlandet (Svalbard), acquired at two different polarizations. The images cover an area of 100 km x 100 km. The area in the upper left corner is to large part open water. It appears bright at HH-polarization and dark at HV-polarization. "H" and "V" denote horizontal and vertical polarization of the radar signal, respectively; "HV", for example, means that the transmitted signal is horizontally and the received signal vertically polarized (Copyright: ESA).

Abb. 16: Envisat ASAR-Bilder, aufgenommen über der nordöstlichen Spitze von Nordaustlandet (Spitzbergen). Das Bild zeigt Meereis (Grautöne) und Landeis (hell bis weiß). Die Bilder wurden in zwei verschiedenen Polarisationskombinationen aufgenommen und entsprechen einer Fläche von 100 km x 100 km. Das Gebiet links oben ist zum größten Teil offenes Wasser, das im HH-polarisiertem Bild hell und im HV-polarisierten Bild dunkel erscheint. (H = waagerechte, V = senkrechte Polarisation, "HV" bedeutet z. B., dass das abgestrahlte Signal waagerecht und das empfangene Signal senkrecht polarisiert ist), (Copyright: ESA).

conditions caused large variations in the appearance of young ice in the ERS C-band images. At L-band, for example, the influence of frost flowers on the radar signal is much weaker (DIERKING 2010).

Figures 14 and 16 show examples of radar images taken over sea ice that differ in frequency and polarization. If they are combined, more ice classes can be distinguished than with single-frequency single-polarization radar. It is also easier to separate open water and ice (Fig. 16). Hence it is in principle beneficial for operational sea-ice mapping to combine the imagery of different satellite radars. But economical questions concerning the costs for data acquisitions, processing, and map production have also to be addressed in this context. Therefore basic research is needed to assess the pros and cons of various combinations of radar imaging configurations. When using two or more satellites to observe a given area on the Earth's surface, the time of over-flight varies from satellite to satellite. Since ice drift-speed may be considerable (dependent on wind and ice conditions; at the ice margin, for example, 30 km d^{-1} are not unrealistic), a temporal difference of a few hours may be too long for a meaningful image combination (in particular for narrow swath width <100 km).

DIERKING & BUSCHE (2006) compared images from two satellites. They focused on data from SAR systems on ERS-1 (C-band) and JERS-1 (L-band) that were acquired at the east coast of Greenland and south of Svalbard with time differences of 25 and 35 minutes, respectively. They had to consider that the instruments did not only differ in frequency but also in their polarization and look angle. Another problem was the lack of any in-situ sea-ice data. Nevertheless, they could demonstrate that the information content of both radar systems is complementary. Zones of ice deformation and smooth level ice floes are much easier to separate at L-band, but first- and multi-year ice can be better distinguished at C-band.

Which ice surface properties can be obtained from SAR images?

The ice surface structure is characterized by, for example, distances between ridges, ridge heights, floe sizes, ice concentration, and ice freeboard. Knowledge about these parameters is valuable for studies of the wind drag and wind turbulence in the atmospheric boundary layer which can be as shallow as 50 m over sea ice (DIERKING 1995, GARBRECHT et al. 1999, GARBRECHT et al. 2002). Building on the experience with laser profiling of the sea-ice surface topography gathered during ARCTIC'91, AWI-scientists focused on the question whether satellite SAR data could be used to derive the mean ridge spacing in a given area. To this end, the intensity variations in ERS-1 images were compared to laser profiles measured from a helicopter (HAAS et al. 1999). It was found that the mean radar intensity was higher when more ridges per unit area were present. However, the correlations between intensity and ridge frequency were unfortunately only poor.

It is not possible to retrieve variations of surface height directly from SAR images. This does not mean that it is not worthwhile to take SAR images as data source for questions related to ice surface structure. One example is to complement height measurements ("vertical structure") from laser profilers (one-dimensional) or laser scanners (two dimensional along a narrow strip) with information about horizontal ice deformation patterns (two-dimensional along a wider strip) from satellite images. If the spatial resolution of a SAR image is sufficiently high, it is possible to identify single ice floes and
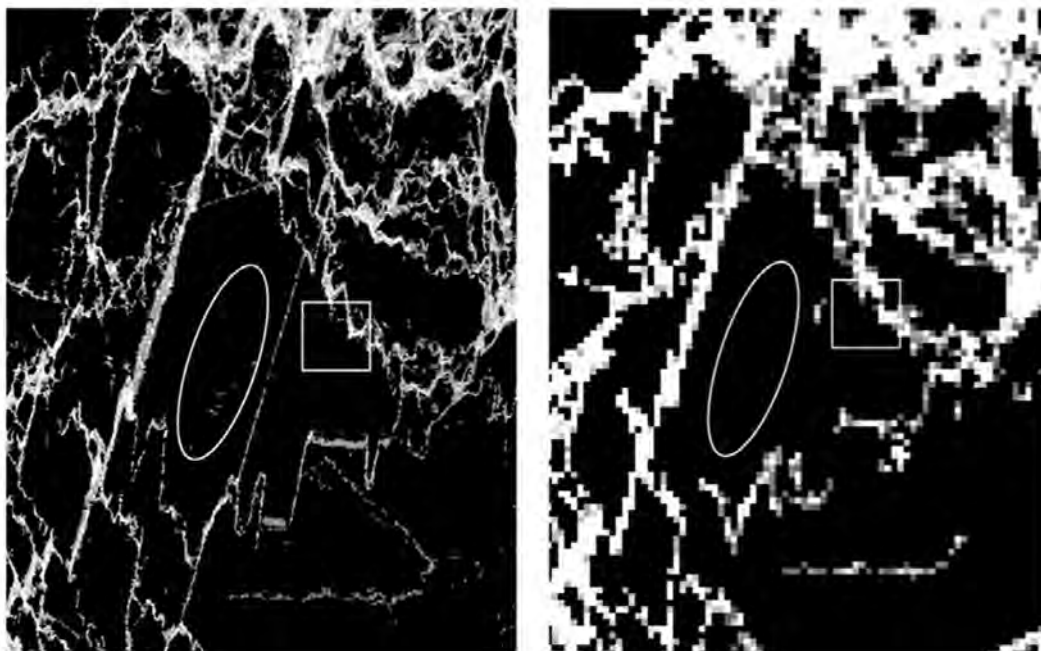
Fig. 17: Ice ridges detected in an airborne L-band SAR image (left = pixel size 5 m, right = 25 m). Demonstrated is the target loss (ellipse) and the image smear (rectangle) at coarser spatial resolution. From DIERKING & DALL (2008).

Abb. 17: Detektierte Eisrücken in einem vom Flugzeug aus aufgenommenen SAR-Bild (Pixelgröße links = 5 m, rechts = 25 m). Gezeigt ist der Verlust eines Objekts (in der Ellipse) und die "Verschmierung" von Bildelementen (Rechteck) in dem Bild mit schlechterer Flächenauflösung (rechts). Aus DIERKING & DALL (2008).

zones of deformation (Figs. 14, 16, 17). Whether the resolution is "sufficient" depends in general on which spatial scales the parameter of interest changes its value. The size of ice floes, for example, lies between about 10 m ("small floe") and more than 10 km across ("giant floe"). The width of ridges (as seen on the ice surface) can vary from less than a meter up to more than 20 meters. DIERKING & DALL (2007, 2008) found that ice ridges and rafting zones (which occur in thin ice) are preferably mapped using L-band SAR images at high spatial resolution of 5–10 m (Fig. 17). However, even at coarser resolution (25–30 m), the major deformation patterns can be clearly distinguished, although narrow ridges and rafting zones are lost in the image, whereas the remaining structures appear broader due to image "smear". The influence of radar polarization and incidence angle on detection is only minor.

Surface properties differ depending on ice conditions and ice types. Hence, the information on ice types, as discussed above, is useful for categorizing the ice surface structure. Also valuable in this context is ice freeboard that can be obtained if the ice thickness is known. One question of interest has been whether it is possible to relate ice thickness or freeboard to the measured radar intensity? Among remote sensing specialists it was clear from the beginning that a direct relationship does not exist. Radar signatures are predominantly influenced by millimetre-to-decimetre scale surface and volume properties of sea ice. So the question is whether such properties differ between different ice types. (One criterion for separating ice types is their thickness). BUSCHE et al. (2005) compared thickness measurements carried out with an EM-bird attached to a helicopter with the radar signatures along the flight path obtained from a satellite SAR image (Fig. 18). The problem was to compensate the effect of the ice drift that occurred between helicopter measurements and satellite over-flight, since no corresponding information was available. The direct correlation between radar intensity and ice thickness revealed only a low correlation. With modern SAR systems it is also possible to use the intensity ratio between differently polarized signal channels (specifically HH- and VV-polarization; see Fig. 14 for an explanation of the denotation). In one study, ice thickness could be retrieved from ENVISAT ASAR C-band data based on the polarization ratio VV/HH (NAKAMURA et al. 2009), but only for ice that was less than 1.2 m thick. In general, multi-polarization SAR systems operated at L-band are better suited for thickness retrievals (NAKAMURA et al. 2006) but the restriction to thinner ice applies also in this case. All in all, no robust, generally valid method exists to determine the ice thickness directly from SAR data.

THE MELTING SEASON

A large part of the ARCTIC 91 cruise was carried out under melting conditions

as Figure 6 demonstrates. How do such conditions affect the microwave properties of sea ice? In fact, the change of microwave properties is significant. WINEBRENNER et al. (1994) observed a distinct decrease of the radar intensity scattered from multi-year ice at the onset of melt such as shown in Figure 19. Multi-year ice is character-ized by the presence of air bubbles in the upper ice layers. Radar waves that penetrate into the ice are scattered by those bubbles. However, radar signals of perceptible intensity propagate through the ice volume only if temperatures are below freezing and the ice surface is dry. When the ice surface starts to melt, the radar penetration depth is drastically reduced and the level of volume scattering from air bubbles is very low. This decrease of the received radar intensity is also visible in the images of SAR systems operated at other frequencies. The reverse process is observed during autumn. When temperatures fall below freezing, the volume scattering contribution increases strongly and rapidly (WINE-BRENNER et al. 1996). KWOK et al. (2003) used images from the Canadian RADARSAT to study the timing of melt-onset over the entire Arctic sea-ice area. They found that the radar intensity from first-year ice increases with the onset of melt. For melt detection, they developed an algorithm that uses not only changes of radar intensity but also additional criterions related to the distribution of radar intensity values in an area of 5×5 km^2 (including 2500 pixels). The algorithm was validated by comparing the timing of melt onset obtained from RADARSAT data with the zero crossings of buoy temperature records. The corresponding dates differed by 1–2 days. KWOK et al. (2003) noted that the timing of melt onset derived from passive microwave data occurs later, i.e. it is biased to a
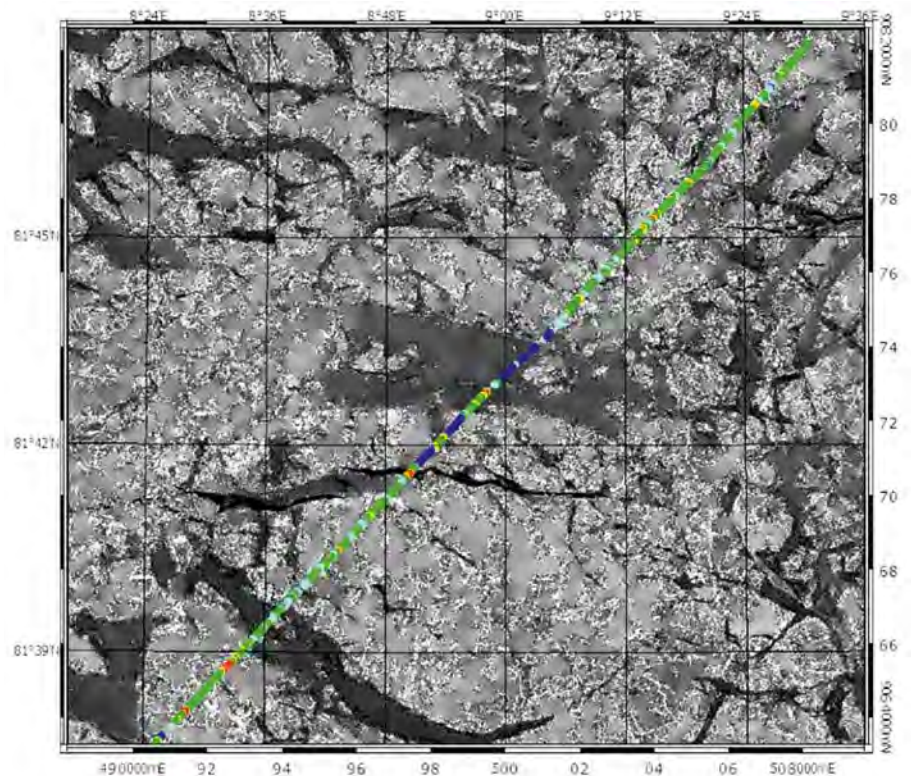
Fig. 18: Radarsat-1 SAR image showing a mix of first- and multiyear ice in Fram Strait, with ice thickness obtained by helicopterborne EM sounding overlayed (from BUSCHE et al. 2005).

Abb. 18: Radarsat-1 SAR Bild aufgenommen über ein- und mehrjährigem Eis in der Framstraße. Die mittels elektromagnetscher Sondierung vom Hubschrauber gemessene Eisdicke ist als farbiges Profil darüber gelegt (aus BUSCHE et al. 2005).
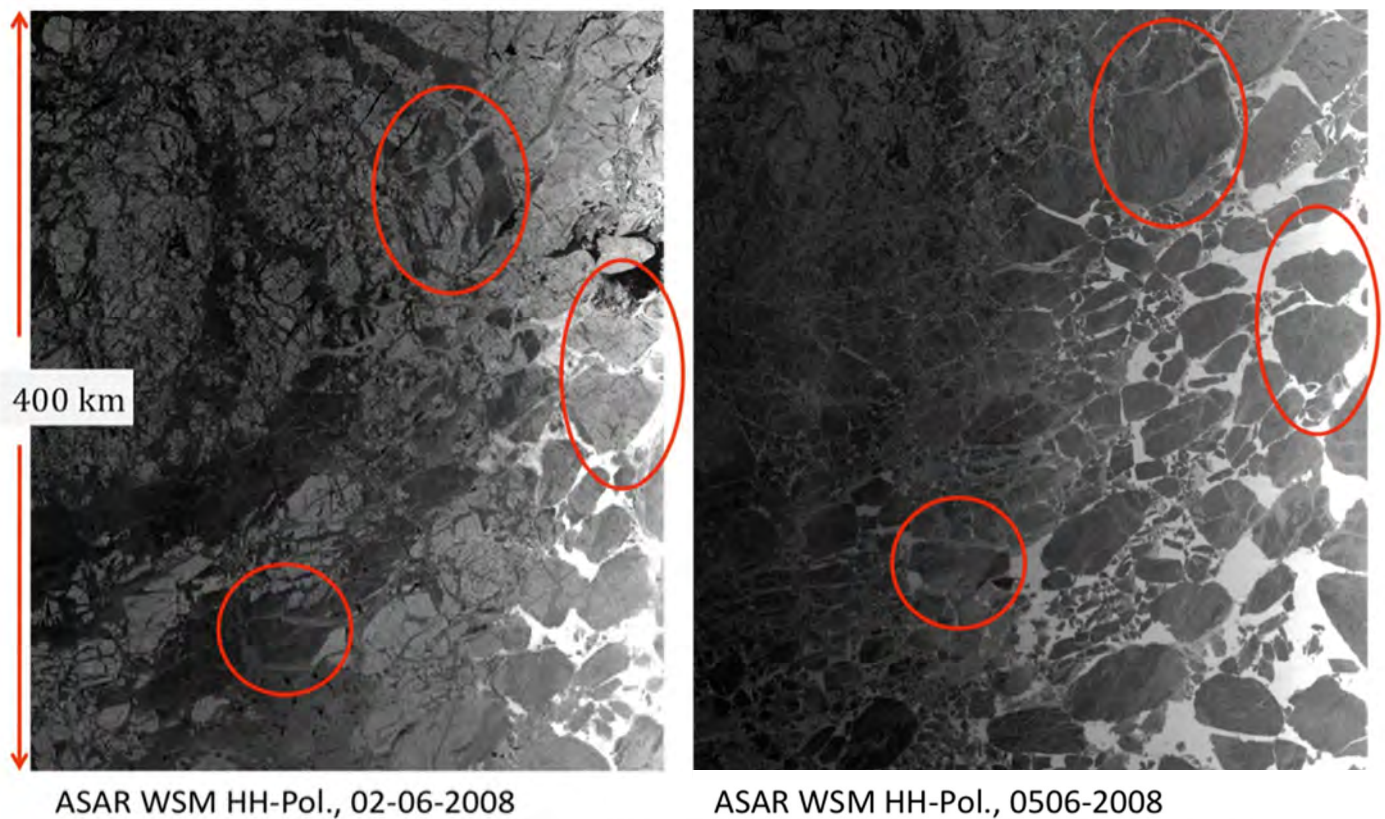
Fig. 19: Sea ice in the Beaufort Sea (71-76° N, 130–150° W). The left image was acquired in the beginning of June 2008, when air temperatures were below zero; the right image was acquired three days later after the onset of melting conditions. The red ellipses mark arbitrarily selected ice structures as references in both images for ease of comparison. Under melting conditions, the radar intensity backscattered from the ice changes, and the separation of young and old ice becomes more difficult. (Copyright: ESA).

Abb. 19: Meereis in der Beaufort-See im Frühjahr 2008. Das linke Bild stammt von Anfang Juni, als die Temperaturen unter Null Grad lagen. Das rechte Bild wurde drei Tage später aufgenommen, nachdem die Eisschmelze eingesetzt hatte. Die roten Ellipsen kennzeichnen willkürlich gewählte Eisstrukturen, um die Orientierung in beiden Bildern zu erleichtern. Unter Schmelzbedingungen ändert sich die empfangene Radarintensität, und die Unterscheidung von jungem und altem Eis wird schwieriger. (Copyright: ESA).

later stage of melt. This has to be considered when comparing dates of melt onset and freeze-up obtained from SAR and microwave radiometer data. The latter proved to be extremely useful for deriving an Arctic-wide view of melting patterns covering the last three decades. MARKUS et al (2009) used passive microwave data to determine the timing of melt onset and freeze-up and the length of the melt season from 1979 to 2007. For the entire Arctic, the melt season length increased on average by 20 days, but regional differences are relatively large (Fig. 20). The largest trends of more than ten days per decade were found in the East Greenland Sea, Laptev Sea, and East Siberian Sea, Chuckchi and Beaufort Sea, and Hudson Bay.

THE FUTURE

Sea ice is one of the "Essential Climate Variables" (ECVs) as defined by the Global Climate Observing System (GCOS) Steering Committee. In the report "The Changing Earth" (ESA 2006), the main research challenges listed for sea-ice research are
• to quantify the distribution of sea ice mass and freshwater equivalent;
• to assess the sensitivity of sea ice to climate change, and

• to understand thermodynamic and dynamic feedbacks between ocean, sea ice, and atmosphere.

The importance of improved sea-ice observations (in-situ, airborne, from space) is mentioned also in other documents, among them the "IPCC Report on Climate Change" (LEMKE et al. 2007), the "Arctic Climate Impact Assessment" report (ACIA 2004), and the" Cryosphere Theme Report of the Integrated Global Observing Strategy" (IGOS 2007).

Sea-ice observations need to include ice extent, the ice edge, ice concentration, ice type distribution, leads and polynyas, ice thickness, snow depth on sea ice, and ice drift. Since sea ice is subject to rapid temporal and spatial variations, monitoring from space is required, which enables a complete coverage of the Arctic (or Antarctic) and short repeat intervals at medium to low spatial resolution (100 m - 10 km). For future sea-ice observations, various space missions will be employed, among them:
• Sentinel-1 (SAR),
• MetOp-SG (scatterometer, radiometers operating in the visible, infrared and microwave range),
• Cryosat-2 and Sentinel-3 (radar altimeters), and
• ICESat-2 (laser altimeter).
The Sentinel missions have been developed by ESA specifi-

Melt Season Length Trend
(Days per Decade)

-40 -20 0 20 40
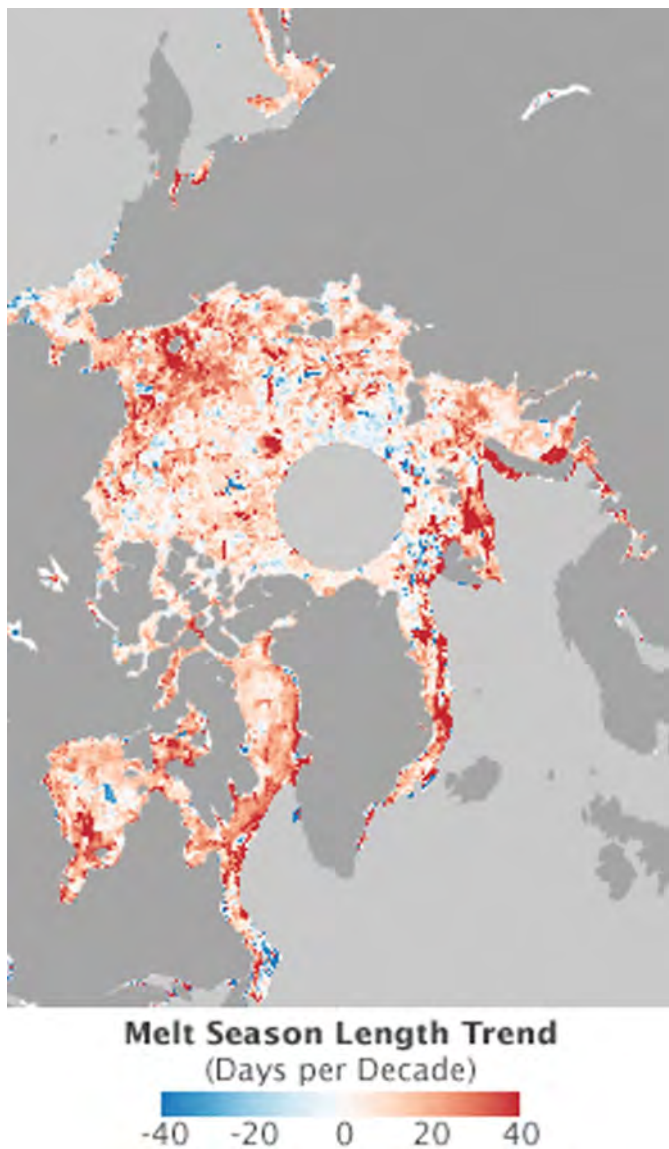
Fig. 20: Regional changes of melt season length over the Arctic from 1979 to 2007, derived from passive microwave data over sea ice (NASA Earth Observatory, http://earthobservatory.nasa.gov/IOTD/view.php?id=42456).

Abb. 20: Regionale Änderungen der Dauer der Schmelzsaison in der Arktis zwischen 1979 und 2007, abgeleitet aus über dem Meereis aufgenommenen Daten von passiven Mikrowellenradiometern (Quelle: NASA Earth Observatory).

cally for the needs of the GMES (Global Monitoring for Environment and Security) initiative. They are based on a constellation of two satellites to fulfill the GMES revisit and coverage requirements. There are five different Sentinels for monitoring of land, oceans, and atmosphere. The launches of the first satellites for Sentinels 1–3 are scheduled for 2013. The MetOp (Meteorological Operational satellite) series, consisting of satellites A to C (launches 2006, 2012, and 2016) and MetOp-SG (Second Generation, starting 2018) provide space observations of temperature, humidity, ocean surface wind speed, sea ice drift, and ozone and trace gases at global scale. The "Ice, Cloud and land Elevation Satellite-2" (ICESat-2) will be used for the estimation of sea ice thickness and ice sheet elevation changes, among other tasks. It will be launched in 2016. For local and regional studies, which require a higher spatial resolution, a number of missions already operational

(such as RADARSAT-2) or under development will provide the necessary data.

Among those sea-ice parameters that need to be determined from satellite data, ice thickness is still most demanding with respect to the robustness and accuracy of the retrieval methods. Ice thickness will be monitored by means of radar and laser altimetry missions (see above). Radar altimeter measurements result in relatively large errors for ice that is thinner than 1 m (LAXON et al. 2003). Estimates of ice thickness from freeboard measurements using laser systems reveal errors of ±0.5 m (KWOK et al. 2009). Altimeters may be favourably complemented by passive microwave radiometers operated at L-band, such as ESA's SMOS (Soil Moisture and Ocean Salinity) mission. It was demonstrated with SMOS data that the change of emission during the different stages of sea-ice growth is large enough to retrieve ice thickness up to 0.5 m if air temperatures are below -10 °C (KALESCHKE et al. 2012). The accuracy of thickness retrievals from satellite instruments depends on the knowledge of snow thickness and snow and ice density, as mentioned above. Their actual values at the timing of data acquisition are usually not known. Another problem is that the spatial resolution of the satellite radar altimeters (Cryosat-2: about 250 m along-track but up to 1 km across-track in the so-called SAR mode) is moderate, and for radiometers (SMOS: 35–45 km) it is coarse. This means that insights into the mechanisms of ice thickness variations cannot easily be gained because pressure ridges and narrow leads can hardly be separated from level ice.

This example shows that high-resolution airborne data acquisitions or in-situ measurements during ship expeditions remain mandatory also in the future for providing detailed data on sea-ice properties and processes. Other examples are the various physical and biogeochemical interaction mechanisms between the sea-ice cover and the atmospheric boundary layer, and between sea ice and the underlying water column. The authors expect that the availability of modern icebreaker technology and the better accessibility of the Arctic Ocean due to its thinner ice cover will make it possible to extend the time window for field campaigns from early spring to late autumn. This would mean that the sea-ice data measured in-situ, which hitherto are mainly from summer seasons, can be extensively supplemented by ice properties data that also reflect colder conditions.

SUMMARY

This brief and incomplete historic journey through sea-ice research and sea-ice remote sensing during the past twenty years touched topics that have been keeping the authors (and many others) busy since 1991. Those topics included in particular the ground-based and airborne measurements of sea-ice thickness and the use of satellite data for mapping sea-ice conditions, for characterizing the ice surface structure, and for determining melt-onset and freeze-up in the Arctic. Many other important issues could not be mentioned here. But the authors hope that they could provide at least a basic idea on how measurement technologies developed, and how the knowledge about sea-ice properties and interaction mechanisms between atmosphere, sea ice, and ocean has been extended during the past twenty years.

ACKNOWLEDGMENT

References

ACIA (2004): Impacts of a warming Arctic: Arctic Climate Impact Assessment. - Cambridge University Press, 1-140.

Bourke, R.H. & Garrett R.P. (1987): Sea ice thickness distribution in the Arctic Ocean.- Cold Reg. Sci. Technol. 13(3): 259-280.

Busche, T., Saldern, C., Haas, C. & Dierking, W. (2005): Comparison of helicopter-borne measurements of sea ice thickness and surface roughness with SAR signatures.- Proc. 2004 Envisat & ERS Symposium, European Space Agency, ESA SP572.

Carlström, A. & Ulander, L.M.H. (1993): C-band backscatter signatures of old sea ice in the central Arctic during freeze-up.- IEEE Transact. Geosci. Remote Sensing 31: 819-829.

Comiso, J.C. (2012): Large decadal decline of the Arctic multiyear ice cover.- J. Climate 25: 1176-1193, doi: 10.1175/JCLI-D-11-00113.1.

Dierking, W. (1995): Laser profiling of the ice surface topography during the Winter Weddell Gyre Study 1992.- J. Geophys. Res. 100(C3): 4807-4820.

Dierking, W. (2010): Mapping of different sea ice regimes using images from Sentinel-1 and ALOS synthetic aperture radar.- IEEE Transact. Geosci. Remote Sensing 48(3): 1045-1058, doi:10.1109/TGRS.2009.2031806.

Dierking, W. & Busche, T. (2006): Sea ice monitoring by L-Band SAR: an assessment based on literature and comparisons of JERS-1 and ERS-1 imagery.- IEEE Transact. Geosci. Remote Sensing 44(2): 957-970, doi:10.1109/TGRS.2005.861745.

Dierking, W., Carlström, A. & Ulander, L. (1997): The effect of inhomogeneous roughness on radar backscattering from slightly deformed sea ice.- IEEE Transact. Geosci. Remote. Sensing 35(1): 147-159.

Dierking, W. & Dall, J. (2007): Sea ice deformation state from synthetic aperture radar imagery - part I: comparison of C- and L-band and different polarizations. -IEEE Transact. Geosci. Remote Sensing 45(11): 3610-3622, doi:10.1109/TGRS.2007.903711.

Dierking, W. & Dall, J. (2008): Sea ice deformation state from synthetic aperture radar imagery part II: effects of spatial resolution and noise level.- IEEE Transact. Geosci. Remote Sensing 46(8): 2197-2207, doi:10.1109/TGRS.2008.917267.

Dierking, W., Pettersson, M. & Askne, J. (1999): Multifrequency scatterometer measurements of Baltic Sea ice during EMAC-95.- Internat. J. Remote Sensing 20: 349-372.

Eicken, H. (1994): Structure of under-ice melt ponds in the central Arctic and their effect on the sea-ice cover.- Limnol. Oceanogr. 39(3): 682-694.

Eicken, H., Lensu, M., Leppäranta, M., Tuckeriii, W., Gow, A. & Salmela, O. (1995): Thickness, structure, and properties of level summer multiyear ice in the Eurasian sector of the Arctic Ocean.- J. Geophys Res. 100(C11): 22697-22710.

ESA (2006): ESA Living Planet Scientific Challenges.- ESA-SP-1304.

Fetterer, F. M., Gineris, D. & Kwok, R. (1994): Sea ice type maps from Alaska synthetic aperture radar facility imagery: an assessment.- J. Geophys. Res. 99(C11): 22443-22458.

Frolov, I., Gudkovich, Z.M., Radionov, V.F., Shirochkov, A.V. & Timokhov, L.A. (2005): The Arctic Basin – results from the Russian drifting stations. - Springer Verlag, Berlin, Heidelberg, 1-272.

Fütterer, D.K. (ed) (1992): Arctic'91: The Expedition ARK-VIII/3 of RV "Polarstern" in 1991.- Reports Polar Res. 107: 1 267.

Garbrecht, T., Lüpkes, C., Augstein, E. & Wamser, C. (1999): The influence of a sea ice ridge on the low-level air flow.- J. Geophys. Res. 104(D20): 24499-24507.

Garbrecht, T., Lüpkes, C., Hartmann, J. & Wolff, M. (2002): Atmospheric drag coefficients over sea ice – validation of a parameterisation concept.- Tellus 54A: 205-219.

Giles, K.A., Laxon, S.W. & Ridout, A.L. (2008): Circumpolar thinning of Arctic sea ice following the 2007 record ice extent minimum.- Geophys. Res. Lett. 35: L22502, doi:10.1029/2008GL035710.

Haas, C. (1997): Sea-ice thickness measurements using seismic and electro-magnetic-inductive techniques.- PhD thesis Univ. Bremen, Rep. Polar Res. 223, 1-161.

Haas, C. (1998): Evaluation of ship-based electromagnetic-inductive thickness measurements of summer sea-ice in the Bellingshausen and Amundsen Seas, Antarctica.- Cold Regions Sci. Technol. 27: 1-16.

Haas, C. (2004): Late-summer sea ice thickness variability in the Arctic Transpolar Drift 1991-2001 derived from ground-based electromagnetic sounding.- Geophys. Res. Lett. 31, L09402, doi:10.1029/2003GL019394

Haas, C. & Eicken, H. (2001): Interannual variability of summer sea ice thickness in the Siberian and central Arctic under different atmospheric circulation regimes.- J. Geophys. Res. 106(C3): 4449-4462, doi:10.1029/1999JC000088.

Haas, C., Gerland, S., Eicken, H. & Miller, H. (1997): Comparison of sea-ice thickness measurements under summer and winter conditions in the Arctic using a small electromagnetic induction device.- Geophys. 62: 749-757.

Haas, C., Hendricks, S., Eicken, H. & Herber, A. (2010): Synoptic airborne thickness surveys reveal state of Arctic sea ice cover.- Geophys. Res. Lett. 37, L09501, doi:10.1029/2010GL042652.

Haas, C., Liu, Q. & Martin, T. (1999): Retrieval of Antarctic sea-ice pressure ridge frequencies from ERS SAR imagery by means of in-situ laser profiling and usage of a neural network.- Internat. J. Remote Sensing 20(15): 3111-3123 .

Haas, C., Pfaffling, A., Hendricks, S., Rabenstein, L., Etienne, J.-L. & Rigor, I. (2008): Reduced ice thickness in Arctic Transpolar Drift favours rapid ice retreat.- Geophys. Res. Lett., 35, L17501, doi:10.1029/ 2008GL034457.

Hvidegaard, S.M. & Forsberg, R. (2002): Sea-ice thickness from airborne laser altimetry over the Arctic Ocean north of Greenland.- Geophys. Res. Lett. 29(20), 1952, doi:10.1029/2001GL014474.

IGOS (2007): Integrated Global Observing Strategy (IGOS).- Cryosphere Theme Rep., August 2007, WMO/TD-No. 1405. http://igos-cryosphere.org/

Kaleschke, L., Tian-Kunze, X., Maaß, N., Mäkynen, M. & Drusch, M. (2012): Sea ice thickness retrieval from SMOS brightness temperatures during the Arctic freeze-up period.- Geophys. Res. Lett. doi: 10.1029/2012GL050916.

Kay, J.E., Holland, M.M. & Jahn, A. (2011): Inter-annual to multi-decadal Arctic sea ice extent trends in a warming world.- Geophys. Res. Let. 38, L15708, doi: 10.1029/2011GL048008.

Koerner, R.M. (1973): The mass balance of the sea ice of the Arctic Ocean. - J. Glaciol. 12: 173-185.

Kwok, R., Cunningham, G.F. & Nghiem, S.V. (2003): A study of the onset of melt over the Arctic Ocean in RADARSAT synthetic aperture radar data.- J. Geophys. Res. 108(C11), 3363, doi: 10.1029/2002JC001363, 2003

Kwok, R., Cunningham, G.F., Wensnahan, M., Rigor, I., Zwally, H.J. & Yi, D. (2009): Thinning and volume loss of the Arctic Ocean sea ice cover: 2003-2008.- J. Geophys. Res. 114:C07005.

Kwok, R., Cunningham, G.F., Manizade S.S. & Krabill, W.B. (2012): Arctic sea ice freeboard from IceBridge acquisitions in 2009: estimates and comparisons with ICESat.- J. Geophys. Res. 117, C02018, doi: 10.1029/2011JC007654.

Laxon, S., Peacock, N. & Smith, D. (2003): High interannual variability of sea ice thickness in the Arctic region.- Nature 425: 947-950.

Lemke, P., Ren, J., Alley, R., Allison, I., Carrasco, J., Flato, G., Fujii, Y., Kaser, G., Mote, P., Thomas, R. & Zhang, T. (2007): Observations: changes in snow, ice and frozen ground.- In: Climate Change 2007: The Physical Science Basis. Contrib. WG I to the Fourth Assessm. Rep. IPCC. Cambridge Univ. Press, Cambridge, UK and New York, NY, USA.

Lubin, D. & Massom, R. (2006): Polar Remote Sensing, Vol. I: Atmosphere and Oceans. Springer Praxis, Chichester, UK, 1-756.

Markus, T., Stroeve, J.C. & Miller, J. (2009): Recent changes in Arctic sea ice melt onset, freeze-up, and melt season length.- J. Geophys. Res. 114, C12024, doi: 10.1029/2009JC005436.

Maslanik, J., Stroeve, J., Fowler, C. & Emery, W. (2011): Distribution and trends in Arctic sea ice age through spring 2011.- Geophys. Res. Lett. 38, L13502, doi:10.1029/2011GL047735.

Nakamura, K., Wakabayashi, H., Uto, S., Naoik, K., Nishio, F. & Uratsuka, S. (2006): Sea ice thickness retrieval in the Sea of Okhotsk using dual-polarization data.- Annals Glaciol. 44: 261-268.

Nakamura, K., Wakabayashi, H., Uto, S., Ushio, S. & Nishio, F. (2009): Observation of sea ice thickness using ENVISAT data from Lützow-Holm Bay, East-Antarctica.- IEEE Geosci. Remote Sensing Lett. 6(2): 277-281.

Nansen, F. (1897): Farthest North, 2 vols., New York, Harper, 1897. (Fram over Polhavet: Den norske polarfaerd, 1893-1896. 2 vols. Oslo, Aschehoug, 1897.)

Perovich, D.K., Grenfell, T.C., Light, B., Elder, B.C., Harbeck, J., Polashenski, C., Tucker III, W.B., & Stelmach, C. (2009): Transpolar observations of the morphological properties of Arctic sea ice.- J. Geophys. Res. 114, C00A04, doi:10.1029/ 2008JC004892.

Prinsenberg, S., Holladay, S. & Lee, J. (2002): Measuring ice thickness with EISFlow^{TM}, a fixed-mounted helicopter electromagnetic laser system.- Proceed. Twelfth Internat. Offshore and Polar Engineering Conference, Kitakyushu, Japan, May 26-31: 737-740.

Romanov, I.P. (1995): Atlas of Ice and Snow of the Arctic Basin and Siberian Shelf Seas. - Dr. Alfred Tunik, translator and editor. Second edition of atlas and monograph. Revised and expanded. ISBN 0-9644311-3-0. Backbone Publishing Company.

Steffen, K. & Heinrichs, J. (1994): Feasibility of sea ice typing with synthetic aperture radar (SAR): merging of Landsat thematic mapper and ERS-1 SAR satellite imagery.- J. Geophys. Res. 99(C11): 22 413-22 424.

Stroeve, J., Sereze, M., Drobot, S., Gearheard, S., Holland, M., .Maslanik, J., Meier, W. & Scambos, T. (2008): Arctic sea ice extent plummets in 2007.- Eos Trans. AGU 89(2).

Tucker III, W.B., Gow, A.J., Meese, D.A., Bosworth, H.W. & Reimnitz, E. (1999): Physical characteristics of summer sea ice across the Arctic Ocean.- J. Geophys. Res. 104(C1): 1489-1504, doi: 10.1029/98JC02607.

Turner, J., Comiso, J.C., Marshall, G.J., Lachlan-Cope, T.A., Bracegirdle, T., Maksym, T., Meredith, M.P., Wang, Z. & Orr, A. (2009): Non-annular atmospheric circulation change induced by stratospheric ozone depletion and its role in the recent increase of Antarctic sea ice extent. - Geophys. Res. Lett. 36, L08502, doi: 10.1029/2009GL037524.

Ulander, L.M.H., Carlström, A. & Askne, J. (1995): Effect of frost flowers, rough saline snow and slush on the ERS-1 backscatter of thin arctic sea ice. - Internat. J. Remote Sensing 16(17): 3287-3305.

Untersteiner, N, Thorndike, A.S., Rothrock, D.A. & Hunkins, K.L. (2007): AIDJEX revisited: a look back at the U.S.-Canadian Arctic Ice Dynamics Joint Experiment 1970-78.- Arctic 60(3): 327-336.

Viehoff, T. (1990): A shipborne AVHRR-HRPT receiving and image processsing system for polar research.- Internat. J Remote Sensing 11(5): 877-886 .

Wadhams, P. (2000): Ice in the ocean.- Gordon & Breach Science Publishers, Singapore, 1-351.

Wang, M. & Overland, J.E. (2009): A sea-ice free summer Arctic within 30 years?- Geophys. Res. Lett. 36, L07502, doi: 10.1029/2009GL037820.

Winebrenner, D.P., Holt, B. & Nelson, E.D. (1996): Observation of autumn freeze-up in the Beaufort and Chukchi Seas using the ERS-1 synthetic aperture radar.- J. Geophys. Res. 101(C7): 16 401-16419.

Winebrenner, D.P., Nelson, E.D., Colony, R. &West, R.D. (1994): Observation of melt onset on multiyear arctic sea ice using the ERS-1 synthetic aperture radar.- J. Geophys. Res. 99(C11): 22 425-22 441.

Wingham, D.J., Francis, C.R., Baker, S., Bouzinac, C., Brockley, D., Cullen, R., de Chateau-Thierry, P., Laxon, S.W., Mallow, U., Mavrocordatos, C., Phalippou, L., Ratier, G., Rey, L., Rostan, F., Viau, P. & Wallis, D.W. (2006): Cryosat: a mission to determine the fluctuations in the Earth's land and marine ice fields.- Advances Space Res. 37: 841-871.

History of Atlantic Water Advection to the Arctic Ocean:
A Review of 20 Years of Progress
Since the "Oden"–"Polarstern" Expedition   ARCTIC 91*

by Robert F. Spielhagen[1]

Abstract: The variability of Atlantic Water advection to the Arctic Ocean is described for the last about 50 million years based on available published sources. Until the opening of the Fram Strait as a deep-water passage at about 17 million years before present the inflow of Atlantic Water may have occurred through gaps in morphologic barriers, but results from microfossil findings are in part contradictory and difficult to interpret. After the opening, brownish deep-sea Arctic sediments reflect well-oxygenated deep-sea conditions and an improved exchange with the North Atlantic. The build-up of first ice sheets on northern Eurasian continental and shelf areas in the Late Tertiary may have resulted in intensive brine formation at the ice sheet margins and a significantly weaker influence of Atlantic Water on the Arctic intermediate waters. The history of Quarternary glacial-interglacial variability in the central Arctic is not well understood for most of the last 2 million years due to the lack of carbonate microfossils. For the last 200,000 years, however, short intervals of intensive Atlantic Water advection during interglacials and inter-stadials can be clearly identified in a number of sediment cores. Seasonally open water conditions (i.e., reduced sea ice) during these periods and even during maximum glaciation at Arctic continental margins probably made additional moisture available for the (re)growth of adjacent ice sheets. After the last deglaciation, Atlantic Water quickly returned to the Arctic and established conditions close to the modern ones. High-resolution records from the Fram Strait, however, indicate a rapid temperature rise of the Atlantic Water layer during the last 100 years, which most probably reflects on-going global warming and the so-called "Arctic Amplification".

Zusammenfassung: In diesem Artikel wird die Veränderlichkeit des Ein-stroms von Atlantikwasser in die Arktis für die letzten ca. 50 Millionen Jahre beschrieben, basierend auf publizierten Quellen. Bis zur Öffnung der Framstraße vor ca. 17 Millionen Jahren konnte Atlantikwasser höchstens durch Lücken in morphologischen Barrieren in den Arktischen Ozean einströmen, doch sind die Ergebnisse von Mikrofossilfunden in dieser Hinsicht z. T. widersprüchlich und nicht eindeutig interpretierbar. Bräunliche arktische Tiefseesedimente sind ein deutlicher Hinweis auf gut durchlüftete Wassermassen in der Tiefsee in der Zeit nach der Öffnung und auf einen verbesserten Austausch mit dem Nordatlantik. Der Aufbau erster Eisschilde auf den Land- und Schelfgebieten im nördlichen Eurasien im Spätquartär (letzte 200.000 Jahre) hatte womöglich eine intensive Bildung dichter, salz-reicher Wassermassen an der Eiskante zur Folge, was in einem schwächeren Einfluss des Atlantikwassers auf das arktische Zwischenwasser resultierte. Über die Geschichte quartärer Eiszeit-Warmzeit-Zyklen ist wegen des weit-gehenden Fehlens kalkiger Mikrofossilien in entsprechenden Ablagerungen bisher wenig bekannt. In Warmzeiten und Interstadialen im Spätquartär erfolgte jedoch jeweils ein vergleichsweise starker Einstrom von Atlantik-wasser. Im Sommer auftretende offene Wasserflächen trugen vermutlich über verstärkte Verdunstung und entsprechende Niederschläge zum Aufbau zirkumarktischer Eisschilde bei. Nach dem Ende der letzten Eiszeit drang das Atlantikwasser rasch wieder in den Arktischen Ozean vor, verbunden mit Umweltbedingungen ähnlich den heutigen Verhältnissen. Zeitlich hochauflö-sende Datenserien aus der Framstraße haben jedoch gezeigt, dass es in den letzten 100 Jahren im Atlantikwasser einen besonders raschen Temperatur-anstieg gab der vermutlich mit der „Arktischen Verstärkung" der globalen Erwärmung zusammenhängt.

––––––––––

INTRODUCTION

On September 7, 1991, the Swedish icebreaker "Oden" and the German research icebreaker "Polarstern" together reached the geographic North Pole as the first non-nuclear powered ships, after several weeks of struggle through the Arctic sea ice. The data and samples collected on this ARCTIC 91 expe-dition helped to greatly expand our knowledge about past and present processes and developments in the Arctic Ocean. On the occasion of the 20th anniversary of that magic day when both ships had reached the northernmost point on earth, crew members and scientists from 1991 gathered in Kiel for a symposium to commemorate the epic voyage and to discuss the progress in science that has been made since. This manu-script, which is based on a presentation given at the sympo-sium, is intended to summarize our knowledge of the history of the advection of Atlantic Water to the Arctic Ocean.

The Arctic and North Atlantic ocean basins are connected via three gateways (Fig. 1). The Fram Strait (~500 km wide) is the only deep-water passage with a sill depth of >2500 m while the NW Barents Sea is a shallow seaway (50-500 m). Various narrow straits through the Canadian Arctic archipelago serve mainly as pathways for the export of sea ice and Arctic surface waters. Waters of the ice-covered, 50-200 m thick low-salinity surface water layer in the Arctic Ocean (S <34) contain large amounts of freshwater, which are supplied by the large rivers entering the ocean in Siberia and North America, and to a lesser extent to the influx of low-salinity Pacific waters and the melting of sea ice. Atlantic Water is advected to the Arctic Ocean today both through the Fram Strait and across the Barents Sea. In these gateways it is characterized by rela-tively high temperatures (maxima of 6–8 °C in summer) and salinities of >35 (SCHAUER et al. 2002). As a result of heat loss and mixing, values are lower in the Arctic interior but remain >0 °C and >34.7 throughout the entire Arctic basin. Thus, Atlantic Water is the main source of salt and heat for waters in the deep-sea Arctic Ocean. The influence of the Atlantic Water is seen in the occurrence of typical Atlantic faunas along its pathway in the Arctic Ocean (CARMACK & WASSMANN 2006). This pathway can be traced eastward along the Siberian conti-nental margin (WOODGATE et al. 2001) and into the interior Arctic basins (MCLAUGHLIN et al. 2004).

Advection of Atlantic Water to and into and within the Arctic Ocean is part of the Atlantic meridional overturning circula-tion (AMOC, KUHLBRODT et al. 2007). The strong tempera-ture and salinity contrasts between the Arctic and Atlantic oceans are an important boundary condition for the thermoha-line convection in the North Atlantic, which is a major driver
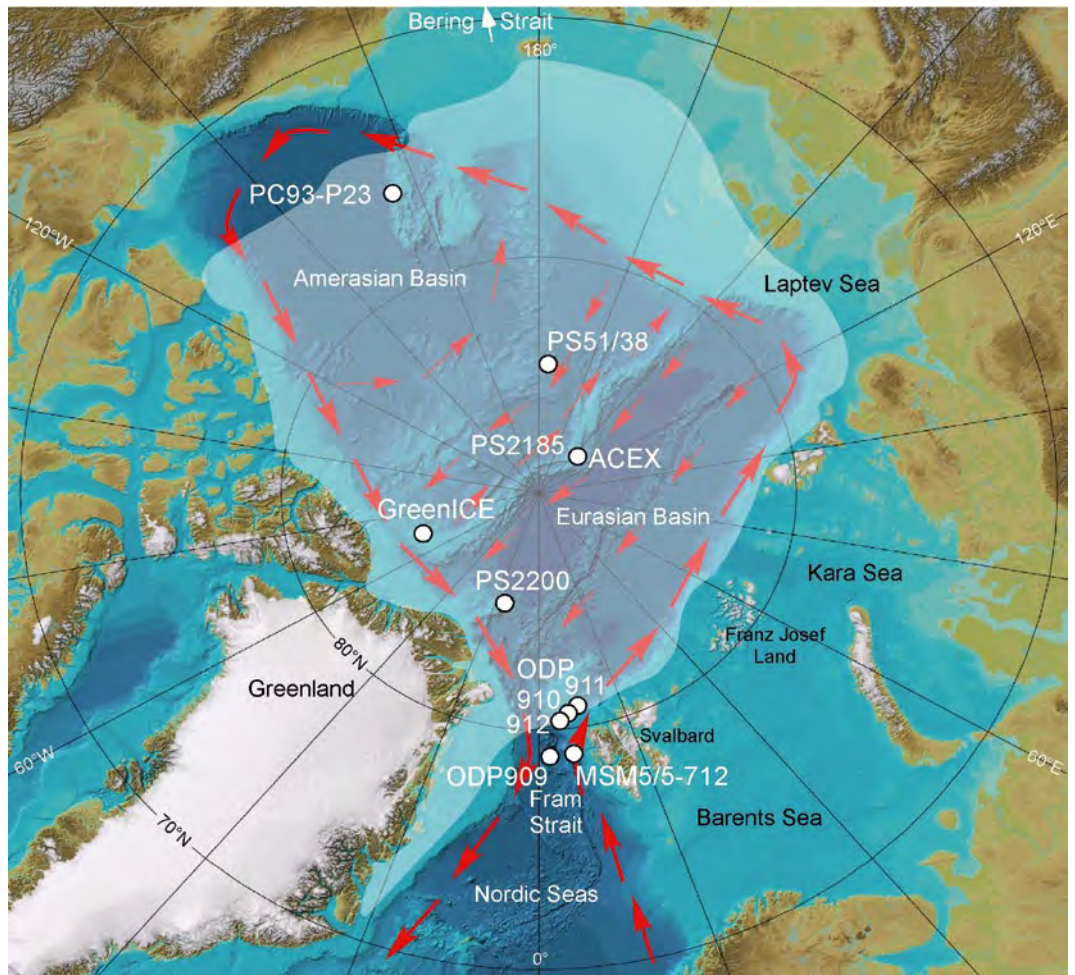
of the AMOC. Geological data and modelling experiments have shown that the AMOC is sensitive to freshwater perturbbations (BOND et al. 1993, RAHMSTORF 1995) and was significantly weakened at times in the Late Quaternary, with profound consequences for global climate (e.g., CLARK et al. 2002). Until about three decades ago, the history of Atlantic Water in the Arctic could be reconstructed only indirectly, based on marine sediment cores from the Nordic Seas. Several thin (3 cm) sediment cores obtained from ice islands in the Amerasian part of the Arctic Ocean in the 1960s and 1970s were studied intensively (e.g., CLARK et al. 1980, HERMAN & HOPKINS 1980, CLARK 1982). However, the age models established for these cores indicated extremely low sedimentation rates (mm per 1000 years, mm ky-1) for the western Arctic, which rendered the detection of short-term events difficult. Much later it could

Fig.1: Bathymetric map of the Arctic Ocean (www.ibcao.org); average summer ice coverage (light shading); circulation of Atlantic Water (red arrows, after RUDELS et al. 1994), and core sites mentioned in the text (white dots).

Abb. 1: Bathymetrische Karte (www.ibcao.org) des Arktischen Ozeans, durchschnittliche sommerliche Eisbedeckung (helle Schattierung), Zirkulation des Atlantikwassers (nach RUDELS et al. 1994) und im Text erwähnte Lokationen von Sedimentkernen (weiße Kreise).

be shown that sedimentation rates were indeed higher than previously assumed (DARBY et al. 1997, JAKOBSSON et al. 2000, BACKMAN et al. 2004) and that the older stratigraphic models had to be revised. In the meantime, newly developed ice-going research vessels and icebreakers with capabilities to deploy heavy research equipment including large-volume sediment corers had performed several geoscientific expeditions to the major Arctic Ocean basins. In 2004, the first successful deep-sea drilling effort in the central Arctic Ocean during Integrated Ocean Drilling Program Leg 302 recovered a 425 m long sedimentary sequence, which helped to unveil the Arctic Ocean history since the Paleocene (BACKMAN et al. 2005, MORAN et al. 2006) and closed a gap in our knowledge of earth history.

This manuscript reviews the history of the oceanic connection between the northern North Atlantic and the Arctic Ocean, from its initiation in the Tertiary to its variability in historical times. Ages for the youngest part of the Cenozoic are given as calibrated years before present (1950 CE). The oceanic history is reconstructed from various sediment cores obtained in the Arctic Ocean in the last 20 years – the first decades of modern central Arctic geoscientific exploration.

TERTIARY ONSET OF DEEP-WATER EXCHANGE

A few of the sediment cores taken from ice island T-3 in the deep-sea of the Western Arctic Ocean in the 1960s and 1970s contained Late Cretaceous and Early Tertiary sediments, but no continuous sequences (CLARK 1974). The recovered black muds were rich in siliceous microfossils and dinocysts, indicating warm surface water temperatures (CLARK et al. 1986, CLARK 1988). On the other hand, it became clear that at these times the deep Arctic Ocean basins were poorly ventilated, a fact that precludes an extensive exchange with the deep North Atlantic at the time of formation and points to an Arctic estuary-type environment where deep-water ventilation may have occurred by seasonal convection (JAKOBSSON et al. 2007). No sedimentary records were found to document the transition to the modern, ice-covered and well-ventilated Arctic Ocean. Only in 2004, during the Arctic Coring Expedition (ACEX, IODP Leg 302), was the first continuous sedimentary profile from the interior Arctic recovered from the top of the Lomonosov Ridge (Fig. 1). The lower half of the 415 m sequence was grey or dark grey with mostly 1.5 % of organic carbon (Fig. 2), but at 193 m core depth a remarkable change to brownish muds with ~0.5 % organic carbon was
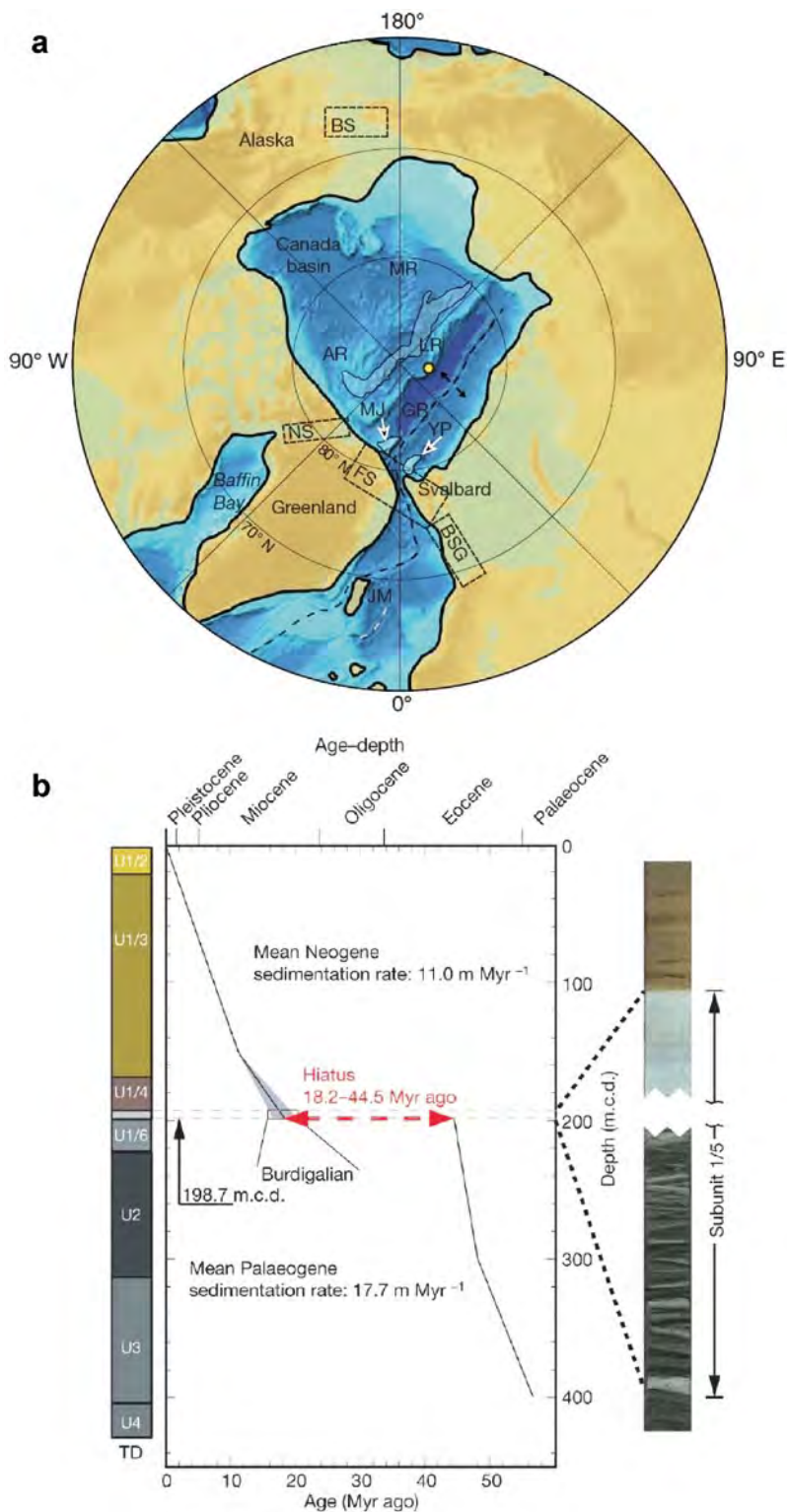
Fig. 2: (a) Paleogeographic map of the Arctic in the Miocene (from JAKOBSSON et al. 2007), AR = Alpha Ridge, BS = Bering Strait, BSG = Barents Sea Gateway, FS = Fram Strait, GR = Gakkel Ridge, JM = Jan Mayen, MJ = Morris Jesup Plateau, MR = Mendeleyev Ridge, NS = Nares Strait, LR = Lomonosov Ridge, YP = Yermak Plateau. (b) Generalized sediment types and age-depth profile from the ACEX drill site on the Lomonosov Ridge (yellow dot in (a)). Details of sedimentary subunit 1/5 are displayed on the right. From JAKOBSSON et al. (2007).

Abb. 2: (a) Paläogeographische Karte des Arktischen Ozeans im Miozän (aus JA-KOBSSON et al. 2007), AR = Alpharücken, BS = Beringstraße, BSG = Barentssee-Mee-resverbindung, FS = Framstraße, GR = Gakkelrücken, JM = Jan Mayen, MJ = Morris-Jesup-Plateau, MR = Mendelejewrücken, NS = Naresstraße, LR = Lomonosowrücken, YP = Yermak-Plateau. (b) Vereinfachtes Diagramm der Sedimenttypen und Alters-Tiefen-Profil für die ACEX-Bohrung auf dem Lomonosowrücken (gelber Punkt in (a)). Details der Untereinheit 1/5 sind rechts dargestellt. Aus JAKOBSSON et al. (2007).

found (MORAN et al. 2006). Age determinations for the very uppermost greyish sediments just below this colour change reveal an apparent gap in the sediment ages whose nature and extent are still under debate. It may represent either a hiatus from about 44.5 to 18.2 million years before present (Ma) (BACKMAN et al. 2006, JAKO-BSSON et al. 2007) or an interval of extremely slow deposition (POIRIER & HILLAIRE-MARCEL 2009, 2011). Depending on the age model used, the prominent colour change of the sediments dates to ~17.5 Ma (Jakobsson et al., 2007) or 36 Ma (POIRIER & HILLAIRE-MARCEL 2011). Unequivocally, however, it is correlated to the opening of the Fram Strait as a deep-water passage, which allowed the intrusion of saline Atlantic Water into the Arctic and, through the establishment of stronger salinity contrasts, the ventilation of deep-water in the Arctic basins (JAKOBSSON et al. 2007). The transition from the "Arctic Esturary" stage to the "Ocean" stage may have taken 0.7-2 million years (My) and resulted in a ventilated Arctic Ocean although it is difficult to estimate the volume flux of Atlantic Water in the early phase of Fram Strait opening (JAKOBSSON et al. 2007).

The Neogene development of Atlantic Water in the Arctic Ocean still remains poorly known in detail. There is evidence from probably ice-rafted heavy minerals, clay minerals, and detrital iron oxide grains that a sea-ice cover developed ~13–14 Ma (DARBY 2008, KRYLOV et al. 2008). The low temperatures required to maintain such an ice cover rule out warm Atlantic Water near the surface. Results about any Atlantic Water contribution to the Arctic intermediate water (i.e., the water at the paleo-depth of the ACEX drill site) which today consists almost entirely of Atlantic Water, appear controversial. HALEY et al. (2008) analyzed the Neodymium isotope composition (εNd ~^{143}Nd/^{144}Nd) of authigenic coatings on minerals grains from ACEX sediments of the last 15 My, which are assumed to form at the ocean-seafloor interface and store the εNd value of the bottom water. High ("radiogenic") εNd values are typical for water masses that attained their Nd signature from erosion of magmatic rocks while low ("non-radiogenic") εNd values are typical for waters from sedimentary rock sources. The results (Fig. 3) reveal a dominant radiogenic εNd signature until ~2 Ma. The most likely source rocks for such high values are found in the Siberian Putorana Plateau, which consists of trap basalts and is drained to the North by major Siberian rivers. It is the only major complex of magmatic rocks on the circum-Arctic continents. However, to explain the high εNd values in the intermediate water at the ACEX site, a vigorous mechanism is needed to transport high -εNd waters from surface to depth. HALEY et al. (2008) proposed brine formation as the responsible process, i.e., the rejection of salt during freezing of sea-water and formation of sea ice. This process is especially effective where katabatic winds flowing down large ice sheets can permanently cool the adjacent ocean surface and at the same time induce an offshore drift of the newly formed ice (GILL 1973, MARSLAND et al. 2004). Accordingly, large-scale North Siberian glaciations in the Late Tertiary were proposed and a strong influence of North Atlantic-derived waters on Arctic intermediate water was largely excluded (HALEY et al. 2008). A Late Miocene onset
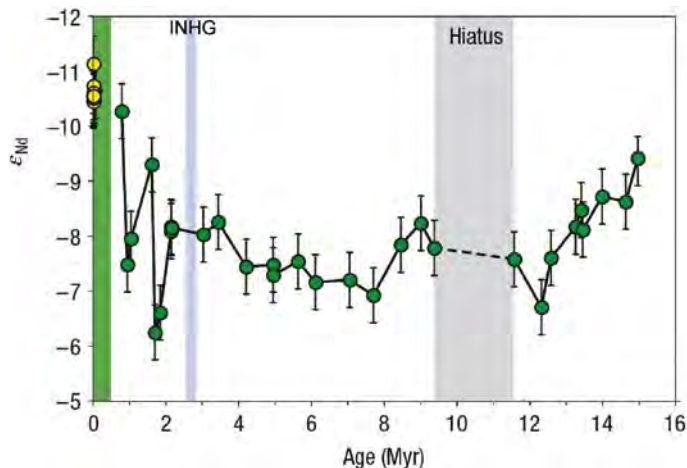
Fig. 3: Neodymium isotope (εNd) record (HALEY et al. 2008) of the last 15 My at the ACEX drill site (cf. Figs. 1, 2). Green circles = Record from sediment leaches (incl. 2s error); yellow circles = Data from deep-sea Arctic core-top samples; green box = The range of data from site PS2185 close to ACEX, covering the last ~400 ky. INHG = Intensification of Northern Hemisphere Glaciation.

Abb. 3: Neodymisotopen-Datensatz (εNd) für Sedimente der letzten 15 Mio. Jahre (HALEY et al. 2008) aus der ACEX-Bohrung (vgl. Abb. 1, 2). Grüne Kreise = Werte aus Laugungslösungen (inkl. 2s-Fehlerbereich); gelbe Kreise = Daten aus arktischen Sedimentoberflächenproben; grünes Rechteck = Wertebereich von Sedimentkern PS2185 (nahe ACEX entnommen) für die letzten 400.000 Jahre. INHG = Intensivierung der Nordhemisphären-Vereisung.

of glaciations on the northern Eurasian shelf (Barents Sea) was also suggested by KNIES & GAINA (2008) based on IRD, organic carbon and clay mineral data from ODP Leg 909 in the central Fram Strait. However, the authors also proposed the coeval northward intrusion of Atlantic waters into the Arctic.

Benthic foraminiferal associations in Neogene sediments from the ACEX site apparently tell a different story than the Neodymium isotopes. Deep-water agglutinated foraminifers found in the lowermost brownish layers clearly have Atlantic/Norwegian Sea affinities and point to an Atlantic source of the intermediate water on the Lomonosov Ridge (KAMINSKI et al. 2009). This finding is in line with the conclusion of JAKOBSSON et al. (2007) about the onset of deep-water ventilation in the Arctic. On the other hand, KAMINSKI et al. (2009)

pointed out that Early Miocene sediments from ODP Site 909 in the central Fram Strait (Fig. 1) contain deep-water agglutinated foraminifers of presumably Atlantic origin. Furthermore, similar "Atlantic" associations were found in Oligocene deposits obtained from exploration wells in the northern Canadian Beaufort-Mackenzie Basin (MCNEIL 1996, 1997). Based on these data, KAMINSKI et al. (2009) speculate on a faunal exchange of deep-water species already in the Oligocene. They conclude that "these faunal connections were certainly in place by the Early Miocene".

At first sight, the results of KAMINSKI et al. (2009) are difficult to reconcile with those of HALEY et al. (2008) and with a Fram Strait opening in the late Early Miocene (JAKOBSSON et al. 2007). Recent geophysical results, however, suggest that sediments found today on the Yermak Plateau were deposited in the last 33–35 My and that the present-day barrier to deep-water flow was a gateway in the Oligocene (GEISSLER et al. 2011). Due to the hiatus in the ACEX core, this interval is not recorded on the Lomonosov Ridge (BACKMAN et al. 2006). Successive filling of the gateway in the present-day Yermak Plateau (GEISSLER et al. 2011) may have cut off the Arctic Ocean from the Atlantic and weakened deep-water ventilation in the Arctic. Only when the separation of Greenland and Svalbard allowed a penetration of Atlantic-derived deep-water to the Fram Strait (in the Early(?) Miocene) and a true deep-water connection with the Arctic (in the early Late Miocene), deep-water agglutinated foraminifers could be exchanged between both basins. The proposed onset of large-scale glaciations on northern Siberia and associated deep-water renewal from brine formation around 15 Ma (HALEY et al. 2008) are largely coeval with a decline in the preservation of deep-water agglutinated foraminifers at the seafloor on the Lomonosov Ridge (cf. KAMINSKI et al. 2009). According to HEMLEBEN & KAMINSKI (1990), the preservation potential largely depends on the availability of silica, which replaces the organic cement in deep-water agglutinated foraminifers after death. Present deep-water environments off the Weddell Sea in the Antarctic, which may serve as a possible modern analog for the Late Tertiary ice sheet scenario of HALEY et al. (2007), are both brine-enriched and rich in silica (BAUCH & BAUCH 2001, RUTGERS VAN DER LOEFF & VAN BENNEKOM 1989). Transfer
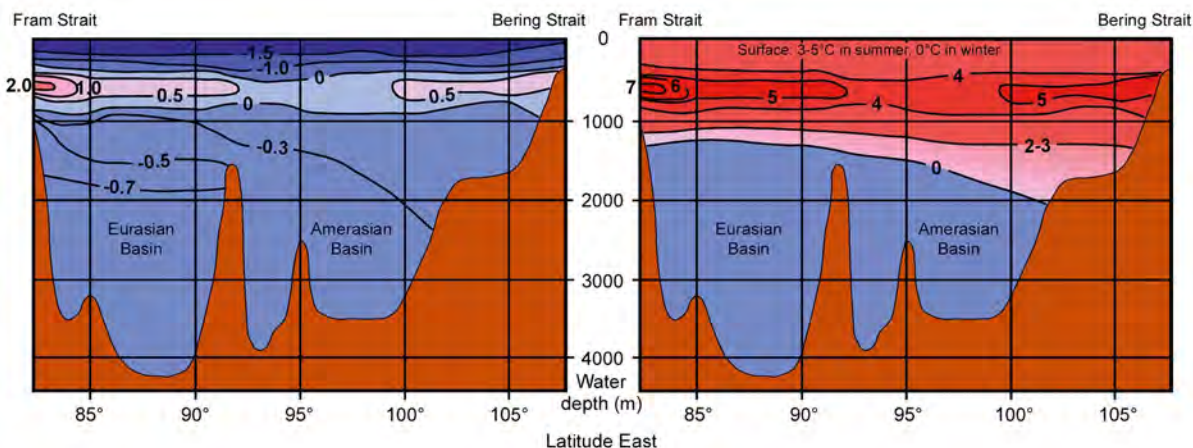
Fig. 4: Modern water temperature profile across the Arctic Ocean (left) and reconstruction of Pliocene conditions (redrawn from CRONIN et al. 1993).

Abb. 4: Heutige Wassertemperaturen im Arktischen Ozean (links) und Rekonstruktion für das Pliozän (umgezeichnet nach CRONIN et al. 1993).

of this analog certainly depends on the availability of silica in the Late Tertiary deep Arctic Ocean – a factor unknown so far. Thus, further research is necessary to understand how an Atlantic-type deep-water fauna could survive when deep-waters in the Arctic Ocean were mainly renewed within the Arctic Ocean and not by massive advection of Atlantic Water from the south. On the other hand, further research on the Neodymium transfer to deeper waters in the Arctic may find an alternative explanation for the radiogenic εNd signal in Miocene and Pliocene sediments at the ACEX site. This alternative explanation must permit to reconcile these data with the paleontological evidence for warmer temperatures than today in the Late Tertiary Arctic Ocean, especially in the Pliocene, as elaborated below.

PLIOCENE AND EARLY QUATERNARY VARIABILITY

From the central Arctic Ocean drill site ACEX there is little micropaleontological information on the variability of Atlantic Water advection to the Arctic during the Pliocene and the transition to the Pleistocene (~5.3–1.8 Ma). What were thought to be Pliocene deposits in a large number of sediment cores from the western and central Arctic Ocean (e.g., CLARK et al. 1980, HERMAN & HOPKINS 1980, CLARK 1982, 1996, SCOTT et al. 1989, SPIELHAGEN et al. 1997) must now be regarded as Quaternary sediments, according to the revised model of BACKMAN et al. (2004) for sedimentation rates in the Arctic Ocean. On the Northwind Ridge in the Western Arctic Ocean, MULLEN & MCNEIL (1995) found a distinct Early Pliocene assemblage of benthic foraminifers at the base of piston core 93-P23. They noted that although paleogeographic affinities of the bulk of the assemblage are indicative of connections to the Atlantic, the occurrence of some Arctic endemic species suggests environmental differences or a partial isolation of the western Arctic Ocean.

A series of Pliocene paleoclimatic data from terrestrial and onshore marine deposits in northernmost North America and Greenland consistently suggests a climate with mean annual air temperatures up to 15–20 °C warmer than today. Evidence comes from, e.g., beetle findings (ELIAS & MATTHEWS 2002, ELIAS et al. 2006), plant remains (e.g., BENNIKE et al. 2002, BALLANTYNE et al. 2006, 2010), macro- and microfossils (e.g., FUNDER et al. 1984, 2001), aminoacid (KAUFMAN & BRIGHAM-GRETTE 1993) and isotopic data (CSANK et al. 2011) and can only be explained by strong northward heat transport from the Atlantic. A conceptual model approach to estimate Late Pliocene to Early Quaternary (3.5–2.0 Ma) water temperatures in the Arctic Ocean was put forward by CRONIN et al. (1993). They compared Pliocene marine ostracod assemblages from 13 sites in NW Europe, the American Arctic, and the NW Pacific with a database of assemblages from more than 800 sediment surface samples, which are thought to reflect modern environmental conditions. Although the age control for some of the Late Pliocene sites holds uncertainties of several hundred thousand years and limits the possibilities to present a chronological order of paleoenvironmental changes, the results suggest a relatively strong influx of warm waters from the Atlantic, at least during interglacials. The conceptual model of water temperatures in the Late Pliocene to Early Quaternary Arctic Ocean, as presented by CRONIN et al. (1993), shows a similar structure as today, but significantly

higher temperatures (up to 6 °C), at least in the upper ca. 1200 m (Fig. 4). Surface water temperatures were estimated to be 3–5 °C in summer and around 0 °C in winter, which is largely incompatible with a perennial sea ice cover. The authors conclude on an increased heat supply from a strong North Atlantic Drift reaching the Arctic Ocean as the most likely mechanism to facilitate a temperature regime well above the present-day level.

Recently, improved stratigraphic models and partly new IRD, clay mineral, and seismic data from the ODP drill sites on the Yermak Plateau and in the Fram Strait have revealed new details of the onset of glaciation in the Barents Sea-Svalbard region (KNIES et al. 2009, LABERG et al. 2010). According to this reconstruction, ice accumulation in the northernmost Barents Sea started in the Late Pliocene (~3.5 Ma), contributing to the increasing northern hemisphere glaciation (cf. RAYMO 1994). It intensified in two steps at ~2.4 and 1.0 Ma, eventually merging with the Scandinavian ice sheet. It is important to note, however, that there were large variations within all three glaciation phases. KNIES et al. (2009) surmise that the glaciers were waxing and waning between their maximum size and an almost complete absence. Evidence for warmer intervals comes from microfossil findings in sediments from ODP sites 910–912 on the Yermak Plateau. Variable planktic foraminifer associations point to several short warm-temperate to subtropical surface-water ingressions (SPIEGLER 1996). Unusually high abundances of the dinoflagellate cyst *Operculodinum centrocarpum* (Fig. 5), which is considered as an indicator of enhanced advection of warm surface water from the Atlantic, were found in ODP Hole 911A (KNIES et al. 2002). According to the revised stratigraphic model (KNIES et al. 2009), the most prominent warm interval was largely coeval with the Pliocene Climate Optimum at ~3 Ma (MATTHIESSEN et al. 2009). Sea surface temperature (SST) estimates from Mg/Ca measurements on planktic foraminifers and alkenone ($U^{k'}37$) data from lipids from ODP sites 909 (Fram Strait) and 911 gave values of up to 19 °C (ROBINSON 2009) which is about 10 °C higher than present day temperatures. Although these values likely represent peak temperatures during summer and are possibly biased by uncertainties regarding preservation effects and SST calibration, they are in support of Pliocene intervals in the Arctic with temperatures significantly higher than today.

As a whole, there is compelling evidence both for a build-up of ice sheets on the Barents Sea and for a relatively strong Atlantic Water advection to the Arctic in the (Late) Pliocene and Early Quaternary. The results – though contradictory at first sight – suggest that climatic variability similar to the Middle and Late Quaternary glacial/interglacial cycles had developed already in the Pliocene. Stratigraphic and sampling resolution often limits possibilities to unambiguously determine the length of warm and cool periods. Possibly, these periods of strong Atlantic Water advection to the Arctic lasted much longer in the "41 ky world" (RAYMO et al. 2006) than the relatively short interglacial periods of the last 0.7–1.0 My.

QUATERNARY GLACIAL-INTERGLACIAL CYCLES

High-resolution records documenting Early Quaternary (~1.8–0.8 Ma) Milankovitch-type climatic variability in the Arctic are still rare and restricted mostly to sequences from

Dinoflagellate cysts (%)

Fig. 5: Dinocyst distribution in sediments from ODP site 911A (redrawn from MATTHIESSEN et al. 2009). Note the relative abundance of species *Operculodinum centrocarpum*, which is considered to be indicative of warm water masses of Atlantic origin especially in the Pliocene climate optimum (PCO).
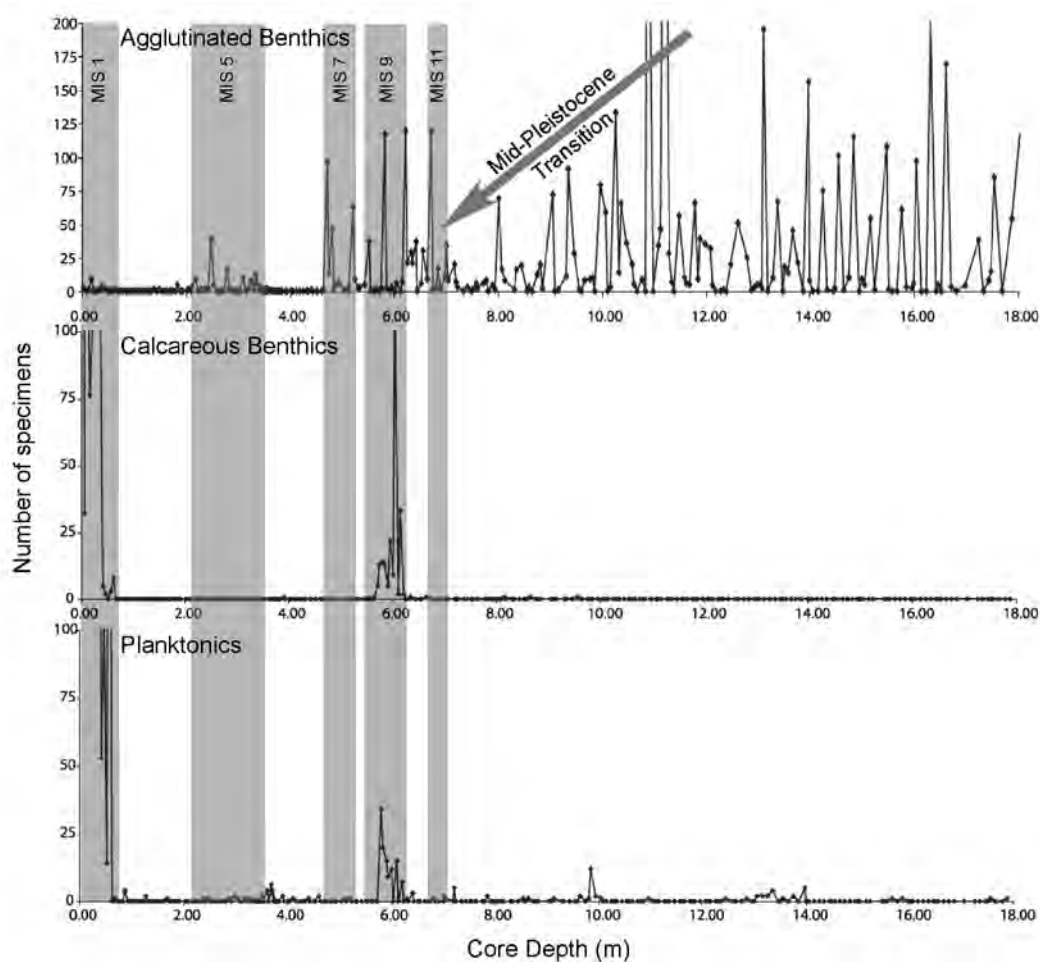
Abb. 5: Dinozystenverteilung in Sedimenten von ODP-Site 911A (umgezeichnet nach MATTHIESSEN et al. 2009). Auffällig ist der hohe relative An–teil der Art *Operculodinum centrocarpum* besonders in Sedimenten aus dem pliozänen Klimaoptimum (PCO); diese Art gilt als Anzeiger für relativ warme Wassermassen atlantischen Ursprungs.

CRONIN et al. (2008) analyzed the foraminiferal fauna in the uppermost 18 m of sediments from ACEX Hole 4C which were deposited in the last 1.5 My (O'REGAN et al. 2008). Only the upper few meters contain layers with abundant planktic and calcareous benthic foraminifers – a feature seen also in other central Arctic Ocean cores (AKSU 1985, POORE et al. 1994, ISHMAN et al. 1996, SPIELHAGEN et al. 1997, 2004, POLYAK et al. 2004, NØRGAARD-PEDERSEN et al. 2007). Below, agglutinated benthic foraminifers are strongly dominating the foraminiferal fauna, but show a high variability in abundance (Fig. 6). According to the latest ACEX age model for the Pleistocene sequence (O'REGAN et al. 2008), abundance peaks result from interglacials. CRONIN et al. (2008) speculate that the almost equal numbers of interglacials and agglutinated benthic foraminifer peaks may suggest a downcore extrapolation of this pattern to the MIS 64/65 boundary (~1.8 Ma). The dark brownish colour of the interglacial and interstadial layers in the ACEX Quaternary sediment sequence and other sediment cores from the Lomonosov Ridge had previously been attributed to the enhanced manganese oxide contents measured in the respective layers (JAKOBSSON et al. 2000, POLYAK et al. 2004, O'REGAN et al. 2008). Diminished deep-water ventilation from decreased Atlantic Water advection had been discussed earlier as a possible cause of low MnO in glacial sediments (JAKOBSSON et al. 2000). A combination of geochemical results published by O'REGAN et al. (2010), however, suggests that the variable MnO content is most likely a primary sedimentary signal, resulting from variable Mn input to the Arctic Ocean. Nevertheless, the finding of low (Atlantic Water type) εNd values in dark brownish interstadial and interglacial sediments of the last 350 ky on the Lomonosov Ridge (HALEY et al. 2008), taken together with the foraminifer findings (CRONIN et al. 2008), may suggest that Atlantic Water advection and enhanced intermediate/deep-water ventilation were characteristic features of the warmer intervals in the entire Quaternary.

The foraminiferal faunas in the ACEX core indicate two intervals with significant changes in the Quaternary Arctic Ocean climate system (CRONIN et al. 2008). Sediments from the mid-Pleistocene transition (~1.2–0.9 Ma) contain several intervals, which hold very few or no agglutinated foraminifers (Fig. 6) and are thought to represent severe glacial events with perennial sea ice (CRONIN et al. 2008). Although better knowledge of their ecology may be necessary for detailed paleoenvironmental reconstructions, the lack of foraminifers may also indicate that there was no (or weak) Atlantic Water advection at depth during these glacials. The second important change occurred at the εNd of the so-called "mid-Brunhes event" (~0.6–0.2 Ma), which represents a period of unusually strong carbonate dissolution in the world ocean, related to changes in the carbon cycle (cf. BARKER et al. 2006). The transition to conditions resembling the modern Arctic Ocean may have occurred at ~300,000–250,000 before present (~300–250 ka), as shown by changes in benthic foraminiferal faunas in the Amerasian Basin indicating a stronger Atlantic Water inflow (ISHMAN et al. 1996). Deposits from the last ~200,000 years (~200 ky) in sediment cores from Arctic submarine highs (Lomonosov Ridge, Alpha Ridge, Morris Jesup Rise) contain several layers with abundant planktic foraminifers (SPIELHAGEN et al. 2004, CRONIN et al. 2008). This indicates a significant amelioration of the carbonate preservation potential in Arctic intermediate waters, which are today fed mostly

ODP/ IODP drillholes. KNIES et al. (2007, 2009) compiled a quasi-contin-uous planktic oxygen isotope record from ODP Hole 910A (Yermak Plateau), which exhibits a distinct variability interpreted by the authors as glacial-interglacial cycles. Maxima in the $\delta^{18}O$ record are increasing from 1.3 to 0.95 Ma (a hiatus covers 0.95-0.79 Ma), eventually reaching values of 4.0 ‰. Modern (interglacial) values are 2.9–3.4 ‰ in this area (SPIELHAGEN & ERLENKEUSER 1994) while glacial maximum values from marine isotope (sub) stages (MIS) 2 and 6.2 are 4.5–4.9 ‰ (SPIELHAGEN et al. 2004). Both ranges are thought to reflect mostly Atlantic Water (NØRGAARD-PEDERSEN et al. 2003, SPIELHAGEN et al. 2004). According to LIESICKI & RAYMO (2004), the global ice volume increase between glacial maxima in the 1.5–1.0 Ma interval and in MIS 2 and 6.2 was equivalent to ~0.8 ‰. When subtracting this 0.8 ‰, the Early Quaternary planktic $\delta^{18}O$ values on the Yermak Plateau (KNIES et al. 2007, 2009) come out comparable to MIS 2 and 6.2 values. This may indicate that Atlantic Water was present in the Arctic Gateway not only during interglacials but also during Early Quaternary glacial maxima.

Fig. 6: Distribution of foraminifers of Quaternary ACEX drill site sediments (modified from CRONIN et al. 2008). The mid-Pleistocene transition is reflected in a decrease of agglutinated benthic specimens between 12 and 7 m core depth. Sections from interglacials of marine isotope stages (MIS) 1-11 are indicated according to age model of O'REGAN et al. (2010).

Abb. 6: Verteilung der Foraminiferen im Quartär der ACEX-Bohrung (verändert aus CRONIN et al. 2008). Die mittelpleistozäne Übergangszone ist durch einen Rückgang agglutinierender benthischer Foraminiferen zwischen 12 und 7 m Kernteufe charakterisiert. Grau markiert = interglaziale Kernintervalle der marinen Isotopenstadien (MIS) 1-11 (Alter nach O'REGAN et al. 2010).

by Atlantic Water advection. In summary, it must be stated that there is only indirect evidence of Atlantic Water advection for most of the Quaternary, owing to the lack of undoubtedly indicative microfossil contents. On the other hand, the changes towards more negative (non-radiogenic) Nd isotope values after 2 Ma (Fig. 3) and the variability seen in the benthic foraminiferal record make a relatively strong Atlantic Water inflow during interglacials more likely than the opposite.

VARIABILITY AND INTERACTIONS OF ATLANTIC WATER INFLOW AND EURASIAN ICE SHEETS IN THE LAST 200 KY

Arctic Ocean deposits from the last two glacial interglacial cycles show a much higher variability in a number of important parameters than those from the older part of the Quaternary. Typically, sediments from MIS 6 are almost barren of calcareous microfossils and have a high coarse fraction content interpreted as the result of intensive iceberg rafting (JAKOBSSON et al. 2000, SPIELHAGEN et al. 2004, O'REGAN et al. 2010). Very similar IRD-rich layers also appear further up in the sequence and were shown to be deposited in MIS

5b (~90–80 ka), in late MIS 5a (~75 ka), and at the MIS 3/4 boundary (~65–50 ka)(SPIELHAGEN et al. 2004). The source area of the IRD can be traced to the area of the Barents-Kara Sea shelf by the unusually high smectite contents in the IRD-rich layers (VOGT et al. 2001, SPIELHAGEN et al. 2004) and by coal particles found in the oldest and the youngest of these layers (BISCHOF et al. 1990). Relatively high (radiogenic) εNd values (Fig. 7) determined for authigenic precipitates on sediment grains from the IRD-rich layers on the Lomonosov Ridge largely exclude a strong inflow of Atlantic Water during the periods of extensive glaciations on northern Eurasia between 200 and 50 ka (HALEY et al. 2008).

In contrast to the IRD-rich deposits, the intercalated sediments from interglacials and interstadials, as well as those from the last 50 ky (all ages <50 ka are given in calendar years before present), hold evidence for a relatively strong inflow of Atlantic Water to the Arctic Ocean. The εNd values of precipitates on the Lomonosov Ridge are relatively low (non-radiogenic) and in the range of typical Atlantic Water (HALEY et al. 2008). Furthermore, the sediments hold unusually high amounts of calcareous microfossils (Fig. 7). Both coccoliths and planktic foraminifers show peak abundances

especially in MIS 7a, 5e (last interglacial, "Eemian"), 5c, 5a, and in the Holocene (GARD 1993, BAUMANN 1990, JAKOBSSON et al. 2000, BACKMAN et al. 2004, SPIELHAGEN et al. 2004, NØRGAARD-PEDERSEN et al. 2007). These abundance peaks can be traced southward to the Fram Strait (e.g., GARD 1987, HEBBELN & WEFER 1997, SPIELHAGEN et al. 2004). Being remains of photoautotrophic algae, the coccoliths are indicative of at least seasonally open ice cover. The same accounts for the heterotrophic planktic foraminifers which feed on phototrophic phytoplankton. Organic geochemical components and findings of dinoflagellate cysts in interglacial and interstadial deposits of the last 150 ky in sediment cores from the northern Eurasian continental margin also indicate a direct relationship of strong Atlantic Water inflow and seasonally open waters in the Arctic Ocean (KNIES et al. 2000, MATTHIESSEN & KNIES 2001, MATTHIESSEN et al. 2001). Relatively high amounts of subpolar planktic foraminifers (up to 50 % of all foraminifers in the >63 μm fraction) were found in Eemian and MIS 5a deposits in the GreenICE sediment cores from 85° N off Ellesmere Island and northern Greenland (Fig. 1). Although such high abundances in Arctic sediments are usually interpreted as strong evidence of Atlantic Water, NØRGAARD-PEDERSEN et al. (2007) relate them more cautiously to a reduced ice cover in an area which today is densely ice-covered around the year even in times of a generally shrinking Arctic sea-ice cover. In summary, several different and independent proxies in Arctic sediment cores unequivocally point to a significant inflow of Atlantic Water to the Arctic Ocean and its spread throughout the basin during at least six periods of the last 200 ky. The length of these periods probably varied between 5 and 10 ky, except

for the last 50 ky which apparently had continuous Atlantic Water inflow and will be discussed later. From the available data it seems difficult to draw quantitative conclusions on the volumes and temperatures of Atlantic Water inflow. Detailed oceanographic measurements in the Fram Strait in the last few decades showed these parameters to be positively correlated (RUDELS et al. 1994, KARCHER et al. 2003, DMITRENKO et al. 2010). However, the peaks in microfossil abundances in sediments from MIS 5a and 5e (BAUMANN 1990, JAKOBSSON et al., 2000, MATTHIESSEN et al. 2001, BACKMAN et al. 2004, SPIELHAGEN et al. 2004, NØRGAARD-PEDERSEN et al. 2007) may indicate that open water conditions in summer occurred more frequently in these intervals than at other times.

The abundance of microfossils (especially planktic foraminifers) in sediments from ~50–30 ka (Fig. 7) appears somewhat unusual and its interpretation in terms of Atlantic Water inflow may be ambiguous. An abundance peak building up already in the uppermost sediments of the youngest IRD-rich layer from the 60–50 ka glaciation in northern Eurasia indicates an Atlantic Water inflow and warming event possibly related to the Dansgaard-Oeschger events 17–14 in Greenland ice cores which mark a time of climatic amelioration in the northern hemisphere in the first half of MIS 3. Firm stratigraphic constraints are difficult to establish for this interval in central Arctic sediment cores (NØRGAARD-PEDERSEN et al. 1998, SPIELHAGEN et al. 2004, HANSLICK et al. 2010). Since higher-resolution cores from the Atlantic Water inflow path in the eastern Fram Strait and Yermak Plateau hold only a thin foraminifer-rich layer at ~52 ka and are almost barren for the 50–35 ka interval (HEBBELN & WEFER 1997, SPIELHAGEN et
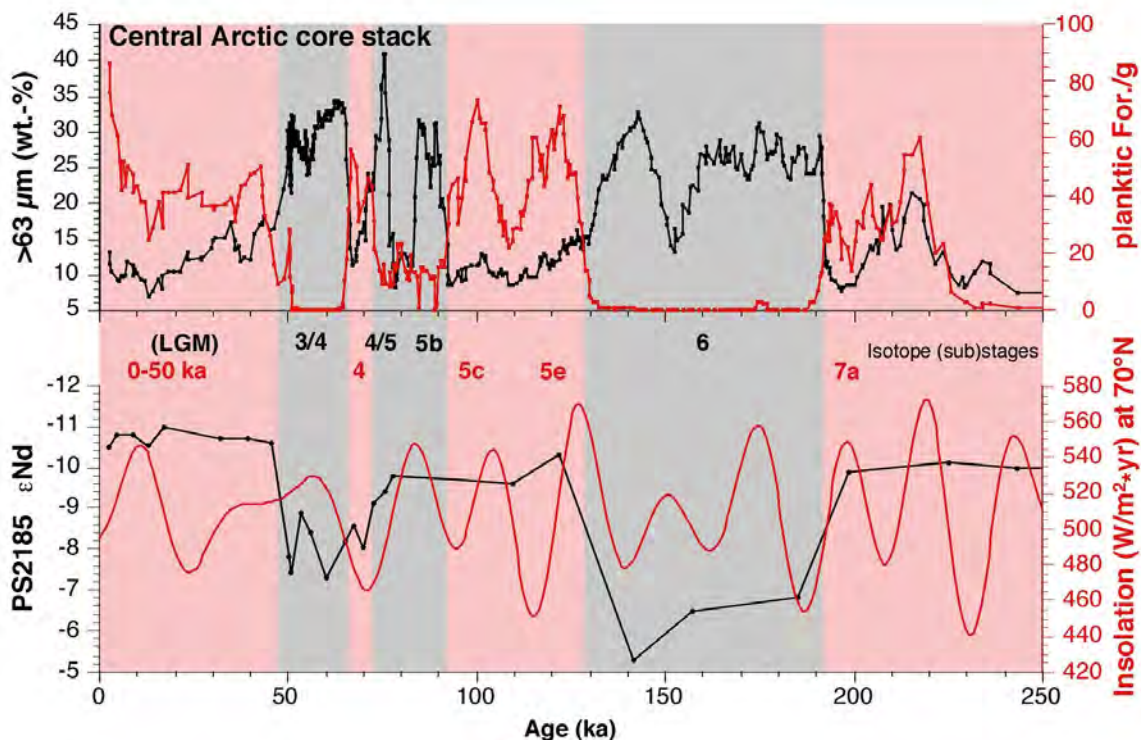
Fig. 7: Stacked coarse fraction and planktic foraminifer abundance records from cores PS2185, PS2200, and PS51/038 (data from SPIELHAGEN et al. 2004); εNd record from PS2185 (HALEY et al. 2008), and summer peak insolation (June 21st) at 70° N (from LASKAR et al. 2004) for the last 200 ky.

Abb. 7: Zusammengesetzte Häufigkeitsverteilungen von Grobfraktion und planktischen Foraminiferen der Sedimentkern PS2185, PS2200 und PS51/038 (nach SPIELHAGEN et al. 2004); εNd-Daten von PS2185 (aus HALEY et al. 2008) und max. Insolation (für 21. Juni) bei 70° N (aus LASKAR et al. 2004) für die letzten 200.000 Jahre.

al. 2004), the apparent continuous distribution of foraminifers in central Arctic MIS 3 sediments may in fact result from very low sedimentation rates and bioturbation. This could mean that a strong inflow was in fact restricted to short events just before 50 ka and after ~35 ka. On the other hand, very homogeneous and non-radiogenic εNd values from the Lomonosov Ridge suggest a continuous influence of Atlantic Water on Arctic Ocean intermediate waters after 50 ka (HALEY et al. 2008). At first sight, it seems difficult to reconcile this finding with the low sedimentation rates from MIS 3 in the central Arctic. Particularly low sedimentation rates in Arctic environments are usually associated with a dense sea-ice coverage (HEBBELN & WEFER 1991) but not with strong Atlantic Water advection. Recent faunal and geochemical data from ostracods, however, point to an Atlantic Water layer significantly warmer than at present during or just before millenial scale Heinrich events in MIS 3 (POIRIER et al. 2012, CRONIN et al. 2012). During these intervals, decreased freshwater run-off from the continents may have resulted in a thickening of the Arctic halocline layer which caused the warm Atlantic Water layer to reach deeper than today. The observed low sedimentation rates and lack of planktic foraminifers in MIS 3 sequences may then be explained by a dense and thick sea-ice cover and salinities which were too low for foraminifers to dwell.

Considering the interlayering of foraminifer-rich and IRD-poor intervals with foraminifer-poor and IRD-rich central Arctic deposits from the last 200 ky, the role of Atlantic Water advection to the Arctic in the build-up of ice sheets needs special attention. A first detailed analysis of sediment cores with high temporal resolution from the eastern Fram Strait (HEBBELN et al. 1994, ELVERHØI et al. 1995) revealed a complex relationship between both processes during the growth and decay of the Svalbard-Barents Sea ice sheet around and in the last glacial maximum (LGM). The ice sheet grew when seasonally open waters, identified by high contents of planktic foraminifers in the sediments, served as a moisture source for oceanic evaporation and subsequent terrestrial precipitation (Fig. 8). When the ice sheet had reached the shelf break, it supplied icebergs with IRD and freshwater to the Fram Strait and the Atlantic Water advection ceased. The Fram Strait data suggest that this pre-LGM cycle was repeated, as a second step of ice sheet growth, around 20 ka during the LGM proper. Organic geochemical and IRD data from the northern Eurasian continental margin suggest a similar linkage of Atlantic Water inflow, seasonally open waters, and ice-sheet build-up also for earlier glaciations in the last 150 ky (KNIES et al. 1999, 2000, 2001), possibly in a polynya-like situation. For the large northern Eurasian ice sheet KNIES et al. (2001) point out the importance of advection of moisture-laden air from more southerly sources in the North Atlantic.

Close inspection of the central Arctic deposits shows that foraminifer-rich layers occur both directly below and directly above the IRD-rich deposits (Fig. 7). Although bioturbation may have played a role in mixing of both sediment components at the interfaces of the layers, it becomes clear that there was apparently only a very short time offset in deposition of both facies. Concerning the coarse layers, it is important to note that the basin-scale IRD deposition, as indicated by the very similar IRD content pattern in sediment cores several hundred kilometres apart from each other (Fig. 1), could occur only when the large northern Arctic ice sheets had reached
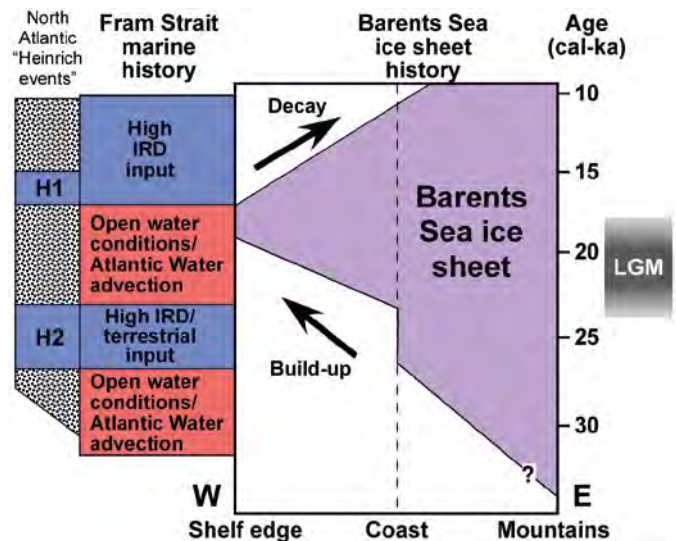

Fig. 8: Correlation of Atlantic Water advection and growth of the Barents Sea ice sheet near the western Svalbard continental margin during the last glaciation (modified from HEBBELN et al. 1994).

Abb. 8: Korrelation der Advektion von Atlantkwasser und Wachstum des Barentssee-Eisschildes nahe dem westlichen Kontinentalrand von Svalbard während der letzten Eiszeit (umgezeichnet nach HEBBELN et al. 1994).

the coastline. Several critical factors determine the growth of ice sheets on land, and model results suggest that a time span of several thousand years was necessary for the ice sheet to reach the northern shelf break (SIEGERT & DOWDESWELL 2004) as a long ice sheet front from where icebergs could be discharged to the Arctic Ocean. This implies that seasonally open water conditions were still present also in the central Arctic when ice sheet growth had already started in the hinterland. This situation most likely was facilitated by relatively strong but decreasing insolation in the northern high latitudes (Fig. 7) and a relatively strong advection of Atlantic Water to the Arctic (Fig. 9) and may have persisted for several thousand years during interglacials and interstadials, assuming that average sedimentation rates of ~1 cm ky^{-1} can be applied. In essence, seasonally open waters in a large part of the Arctic Ocean, reaching well into the Amerasian Basin, were available as a moisture source for precipitation on the nearby Arctic continents when ice sheet growth was initiated there. Apparently, Atlantic Water advection ceased when the ice sheet had reached sea level and discharged icebergs and freshwater. Alternatively, the Atlantic Water layer may have dived below a thickened freshwater-rich surface layer. No data are available, though, to support the latter scenario for the time intervals before 50 ka when ice sheets on the Eurasian continent reached a significantly larger size than thereafter.

The foraminifer-rich layers directly overlying the IRD deposits suggest that seasonally open waters and Atlantic Water returned quickly to the central Arctic after and probably already during the major deglaciations. However, increasing insolation in the northern high latitudes (Fig. 7) and rising global sea level were now in support of a rapid decay of the northern Eurasian ice sheet. All these factors, in addition to atmospheric heat transport by westerly winds from the North Atlantic, led to the deglaciations and to the establishment of interglacial or interstadial conditions with almost no or only minor remnants of ice sheets on land.
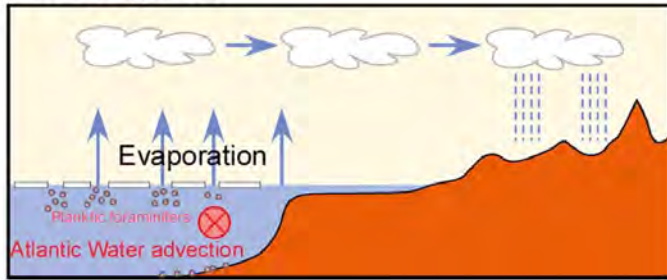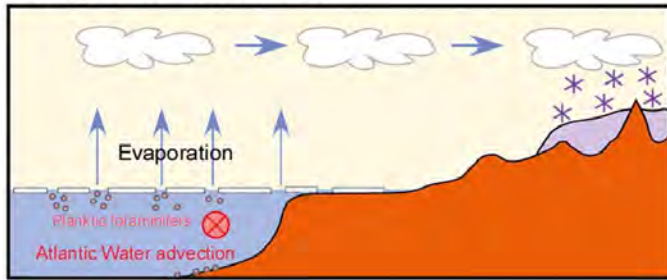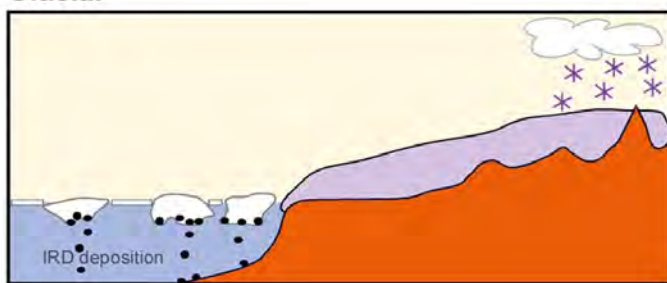
Fig. 9: Conceptual model displaying the role of Atlantic Water for ice sheet build-up on the northern Eurasian continental shelves and hinterland. It is proposed that evaporation from partly ice-free waters in summer supported the growth of ice sheets until the ice eventually reached the shelf break/coastline as a continuous ice sheet front from where icebergs and ice-rafted detritus were discharged to the deep-sea. See text for further explanation and discussion.

Abb. 9: Konzeptuelle Darstellung für die Rolle des Atlantikwassereinstroms beim Aufbau der Eisschilde auf dem eurasischen Schelf und im Hinterland. Danach verstärkte die im sommerlich offenen Meerwasser verdunstete Feuchtigkeit die Niederschläge an Land und das Wachstum der Eisschild bis eine kontinuierliche Gletscherfront die Schelfkante erreicht hat und Eisberge mit dem in ihnen enthaltene Gesteinsmaterial in den Ozean freigesetzt wurden. Siehe Text für weitere Details und Diskussion.

ATLANTIC WATER ADVECTION DURING THE LAST GLACIAL MAXIMUM (LGM)

The role of Atlantic Water advection to the Arctic is known particularly well for the last glacial maximum (LGM, ~21.5–18 ka) because LGM deposits are usually contained in the large number of analysed short sediment cores (multi-cores and box cores) from the Arctic and because these can be dated precisely by radiocarbon accelerator mass spectrometry (^{14}C-AMS). When the first (conventional) radiocarbon dates of Arctic Ocean deep-sea cores were performed, it became clear that LGM sedimentation rates in the central Arctic had been extremely low (OLSON & BROECKER 1961, HUNKINS & KUTSCHALE 1965, KU & BROECKER 1967). AMS radiocarbon datings from Alpha Ridge sediments (CLARK et al. 1986),

Gakkel Ridge cores obtained during the 1987 expedition of RV "Polarstern" (MIENERT et al. 1990, KÖHLER 1992) and short cores obtained on a transect acoss the Eurasian Basin during the "Oden"-"Polarstern" expedition in 1991 (STEIN et al. 1994a, b) supported this conclusion. On the other hand, cores from inside and north of the Fram Strait were known to hold several centimetres of LGM sediments (MARKUSSEN et al. 1985, ZAHN et al. 1985, MARQUARD & CLARK 1987, JONES & KEIGWIN 1988, KÖHLER & SPIELHAGEN 1990). In a synoptic study of 52 sediment cores from the Greenland Sea to the Lomonosov Ridge, NØRGAARD-PEDERSEN et al. (2003) could locate an abrupt transition at 84–85° N in the Eurasian Basin (Fig. 10). In the north, LGM sediments were hardly detectable by ^{14}C-AMS datings of sediment cores (e.g., STEIN et al. 1994a,b, DARBY et al. 1997, SPIELHAGEN et al. 1997, NØRGAARD-PEDERSEN et al. 1998, ADLER et al. 2009, HANSLIK et al. 2010). Either an age jump from ~27–30 to ~14 ka was found within 1–2 centimetres or the LGM interval was masked by apparent age reversals. South of 84–85° N, sediment cores revealed a regular sequence of radiocarbon dates and sedimentation rates of 1–3 cm ky^{-1} in the LGM (Fig. 11), increasing towards the Barents Sea continental margin. Two other features were different in both regions. Cores from the north had a minimum in coarse fraction and planktic foraminifer contents in sediments from the tentatively located LGM interval, and the few foraminifers had relatively low oxygen isotope values (Fig. 11). In contrast, cores from south of 84–85° N had a (local) maximum in planktic foraminifer abundances in LGM sediments, and these foraminifers had relatively heavy oxygen isotope values. Values of 4.5–4.7 ‰, with only very little regional variation (Fig. 10), were found to be typical of Atlantic Water, which had spread all over the Nordic Seas in the LGM (SARNTHEIN et al. 1995). The results from NØRGAARD-PEDERSEN et al. (2003) allow expansion of earlier, more regional environmental reconstructions (HEBBELN et al. 1994, ELVERHØI et al. 1995, KNIES & STEIN 1998, KNIES et al. 1999, 2000, 2001). The current picture, complemented by more recent work on cores from the Svalbard continental margin (RASMUSSEN et al. 2007, JESSEN et al. 2010) is as follows: During the LGM Atlantic Water reached the eastern Fram Strait and flowed around Svalbard eastward along the northern Barent Sea continental margin. It can be traced without doubt to ~30° E (e.g., KNIES & STEIN 1998, MATTHIESSEN et al. 2001) and probably to ~45° E (KNIES et al. 1999, 2000), but cores further to the east do not hold clear evidence (MATTHIESSEN et al. 2001). North of Fram Strait, Atlantic Water spread as a subsurface water mass to 84–85° N from where it may have turned westward and then southward to eventually exit through the western Fram Strait. The boundary to the north is surprisingly narrow. Within ~100 km calculated LGM sedimentation rates in the analysed cores drop almost by an order of magnitude and the peak in planktic foraminifer abundances disappears. Recent results from ostracod geochemistry and faunal distributions (POIRIER et al. 2012, CRONIN et al. 2012) suggest an alternative explanation for the changes observed in the transition zone. Similar to earlier periods with Atlantic Water advection to the Arctic in MIS 3, the warm, saline water may penetrated farther into the Arctic Basin than anticipated by NØRGAARD-PEDERSEN et al. (2003), thereby diving below a thickened halocline at 84-85° N. In this case, the typical isotopic signature of Atlantic Water may not have been recorded in the geochemistry of planktic foraminifers because their habitat was too shallow. Whether
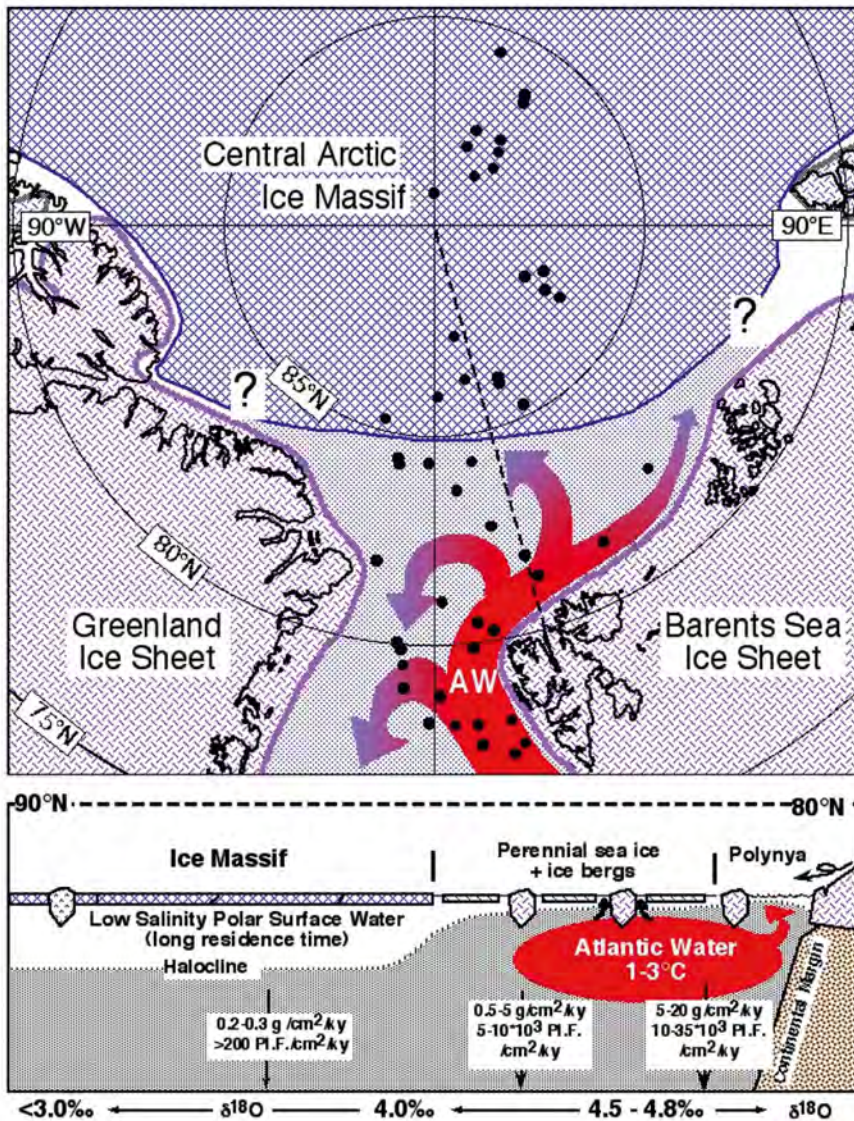
Fig. 10: Spread of Atlantic Water (AW) and distribution of environmental provinces and planktic oxygen isotope values in the last glacial maximum in the Fram Strait and the Arctic Ocean displayed in a map and along a transect from northern Svalbard to the North Pole (modified from NØRGAARD-PEDERSEN et al. 2003). Fluxes of bulk sediment and planktic foraminifers (Pl.F.) are indicated in the white boxes.

Abb. 10: Ausbreitungt des Atlantikwassers (AW) und Verteilung von Umweltmilieus und planktischen Isotopenwerten zum letzten glazialen Maximum in der Framstraße und im Arktischen Ozean in Kartendarstellung und entlang eines Schnitts von Nord-Svalbard bis zum Nordpol (nach NØRGAARD-PEDERSEN et al. 2003). Stoffflüsse von Gesamtsediment und planktischen Foraminiferen (Pl.F.) sind in den weißen Rechtecken aufgeführt.

or not there really is a hiatus present for the LGM period (i.e., non-deposition, cf. POLYAK et al. 2009, ADLER et al. 2009) or rather extremely slow sedimentation in the range of 1-2 mm ky⁻¹, later mixed by bioturbation with pre- and post-LGM sediments, seems almost impossible to determine.

VARIABLE ATLANTIC WATER ADVECTION DURING THE LAST DEGLACIATION

According to published results, the last deglaciation was highly complex in the Arctic Ocean. This holds true especially for the marginal areas which were influenced by interfering factors like Atlantic Water advection, continental ice break-

up, meltwater discharge, isostatic rebound of previously glaciated shelves, and global sea level rise. Not necessarily these developments occurred synchronously around the Arctic Ocean. In this paper, only the available evidence for Atlantic Water advection will be discussed.

Until the decay of the large Barents Sea ice sheet into several local ice caps at ~15 ka (WINSBORROW et al. 2010), Atlantic Water could enter the Arctic Ocean only through the Fram Strait. Based on a multiproxy study of sediment cores from the southwestern Svalbard continental slope and shelf (76° N), RASMUSSEN et al. (2007) demonstrated that Atlantic Water has been continuously present in this area since at least 20 ka. Relatively high abundances of subpolar planktic foraminifers in LGM sediments indicate Atlantic Water temperatures only slightly lower than today, but decreasing numbers and percentages of the total planktic foraminifer fauna, as well as increasing planktic oxygen isotope values reveal a cooling trend towards the deglaciation (RASMUSSEN et al. 2007). This suggests that the strength of the northward flow had ceased in the late LGM, possibly due to early deglacial effects and meltwater discharge further upstream. Rather abrupt changes in sedimentological and faunal parameters (e.g., planktic and benthic foraminifers) in a variety of cores obtained from the western and northern Svalbard margins and shelves are interpreted as evidence of a rapid return of (subsurface) Atlantic Water around 15 ka (KOÇ et al. 2002, ŚLUBOWSKA et al. 2005, RASMUSSEN et al. 2007, ŚLUBOWSKA-WOLDENGEN et al. 2007, 2008). It must have spread quickly along the northern Eurasian margin and may have reached the Laptev Sea continental margin already before 15.4 ka (TALDENKOVA et al. 2010). Apparently contradictory age differences may in part be related to variable reservoir ages of the water masses.

While Atlantic Water was present in the troughs northwest and northeast of Franz Josef Land and at the Laptev Sea margin only intermittently until ~12 ka (LUBINSKI et al. 2001, TALDENKOVA et al. 2010), faunal records from the western and northern Svalbard margins suggest a continuous presence as a subsurface water mass below cool and fresh surficial waters after ~15 ka, with a possibly weakened advection around 13.4 ka (RASMUSSEN et al. 2007, ŚLUBOWSKA-WOLDENGEN et al. 2007, 2008). This is corroborated by organic-geochemical data from sediment cores obtained in the Fram Strait and on Yermak Plateau which indicate seasonally open water conditions and enhanced biologic productivity, especially pronounced in the Bølling interstadial (BIRGEL & STEIN 2003, BIRGEL & HASS 2004). For the Younger Dryas stadial (~12.6–11.5 ka), faunal changes in cores from
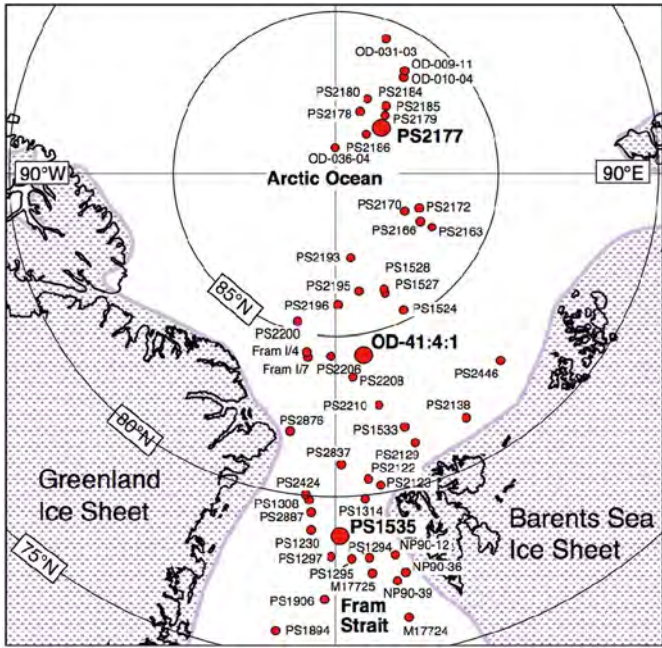
Fig. 11: Oxyen isotope records of *Neogloboquadrina pachyderma* (sin.) and abundance of planktic foraminifers in three representative sediment cores (large red dots in map) from the Fram Strait and the Arctic Ocean (data from NØRGAARD-PEDERSEN et al. 2003). LGM marks the last glacial maximum. Also shown are sites of other cores used in the LGM reconstruction (see Fig. 10).

Abb. 11: Sauerstoff Isotopenwerte von *Neogloboquadrina pachyderma* (sin.) und Häufigkeit planktischer Foraminiferen in drei repräsentativen Sediment-kernen (große rote Kreise) aus der Framstraße und dem Arktischen Ozean (Daten aus NØRGAARD-PEDERSEN et al. 2003). Das letzte glaziale Maximum (LGM) ist markiert. Ebenfalls eingezeichnet sind die Positionen weiterer für die LGM-Rekonstruktion (siehe Abb. 10) genutzter Sedimentkerne.

the Svalbard margins provide clear evidence for cooler and fresher conditions, probably with diminished Atlantic Water inflow (RASMUSSEN et al. 2007, ŚLUBOWSKA-WOLDENGEN et al. 2007, 2008). This scenario is not easily reconciled with open water conditions and relatively high bioproductivity, as suggested by organic-geochemical data from the Yermak Plateau (BIRGEL & HASS 2004). More high-resolution multi-proxy data sets are needed from the deeper waters around Svalbard to get a broader picture of environmental conditions in this area during the Younger Dryas.

ATLANTIC WATER ADVECTION FROM THE EARLY HOLOCENE THERMAL MAXIMUM TO PRESENT

By a correlation of foraminiferal, isotope, and $U^{k'}37$ data series from sediment cores obtained along a transect from the North Sea to the western Svalbard continental margin and the Barents Sea, HALD et al. (2007) and RISEBROBAKKEN et al. (2011) revealed an enhanced flow Atlantic Water which rapidly advanced northwards after the Younger Dryas. A series of studies (EBBESEN et al. 2007, HALD et al. 2007, RASMUSSEN et al. 2007, ŚLUBOWSKA-WOLDENGEN et al. 2007, 2008) showed that in the middle Preboreal (~11 ka) it had reached the eastern Fram Strait and remained the dominant near-surface water mass until shortly after 9 ka when a rapid change from subpolar to polar planktic foraminifers in the sediments indicates a return of colder surface waters to the area. This interval, termed the (Early) Holocene Thermal Maximum (HTM; KAUFMAN et al. 2004), is generally attributed to the summer insolation maximum in the northern high latitudes peaking between 9 and 11 ka (BERGER & LOUTRE 1991).

Microfossil data from a number of cores obtained on Arctic Ocean continental margins and nearby slopes and shelves show that the Atlantic Water reached far into the basin (Fig. 12), probably following its present-day path eastward from the northern Barents Sea margin. Isostatic depression of
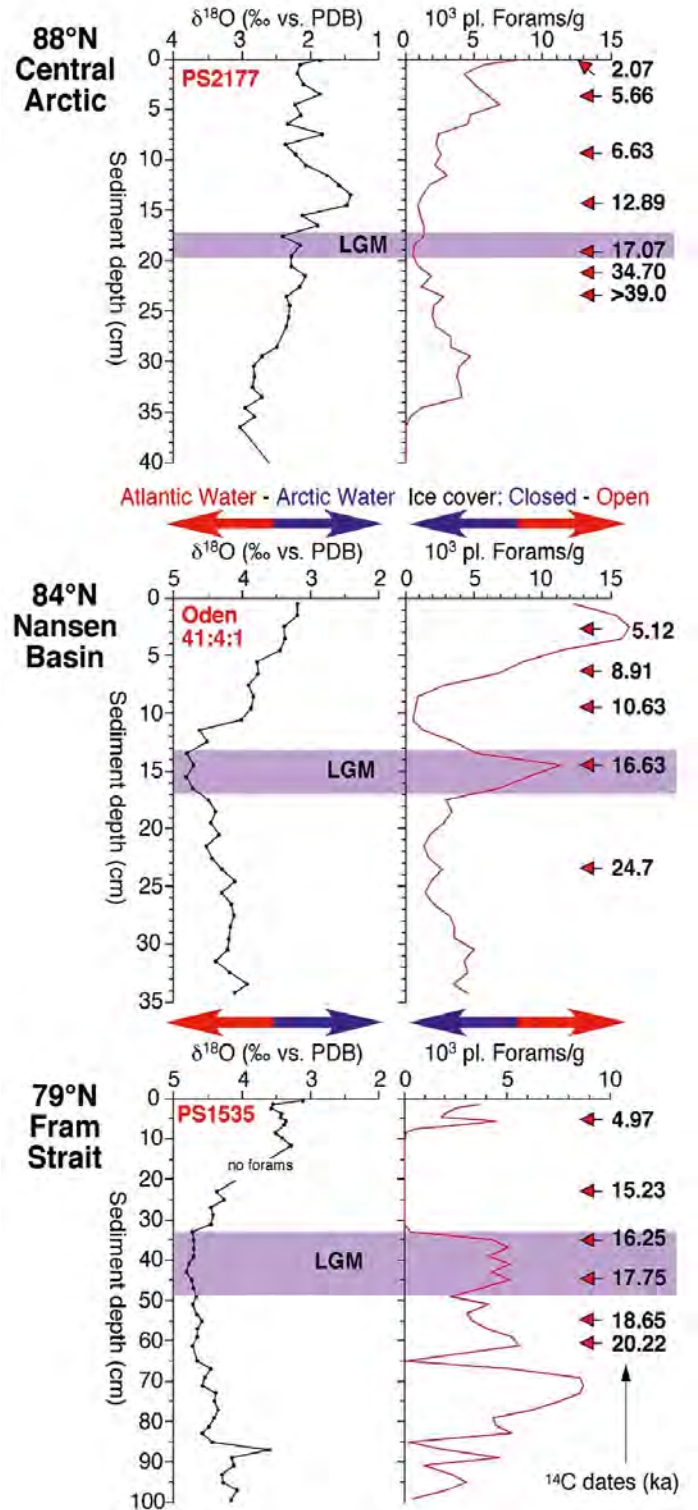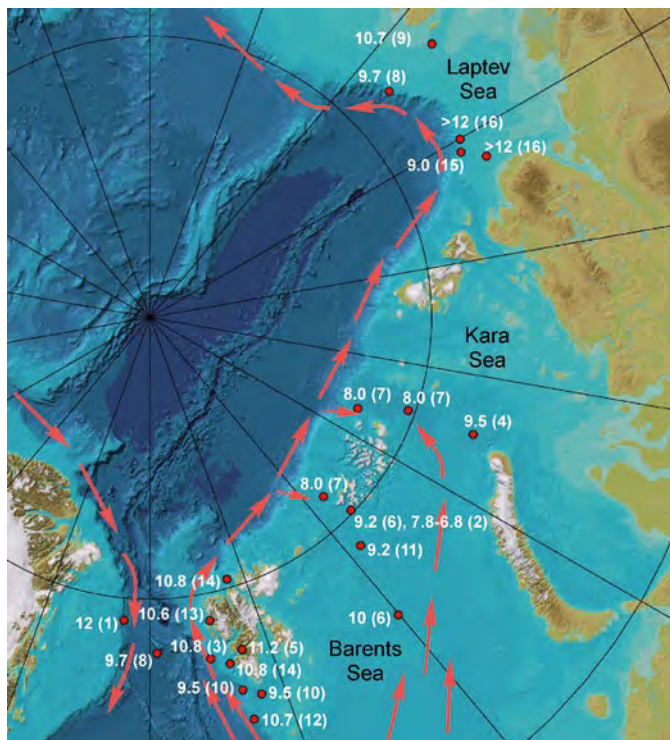
Fig. 12: Variable timing for the onset of strong Early Holocene Atlantic Water advection to sites in the Fram Strait and at the northern Eurasian continental margin. Data were obtained from various types of records, most of which are microfossil distributions. The relatively wide range of data displays the problem to clearly define this onset.
Data sources are given in parantheses: (1) = BAUCH et al. (2001), (2) = DUPLESSY et al. (2001, 2005), (3) = EBBESEN et al. (2007), (4) = HALD et al. (1999), (5) = HALD et al. (2004), (6) = IVANOVA et al. (2002), (7) = LUBINSKI et al. (2001), (8) = MATTHIESSEN et al. (2001), (9) = POLYAKOVA et al. (2005), (10) = RASMUSSEN et al. (2007), (11) = RISEBROBAKKEN et al. (2011), (12) = SARNTHEIN et al. (2003), (13) = SKIRBEKK et al. (2010), (14) = ŚLUBOWSKA-WOLDENGEN et al. (2007), (15) = STEIN & FAHL (2000), (16) = TALDENKOVA et al. (2008, 2010).

Abb. 12: Darstellung des uneinheitlichen Beginns der starken frühholozänen Advektion von Atlantikwasser an verschiedenen Kernstationen in der Framstraße und am eurasischen Kontinentalrand. Die Daten entstammen unterschiedlichen Datensätzen (meist Mikrofossilien); die Datenquellen sind in Klammern genannt: (1) = BAUCH et al. (2001), (2) = DUPLESSY et al. (2001, 2005), (3) = EBBESEN et al. (2007), (4) = HALD et al. (1999), (5) = HALD et al. (2004), (6) = IVANOVA et al. (2002), (7) = Lubinski et al. (2001), (8) = MATTHIESSEN et al. (2001), (9) = POLYAKOVA et al. (2005), (10) = RASMUSSEN et al. (2007), (11) = RISEBROBAKKEN et al. (2011), (12) = SARNTHEIN et al. (2003), (13) = SKIRBEKK et al. (2010), (14) = ŚLUBOWSKA-WOLDENGEN et al. (2007), (15) = STEIN & FAHL (2000), (16) = TALDENKOVA et al. (2008, 2010).

the Barents Sea, which was by then ice-free, was probably supportive of an enhanced Atlantic Water inflow to the Arctic Ocean (LUBINSKI et al. 2001). At least in areas where this water was at the surface (e.g. at 75° N on the western Barents Sea margin) it may have been warmer than today (SARNTHEIN et al. 2003). On its cyclonic path around the Arctic it was recorded by occurrences of subpolar microfossils, indicative benthic foraminifer species, unique isotopic compositions, and organic sediment parameters around Franz Josef Land (e.g., LUBINSKI et al. 1996, 2001, HALD et al. 1999, DUPLESSY et al. 2001, 2005, IVANOVA et al. 2002, RISEBROBAKKEN et al. 2011), at the Laptev Sea continental margin (e.g., BOUCSEIN et al. 2000, MATTHIESSEN et al. 2001, STEIN & FAHL 2000, POLYAKOVA et al. 2005, TALDENKOVA et al. 2008, 2010) and on the upper slope off northern Alaska (ANDREWS & DUNHILL

2004). The timing of the HTM apparently varied spatially; some records reveal maximum warmth as late as 7.8–6.8 ka southwest of Franz-Josef Land (DUPLESSY et al. 2001). Sites from the shelf and upper slope of western and northern Svalbard generally show a noticable but more limited influence of Atlantic WATER (ŚLUBOWSKA et al. 2005, ŚLUBOWSKA-WOLDENGEN et al. 2007), which is probably due to the influence of colder and less saline surface waters originating from the remaining ice caps over Svalbard.

High abundances of subpolar planktic foraminifers in a sediment core from the Greenland slope in the Fram Strait (79° N) indicate the presence of Atlantic Water between ~12 and ~8.5 ka (BAUCH et al. 2001). However, these specimens were probably not transported loopwise through the entire Arctic. Most likely they originate from a westward expansion of Atlantic Water in the Early Holocene and a shallower halocline in the Fram Strait which allowed subpolar planktic foraminifers to dwell in an area which after 8 ka was populated only by polar foraminifers. Although apparently not fully time-equivalent, the Atlantic Water advection to the western Fram Strait and the related heat transfer may have played a major role in the establishment of reduced sea ice conditions at Northeast Greenland coasts at ~8.5–6.0 ka (FUNDER et al. 2011).

Cores from the deep Arctic basins and contained bathymetrical highs usually do not resolve the deglacial and Early Holocene interval in such detail as cores from the Arctic margins do. Nevertheless, Early Holocene Arctic deep-sea sediments are often characterized by higher microfossil and carbonate contents than younger deposits (e.g., BAUMANN 1990, GARD 1993, STEIN et al. 1994, SPIELHAGEN et al. 1997, 2004, NØRGAARD-PEDERSEN et al. 1998, 2003, POORE et al. 1999, POLYAK et al. 2004, HANSLIK et al. 2010). In other cases – especially when very low sedimentation rates are noted – the carbonate and microfossil contents increase more or less gradually from LGM towards Holocene sediments, probably caused by bioturbation and mixing of fossil-poor (de) glacial and relatively fossil-rich Holocene deposits. A study by BAUCH (1999) showed that subpolar species are absent in Holocene sediments on the Lomonosov Ridge at 87.5° N, except for <5 % Neogloboquadrina pachyderma (dex.) which may, however, represent aberrant forms of the sinistral coiling species (cf. BAUCH et al. 2003). In summary, the elevated microfossil abundances in Early Holocene Arctic Ocean sediments all over the basin suggest an extraordinarily vigorous inflow from the south during the HTM, probably both through the Fram Strait and across the Barents Sea.

Arctic deep-sea sediments younger than the HTM usually contain lower amounts of microfossils (e.g., SPIELHAGEN et al. 1997, 2004, NØRGAARD-PEDERSEN et al. 1998, 2003, BAUCH 1999, POLYAK et al. 2004, HANSLIK et al. 2010), although some cores may show a maximum at the surface. The latter feature may again result from bioturbation and/or a better preservation of carbonate in oxygenated near-surface sediments. A trend towards lower near-surface or subsurface water temperatures is seen in almost all Holocene sediment records from the circum-Arctic continental margins and shelves for the times after the HTM (e.g., HALD et al. 1999, 2007, STEIN & FAHL 2000, DUPLESSY et al. 2001, 2005, Lubinski et al. 2001, MATTHIESSEN et al. 2001, IVANOVA et al. 2002, ANDREWS & DUNHILL 2004, POLYAKOVA et al. 2005, TALDENKOVA et al.

2010, RISEBROBAKKEN et al. 2011). The overall picture shows the establishment of conditions close to modern around 5 ka, followed by some minor variability.

Measurements of Atlantic Water temperatures and flux (i.e., volume per time) in the last few decades have revealed a close positive correlation between both parameters (KARCHER et al. 2003, SCHAUER et al. 2004). Recent sediment core data from the upper continental margin north of Alaska (160° W) show that several centennial-scale periods within the last 8,000 years were characterized by unusually warm Atlantic Water and reduced ice cover (FARMER et al. 2011). Most likely, these were intervals with a stronger Atlantic inflow to the Arctic. Further upstream, high-resolution sediment records from core MSM5/5-712 in the eastern Fram Strait (Fig. 1) revealed a multi-centennial temperature variability of Atlantic Water on its way to the Arctic Ocean which thus most probably was concurrent with a stronger advection of warm and saline waters (SPIELHAGEN et al. 2011, WERNER et al. 2011). Temperature reconstructions were based on transfer functions utilizing planktic foraminifer associations and on Mg/Ca measurements of planktic foraminifers. Both methods gave very similar results (Fig. 13). It could be shown that Atlantic Water temperatures in the last two millennia (average ~3.5 °C at 50 m water depth) were elevated by ~0.5–1 °C during warmest intervals of the Medieval Climate Anomaly (~800–1400 CE) and lower than average during the Dark Ages Cold Period (~500–800 CE) and the Little Ice Age (~1400–1900 CE). The last ~100 years, however, showed an unprecedented temperature rise by >2 °C, eventually resulting in modern values of ~6 °C. Most likely, this temperature increase is one of the various aspects of a rapid response of the Arctic to Global Warming. Both atmospheric data series (KAUFMAN et al. 2009) and the record of oceanic heat advection by Atlantic Water through Fram Strait (SPIELHAGEN et al. 2011) show that warming in the Industrial Period has reversed a cooling trend in the Arctic which has lasted (with internal variations) for at least 2000 years and probably for several thousand years more. Model-based scenarios, e.g., in the IPCC REPORT (2007), predict a progressive sea-ice loss in the Arctic caused mainly by atmospheric warming over the Arctic. The recent results from the Fram Strait, however, suggest that warmer and intensified Atlantic Water advection to the Arctic and the increased temperature difference between the Atlantic Water layer and the surface may also contribute to a development, which may eventually lead to an ice-free Arctic.

ATLANTIC WATER, ARCTIC OCEAN CIRCULATION TYPES, AND THE ROLE OF THE ARCTIC IN PAST CLIMATE CHANGES

Geoscientific research in the last 20 years has revealed that Atlantic Water advection to the Arctic was quite variable in the 50 million years. Until the opening of the Fram Strait as a passage for intermediate and deep water exchange which occurred either at 17.5 Ma (JAKOBSSON et al. 2007) or at 36 Ma (POIRIER & HILLAIRE-MARCEL 2011), bathymetry of the gateway, erosion of nearby land areas and filling of morphologic gaps as well as eustatic sea-level changes were probably the major factors controlling the exchange with the North Atlantic. Thereafter, a free exchange was physically possible but climate-related developments on the surrounding conti-
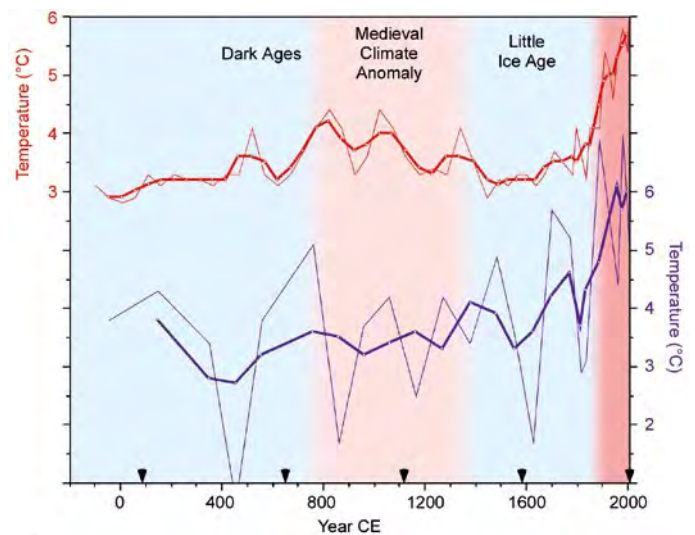
Fig. 13: Temperature reconstructions of the Atlantic Water layer at ca. 50 m water depth in the eastern Fram Strait at 79° N based on planktic foraminifer species distributions (red) and Mg/Ca ratios (blue) in core MSM5/5-712-1 for the last ca. 2,000 years (data from SPIELHAGEN et al. 2011). Thick lines are 3-point running means, black triangles mark radiocarbon dates (converted to calendar years).

Abb. 13: Temperaturrekonstruktion für die Atlantikwasserschicht in 50 m Wassertiefe in der östlichen Framstraße (79° N) in den letzten ca. 2000 Jahren, basierend auf der Artenverteilung (rot) und Mg/Ca-Verhältnissen (blau) planktischer Foraminiferen in Sedimentkern MSM5/5-712-1 (Daten aus SPIELHAGEN et al. 2011). Fette Linien zeigen Dreijahresmittelwerte; schwarze Dreiecke markieren mittels Radiokarbonmethode gemessene Alter in Kalenderjahren (CE).

nents apparently controlled the inflow and outflow. In times of extended glaciations water masses in the upper half of the water column did not show signs of intensive Atlantic Water advection and an estuarine circulation type may have developed. This type of circulation was characterized by a dominating export of surface, subsurface and intermediate waters which contained variable, but significant contributions of brines that had formed at the northern ice sheet margin and can be traced by relatively high εNd values (HALEY et al. 2008). Such scenarios apparently developed both in the Miocene-Pliocene and in the Late Quaternary. On the other hand, in intervals with significantly reduced glaciation (e.g., in parts of the Pliocene and in various interglacials and interstadials of the Late Quaternary, including the Holocene), an anti-estuarine circulation type persisted, with a strong inflow from the Atlantic which filled the Arctic Basin below a halocline separating cold, low saline riverwater-fed outflowing surface waters from underlying warmer, saline Atlantic Water. The change from one circulation type to the other may often have been somewhat "chaotic": Freshwater contributions from melting ice on the continents and icebergs in the ocean, as well as from previously ice-dammed lakes probably induced a "super-estuarine" circulation type which then, during a deglacial interval of climatic amelioration, switched to the anti-estuarine type. Details of these changes are still poorly understood and need further research and modelling.

While the prominent role of the Arctic Ocean in the present-day ocean circulation system seems undoubted, there is significantly less knowledge about an active role in climate changes of the past. The opening of the Fram Strait in the Tertiary may

have seen the initiation of such a role. It induced the transition from a freshwater-dominated environment with presumably relatively little exchange with the world ocean to a ventilated subbasin of the North Atlantic and possibly the establishment of stronger E-W contrasts there. However, little is known in detail about this transition and even its timing is uncertain. Somewhat better understood is the role of Atlantic Water inflow in interglacial-to-glacial changes (and vice versa) in the Late Quaternary. The rapid change from foraminifer-bearing to IRD-bearing sediments reveals a persisting Atlantic Water inflow to the Arctic Ocean while ice sheets were already growing on the circum-Arctic continents. The inflow may have supported seasonally open water conditions along the continental margins from where evaporation could foster ice sheet growth. In sediments from glacial-interglacial transitions, microfossil-based evidence for Atlantic Water inflow shows up when the IRD content is still relatively high. At these times, heat advection by Atlantic Water may have helped to raise atmospheric temperatures and enforce ice sheet melt. Thus, ice sheet history and Atlantic Water development seem closely tied, at least in the Late Quaternary. A third stage for an active role of the Arctic in climate change was apparently opened when large amounts of freshwater entered the Arctic Ocean during the collapse of ice sheets and release of freshwater from ice-dammed lakes, e.g. at the MIS 6/5 and MIS 4/3 transitions. The contemporaneous breakdown of deep-water ventilation in the North Atlantic (e.g., CHAPMAN et al. 2000) may suggest that freshwater export from the Arctic disturbed vertical convection in the Nordic Seas and the North Atlantic and thereby stopped the advection of Atlantic Water to the Arctic for a few thousand years and cooled northwestern Europe.

The above examples show that Atlantic Water advection to the Arctic was both active and passive during climate change of the past. While the term of "Arctic Amplification" of global warming suggests a passive role of the Arctic, the ongoing changes in the Arctic related to the temperature increase may relatively soon allocate a more active role to this area when increased freshwater fluxes and a disappearing ice cover will potentially interact strongly with global oceanic and atmospheric circulation. Further geoscientific research on the geological history of the Arctic will certainly help to improve our understanding of past, present, and future changes in this highly vulnerable part of our planet.

ACKNOWLEDGMENT

References

Adler, R.E., Polyak, L., Ortiz, J.D., Kaufman, D.S., Channell, J.E.T., Xuan, C., Grottoli, A.G., Sellen, E. & Crawford, K.A. (2009): Sediment record from the western Arctic Ocean with an improved Late Quaternary age resolution: HOTRAX core HLY0503-8JPC, Mendeleev Ridge.- Global Planet. Change 68: 18-29.

Aksu, A.E. (1985): Paleomagnetic stratigraphy of the CESAR cores.- In: H.R. JACKSON, P.J. MUDIE & S.M. BLASCO (eds), Geological Report on CESAR: The Canadian Expedition to Study the Alpha Ridge, Arctic Ocean.- Geol. Soc. Canada Paper 84-22: 101-114.

Andrews, J.T. & Dunhill, G. (2004): Early to mid-Holocene Atlantic water influx and deglacial meltwater events, Beaufort Sea slope, Arctic Ocean.- Quat. Res. 61(1): 14-21.

Backman, J., Jakobsson, M., Løvlie, R., Polyak, L. & Febo, L.A. (2004): Is the central Arctic Ocean a sediment starved basin?- Quat. Sci. Rev. 23: 1435-1454.

Backman, J., Moran, K., McInroy, D. & IODP Exp. 302 Scientists (2005): IODP Expedition 302, Arctic Coring Expedition (ACEX): A first look at the Cenozoic paleoceanography of the central Arctic Ocean.- Sci. Drilling. 1: 12-17.

Backman, J., Moran, K., McInroy, D.B., Mayer, L.A. & the Expedition 302 Scientists (2006): Expedition 302 Summary. Proc. IODP 302, doi:10.2204/iodp.proc.302.101.2006

Ballantyne, A.P., Greenwood, D.R., Sinninghe-Damsté, J.S., Csank, A.Z., Eberle, J.J. & Rybczynski, N. (2010): Significantly warmer Arctic surface temperatures during the Pliocene indicated by multiple independent proxies.- Geology 38(7): 603-606.

Ballantyne, A.P., Rybczynski, N., Baker, P.A., Harington, C.R. & White, D. (2006): Pliocene Arctic temperature constraints from the growth rings and isotopic composition of fossil larch.- Palaeogeogr. Palaeoclimatol. Palaeoecol. 242 (3-4): 188-200.

Barker, S., Archer, D., Booth, L., Elderfield, H., Henderiks, J. & Rickaby, R.E.M. (2006): Globally increased pelagic carbonate production during the mid-Brunhes dissolution interval and the CO_2 paradox of MIS 11.- Quat. Sci. Rev. 25: 3278-3293.

Bauch, D. & Bauch, H.A. (2001): Last glacial benthic foraminiferal $\delta^{18}O$ anomalies in the polar North Atlantic: a modern analogue evaluation.- J. Geophys. Res. 106: 9135-9143.

Bauch, D., Darling, K., Simstich, J., Bauch, H.A., Erlenkeuser, H. & Kroon D. (2003): Palaeoceanographic implications of genetic variation in living North Atlantic, *Neogloboquadrina pachyderma*.- Nature 424: 299-302.

Bauch, H.A. (1999): Planktic foraminifera in Holocene sediments from the Laptev Sea and the Central Arctic Ocean: species distribution and paleobiogeographical implication.- In: H. KASSENS, H.A. BAUCH & I. DMITRENKO, H. EICKEN, H.-W. HUBBERTEN, M. MELLES, J. THIEDE & L.A. TIMOKHOV (eds), Land-Ocean System in the Siberian Arctic: Dynamics and History.- Springer-Verlag, Berlin, 601-615.

Bauch, H.A., Erlenkeuser, H., Spielhagen, R.F., Struck, U., Matthiessen, J., Thiede, J. & Heinemeier, J. (2001): A multiproxy reconstruction of the evolution of deep and surface waters in the subarctic Nordic seas over the last 30,000 yr.- Quat Sci. Rev. 20: 659-678.

Baumann, M. (1990): Coccoliths in sediments of the Eastern Arctic Basin. In: U. BLEIL & J. THIEDE (eds), Geological History of the Polar Oceans: Arctic *versus* Antarctic, NATO ASI Series C, Kluwer Academic Publishers, Dordrecht, 308: 437-445.

Bennike, O., Abrahamsen, N., Bak, M., Israelson, C., Konradi, P., Matthiessen, J. & Witkowski, A. (2002): A multi-proxy study of Pliocene sediments from Ile de France, North-East Greenland.- Palaeogeogr. Palaeoclimatol. Palaeoecol. 186: 1-23.

Berger, A. & Loutre, M.F. (1991): Insolation values for the climate of the last 10 million years.- Quat. Sci. Rev. 10: 297-317.

Birgel, D. & Hass, H.C. (2004): Ocean and Atmospheric variations during the last deglaciation in the Fram Strait (Arctic Ocean): a coupled high-resolution organic-geochemical and sedimentological study.- Quat. Sci. Rev. 23: 29-47.

Birgel, D. & Stein, R. (2003): Northern Fram Strait and Yermak Plateau: distribution, sources, variability and burial of organic carbon.- In: R. STEIN & R.W. MACDONALD (eds), The Organic Carbon Cycle of the Arctic Ocean, Springer, New York, 279-294.

Bischof, J., Koch. J., Kubisch, M., Spielhagen, R.F. & Thiede, J. (1990): Nordic Seas surface ice drift reconstructions - evidence from ice rafted coal fragments during oxygen isotope stage 6.- In: J.A. DOWDESWELL & J.D. SCOURSE (eds), Glacimarine Environments: Processes and Sediments, Geol. Soc. Spec. Publ., London, 53: 275-291.

Bond, G.C., Broecker, W., Johnsen, S., McManus, J., Labeyrie, L., Jouzel, J. & Bonani, G. (1993): Correlations between climate records from North Atlantic sediments and Greenland ice.- Nature 365: 143-147.

Boucsein, B., Fahl, K. & Stein, R. (2000): Late Quaternary organic matter records from the Laptev Sea continental margin: evidence for the variability of river discharge during the last 15000 years BP.- Internat J. Earth Sci. 89: 578-591.

Carmack, E. & Wassmann, P. (2006): Food webs and physical-biological coupling on pan-Arctic shelves: Unifying concepts and comprehensive perspectives.- Progr. Oceanogr. 71: 446-477.

Chapman, M.R., Shackleton, N.J. & Duplessy, J.-C. (2000): Sea surface temperature variability during the last glacial-interglacial cycle: assessing the magnitude and pattern of climate change in the North Atlantic.- Palaeogeogr. Palaeoclimatol. Palaeoecol. 157: 1-25.

Clark, D.L. (1974): Late Mesozoic and early Cenozoic sediment cores from the Arctic Ocean.- Geology 2: 41-44.

Clark, D.L. (1982): Origin, nature and world climate effect of Arctic Ocean ice-cover.- Nature 300: 321-325.

Clark, D.L. (1988): Early history of the Arctic Ocean.- Paleoceanography: 3(5): 539-550.

Clark, D.L. (1996): The Pliocene record in the central Arctic Ocean.- Mar. Micropal. 27: 157-164.

Clark, D.L., Andree, M., Broecker, W.S., Mix, A.C., Bonani, G., Hofmann, H.J., Morenzoni, E., Nessi, M., Suter, M. & Woelfli W. (1986): Arctic Ocean chronology confirmed by accelerator ^{14}C dating.- Geophys. Res. Lett. 13(4), 319-321, doi:10.1029/GL013i004p00319.

Clark, D.L., Byers, C.W. & Pratt, L.M. (1986): Cretaceous black mud from the central Arctic Ocean.- Paleoceanography, 1(3): 265-271.

Clark, D.L., Whitman, R.R., Morgan, K.A. & Mackey, SD. (1980): Stratigraphy and glacial-marine sediments of the Amerasian Basin, central Arctic Ocean.- Geol. Soc. Amer. Spec. Pap. 181: 1- 57.

Clark, P.U., Pisias, N.G., Stocker, T.F. &Weaver, A.J. (2002): The role of the thermohaline circulation in abrupt climate change.- Nature 415: 863-869.

Cronin, T.M., Dwyer, G.S., Farmer, J., Bauch, H.A., Spielhagen, R.F., Jakobsson, M., Nilsson, J., Briggs, W.M.Jr., & Stepanova, A. (2012): Arctic Ocean Warming and Halocline Deepening during the last Glacial Cycle.- Nature Geosci. 5: 631-634, doi:10.1038/NGEO1557.

Cronin, T.M., Smith, S.A., Eynaud, F., O'Regan, M. & King, J. (2008): Quaternary paleoceanography of the central Arctic based on IODP ACEX 302 foraminiferal assemblages.- Paleoceanography 23: PA1S18.

Cronin, T.M., Whatley, R.C., Wood, A., Tsukagoshi, A., Ikeya, N., Brouwers, E.M. & Briggs W.M. (1993): Microfaunal evidence for elevated mid-Pliocene temperatures in the Arctic Ocean.- Paleoceanography 8: 161-173

Csank, A.Z., Tripati, A., Patterson, W.P., Eagle, R.A., Rybczynski, N., Ballantyne, A. & Eiler J.M. (2011): Estimates of Arctic land surface temperatures during the Early Pliocene from two novel proxies.- Earth Planet. Sci. Lett. 304: 291299.

Darby, D.A. (2008): Arctic perennial ice cover over the last 14 million years.- Paleoceanography 23: PA1S07

Darby, D.A., Bischof, J.F. & Jones, G.A. (1997): Radiocarbon chronology of depositional regimes in the western Arctic Ocean.- Deep Sea Res. II 44(8): 1745-1757.

Dmitrenko, I.A., Kirillov, S.A. Tremblay, L.B. Bauch, D. Hölemann, J.A. Krumpen, T. Kassens, H. Wegner, C. Heinemann, G. & Schröder D. (2010): Impact of the Arctic Ocean Atlantic water layer on Siberian shelf hydrography.- J. Geophys. Res. 115: C08010, doi: 10.1029/2009JC006020.

Duplessy, J.C., Cortijo, E., Ivanova, E., Khusid, T., Labeyrie, L., Levitan, M., Murdmaa, I. & Paterne, M. (2005): Paleoceanography of the Barents Sea during the Holocene.- Paleoceanography 20: PA4004, doi: 10.1029/2004PA001116.

Duplessy, J.-C., Ivanova, E., Murdmaa, I., Paterne, M. & Labeyrie, L. (2001): Holocene paleoceanography of the northern Barents Sea and variations of the northward heat transport by the Atlantic Ocean.- Boreas 30(1): 2-16.

Ebbesen, H., Hald, M. & Eplet, T.H. (2007): Lateglacial and Early Holocene climatic oscillations on the western Svalbard margin, European Arctic.- Quat. Sci. Rev. 26: 1999-2011.

Elias, S.A., Kuzmina, S. & Kiselyov, S. (2006): Late Tertiary origins of the Arctic beetle fauna.- Palaeogeogr. Palaeoclimatol. Palaeoecol. 241: 373-392.

Elias, S.A. & Matthews Jr., J.V. (2002): Arctic North American seasonal temperatures in the Pliocene and Early Pleistocene, based on mutual climatic range analysis of fossil beetle assemblages.- Can. J. Earth Sci. 39: 911-920.

Elverhøi, A., Andersen, A.E., Dokken, T., Hebbeln, D., Spielhagen, R.F., Svendsen, J.I., Sørflaten, M., Rørnes, A., Hald, M. & Forsberg, C.F. (1995): The growth and decay of the Late Weichselian ice sheet in western Svalbard and adjacent areas based on provenance studies of marine sediments.- Quat. Res. 44: 303-316.

Farmer, J.R., Cronin, T.M., de Vernal, A., Dwyer, G.S., Keigwin, L.D. & Thunell, R.C. (2011): Western Arctic Ocean temperature variability during the last 8000 years.- Geophys. Res. Lett. 38: L24602. doi: 10.1029/2011GL049714.

Funder, S., Bennike, O., Böcher, J., Israelson, C., Petersen, K.S. & Símonarson, L.A. (2001): Late Pliocene Greenland: The Kap København Formation in North Greenland.- Bull. Geol. Soc. Denmark 48: 117-134.

Funder, S., Bennike, O., Mogensen, G.S,. Noe-Nygaard, B., Pedersen, S.A.S. & Petersen, K.S. (1984): The Kap København Formation, a Late Cainozoic sedimentary sequence in North Greenland.- Rapp. Grønlands Geol. Unders. 120: 9-18.

Funder, S., Goosse, H., Jepsen, H., Kaas, E., Kjær, K.H., Korsgaard, N.J., Larsen, N.K., Linderson, H., Lyså, A., Möller, P., Olsen, J. & Willerslev, E. (2011): A 10,000-year record of Arctic Ocean sea-ice variability - view from the Beach.- Science 333(6043): 747-750, doi: 10.1126/science.1202760].

Gard, G. (1987): Late Quaternary calcareous nannofossil biostratigraphy and sedimentation patterns: Fram Strait, Arctica.- Paleoceanography 2 (5): 519, doi: 10.1029/PA002i005p00519.

Gard, G. (1993): Late Quaternary coccoliths at the North Pole: Evidence of ice-free conditions and rapid sedimentation in the central Arctic Ocean.- Geology 21(3): 227-230.

Geissler, W.H., Jokat, W. & Brekke, H. (2011): The Yermak Plateau in the Arctic Ocean in the light of reflection seismic data - implication for its tectonic and sedimentary evolution.- Geophys. J. Int. 187: 1334-1362.

Gill, A.E. (1973): Circulation and bottom water production in theWeddell Sea.- Deep-Sea Res. 20: 111-140.

Hald, M., Andersson, C., Ebbesen, H., Jansen, E., Klitgaard-Kristensen, D., Risebrobakken, B., Salomonsen, G.R., Sarnthein, M., Sejrup, H.P. & Telford R.J. (2007): Variations in temperature and extent of Atlantic Water in the Northern North Atlantic during the Holocene.- Quat. Sci. Rev. 26: 3423-3440, doi: 10.1016/j.quascirev.2007.10.005.

Hald, M., Ebbesen, H., Forwick, M., Godtliebsen, F., Khomenko, L., Korsun, S., Ringstad Olsen. L. & Vorren, T.O. (2004): Holocene paleoceanography and glacial history of the West Spitsbergen area, Euro-Arctic margin.- Quat. Sci. Rev. 23: 2075-2088.

Hald, M., Kolstad, V., Polyak, L., Forman, S.L., Herlihy, F.A., Ivanov, G. & Nescheretov, A. (1999): Late-glacial and Holocene paleoceanography and sedimentary environments in the St. Anna Trough, Eurasian Arctic Ocean margin.- Palaeogeogr. Palaeoclimatol. Palaeoecol. 146: 229-249.

Haley, B.A., Frank, M., Spielhagen, R.F. & Eisenhauer, A. (2008): Influence of brine formation on Arctic Ocean circulation over the past 15 million years.- Nature Geosci. 1: 68-72, doi: 10.1038/ngeo.2007.5.

Hanslik, D., Jakobsson, M., Backman, J., Björck, S., Sellén, E., O'Regan, M., Fornaciari, E. & Skog, G. (2010): Quaternary Arctic Ocean sea ice variations and radiocarbon reservoir age corrections.- Quat. Sci. Rev. 29: 3430-3441.

Hebbeln, D., Dokken, T., Andersen, E.S., Hald, M. & Elverhoi, A. (1994): Moisture supply to northern ice-sheet growth during the Last Glacial Maximum.- Nature 370: 357-360.

Hebbeln, D. & Wefer, G. (1991): Effects of ice coverage on sedimentation in the Fram Strait.- Nature 350:409-411.

Hebbeln, D. & Wefer, G. (1997): Late Quaternary paleoceanography in the Fram Strait.- Paleoceanography 12(1): 65-78.

Hemleben, C. & Kaminski, M.A. (1990): Agglutinated Foraminifera: an introduction.- In: C. HEMLEBEN, M.A. KAMINSKI, W. KUHNT & D.B SCOTT (eds), Paleoecology, biostratigraphy, paleoceanography and taxonomy of agglutinated foraminifera, NATO ASI Series, Kluwer Academic Publishers, Dordrecht, 3-11.

Herman, Y. & Hopkins, D.M. (1980): Arctic Oceanic Climate in Late Cenozoic Time.- Science 209: 557-562.

Hunkins, K. & Kutschale, H. (1965): Quaternary sedimentation in the Arctic Ocean.- Progr. Oceanogr. 4: 89-94.

Ishman, S.E., Polyak,L. & Poore, R.Z. (1996): An expanded record of Pleistocene deep Arctic change: Canada Basin, western Arctic Ocean.- Geology 24: 139-142.

Ivanova, E.V., Murdmaa, I.O., Duplessy, J.-C. & Paterne, M. (2002): Late Weichselian to Holocene Paleoenvironments of the Barents Sea.- Global Planet. Change 34(3-4): 69-78.

Jakobsson, M., Backman, J., Rudels, B., Nycander, J., Frank, M., Mayer, L., Jokat, W., Sangiorgi, F., O'Regan, M., Brinkhuis, H., King, J., & Moran, K. (2007): The Early Miocene Onset of a Ventilated Circulation Regime in the Arctic Ocean.- Nature 447(21): 986-990.

Jakobsson, M., Løvlie, R., Al-Hanbali, H., Arnold, E., Backman, J. & Mörth M. (2000): Manganese and color cycles in Arctic Ocean sediments constrain Pleistocene chronology.- Geology 28: 23-26.

Jessen, S.P., Rasmussen, T.L., Nielsen, T. & Solheim, A. (2010): A new Late Weichselian and Holocene marine chronology for the western Svalbard slope 30,000 - 0 cal years BP.- Quat. Sci. Rev. 29: 1301-1312, doi: 10.1016/j.quascirev.2010.02.020.

Jones, G.A., & Keigwin, L.D. (1988): Evidence from Fram Strait (78N) for early deglaciation.- Nature 336: 56-59.

Kaminski, M.A., Silye, L. & Kender, S. (2009): Miocene deep-water agglutinated foraminifera from the Lomonosov Ridge and the opening of the Fram Strait.- Micropaleontology 55(2-3): 117-135.

Karcher, M.J., Gerdes, R., Kauker, F. & Köberle, C. (2003): Arctic warming - Evolution and Spreading of the 1990s warm event in the Nordic Seas and the Arctic Ocean.- J. Geophys. Res. 108: 3034, doi: 10.1029/.2001JC001265.

Kaufman, D.S., Ager, T.A., Anderson, N.J., Anderson, P.M., Andrews, J.T., Bartlein, P.J., Brubaker, L.B., Coats, L.L., Cwynar, L.C., Duvall, M.L., Dyke, A.S., Edwards, M.E, Eisner, W.R., Gajewski, K., Geirsdóttir, A.,

Hu, F.S., Jennings, A.E., Kaplan, M.R., Kerwin, M.W., Lozhkin, A.V., MacDonald, G.M., Miller, G.H., Mock, C.J., Oswald, W.W., Otto-Bliesner, B.L., Porinchu, D.F., Rühland, K., Smol, J.P., Steig, E.J. & Wolfe, B.B. (2004): Holocene thermal maximum in the western Arctic (0-180° W).- Quat. Sci. Revi. 23: 529-560.

Kaufman, D.S. & Brigham-Grette, J. (1993): Aminostratigraphic correlations and paleotemperature implications, Pliocene–Pleistocene high sea level deposits, northwestern Alaska.- Quat. Sci. Rev. 12: 21-33.

Koç, N., Klitgaard Kristensen, D., Hasle, K., Forsberg, C.F. & Solheim, A. (2002): Late glacial paleoceanography of Hinlopen Strait, northern Svalbard.- Polar Res. 21: 307-314.

Köhler, S.E.I. (1992): Spätquartäre paläo-ozeanographische Entwicklung des Nordpolarmeeres und Europäischen Nordmeeres anhand von Sauerstoff- und Kohlenstoff-Isotopenverhältnissen der planktischen Foraminifere Neogloboquadrina pachyderma (sin.).- GEOMAR Rep. 13: 1-104.

Köhler, S.E.I. & Spielhagen, R.F. (1990): The enigma of oxygen isotope stage 5 in the central Fram Strait.- In: U. BLEIL & J. THIEDE (eds), Geological History of the Polar Oceans: Arctic versus Antarctic, NATO ASI Series C, Kluwer Academic Publishers, Dordrecht, 308: 489-497.

Knies, J. & Gaina, C. (2008): Middle Miocene ice sheet expansion in the Arctic: views from the Barents Sea.- Geochem. Geophys. Geosyst. 9: Q02015, doi: 10.1029/2007GC001824.

Knies, J., Kleiber, H.P., Matthiessen, J., Müller, C. & Nowaczyk, N.R. (2001): Marine ice-rafted debris records constrain maximum extent of Saalian and Weichselian ice sheets along the northern Eurasian margin.- Global Planet. Change 31: 45-63.

Knies, J., Matthiessen, J., Mackensen, A., Stein, R., Vogt, C., Frederichs, T. & Nam S.-I. (2007): Effects of Arctic freshwater forcing on thermohaline circulation during the Pleistocene.- Geology 35: 1075-1078.

Knies, J., Matthiessen, J., Vogt, C., Laberg, J.S., Hjelstuen, B.O., Smelror, M., Larsen, E., Andreassen, K., Eidvin T. & Vorren T.O. (2009): The Plio-Pleistocene glaciation of the Barents Sea - Svalbard region: a new model based on revised chronostratigraphy.- Quat. Sci. Rev. 28(9-10): 812-829.

Knies, J., Matthiessen, J., Vogt, C. & Stein R. (2002): Evidence of 'Mid-Pliocene (~3 Ma) global warmth' in the eastern Arctic Ocean and implications for the Svalbard/Barents Sea ice sheet during the late Pliocene and early Pleistocene (~3–1.7 Ma).- Boreas 31: 82-93.

Knies, J., Nowaczyk, N., Müller, C., Vogt, C. & Stein, R. (2000): A multiproxy approach to reconstruct the environmental changes along the Eurasian continental margin over the last 150000 years.- Mar. Geol. 163: 317-344.

Knies, J. & Stein, R. (1998): New aspects of organic carbon deposition and its paeoceanographic implications along the northern Barents Sea margin during the last 30,000 years.- Paleoceanography 13(4): 384-394, doi: 10.1029/98PA01501.

Knies, J., Vogt, C. & Stein, R. (1999): Growth and decay patterns of the Svalbard - Barents Sea ice sheet and paleoceanographic evolution during Saalian and Weichselian glaciations.- Geo-Mar. Lett. 18: 195-202.

Krylov, A.A., Andreeva, I.A., Vogt, C., Backman, J., Krupskaya, V.V., Grikurov, G.E., Moran, K. & Shoji H. (2008): A shift in heavy and clay mineral provenance indicates a middle Miocene onset of a perennial sea ice cover in the Arctic Ocean.- Paleoceanography 23: PA1S06, doi: 10.1029/2007PA001497.

Ku, T.L. & Broecker, W.S. (1967): Rates of sedimentation in the Arctic Ocean.- Progr. Oceanogr. 4: 94-104.

Kuhlbrodt, T., Griesel, A., Montoya, M., Levermann, A., Hofmann, M. & Rahmstorf, S. (2007): On the driving processes of the Atlantic meridional overturning circulation.- Rev. Geophys. 45: RG2001, doi: 10.1029/2004RG000166.

Laberg, J.S., Andreassen, K., Knies, J., Vorren, T.O. & Winsborrow, M. (2010): Late Pliocene-Pleistocene development of the Barents Sea Ice Sheet.- Geology 38(2): 107-110.

Laskar, J., Robutel, P., Joutel, F., Gastineau, M., Correia A.C.M. & Levrard, B. (2004): A long-term numerical solution for the insolation quantities of the Earth.- Astron. Astrophys. 428 (1): 261. DOI: 10.1051/0004-6361:20041335.

Lubinski, D.J., Korsun, S., Polyak, L., Forman, S. L., Lehman S.J., Herlihy, F.A. & Miller, G.H. (1996): The last deglaciation of the Franz Victoria Trough, northern Barents Sea.- Boreas 25: 89-100.

Lubinski, D.J., Polyak, L. & Forman, S.L. (2001): Freshwater and Atlantic water inflows to the deep northern Barents and Kara seas since ca 13 14C ka: foraminifera and stable isotopes.- Quat. Sci. Rev. 20: 1851-1879.

Markussen, B., Zahn, R. & Thiede, J. (1985): Late Quaternary sedimentation in the Eastern Arctic Basin: stratigraphy and depositional environment.- Paleogeogr. Paleoclimatol. Paleoecol. 50: 271-284.

Marquard, R.S. & Clark, D.L. (1987): Pleistocene paleoceanographic correlations: northern Greenland Sea to central Arctic Ocean.- Mar. Micropaleontol. 12: 325-341.

Marsland, S.J., Bindoff, N.L., Williams, G.D. & Budd, W.F. (2004): Modeling water mass formation in the Mertz Glacier Polynya and Adelie Depression, East Antarctica.- J. Geophys. Res. 109: C11003.

Matthiessen, J. & Knies, J. (2001): Dinoflagellate cyst evidence for warm interglacial conditions at the northern Barents Sea margin during marine oxygen isotope stage 5.- J. Quat. Sci. 16: 727-737.

Matthiessen, J., Knies, J., Nowaczyk, N. & Stein, R. (2001): Late Quaternary dinoflagellate cyst stratigraphy at the Eurasian Continental Margin, Arctic Ocean: indications for Atlantic water inflow in the past 150,000 years.- Global Planet. Change 31: 65-86.

Matthiessen, J., Knies, J., Vogt, C. & Stein, R. (2009). Pliocene Palaeoceanography of the Arctic Ocean and Subarctic Seas.- Phil. Trans. Royal Soc. London A 367(1886): 21-48.

McLaughlin, F.A., Carmack, E.C., Macdonald, R.W., Melling, H., Swift, J.H., Wheeler, P.A., Sherr, B.F. & Sherr, E.B. (2004): The joint roles of Pacific and Atlantic-origin waters in the Canada Basin, 1997-1998.- Deep-Sea Res. I 51: 107-128.

McNeil, D.H. (1996): Distribution of Cenozoic agglutinated benthic foraminifers in the Beaufort-Mackenzie Basin.- In: J. DIXON (ed), Geological Atlas of the Beaufort-Mackenzie Area, Geol. Surv. Canada, Misc. Rep. 1-59.

McNeil, D.H. (1997): New foraminifera from the Upper Cretaceous and Cenozoic of the Beaufort-Mackenzie Basin of Arctic Canada.- Cushman Foundation Foram. Res. Spec. Publ., Washington, DC, 35: 1-95.

Mienert, J., Mayer, L., Jones, G. & King, J. (1990): Physical and acoustic properties of Arctic Ocean deep-sea sediments: paleoclimatic implications.- In: U. BLEIL & J. THIEDE (eds), Geological History of the Polar Oceans: Arctic versus Antarctic, NATO ASI Series C, Kluwer Academic Publishers, Dordrecht, 308: 455-473

Moran, K., Moran, K., Backman, J., Brinkhuis, H., Clemens, S.C., Cronin, T., Dickens, G.R., Eynaud, F., Gattacceca, J., Jakobsson, M., Jordan, R.W., Kaminski, M., King, J., Koc, N., Krylov, A., Martinez, N., Matthiessen, J., McInroy, D., Moore, T.C., Onodera, J., O'Regan, M., Pälike, H., Rea, B., Rio, D., Sakamoto, T., Smith, D.C., Stein, R., St. John, K., Suto, I., Suzuki, N., Takahashi, K., Watanabe, M., Yamamoto, M., Farrell, J., Frank, M., Kubik, P., Jokat, W. & Kristoffersen, Y. (2006): The Cenozoic palaeoenvironment of the Arctic Ocean.- Nature 441: 601-606.

Mullen, M.W. & McNeil, D.H. (1995): Biostratigraphic and paleoclimatic significance of a new Pliocene foraminiferal fauna from the central Arctic Ocean.- Mar. Micropal. 26: 273-280.

Nørgaard-Pedersen, N., Mikkelsen, N., Lassen, S.J., Kristoffersen, Y. & Sheldon E. (2007): Reduced sea-ice concentrations in the Arctic Ocean during the last interglacial period revealed by sediment cores off northern Greenland.- Paleoceanography 22: PA1218, http://dx.doi.org/10.1029/2006PA001283.

Nørgaard-Pedersen, N., Spielhagen, R.F., Erlenkeuser, H., Grootes, P.M., Heinemeier, J., & Knies, J. (2003): Arctic Ocean during the Last Glacial Maximum: Atlantic and polar domains of surface water mass distribution and ice cover.- Paleoceanography 18(3): 1063, doi: 10.1029/2002PA000781.

Nørgaard-Pedersen, N., Spielhagen, R.F., Thiede, J. & Kassens, R. (1998): Central Arctic surface ocean environment during the past 80,000 years.- Paleoceanography 13: 193-204.

Olson, E.A. & Broecker, W.S. (1961): Lamont natural radiocarbon measurements VII.- Radiocarbon 3: 141-175.

O'Regan, M., King, J., Backman, J., Jakobsson, M., Pälike, H., Moran, K., Heil, C., Sakamoto, T., Cronin, T. & Jordan R. (2008): Constraints on the Pleistocene chronology of sediments from the Lomonosov Ridge.- Paleoceanography 23: PA1S19.

O'Regan, M., St. John, K., Moran, K., Backman, J., King, J., Haley, B.A., Jakobsson, M., Frank, M. & Röhl, U. (2010): Plio-Pleistocene trends in ice rafted debris on the Lomonosov Ridge.- Quat. Int. 219 (1-2): 168-176.

Poirier, A. & Hillaire-Marcel, C. (2009): Os-isotope insights into major environmental changes of the Arctic Ocean during the Cenozoic.- Geophys. Res. Lett. 36: L11602, doi:10.1029/2009GL037422.

Poirier, A. & Hillaire-Marcel, C. (2011): Improved Os-isotope stratigraphy of the Arctic Ocean.- Geophys. Res. Lett. 38(14): L14607.

Poirier, R.K., Cronin, T.M., Briggs, W.M. Jr. & Lockwood, R. (2012): Central Arctic paleoceanography for the last 50 kyr based on ostracode faunal assemblages.- Mar. Micropal. 88-89: 65-76.

Polyak, L., Bischof, J., Ortiz, J.D., Darby, D.A., Channell, J.E.T., Xuan, C., Kaufman, D.S., Løvlie, R., Schneider, D.A., Eberl, D.D., Adler, R.E. & Council, E.A. (2009): Late Quaternary stratigraphy and sedimentation patterns in the western Arctic Ocean.- Global Planet. Change 68: 5-17.

Polyak, L., Curry, W.B., Darby, D.A., Bischof, J. & Cronin, T.M. (2004): Contrasting glacial/interglacial regimes in the western Arctic Ocean as exemplified by a sedimentary record from the Mendeleev Ridge.- Palaeogeogr. Palaeoclimatol. Palaeoecol. 203: 73-93.

Polyakova, Y.I., Bauch, H.A. & Klyuvitkina, T.S. (2005): Past changes in Laptev Sea water masses deduced from diatom and aquatic palynomorph assemblages.- Global Planet. Change 48(1-3): 208-222, doi: 10.1016/j.gloplacha.2004.12.014.

Poore, R.Z., Ishman, S.E., Phillips, L. & McNeil, D. (1994): Quaternary stratigraphy and paleoceanography of the Canada Basin, western Arctic Ocean.- US Geol. Survey Bull. 2080: 1-32.

Poore, R.Z., Osterman, L., Curry, W.B. & Phillips R.L. (1999): Late Pleistocene and Holocene meltwater events in the western Arctic Ocean.- Geology 27: 759-762.

Rahmstorf, S. (1995): Bifurcations of the Atlantic thermohaline circulation in response to changes in the hydrological cycle.- Nature 378: 145-149.

Rasmussen, T.L., Thomsen, E., Ślubowska, M.A., Jessen, S., Solheim, A., Koç, N. (2007): Paleoceanographic evolution of the SW Svalbard margin (76° N) since 20,000 ^{14}C yr BP.- Quat. Res. 67: 100-114.

Raymo, M.E. (1994): The initiation of northern hemisphere glaciation.- Ann. Rev. Earth Planet. Sci. 22: 353-383.

Raymo, M.E., Lisiecki, L.E. & Nisancioglu, K.H. (2006): Plio-Pleistocene Ice Volume, Antarctic Climate, and the Global δ^{18}O Record.- Science 313: 492-495.

Risebrobakken, B., Dokken, T., Smedsrud, L.H., Andersson, C., Jansen, E., Moros, M. & Ivanova, E.V. (2011): Early Holocene temperature variability in the Nordic Seas: the role of oceanic heat advection *versus* changes in orbital forcing.- Paleoceanography 26: PA4206, doi: 10.1029/2011PA002117.

Robinson, M.M. (2009): New quantitative evidence of extreme warmth in the Pliocene Arctic.- Stratigraphy 6(4): 265-275.

Rudels, B., Jones, E.P., Anderson, L.G. & Kattner, G. (1994): On the intermediate depth waters of the Arctic Ocean.- In: O.M. JOHANNESSEN, R.D. MUENCH & J.E. OVERLAND (eds), The Polar Oceans and Their Role in Shaping the Global Environment, Amer. Geophy. Union, Washington, DC, 33-46.

Rutgers van der Loeff, M.M. & Van Bennekom, A.J. (1989): Weddell Sea contributes little to silicate enrichment in Antarctic Bottom Water.- Deep-Sea Res. 36: 1341-1357.

Sarnthein, M., Jansen, E., Weinelt, M., Arnold, M., Duplessy, J.-C., Erlenkeuser, H., Flatøy, A., Johannessen, G., Johannessen, T., Jung, S., Koç, N., Labeyrie, L., Maslin, M., Pflaumann, U. & Schultz, H. (1995): Variations in Atlantic surface ocean paleoceanography, 50°-80° N: a time-slice record of the last 30,000 years.- Paleoceanography 10(6): 1063-1094.

Sarnthein, M., van Kreveld, S.A, Erlenkeuser, H., Grootes, P.M., Kucera, M., Pflaumann, U. & Schulz, M. (2003): Centennial-to-millennial-scale periodicities of Holocene climate and sediment injections off western Barents shelf, 75° N.- Boreas 32(3): 447-461, doi: 10.1111/j.1502-3885.2003.tb01227.x

Schauer, U., Fahrbach, E., Osterhus, S. & Rohardt G. (2004): Arctic warming through the Fram Strait: Oceanic heat transport from 3 years of measurements.- J. Geophys. Res. 109: C06026, doi: 10.1029/2003JC001823.

Schauer, U., Loeng, H., Rudels, B., Ozhigin, V. & Dieck, W. (2002): Atlantic water flow through the Barents and Kara Seas.- Deep-Sea Res. I 49(12): 2281-2298.

Scott, D.B., Mudie, P.J., Baki, V., MacKinnon, K.D. & Cole, F.E. (1989): Biostratigraphy and late Cenozoic paleoceanography of the Arctic Ocean: foraminiferal, lithostratigraphic, and isotopic evidence.- Geol. Soc. Amer. Bull. 101: 260-277.

Siegert, M.J. & Dowdeswell, J.A. (2004): Numerical reconstructions of the Eurasian Ice Sheet and climate during the Late Weichselian.- Quat. Sci. Rev. 23: 1273-1283.

Skirbekk, K., Klitgaard-Kristensen, D., Rasmussen, T.L., Koç, N. & Forwick, M. (2010): Holocene climate variations at the entrance to a warm Arctic fjord: evidence from Kongsfjorden trough, Svalbard.- In: J.A. HOWE, W.E.N. AUSTIN, M. FORWICK & M. PAETZEL (eds), Fjords Systems and Archives, Geol. Soc. Spec. Publ., London 344: 289-304.

Ślubowska, M.A., Koç, N., Rasmussen, T.L. & Klitgaard Kristensen, D. (2005): Changes in the flow of Atlantic water into the Arctic Ocean since the last deglaciation: evidence from the northern Svalbard continental margin, 80° N.- Paleoceanography 20: 1-15, doi: 10.1029/2005PA001141.

Ślubowska-Woldengen, M., Koç, N., Rasmussen, T.L., Klitgaard-Kristensen, D., Hald, M. & Jennings, A.E. (2008): Time-slice reconstructions of ocean circulation changes on the continental shelf in the Nordic and Barents Seas during the last 16,000 cal yr B.P.- Quat. Sci. Rev. 27: 1476-1492.

Ślubowska-Woldengen, M., Rasmussen, T.L., Koç, N., Klitgaard-Kristensen, D., Nilsen, F. & Solheim A. (2007): Advection of Atlantic Water to the western and northern Svalbard shelf since 17,500 cal yr BP.- Quat. Sci. Rev. 26: 463-478.

Spiegler, D. (1996): Planktonic foraminifer Cenozoic biostratigraphy of the Arctic Ocean, Fram Strait (Sites 908-909), Yermak Plateau (Sites 910-912), and East Greenland Margin (Site 913).- In: J. THIEDE, A.M. MYHRE, J.V. FIRTH, G.L. JOHNSON & W.F. RUDDIMAN (eds), Proc. Ocean Drilling Program, Sci. Results 151: 153-167.

Spielhagen, R.F., Baumann, K.-H., Erlenkeuser, H., Nowaczyk, N.R., Nørgaard-Pedersen, N., Vogt, C. & Weiel, D. (2004): Arctic Ocean deep-sea record of Northern Eurasian ice sheet history.- Quat. Sci. Rev. 23(11-13): 1455-1483.

Spielhagen, R.F., Bonani, G., Eisenhauer, A., Frank, M., Frederichs, T., Kassens, H., Kubik, P.W., Nørgaard-Pedersen, N., Nowaczyk, N.R., Mangini, A., Schäper, S., Stein, R., Thiede, J., Tiedemann, R. & Wahsner, M. (1997): Arctic Ocean evidence for Late Quaternary initiation of northern Eurasian ice sheets.- Geology 25(9): 783-786.

Spielhagen, R.F. & Erlenkeuser, H. (1994): Stable oxygen and carbon isotopes in planktic foraminifers from Arctic Ocean surface sediments: reflection of the low salinity surface water layer.- Mar. Geol. 119: 227-250.

Spielhagen, R.F., Werner, K., Sørensen, S.A., Zamelczyk, K., Kandiano, E., Budeus, G., Husum, K., Marchitto, T.M. & Hald, M. (2011): Enhanced modern heat transfer to the Arctic by warm Atlantic Water.- Science 331: 450-453. doi: 10.1126/science.1197397.

Stein, R. & Fahl, K. (2000): Holocene accumulation of organic carbon at the Laptev Sea continental margin (Arctic Ocean): sources, pathways, and sinks.- Geo-Mar. Lett. 20: 27-36.

Stein, R., Nam, S.-I., Schubert, C., Vogt, C., Fütterer, D. & Heinemeier, J. (1994a): The last deglaciation event in the eastern central Arctic Ocean.- Science 264: 692-696.

Stein, R., Schubert, C., Vogt, C. & Fütterer, D. (1994b): Stable isotope stratigraphy, sedimentation rates and paleosalinity in the latest Pleistocene to Holocene central Arctic Ocean.- Mar. Geol. 119: 333-355.

Taldenkova, E., Bauch, H.A., Gottschalk, J., Nikolaev, S., Rostovtseva, Y., Pogodina, I., Ovsepyan, Y. & Kandiano, E. (2010): History of ice-rafting and water mass evolution at the northern Siberian Continental Margin (Laptev Sea) during Late Glacial and Holocene times.- Quat. Sci. Rev. 29(27-28): 3919-3935, doi: 10.10116/j.quascirev.2010.09.013.

Taldenkova, E., Bauch, H.A., Stepanova, A., Strezh, A., Dem'yankov, S. & Ovsepyan, Ya. (2008): Postglacial to Holocene benthic assemblages from the Laptev Sea: paleoenvironmental implications.- Quat. Int. 183: 40-60.

Vogt, C., Knies, J., Spielhagen, R.F. & Stein, R. (2001): Detailed mineralogical evidence for two nearly identical glacial/deglacial cycles and Atlantic water advection to the Arctic Ocean during the last 90,000 years.- Global Planet. Change 31: 23-44.

Werner, K., Spielhagen, R.F., Bauch, D., Hass, H.C., Kandiano, E. & Zamelczyk, K. (2011): Atlantic Water advection to the eastern Fram Strait – multiproxy evidence for late Holocene variability.- Palaeogeogr. Palaeoclimatol. Palaeoecol. 308: 264-276. doi: 10.1016/j.palaeo.2011.05.030.

Winsborrow, M.C.M., Andreassen, K., Corner, G.D. & Laberg, J.S. (2010): Deglaciation of a marine-based ice sheet: Late Weichselian Palaeo-ice dynamics and retreat in the southern Barents Sea reconstructed from onshore and offshore glacial geomorphology.- Quat. Sci. Rev. 29: 424-442.

Woodgate, R.A., Aagaard, K., Muench, R.D, Gunn, J., Björk, G., Rudels, B., Roach, A.T. & Schauer U. (2001): The Arctic Ocean boundary current along the Eurasian slope and the adjacent Lomonosov Ridge: Water mass properties, transports and transformations from moored instruments.- Deep-Sea Res. 148: 1757-1792.

Zahn, R., Markussen, B. & Thiede, J. (1985): Stable isotope data and depositional environment in late Quaternary Arctic Ocean.- Nature 314: 433-435.

Proxy Reconstruction of Cenozoic Arctic Ocean Sea-Ice History – from IRD to IP$_{25}$ –[*]

by Ruediger Stein[1], Kirsten Fahl[1] and Juliane Müller[1]

Abstract: This review paper focusses on reconstructions of the long- and short-term history of past Arctic Ocean sea-ice cover. Based on commonly used sedimentological, geochemical and micropaleontological proxies (ice-rafted debris (IRD), mineralogical composition of terrigenous sediment fraction, and abundances of specific diatoms and foraminifers), three examples of reconstructions of glacial history, sea-ice cover and surface-water characteristics are presented and discussed: (1) the onset Arctic Ocean sea-ice cover near 47 Ma and its long-term variability through Cenozoic times; (2) the Quaternary glacial/interglacial variability in Arctic Ocean ice-rafting and its relationship to sea-ice and ice-sheet history; and (3) Last Glacial Maximum (LGM), Deglacial to Holocene changes in Arctic Ocean sea-ice cover and ice-sheet decay.

In the second part of this paper we concentrate on Arctic Ocean sea-ice reconstructions, using a recently developed biomarker approach that is based on the determination of sea-ice diatom-specific highly-branched isoprenoids with 25 carbon atoms (IP$_{25}$) and IP$_{25}$ in combination with phytoplankton biomarkers (PIP$_{25}$). The diene/ IP$_{25}$ ratio might give additional information about sea-surface temperature (SST) in the low temperature Arctic environment. The high potential of these novel biomarker proxies to improve reconstructions of paleo-sea-ice cover and its variability through time is demonstrated in three examples: (a) the sea-ice variability in Fram Strait over the last 30 ka, (b) the deglacial/Holocene variability of central Arctic sea-ice cover with special emphasis on the Younger Dryas Cooling Event, and (c) a comparison of historical sea-ice observations off northern Iceland over the last millennium and a corresponding high-resolution IP$_{25}$ record.

In a pilot study carried out in a sediment core from the Barents Sea continental slope we were able to prove for the first time that IP$_{25}$ is even preserved in Arctic Ocean sediments as old as 130 to 150 ka (MIS 6), i.e., IP$_{25}$ can be used for reconstruction of sea-ice variability during older glacial/interglacial intervals (MIS 6/MIS 5).

In order to establish the IP$_{25}$ approach as a key proxy for reconstruction of past Arctic Ocean sea-ice conditions, more basic information about production, degradation and preservation/burial of the IP$_{25}$ signal is still needed. Furthermore, the hypothesis that the diene/IP$_{25}$ ratio might be used as reliable proxy for SST reconstructions in the low temperature Arctic environments has to be verified by a ground-truth study including the IP$_{25}$ and diene data as well as independent SST proxies like alkenone-derived SST. All these data should be obtained in future investigations of sea-ice, water column, and sediment-trap samples as well as surface sediments and sediment cores with large spatial coverage from different environments of the entire Arctic Ocean.

Zusammenfassung: Meereis ist ein wichtiges Charakteristikum des Arktischen Ozeans und von großer Bedeutung für das globale Klimasystem. Um die Veränderungen der Meereisdecke in jüngster Vergangenheit besser verstehen zu können, ist die Untersuchung der Meerausdehnung in der geologischen Vergangenheit und seiner zeitlichen Variabilität mittels meeresgeologischer Stellvertreterdaten (Proxys) von großem Nutzen. In drei Beispielen werden im ersten Teil Rekonstruktionen der Meereisverteilung und deren zeitliche Änderungen (1) im Verlauf des Känozoikums, (2) im Spätquartär und (3) für den Zeitabschnitt vom Letzten Glazialen Maximum bis heute vorgestellt, die auf der Anwendung herkömmlicher sedimentologischer und mineralogischer Proxys basiert. Hierbei ist insbesondere der Gehalt an eistransportierter Grobfraktion – "ice-rafted debris" oder "IRD" – als Basisparameter hervorzuheben. Im zweiten Teil dieser Arbeit werden neue Biomarkerproxys für Meereis (IP$_{25}$ und PIP$_{25}$) und Temperatur des Oberflächenwassers (Dien/IP$_{25}$-Verhältnis) in drei Beispielen diskutiert: (a) die Meereisverteilung und Meerreisvariabilität in der Framstraße während der letzten 30 ka; (b) die postglaziale Meereisva- riabilität im zentralen Arktischen Ozean vom Bølling-Allerød über Jüngere Dryas bis Heute und (c) ein Vergleich der Meereisbeobachtungen für den historischen Zeitabschnitt 800–1950.

In einer Pilotstudie wird erstmals IP$_{25}$ in arktischen Sedimenten mit einem Alter >30 ka (MIS 6–MIS 1 oder 150–0 ka) nachgewiesen. Um diese neuen Biomarkerproxys als verlässliche Parameter für die quantitative Rekonstruktion von Meereisverbreitung (und Oberflächenwassertemperatur) im Arktischen Ozean zu etablieren, müssen weitere grundlegende Datensätze mit großer räumlicher Verteilung und unter Einbezug von Untersuchungen an Meereisproben, Sedimentfallen, Oberflächensedimenten und Sedimentkernen gewonnen werden.

INTRODUCTION AND BACKGROUND

One of the most important characteristics of the modern Arctic Ocean is the sea-ice cover with its strong seasonal variability in the marginal (shelf) seas (Fig. 1). Satellite data have shown that the area of sea ice decreases from roughly 14–15 million km^2 in March to 6–7 million km^2 in September, as much of the first-year ice melts during the summer (GLOERSEN et al. 1992, CAVALIERI et al. 1997, JOHANNESSEN et al. 2004). The area of multi-year sea ice, mostly over the Arctic Ocean basins and the Canadian polar shelf, is about 4 to 5 million km^2 (e.g., JOHANNESSEN et al. 1999, NGHIEM et al. 2007). In the geological past, changes in sea-ice cover may have been even more extreme ranging from totally ice-free to permanently ice-covered conditions. These variations occurred on very long time scales (e.g., the Paleogene Greenhouse/Icehouse transition) as well as glacial/interglacial and shorter time scales, and were often coinciding with the waxing and waning of circum-Arctic ice sheets (Fig. 1, e.g., SVENDSEN et al. 2004, for reviews see STEIN 2008, POLYAK et al. 2010).

Sea ice, the main focus of this paper, has a large influence on the environment of the Arctic Ocean itself, the Earth system on a global scale, and climate change. Sea-ice formation is strongly controlled by freshwater supply. Freshwater is essential for the maintainance of the low-salinity layer of the central Arctic Ocean and, thus, contributes significantly to the strong stratification of the near-surface water masses, encouraging sea-ice formation (e.g., AAGAARD & CARMACK 1989, MACDONALD et al. 2004). Changes in the freshwater balance would influence the extent of sea-ice cover. The melting and freezing of sea ice results in distinct changes in the surface albedo, the energy balance, and the temperature and salinity structure of the upper water masses. The albedo of open water is as low as 0.10, whereas the sea-ice albedo ranges between 0.6 and 0.8 (Fig. 2, BARRY 1996). Therefore, up to eight times as much of the incoming shortwave radiation is reflected from the ice surfaces as compared to open water, resulting in lower surface temperatures. Furthermore, the sea-ice cover strongly affects the biological productivity, as a more closed sea-ice cover restricts primary production due to low light influx in
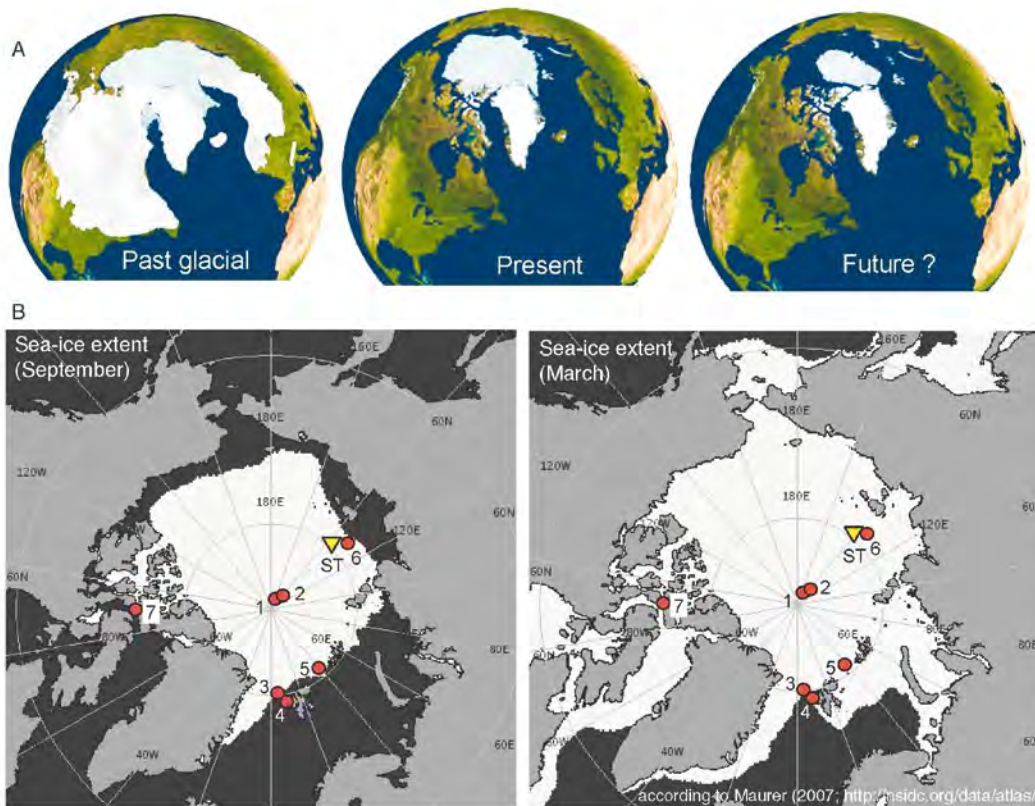
Fig. 1: (A): Distribution of Northern Hemisphere ice sheets and sea ice during past glacials (left), Present (middle) and a possible scenario of the future (right); (Courtesy Martin Jakobsson, Stockholm University, 2012). (B): Maps showing the average distribution of sea ice in the Arctic Ocean in September 1979–2004 (left) and March 1979–2005 (right). Numbers and letters indicate site locations of sediment traps and sediment cores presented and discussed in the text: ST = sediment trap LOMO-2; 1 = IODP-ACEX drill site; 2 = core PS2185: 3 = PS2837-2; 4 = MSM5/5-723-2; 5 = PS2138-1; 6 = PS2458-4; 7 = core ARC-3.

Abb. 1: (A): Verteilung von Meereis und Eisschilden während quartärer Eiszeiten (links), heute (Mitte) und mögliches Szenario in der Zukunft (rechts). (B links): Mittlere minimaler Meereisausbreitung im Spätsommer (September 1979–2004); (B rechts): mittlere maximale Meereisverbreitung im Spätwinter (März) der Jahre 1979–2005. ST und Ziffern 1 bis 6 = im Text diskutierte Lokationen.

the surface waters (Fig. 2). Owing to its light limitation and sea-ice cover, the central Arctic Ocean is the least productive region of the world's oceans, whereas in the marginal ice zone high primary productivity may be reached (SAKSHAUG 2004, WASSMANN et al. 2004, WASSMANN 2011).

Freshwater and sea ice are exported from the Arctic Ocean through the Fram Strait into the North Atlantic. The interplay of the cold Arctic freshwater-rich surface-water layer and its ice cover with the relatively warm and saline Atlantic water is important for the renewal of deep waters driving the global thermohaline circulation (THC) (e.g., BROECKER 1997, 2006, CLARK et al. 2002). Because factors such as the global THC, sea-ice cover and Earth's albedo have a strong influence on the earth's climate system, climate change in the Arctic could cause major pertubations to the global environment.

Over the last decades, the extent and thickness of Arctic sea ice has changed dramatically (Fig. 3) (e.g., JOHANNESSEN et al. 2004, ACIA 2004, 2005, FRANCIS et al. 2005, SERREZE et al. 2007, STROEVE et al. 2007). According to STROEVE et al. (2007), the reduction in the extent of Arctic sea ice observed from 1953 to 2006 is -7.8 ±0.6 % per decade, three times larger than the multi-model mean trend of -2.5 ±0.2 % per decade. For the shorter, yet more reliable period of observations based on modern satellite records (1979–2006), both the observed (-9.1 ±1.5 % per decade) and multi-model mean trend (-4.3

±0.3 % per decade) are larger. The reduction of future sea-ice, however, may be even more rapid. A record-low in minimum sea-ice cover was observed in September 2007, which is about 40 % less than that of 1979, the start of sea-ice observation by satellites (Fig. 3, KERR 2007). Such a minimum was forcasted by modelling to occur in the middle of this century (Fig. 3, JOHANNESSEN et al. 2004, STROEVE et al. 2007).

Observed changes not only included a reduction in total area covered by sea ice (MASLANIK et al. 1996, JOHANNESSEN et al. 1999, 2004, PARKINSON et al. 1999 VINNIKOV et al. 1999, LEVI 2000), but also an increase in the length of the ice melt season (SMITH 1998, STABENO & OVERLAND 2001, RIGOR et al. 2002), a loss of multiyear ice (NGHIEM et al. 2007) and a general decrease in the thickness of ice over the central Arctic Ocean (ROTHROCK et al. 1999, KWOK & ROTHROCK 2009).

Although there is a general consensus that polar regions – and especially the Arctic Ocean and surrounding areas – are (in real time) and were (over historic and geologic time scales) subject to rapid and dramatic change, the causes of the recent changes are a subject of intense scientific and environmental debate. As outlined by JOHANNSSEN et al. (2004), it remains open to debate whether the warming in recent decades is an enhanced greenhouse-warming signal or (at least partly) natural decadal and multidecadal climate variability (POLYAKOV & JOHNSON 2000, POLYAKOV et al. 2002). Here, high-resolution paleo-
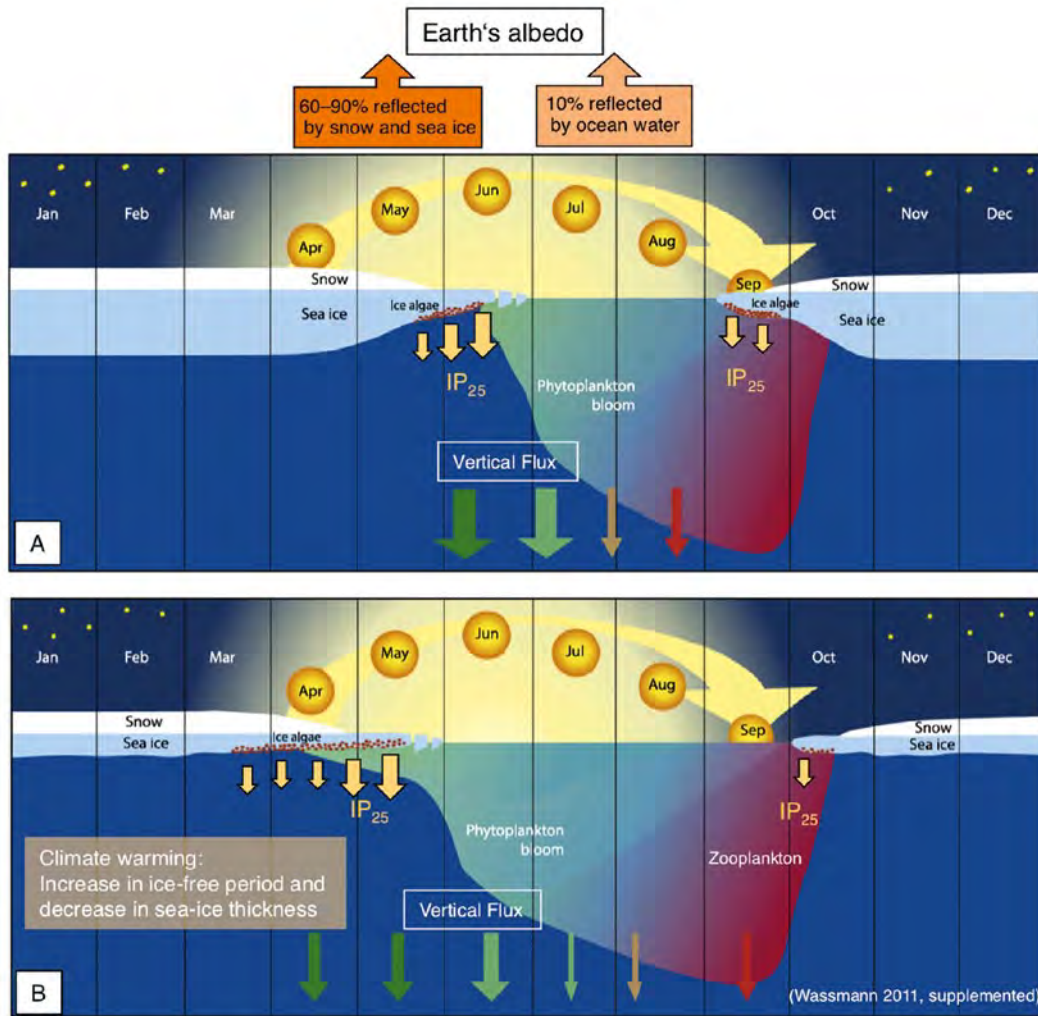
Fig. 2: (A) Schematic illustration of principal processes controlling productivity and carbon flux in the seasonal ice zone. The dark period, height of the sun and changing thickness of snow and ice over the year as well as phytoplankton, zooplankton, and sea-ice algae productivity are indicated. Arrows indicate the changing dominance of autotrophic (green) and heterotrophic (red) processes in the euphotic zone. Flux of sea-ice algae and IP_{25} are indicated by yellow arrows. In addition, Earth's albedo values for snow and sea-ice as well as open ocean conditions are shown (BARRY 1996). (B) Climate warming may result in an increase of the ice-free period and a decrease in sea-ice thickness. Sea-ice algae can start to grow already from mid March, provided that snow cover is not too thick.

Abb. 2: (A) Schematische Darstellung der grundlegenden Prozesse, welche Produktion und Flux von Phytoplankton, Zooplankton und Eisalgen mit Eisalgenproxy "IP_{25}" im jahreszeitlichen Gang von Licht und Meereis beeinflussen. Zusätzlich sind Albedo-Werte für Schnee und Eis gegenüber denen von eisfreier Ozeanoberfläche angegeben (BARRY 1996). (B) Zeigt mögliche Auswirkungen und Veränderungen einer Klimaerwärmung mit verminderter Eisausdehnung und Eisdicke.

climatic records going back beyond the timescale of direct measurements can help reduce some of the uncertainties in the debate of recent climate change. In this context, however, not only high-resolution studies of the most recent (Holocene) climate history are of importance, but also detailed studies of the earlier Earth history characterized by a much warmer (Greenhouse-type) global climate.

The instrumental records of temperature, salinity, precipitation and other environmental observations span only a very short interval (<150 years) of Earth's climate history and provide an inadequate perspective of natural climate variability, as they are biased by an unknown amplitude of anthropogenic forcing. Generally, paleoclimate records document the natural climate, rates of change and variability prior to anthropogenic influence. Paleoclimate reconstructions can be used to assess the sensitivity of the Earth's climate system to changes of different forcing parameters (e.g. CO_2) and to test the reliability of climate models by evaluating their performance under condi-

tions very different from the modern climate. Precise knowledge of past rates and scales of climate change are the only means to separate natural and anthropogenic forcings and will enable us to further increase the reliability of prediction of future climate change. Thus, understanding the mechanisms of natural climate change is one of the major challenges for mankind in the coming years. In this context, the polar regions certainly play a key role, and detailed climate records from the Arctic Ocean spanning time intervals from the Paleogene Greenhouse world to the Neogene-Quaternary Icehouse world (Fig. 4) will give new insight into the functioning of the Arctic Ocean within the global climate system. Here, especially the synchronous versus asynchronous histories of ice-sheet and sea-ice development in the north- and southpolar regions are of special interest.

This paper deals with proxy reconstructions of the long- and short-term history of past circum-Arctic ice sheets and sea-ice cover – with a focus on the latter. Starting with examples of
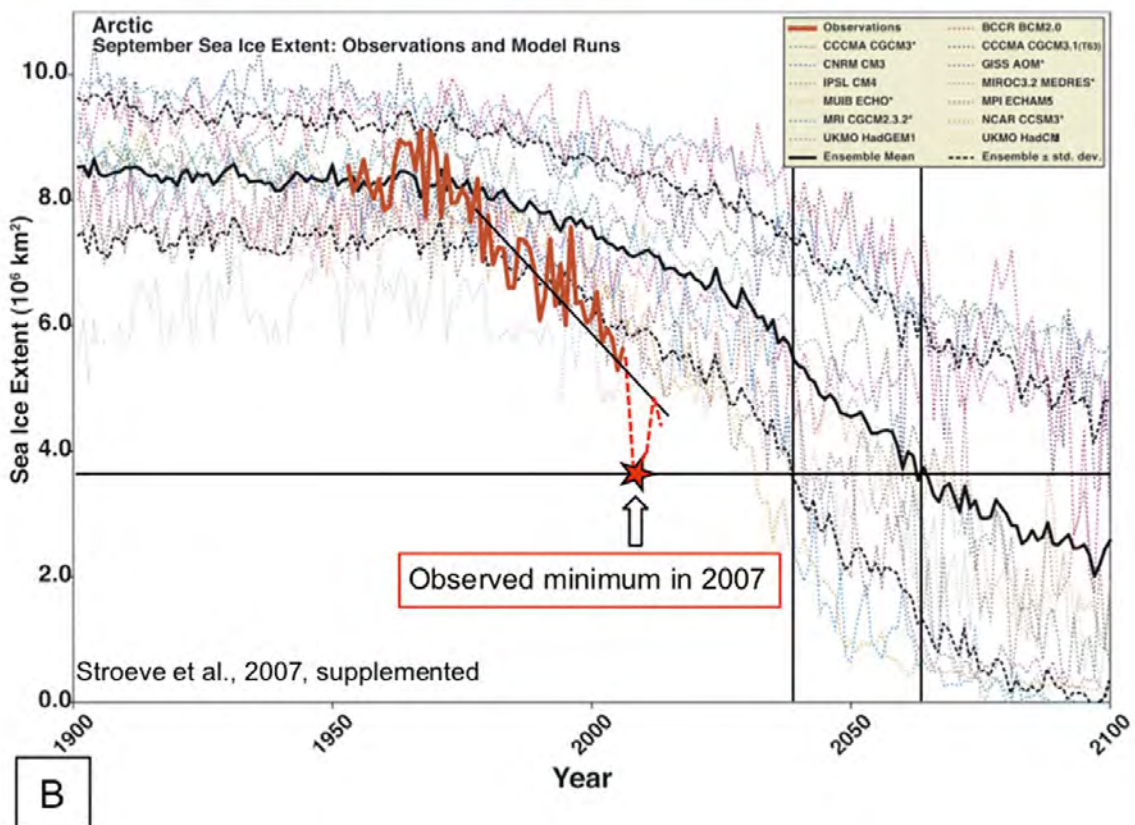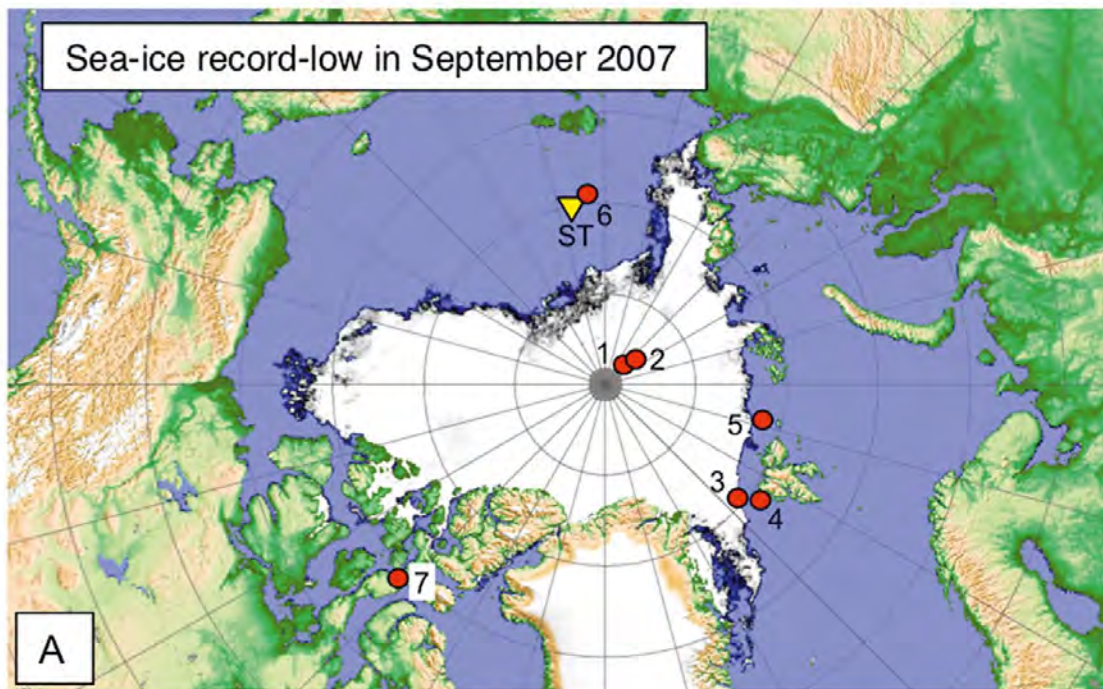
Fig. 3: (A): Distribution of sea-ice cover in the Arctic Ocean on September 12, 2007 (<http://iup.physik. uni-bremen.de:8084/amsr/amsre.html>) and site locations discussed in the text: ST = Sediment trap LOMO-2; sediment cores: 1 = IODP-ACEX drill site; 2 = core PS2185-6; 3 = core PS2837-2; 4 = core MSM5/5-723-2; 5 = core PS2138-1; 6 = core PS2458-4; 7 = core ARC-3. (B) Arctic September sea-ice extent (x10⁶ km²) from observations (thick red line) and 13 IPCC AR4 climate models together with the multi-model ensemble mean (solid black line) and standard deviation (dotted black lines). The absolute minimum of 2007 is highlighted by asterisk.

Abb. 3: (A): Meereisverbreitung im Arktischen Ozean im September 2007 (<http://iup. physik.uni-bremen.de:8084/amsr/amsre.html>) und Lokationen der im Text diskutierten Sedimentfallen und Sedimentkerne: ST = Sedimentfalle LOMO-2. Sedimentkerne: 1 = IODP-ACEX Bohrlokation, 2 = PS2185-6, 3 = PS2837-2, 4 = MSM5/5-723-2, 5 = PS2138-1, 6 = PS2458-4, 7 = ARC-3. (B) Meereisausdehnung im Arktischen Ozean für September (10⁶ km²) für die Zeit 1900 bis 2100, d.h. Beobachtungen und Messwerte (Kurve rot), Mittelwert der Ergebnisse unterschiedlicher Klimamodelle (Kurve fett schwarz) mit Standardabweichung (punktierte schwarze Kurven).

Fig. 4: Smoothed global benthic foraminifer δ¹⁸O time series showing the long-term cooling and the Greenhouse/Icehouse transition through Cenozoic times. The occurrence of Cenozoic ice sheets on the Northern and Southern Hemisphere and Arctic sea-ice are shown. The hiatus in the ACEX record is indicated by a red bar as based on the age model by BACKMAN et al. 2008 (for alternate age model see Fig. 5); periods with anoxic water mass conditions are highlighted by grey bars (STEIN et al. 2006).

Abb. 4: Globale δ¹⁸O-Kurve von benthischen Foraminiferen, welche die langzeitliche Abkühlung und den Wechsel von Treibhaus- zu Eishausbedingungen im Verlauf des Känozoikums anzeigen. Die Ausbreitung von Eisschilden auf der Nord- und Südhemisphäre sowie das Vorkommen von Meereis und anoxischen Bedingungen im Arktischen Ozean sind markiert.
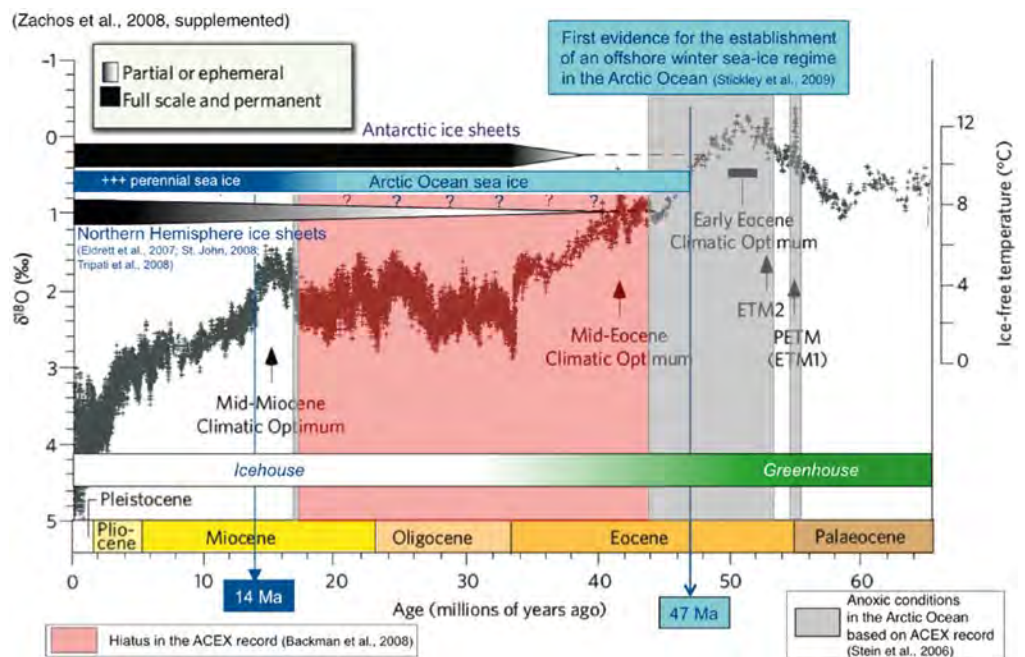
paleoenvironmental reconstructions based on more commonly used sedimentological, micropaleontological and geochemical proxies, the second part of the paper highlights recently developed novel biomarker proxies indicative for modern and past changes in sea-ice cover. These new proxies may allow a more quantitative reconstruction of sea-ice cover and potentially may provide some information about past sea-ice thicknesses.

LONG- AND SHORT-TERM CHANGES IN SEA-ICE COVER: RECONSTRUCTIONS FROM COMMON GEO-PROXIES

Sediment-laden or "dirty" sea ice is a common phenomenon in the Arctic Ocean and its marginal seas and an important transport agent for terrigenous sediments (e.g., PFIRMAN et al. 1989, REIMNITZ et al. 1993b, NÜRNBERG et al. 1994, EICKEN et al. 1997, 2005, DETHLEFF et al. 2000). In areas of sea-ice melting, sediment particles are released and deposited at the sea floor, contributing significantly to the present and past Arctic Ocean sedimentary budget. This sea-ice sediment – or "ice-rafted debris (IRD)" – mainly consists of terrigenous material with clay minerals, quartz, and feldspars as the main components (NÜRNBERG et al. 1994). The mineralogy of sea-ice sediments may be very variable in time and space. Thus, studies of the mineralogical composition may allow the identification of source areas for sea-ice transported sediments and, based on these data, the reconstruction of past and present transport pathways (e.g. NÜRNBERG et al. 1994, WAHSNER et al. 1999, DARBY 2003, STEIN 2008 for review). IRD however, can also be transported by icebergs. If IRD is related to iceberg transport and not sea ice, the IRD proxy record records the existence of extended continental ice sheets reaching the shelf-break. Therefore, a method of distinguishing between sea-ice and iceberg transport is required for paleoenvironmental reconstructions based on the analysis of IRD.

A first-order proxy to discriminate between sea-ice and iceberg-rafted deep-sea sediments is the grain-size distribution. It is generally accepted that very coarse-grained material >250 µm (coarse-sand-, very-coarse-sand, gravel- and pebble-sized particles), are mainly restricted to iceberg transport whereas the dominance of finer-grained (silt and clay sized) sediments are more typical for sea-ice transport (e.g., CLARK & HANSEN 1983, NØRGAARD-PEDERSEN et al. 1998, SPIELHAGEN et al. 2004, DETHLEFF 2005). Grain-size distribution by itself, however, has to be interpreted with caution as other processes (e.g., ocean currents) may overprint the ice-rafted distribution (MANIGHETTI & MCCAVE 1995, HASS 2002).

A large number of studies on the paleodistribution of sea ice are commonly based on sedimentological, mineralogical, and geochemical data (e.g., SPIELHAGEN et al. 1997, 2004, KNIES et al. 2001, DARBY 2003, NØRGAARD-PEDERSEN et al. 2003, POLYAK et al. 2010) and microfossils such as diatoms, dinoflagellates, ostracods, and foraminifers (e.g., CARSTENS & WEFER 1992, KOC et al. 1993, MATTHIESSEN et al. 2001, CRONIN et al. 2010, for most recent review see POLYAK et al. 2010). In particular, sea-ice associated organisms like pennate ice diatoms, are frequently used for reconstructing present and past sea-ice conditions (e.g., KOC et al. 1993, STICKLEY et al. 2009). However, it has also been shown that the preservation of fragile siliceous diatom frustules can be relatively poor in surface sediments from the Arctic realm and the same is also true (if not worse) for calcareous-walled microfossils, thus limiting their applicability (STEINSUND & HALD 1994, SCHLÜTER & SAUTER 2000, MATTHIESSEN et al. 2001). In contrast, radiolarians might be better preserved than diatoms but few data have been published yet (e.g., KRUGLIKOVA et al. 2009). A multi-proxy approach, considering sediment texture in combination with lithology and sediment provenance as well as micropaleontological and geochemical data indicative for surface-water characteristics certainly provides a much sounder interpretation of sea-ice versus iceberg rafting and reconstruction of past sea-ice conditions.

As complimentary approach to reconstructions from marine sediment cores, past sea-ice conditions may also be inferred

41

from driftwood found on Arctic beaches (e.g., DYKE et al. 1997, BENNIKE 2004, ENGLAND et al. 2008, FUNDER et al. 2009). This approach is based on the assumptions that (1) ice is essential for long-distance transport of the wood, which otherwise becomes water-logged and sinks after about a year, and (2) ice-free coastal areas exist to allow the driftwood to strand. JAKOBSSON et al. (2010) have summarized results from different approaches (including results from marine sediment core as well as driftwood studies) to provide a more holistic picture of past Arctic sea-ice conditions during the last about 15 Cal. kyrs. BP (see Fig. 21 and discussion below).

In the following, three example reconstructions of the glacial history, sea-ice cover and surface-water characteristics are presented using common sedimentological, mineralogical, geochemical and micropaleontological proxies. These are:
• Onset and long-term variability of Cenozoic Arctic Ocean ice-rafting: sea-ice versus iceberg transport
• Quaternary glacial / interglacial variability in Arctic Ocean ice-rafting
• LGM, deglacial to Holocene changes in Arctic Ocean sea-ice cover and ice-sheet decay.

Onset and long-term variability of Cenozoic Arctic Ocean ice-rafting: sea-ice versus iceberg transport

During the Arctic Coring Expedition "ACEX" (IODP Expedition 302), the first scientific drilling was carried out successfully in the permanently ice-covered central Arctic Ocean. During ACEX, 428 m of Quaternary, Neogene, Paleogene, and Campanian sediments were penetrated on the crest of Lomonosov Ridge close to the North Pole (Fig. 5, BACKMAN et al. 2006, 2008, MORAN et al. 2006). Numerous outstanding results dealing with the Arctic Ocean climate history came out of studies of ACEX material (BACKMAN & MORAN 2008). Unfortunatey, the ACEX record contains a large hiatus, probably spanning the time interval from late Eocene to middle Miocene (Fig. 5, BACKMAN et al. 2008, O'REGAN 2011). This is a critical time interval, as it spans the time when prominent changes in global climate took place during the transition from the early Cenozoic Greenhouse world to the late Cenozoic Icehouse world (FIG. 4; ZACHOS et al. 2008).

Throughout the upper about 195 m of Miocene-Pleistocene siliclastic silty clays of the ACEX sequence, isolated pebbles and granules interpreted as IRD or "dropstones", were found together with sand lenses, but unexpectedly also in ~50 m of the underlying middle Eocene biosiliceous silty clays and oozes (Fig. 6, BACKMAN et al. 2006). The deepest dropstone, a gneiss of 1 cm in diameter, was found at about 240 m composite depth (mcd). This dropstone was recovered from an undisturbed section of core and was not reworked or moved downward from higher in the sedimentary section. The location of the ACEX site during this time period, although probably in shallow water (~200 m), was distal from the Siberian continental coast and isolated from it by the Gakkel Ridge, suggesting ice transport as the most probable process (MORAN et al. 2006). This dropstone was suggested to represent the onset of Northern Hemisphere glaciation at about 46 million years BP (Ma) (MORAN et al. 2006, using the revised biostratigraphically-derived age model of BACKMAN et al. 2008), i.e., sea-ice formation and/or iceberg transport took place ~30 my earlier than previously thought. When using the alternate chronology based on osmium isotopes (POIRIER & HILLAIRE-MARCEL 2011), the age of the occurrence of the first dropstone at 240 mcd would become about three million years younger (~43 Ma, Fig. 5).

Eocene-age dropstones in the ACEX record provided strong direct evidence for the presence of ice, but are stratigraphically discontinuous, and only about 60 granules and pebbles of ~0.2 to 3.0 cm in diameter were visually identified between 0–240 mcd (BACKMAN et al. 2006). In order to get a more continuous record of the ice-rafting history of the central Arctic Ocean, ST. JOHN (2008) studied the terrigenous coarse (IRD) fractions >150 and >250 μm throughout the entire depth interval 0-275 mcd of the ACEX sequence in much more detail (Fig. 6). Along with information on grain size, composition, and mass accumulation rates of IRD, SEM imaging of represen-
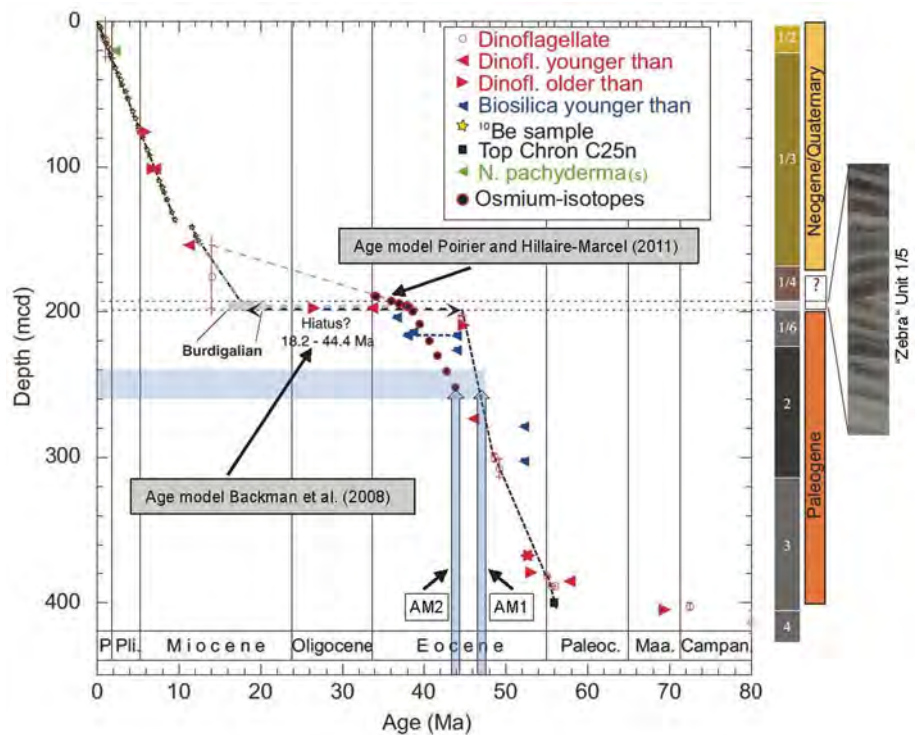
Fig. 5: Age-depth diagram and main lithological units of the ACEX section, based on the biostratigraphic age model AM1 by BACKMAN et al. (2008). Included is chronology AM2 based on osmium isotopes (POIRIER & HILLAIRE-MARCEL 2011). First occurrences of IRD at 240-260 mcd are marked as light blue horizontal bar. Different ages of first occurrence of IRD, obtained by age models AM1 and AM2 are indicated by light blue arrows (from O'REGAN 2011, supplemented).

Abb. 5: Alters-Tiefen-Diagramm AM1 (BACKMAN et al. 2008) und lithologische Einheiten der ACEX-Bohrung. Beigefügt das Altersmodel AM2 nach POIRIER & HILLAIRE-MARCEL (2011). Hellblaue Pfeile = erstes Einsetzen von IRD zwischen 240-260 mcd (ergänzt nach O'REGAN 2011).
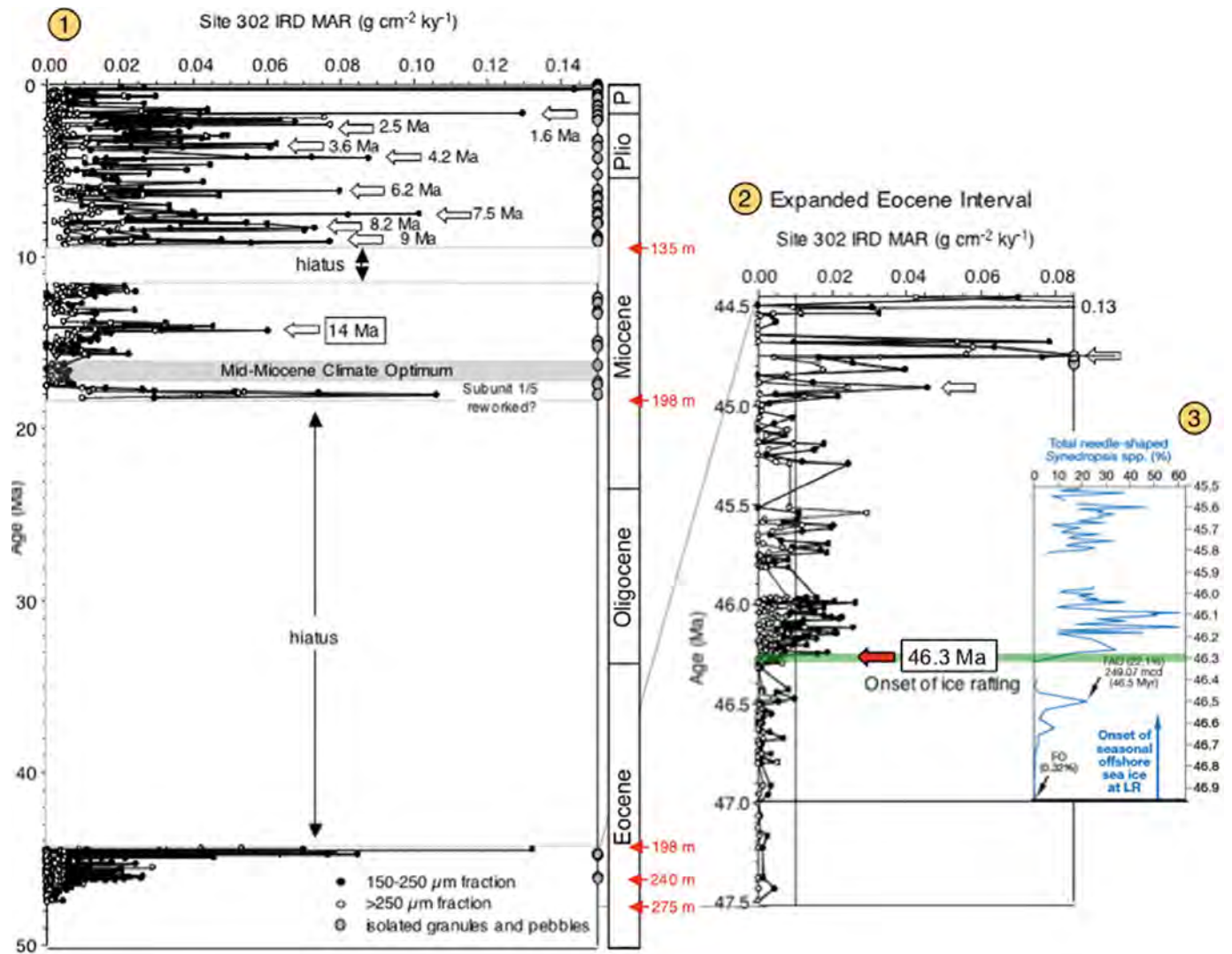
Fig. 6: (1) = IRD mass accumulation rates (g cm⁻² ky⁻¹) in the >250 μm (open circles) and 150-250 μm (solid circles) size fractions of the Eocene to Pleistocene (275 to 0 mcd) section of the IODP-ACEX record (ST. JOHN 2008, supplemented), along with isolated granules and pebbles (large grey circles) (from BACKMAN et al. 2006) *versus* age (Ma). Open arrows indicate major pulses of IRD input. The Mid-Miocene Climate Optimum (e.g., FLOWER & KENNET 1995, ZACHOS et al. 2001) is marked as horizontal grey bar. Red numbers indicate "meters composite depth (mcd)". (2) = blow-up of the middle Eocene interval (44.5-47.5 Ma) of this dataset and (3) = concentrations of needle-shaped sea-ice diatom *Synedropsis* spp. (STICKLEY et al. 2009).

Abb. 6: (1) Akkumulationsraten der terrigenen Grobfraktion >250 μm und 150-250 μm im eozänen-pleistozänen Kernabschnitt (0-275 m bzw. 0-50 Ma) der IODP-ACEX-Bohrung (ST. JOHN 2008). Offene Pfeile heben Maxima mit erhöhtem Eintrag terrigener Grobfraktion = eistransportiertes Material ("ice-rafted debris" = IRD) hervor. Das "Mittel-Miozäne Klimaoptimum" (e.g., FLOWER & KENNETT 1995, ZACHOS et al. 2001) ist als grauer Balken hervorgehoben. Rote Zahlen zeigen Kernteufen an. (2) = Kernabschnitt 47.5-44.5 Ma mit Akkumulationsraten von IRD und (3) = vergrößert dargestellt die Häufigkeit der Meereis-Diatomee *Synedropsis* spp. (nach STICKLEY et al. 2009).

tative quartz grains was used to distinguish between sea-ice and iceberg transport. As outlined by ST. JOHN (2008), surface features of iceberg-transported grains are dominated by those produced by mechanical breakage (e.g., angular edges, high relief, and step-fractures), whereas surface features of sea-ice transported grains show more rounded edges and chemical features, such as silica-dissolution and precipitation (for further information and references see ST. JOHN 2008).

The results from ST. JOHN's (2008) study (Fig. 6) confirm the pebble-based interpretation made by the IODP 302 Scientific Party (BACKMAN et al. 2006, MORAN et al. 2006) that ice initiated in the Arctic in the middle Eocene near 46.3 Ma. At that time, IRD (150-250 μm) percentages and accumulation rates reached values >1 % and 0.02 g cm⁻² ky⁻¹, respectively. Quali-

tatively, the IRD coarse fraction >250 μm mainly composed of quartz, looks very similar in samples from the middle Eocene and from the Pleistocene.

Contemporaneously with the onset of IRD near 46.3 Ma, the abundance of weakly silicified needle-shaped pennate diatoms *Synedropsis* spp. significantly increased, indicating the presence of sea ice and silica-enriched waters (STICKLEY et al. 2009). As the fossil *Synedropsis* spp. found in the ACEX record are uniquely associated with the IRD peaks from the same cores, these authors interpret the IRD being predominantly derived from sea ice (STICKLEY et al. 2009). The first occurrence of these sea-ice related diatoms was at about 47 Ma (or ~43 Ma when using the alternate chronology of POIRIER & HILLAIRE-MARCEL 2011), at times when IRD grains

were found in the ACEX section, albeit in low abundance, suggesting the onset of seasonally paced offshore sea-ice formation at that time (Fig. 6). These sedimentological and micropaleontological data are a strong indication for sea-ice formation in the middle Eocene. Iceberg transport, however, was probably also present in the middle Eocene, as indicated by mechanical surface-texture features on quartz grains from this interval (ST. JOHN 2008).

With the first occurrence of significant amounts of IRD near 46.3 Ma, the alkenone-based sea-surface temperature (SST) estimate in the ACEX record dropped by about 7.5 °C, and temperatures of 10–17 °C were determined for the time interval 46.3–44.8 Ma (WELLER & STEIN 2008). Such SSTs do not seem unrealistic. Assuming that the alkenone SST represents summer SST and considering the strong seasonal temperature variability of >10 °C during the early-middle Eocene (STEIN 2008, WELLER & STEIN 2008), favourable conditions for sea-ice formation may have occurred during wintertime. This could have been a situation similar to that observed in the modern Baltic Sea where summer SSTs of >15 °C and winter SSTs <1 °C with sea-ice formation are typical (WÜST & BROGMUS 1955, KRAUSE 1969).

The records from ACEX (BACKMAN et al. 2006, MORAN et al. 2006, ST. JOHN 2008) as well as similar IRD records from the Greenland Basin ODP Site 913 (ELDRETT et al. 2007, TRIPATI et al. 2008) prove an early onset / intensification of Northern Hemisphere glaciations during Eocene times, as was proposed from changes in oxygen-isotope composition across the Eocene / Oligocene boundary and in late Eocene records from the tropical Pacific and South Atlantic (COXALL et al. 2005, TRIPATI et al. 2005). Furthermore, the increase in IRD in the ACEX and ODP Site 913 records coincided with major decreases in atmospheric CO_2 concentrations (PEARSON & PALMER 2000, PAGANI et al. 2006, LOWENSTEIN & DEMICCO 2006, THOMAS 2008). These data suggest that the Arctic and Antarctic Cenozoic climate evolutions are more closely timed, i.e., the Earth's transition from the "greenhouse" to the "icehouse" world was bipolar (Fig. 4), which points to greater control of global cooling linked to changes in greenhouse gases in contrast to tectonic forcing (MORAN et al. 2006). The decline of atmospheric concentrations of CO_2 in the middle Eocene may have driven both poles across the temperature threshold that enabled the nucleation of glaciers on land and partial freezing of the surface Arctic Ocean, especially during times of low insolation (ST. JOHN 2008).

The ACEX record also provided information about the variability of Northern Hemisphere icesheets and/or sea-ice cover during Neogene times. Between about 17.5 and 16 Ma a distinct minimum in ice-rafting in the central Arctic was found (Fig. 6), which may correspond to the Middle Miocene climate optimum (FLOWER & KENNETT 1995, ZACHOS et al. 2001, MORAN et al. 2006), suggesting minimal ice conditions in the Arctic during this period (ST. JOHN 2008). Between about 15 and 14 Ma, IRD accumulation in the ACEX record distinctly increased, contemporaneously with similar IRD maxima in the Greenland Sea (WOLF-WELLING et al. 1996), the existence of glacially eroded material in sediments recovered at Fram Strait Site 909 (KNIES & GAINA 2008), and the onset of cooling in Baffin Bay (STEIN 1991). This may suggest a shift to larger-scale or permanent sea ice in the Northern Hemisphere high latitudes, which is consis-

tent in timing to the onset of the global mid-Miocene cooling (Fig. 4, ZACHOS et al. 2008), the establishment of more extensive ice sheets in Antarctica and greater Antarctic Bottom Water formation (WRIGHT et al. 1992, FLOWER & KENNETT 1995), and a corresponding eustatic sea-level regression (MILLER et al. 1998). The late Cenozoic maxima in IRD massaccumulation rates found in the ACEX record probably indicate further expansion of sea ice or growth of ice sheets shedding icebergs into the Arctic Ocean (Fig. 6, ST. JOHN 2008), and most of them co-occurred with either initial or intensified ice-rafting events at sub-Arctic sites (WOLF & THIEDE 1991, STEIN 1991, FRONVAL & JANSEN 1996, WOLF-WELLING et al. 1996, THIEDE et al. 1998, 2011, ST. JOHN & KRISSEK 2002). That means ST. JOHN's (2008) data provide a long-term pattern of Arctic ice expansion and decay, on the order of those determined for the sub-Arctic oceans.

A major shift in the composition of heavy minerals in the IRD of the ACEX record is seen at about 13–14 Ma (Fig. 7, KRYLOV et al. 2008). The low-resolution record shows high clinopyroxene (CPx) and low hornblende (Hbl) (amphibole) (high Cpx/Hbl ratios) below 14 Ma, and low clinopyroxene and high hornblende (amphibole) values (low Cpx/Hbl ratios) above 14 Ma. Considering that sea-ice is the main transport agent for the heavy minerals, this points to the western Laptev Sea and Kara Sea as major IRD source prior to about 14 Ma and the eastern Laptev Sea and East Siberian Sea as major IRD source area after 14 Ma, assuming a Transpolar Drift system similar to that of today (KRYLOV et al. 2008). Due to the fact that the distance between the Hornblende (amphibole) source region in the eastern Laptev Sea and East Siberian Sea and the ACEX drill site requires a drift time that exceeds one year when assuming present-day drift trajectories and velocities (Fig. 7), KRYLOV et al. (2008) proposed that the sea-ice transporting this material must have survived a melting season. If this assumption is correct, it may point to the development of a perennial sea-ice cover in the Arctic Ocean at about 13–14 Ma, contemporaneously with the global mid-Miocene cooling (Fig. 4). DARBY (2008) who studied the composition of Fe oxide grains in the ACEX section, came to a similar conclusion that during the last 14 Ma a significant amount of IRD was derived from the northern Canadian islands and Ellesmere Island (Fig. 7), with additional sources in the Eurasian Arctic, and proposed a perennial sea-ice cover since at least about 14 Ma.

The dominance of smectite in the lower part of the ACEX record (Fig. 7) supports the heavy-mineral data, i.e., it indicates a terrigenous sediment input from the western Laptev Sea and Kara Sea. The changes in the clay- and heavy-mineral assemblages, however, do not occur exactly in phase. The decrease in smectite (and increase in illite) already occurred within Unit 1/5, i.e., a few million years earlier (Fig. 7). As outlined by KRYLOV et al. (2008), the reason for this discrepancy could be related to climate-driven changes in weathering conditions in the source regions, that is important for formation of clay in soils, or to different mechanisms of clay- and heavy-minerals transportation.

Concerning the onset of perennial sea-ice cover, there are still some discrepancies that have to be solved. As stated by MATTHIESSEN et al. (2009), a year-round (perennial) sea-ice cover as proposed by DARBY (2008) and KRYLOV et al. (2008) being predominant in the central Arctic Ocean since the
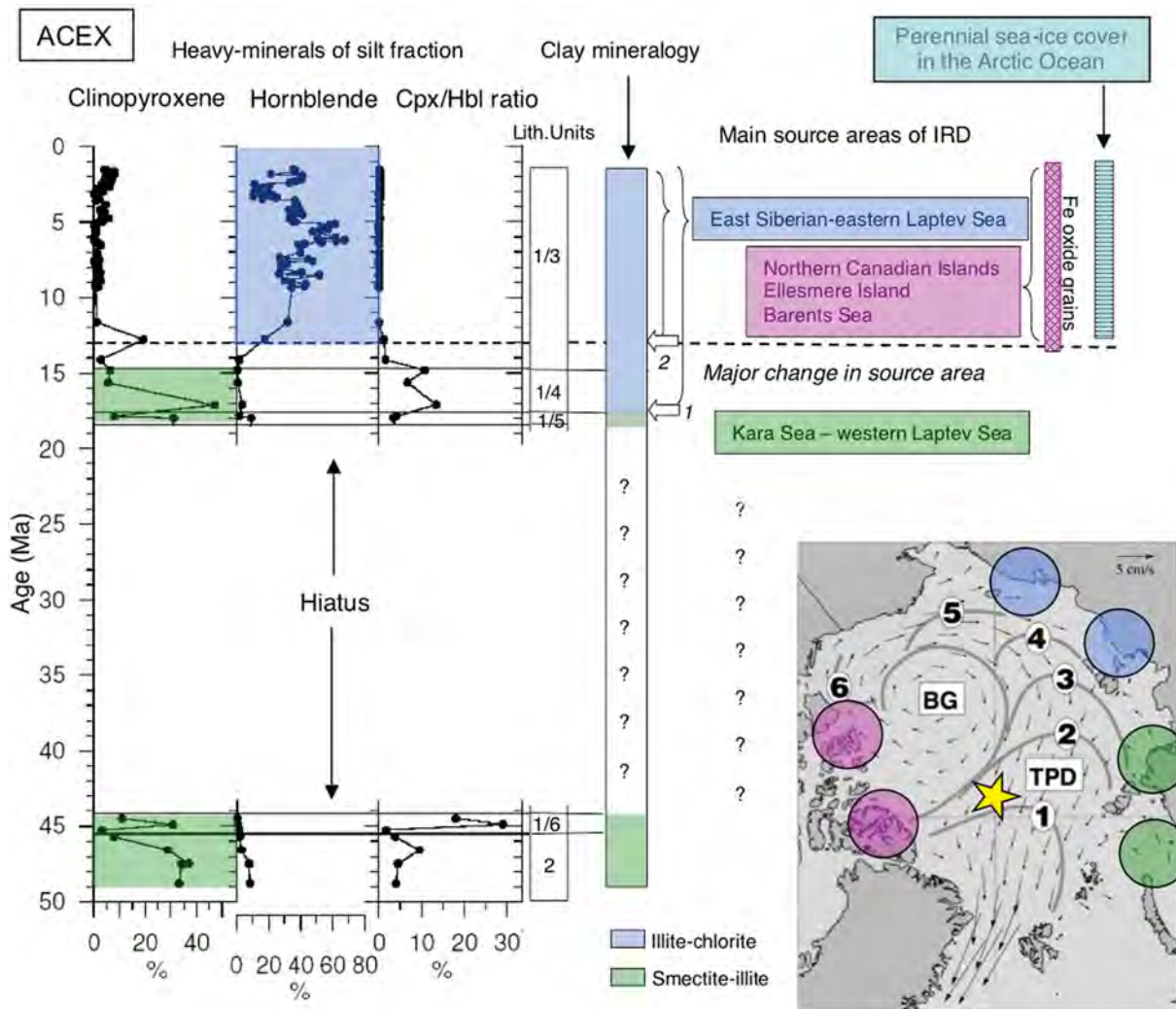
Fig. 7: Percentages of clinopyroxene and hornblende in the heavy mineral silt fraction as well as the clinopyroxene/hornblende (cpx/hbl) ratio, determined in the IODP-ACEX core (KRYLOV et al. 2008), and interpretation in terms of source areas of the terrigenous (IRD) fraction and sea-ice cover. Source-area identification based on Fe-oxide grains (DARBY 2008) and clay-mineral assemblages (KRYLOV et al. 2008) is indicated at right-hand side. Figure from Stein (2008). Inset map (bottom right) shows mean fields of ice drift in the Arctic Ocean derived from buoy drift between 1979 and 1994 (from HOVLAND 2001, supplemented, based on COLONY & THORNDIKE 1985, THORNDIKE 1986, PFIRMAN et al. 1997). Velocities indicated by arrows. Numbered lines indicate the average number of years required for ice in this location to exit the Arctic through the Fram Strait. BG = Beaufort Gyre, TPD = Transpolar Drift. Colour code highlights source areas (pink = Northern Canada, blue = East Siberia/eastern Laptev Sea, green = western Laptev Sea/Kara Sea). Yellow star = location of the ACEX drill site.

Abb. 7: Gehalte an Clinopyroxen und Hornblende in der Schwermineral-Siltfraktion sowie das Clinopyroxen/Hornblende-Verhältnis im eozänen-pleistozänen Kernabschnitt (0-50 Ma) des IODP-ACEX-Kerns (KRYLOV et al. 2008) und Interpretation in Hinblick auf potentielle Liefergebiete der terrigenen (IRD) Sedimentfraktion. Zusätzlich sind Tonmineral- (KRYLOV et al. 2008) und Fe-Oxid-Daten (DARBY 2008) als Anzeiger für Liefergebiete dargestellt. Inset-Karte (unten rechts) zeigt mittlere Driftraten von Meereis im Beaufort-Wirbel (BG) und in der Transpolar-Drift (TPD), Ziffern 1-5 geben die Zeit in Jahren wieder, die Eis an der Position braucht, bis es den Arktischen Ozean durch die Framstraße verlässt (ergänzt aus HOVLAND 2001, nach COLONY & THORNDIKE 1985, THORNDIKE 1986, PFIRMAN et al. 1997).

Middle Miocene, can be ruled out because this would have led to an extremely low production as in the modern Arctic Ocean (e.g., WHEELER et al. 1996) leading to low abundances or absence of aquatic palynomorphs in the sediments. In contrast to this, the co-occurrence of *Nematosphaeropsis* spp. and *Impagidinium* spp. found in the Neogene part of the ACEX sequence, points to seasonally open waters (MATTHIESSEN et al. 2009). Abundance maxima of agglutinated foraminifers in the Early Pleistocene ACEX section also support seasonally ice-free conditions during that time (CRONIN et al. 2008).

On one hand, the discrepancies to Darby's and Krylov et al.'s reconstructions may be explained by their lower temporal resolution. The study by DARBY (2008) has an average

sampling interval of about 0.17 Ma whereas MATTHIESSEN et al. (2009) used samples at an average sample interval of 60 cm in the Late Miocene corresponding to a temporal resolution of approximately 0.04 Ma (based on the age model of FRANK et al. 2008). According to MATTHIESSEN et al. (2009), therefore periods with a reduced seasonal extent of the sea-ice cover (interglacials?) may have alternated with periods of a year-round sea-ice cover (glacials?). On the other hand, applying modern mean drift speeds to argue for perennial ice in the past – as done by DARBY (2008) and KRYLOV et al. (2008) – might also be dangerous, as i) thinner ice may drift faster ii) wind-driven circulation may have been stronger, and iii) there is no modern analysis on how signficant mean speeds are (cf. O'REGAN et al. 2010, O'REGAN 2011).

Concerning the variability of IRD during the Neogene, another prominent phenomenon is the distinct reduction in the amount of IRD in the ACEX record in the early Pleistocene (Fig. 8, O'REGAN et al. 2010, POLYAK et al. 2010). The IRD numbers remain low until a core depth of about 6 mcd. These low IRD values might be explained by (i) a rather stable ice pack, that would reduce the transport and melting of debris-laden sea ice and icebergs across the central Arctic, (ii) a decrease in IRD deposition due to lower inflow of Atlantic-derived intermediate water, that would reduce basal melting of sea ice, or (iii) less icebergs entering the Transpolar Drift from the Eurasian margin (O'REGAN et al. 2010, POLYAK et al. 2010). At 6 mcd, i.e., with the onset of the MIS 6 (Saalian) glaciation, IRD increased significantly in the ACEX record as well as in the neighbouring cores PS2185-6 and 96/12-1PC (Fig. 8, JAKOBSSON et al. 2000, 2001, SPIELHAGEN et al. 2004, O'REGAN et al. 2008, 2010). These distinct maxima in IRD recorded on Lomonosov Ridge are related to advances and retreats of the Barents-Kara Sea Ice Sheet during the last 200 ka (e.g.

SVENDSEN et al. 2004, see discussion below). Whereas the Lomonov Ridge cores display a signal related to the Eurasian ice sheets and IRD input via the Transpolar Drift, started to increase with the onset of MIS 6, a pronounced increase in IRD abundances was recorded in the western Arctic Ocean (Amerasian Basin) significantly earlier than on the Lomonosov Ridge, i.e., probably already during glacial MIS16 at about 650 ka (Fig. 8, POLYAK et al. 2009, STEIN et al. 2010a, 2010b). As outlined by POLYAK et al. (2009), the western Arctic is largely controlled by the Beaufort Gyre circulation system and sediment input from the North American margin. That means, these sedimentary records reflect primarily the history of the Laurentide Ice Sheet and possibly different sea-ice conditions than in the eastern Arctic.

From the discussion above, it is clearly obvious that for the reconstruction of a more complete history of perennial versus seasonal sea ice and ice-free intervals during the past several million years additional well-dated proxy records distributed throughout the Arctic Ocean, are needed (POLYAK et al. 2010, O'REGAN et al. 2010, STEIN et al. 2010b). These proxy records have to be obtained by multidisciplinary studies of long sedimentary sections that can only be recovered by future drilling campaigns to be carried out hopefully within the new phase of IODP (STEIN 2011).

Quaternary glacial / interglacial variability in Arctic Ocean ice-rafting: The last 200 ka

The glacial / interglacial variability in Arctic Ocean ice-rafting may be controlled by different but interrelated factors, i.e., the waxing and waning of circum-Arctic ice sheets, changes in sea-ice cover and changes in oceanic circulation patterns. In detail, however, the interrelationships and the timing of these processes are not fully understood yet (e.g., POLYAK et al. 2004, 2009, STEIN 2008, O'REGAN et al. 2010, O'REGAN 2011). Especially the probably different evolution of ice sheets and sea-ice distribution in the western and eastern Arctic is still a matter of discussion and further studies are needed (see previous chapter). In the following, we will concentrate of the climatic evolution of the last 200 ka.

As shown in several sediment cores from the Eurasian Basin as well as the Amerasian Basin, records of both IRD input and foraminifer abundances from the last 200 thousand years BP (200 ka) clearly demonstrate that sedimentary environments in the central Arctic Ocean were strongly variable. In most of these Arctic Ocean sediment
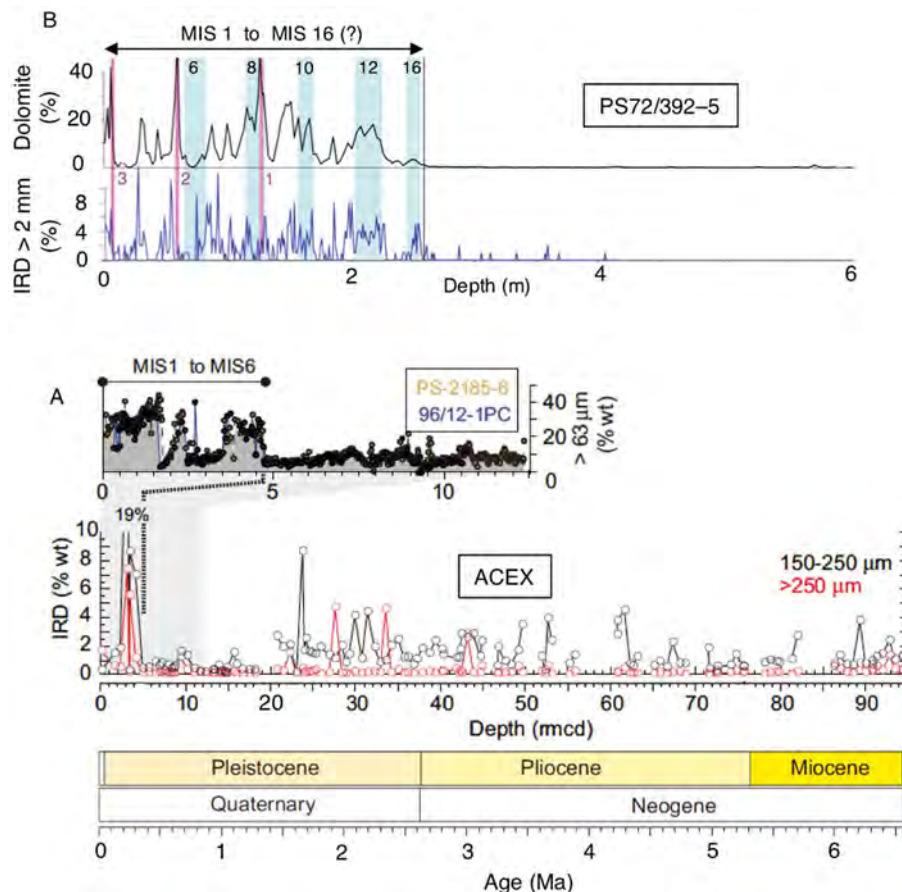
Fig. 8: A = Stratigraphically aligned coarse fraction contents from cores PS-2185-6 and 96/12-1PC shown on the ACEX revised composite depth scale, and the ACEX terrigenous IRD record of the upper 95 mcd (ST. JOHN 2008). Age model based on beryllium stratigraphy (FRANK et al. 2008) (modified after O'REGAN et al. 2010). B = Number of IRD grains >2 mm and content of dolomite (%) determined by XRD and inorganic carbon content, from core PS72/392-5 (for location see Fig. 10; Figure from STEIN et al. 2010a). More sandy intervals are marked by horizontal light blue bars, probably correlating with periods of maximum ice-sheet extend during glacials MIS 6, MIS 8, MIS 10, MIS 12, MIS 16. Main pink-white (1 = PW1 and 2 = PW2) and white (3 = W3) layers are indicated by pink bars.

Abb. 8: A = Gehalte von terrigener Grobfraktion (IRD >63 μm) der Kerne PS2185-6 und 96/12-1PC (Lokationen siehe Fig. 10) und der oberen 95 mcd der ACEX-Abfolge (150-250 μm und >250 μm), aufgetragen gegen revidierte ACEX-Teufenskala (aus O'REGAN et al. 2010, abgeändert). B = Gehalte von IRD >2 mm und Dolomit (Bestimmung mittels Röntgendiffraktometrie und Elementanalyse) von Kern PS72/392-5. Mehr sandige Intervalle sind durch blaue Balken angezeigt, rosa Balken markieren "pink-white layers" (aus STEIN et al. 2010a).

cores, IRD content and abundances of planktonic foraminifers display a general anticorrelation (DARBY et al. 1997, SPIELHAGEN et al. 1997, 2004, NØRGAARD-PEDERSEN et al. 1998, 2003, 2007, POLYAK et al. 2004). As an example, records from core PS2185-6 recovered from Lomonosov Ridge are shown in Figure 9. The foraminifer-rich intervals likely reflect times with an inflow of Atlantic Water of variable strength, temperature, and regional extension, at least a seasonally reduced sea-ice cover (i.e., more open-water conditions), and some increased surface-water productivity (e.g., HEBBELN et al. 1994, NØRGAARD-PEDERSEN et al. 2003, SPIELHAGEN et al. 2004). In core PS2185-6, for example, most prominent peaks in planktonic foraminifer abundance occur in substages MIS 5.5, 5.3, and 5.1 and in the <50 ka interval (Fig. 9, SPIELHAGEN et al. 2004).

Coarse-grained IRD layers contain very few or no foraminifers and are mainly related to iceberg transport of terrigenous material. Distinct maxima in IRD were recorded in uppermost MIS 7 to MIS 6 (190 to 130 ka), upper part of MIS 5 (substage 5.2, about 90 to 80 ka), near the MIS 5/4 boundary (around 75 ka), and in the late MIS 4 to early MIS 3 time interval (65 to 50 ka) (Fig. 9, SPIELHAGEN et al. 2004), indicating major continental glaciations during those times. The central Arctic Ocean sediments from <50 ka show an upward decrease of

IRD content and a minimum in the deposits from the LGM around 20 ka (NØRGAARD-PEDERSEN et al. 1998, 2003, SPIELHAGEN et al. 2004). In general, Holocene deep-sea sediments from the Eurasian Arctic Ocean have a low coarse-fraction content (<10 wt.%, NØRGAARD-PEDERSEN et al. 1998, 2003), which reflects the scarcity of icebergs in the modern Arctic.

Concerning the provenance of the IRD and its variability through time in the Eurasian Arctic, bulk-, clay-, and heavy-mineral associations of core PS2185-6 were used to identify source areas of the terrigenous (IRD) fractions (Fig. 10, e.g., WAHSNER et al. 1999, BEHRENDS et al. 1999, SPIELHAGEN et al. 1997, 2004, STEIN 2008). Here, elevated smectite and kaolinite concentrations as well as high clinopyroxene / amphibole ratios during MIS 6, upper MIS 5, and late MIS 4 early MIS 3, mostly coinciding with IRD maxima (Fig. 9), serve as a tracer for an IRD origin from the area of western Laptev Sea, southeastern Kara Sea, Franz Josef Land and the area of central Barents Sea respectively. High smectite concentrations, however, do not always coincide with high coarse fraction content. In some intervals, e.g. in the uppermost and lowermost MIS 5 (5.1 and 5.5), smectite enrichments correlate with very low terrigenous coarse fraction which may suggest transport by sea ice (or currents) rather than icebergs. Furthermore, the IRD-rich intervals are enriched in quartz, reaching
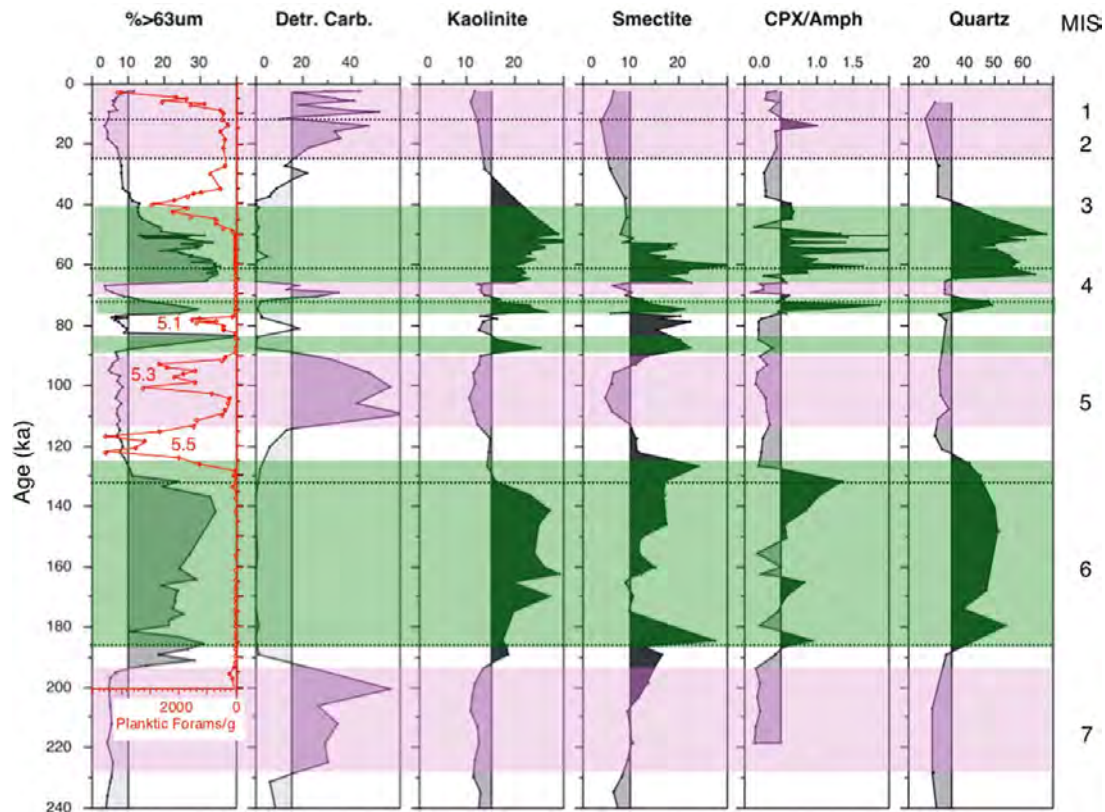
Fig. 9: Summary plots showing coarse-fraction content >63 μm (wt.%), detrital carbonate (% of coarse fraction >500 μm), and kaolinite and smectite (% of clay minerals in the clay fraction <2 μm) (data from SPIELHAGEN et al. 1997) as well as the clinopyroxene/amphibole (CPX/Amph) ratio (data from BEHRENDS 1999) and quartz content (data from VOGT 1997, 2004) in core PS2185 for the last 240 ka (MIS 7 to MIS 1), using the age model of SPIELHAGEN et al. (2004). Marine isotope stages MIS 1 to MIS 7 are indicated. In addition, the concentration of planktic foraminifers per gram sediment is shown (data from SPIELHAGEN et al. 2004). Green and pink bars indicate sediment source areas in Eurasia and northern Canada, respectively. Figure from STEIN (2008).

Abb. 9: Gehalte an Grobfraktion >63 μm, detritischem Karbonat, Kaolinit und Smektit (Daten aus SPIELHAGEN et al. 1997), Verhältnis Clinopyroxen/Amphibol (Daten aus BEHRENDS 1999) und Quarzgehalte (Daten aus VOGT 1997) im Zeitintervall der letzten 240.000 Jahre v.H. (240 ka, MIS 7 bis MIS 1) (Altersmodell nach SPIELHAGEN et al. 2004). Zusätzlich wird der Gehalt an planktischen Foraminiferen gezeigt (Daten aus SPIELHAGEN et al. 2004). Grüne bzw. rosa Balken heben Herkunftsgebiete in Eurasien bzw. Kanada hervor. Abbildung aus STEIN (2008).
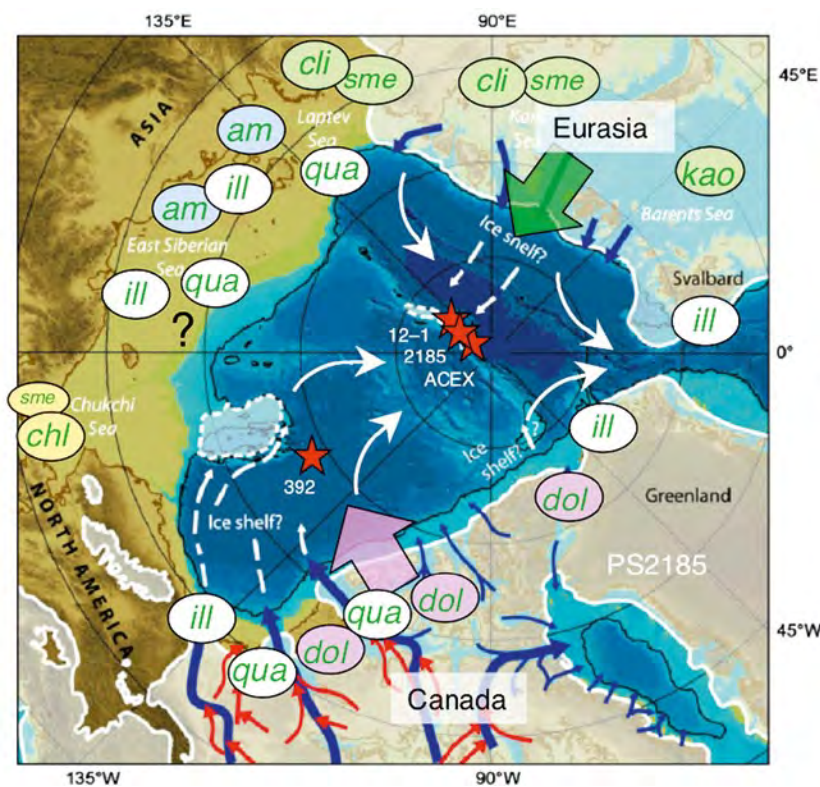
Fig. 10: Bathymetric map of the Arctic Ocean modified to showing lowered sea level of 120 m during LGM maximum glaciation. Limits of the Eurasian and North American ice sheets according to SVENDSEN et al. (2004) and DYKE et al. (2002), respectively; main ice streams (blue arrows) according to DE ANGELES & KLEMAN (2005) and KLEMAN & GLASSER (2007). Red arrows show ice stream tributaries and episodic diversions of ice stream drainage within main ice stream corridors. Projected flow lines of ice shelves and limits of ice rises are mapped based on interpretation of observed glaciogenic seafloor bedforms (figure from JAKOBSSON et al. 2008, supplemented). Main source areas of specific minerals are shown (from STEIN 2008, STEIN et al. 2010 and references therein): qua = quartz; dol = dolomite; ill = illite; sme = smectite; chl = chlorite; kao = kaolinite; am = amphibole; cli = clinopyroxene. Colour codes mark source region: green = western Laptev Sea, Kara Sea, Barents Sea; blue = eastern Laptev Sea, East Siberian Sea; orange = Bering Strait; pink = Canada, northern Greenland; white = no specific source area. Red stars indicate core locations on Lomonosov Ridge ans Canada Basin; large green and pink arrows indicate sediment input from the Eurasian and northern Canadian ice sheets, respectively.

Abb. 10: Modifizierte bathymetrische Karte des Arktischen Ozeans zur Zeit des letzten glazialen Maximums mit einem 120 m abgesenkten Meeresspiegel. Ausdehnung der eurasischen und nordamerikanischen Eisschilde nach SVENDSEN et al. (2004) bzw. DYKE et al. (2002), Eisströme (blaue Pfeile) nach DE ANGELES & KLEMAN (2005) und KLEMAN & GLASSER (2007). Abbildung ergänzt nach JAKOBSSON et al. 2008. Liefergebiete bestimmter Minerale nach STEIN (2008) und STEIN et al. (2010).

values of >50 % (Fig. 9). This is also consistent with an Eurasian source, although quartz alone is not specific enough for a source identification because it also occurs in major abundance in the Canadian Arctic (Fig. 10).

During interglacials, i.e., MIS 7 and the middle part of MIS 5 as well as during the last about 20 ka, increased amounts of detrital carbonate (dolomite) were determined in the record of core PS2185-6, coinciding with very low amounts of terrigenous coarse fraction (Fig. 9). Detrital carbonate, especially dolomite, is related to a sediment source in the Canadian Arctic (Fig. 10, e.g., BISCHOF et al. 1996, PHILLIPS & GRANTZ 2001) whereas the fine-grained terrigenous material points to a transport by sea ice (or currents) rather than icebergs. This may suggest substantial sediment transport towards the Eurasia Basin by sea ice in an extended Beaufort Gyre at those (mainly interglacial) time intervals.

LGM, Deglacial to Holocene changes in Arctic Ocean sea-ice cover and ice sheet decay

In order to reconstruct the Arctic Ocean sea-ice distribution and other surface-water characteristics, NØRGAARD-PEDERSEN et al. (2003) carried out a very detailed study on a large number of well-dated sediment cores from the Eurasian sector of the Arctic Ocean, representing the MIS 2/1 time interval. Based on sedimentological, micropaleontological, and stable isotope data, these authors were able to characterize and map regions of different paleoceanographic conditions for the Last Glacial Maximum (LGM) time slice (18.0–21.5 Cal. kyrs. BP according to GLAMAP (SARNTHEIN et al. 2003b)). This reconstruction is based on (1) the spatial distribution of $\delta^{18}O$ values as proxy for the distribution of Atlantic and polar water masses, (2) flux records of planktic foraminifers as productivity proxy reflecting nutrient supply and degree of ice cover (e.g., HEBBELN & WEFER 1991, HEBBELN et al. 1994), and (3) the IRD content >500 μm as a proxy to estimate the input of terrigenous sediments transported by icebergs derived from continental ice sheets calving into the Arctic Ocean. As a result, NØRGAARD-PEDERSEN et al. (2003) could separate three areas characterized by different sedimentation regimes and surface ocean properties during the LGM (Fig. 11):

Area (1), the eastern Fram Strait and the northern Barents Sea margin;

Area (2), the western Fram Strait and the southwestern Eurasian Basin up to about 84-85° N, and

Area (3), the central Arctic Ocean (north of 85° N in the Eurasian Basin).

In summary, these areas have the following characteristics (Fig. 11, detailed discussion see NØRGAARD-PEDERSEN et al. 2003):

Area (1), the eastern Fram Strait and the northern Barents Sea margin area, is characterized by high sedimentation rates of 2–10 cm ky^{-1} and high abundances of planktic foraminifers (about 4000–6000 specimens g^{-1} sediment). Today, such environments are found in areas of seasonally changing ice cover like the central Fram Strait (HEBBELN & WEFER 1991). The high $\delta^{18}O$ values of *N. pachyderma* (sin.) of 4.5–4.8 % and the estimates of summer sea-surface temperatures (SST) of about 1.6–3.0 °C (PFLAUMANN et al. 2003) suggest a strong inflow of Atlantic Water. The high abundances of planktic foraminifers (and fluxes of 10–35 10^3 specimens cm^{-2} ky^{-1}, NØRGAARD-PEDERSEN et al. 2003) correspond to the glacial "high productive zones" (HPZ) first reported from the eastern Fram Strait and the Norwegian Sea by HEBBELN et al. (1994) and DOKKEN & HALD (1996).

Area (2), the western Fram Strait and the southwestern Eurasian Basin up to about 84-85° N, is characterized by lower sedimentation rates of 1–2 cm ky^{-1} and moderately high abundances and fluxes of planktic foraminifers, high $\delta^{18}O$ values of *N. pachyderma* (sin.), and summer SST estimates slightly lower than in Area (1). This region may have been characterized by the pres-

48

ence of ice cover with some open leads in summer, similar to the present interior Arctic Ocean. NØRGAARD-PEDERSEN et al. (2003) suppose that Area 2 was under the steady influence of Atlantic subsurface waters advected from Area (1). The impact of recirculating saline and relatively warm Atlantic Water over a large area of the southwestern Eurasian Basin was the decisive factor causing a break-up of the ice cover, relatively high sedimentation rates and a comparatively high planktic foraminiferal flux (about 5-10 x 10^3 specimens cm^{-2} ky^{-1}, Fig. 11, NØRGAARD-PEDERSEN et al. 2003).

Area (3), the central Arctic Ocean north of 85° N in the Eurasian Basin, is characterized by extremely low sedimentation rates (dominantly <1 cm ky^{-1}), low abundances and fluxes
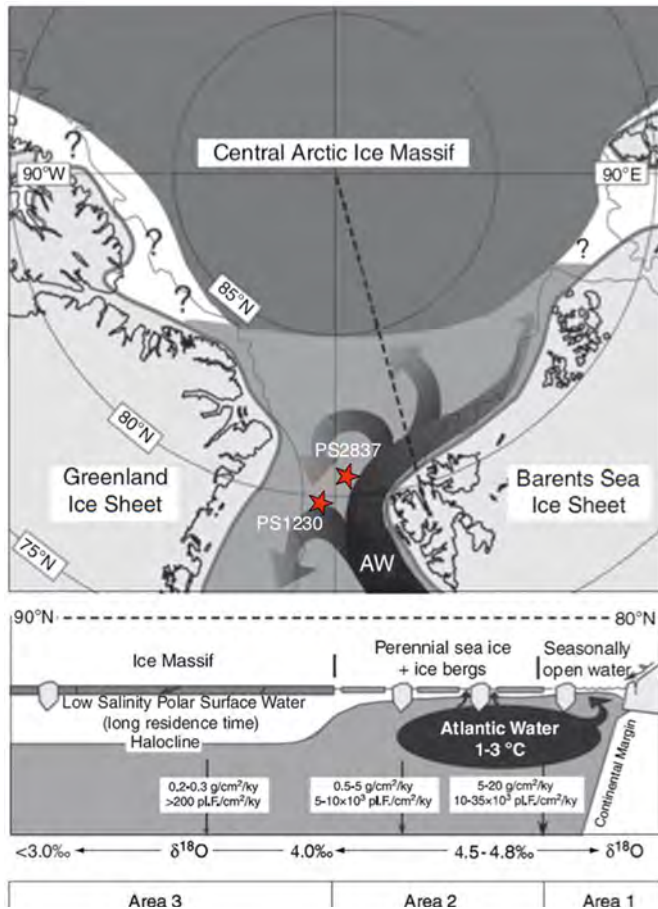
Fig. 11: Simplified model of sea-ice and surface-ocean characteristics in the Fram Strait to central Arctic Ocean region during the LGM (from NØRGAARD-PEDERSEN et al. 2003, supplemented). On the latitudinal transect from the northern Svalbard continental margin to the North Pole, related proxy data such as sedimentation rates, planktic foraminiferal flux, planktic δ^{18}O values, and mean summer SST values of the Atlantic Water mass are shown. Advection and recirculation of relatively warm and saline Atlantic Water in the Fram Strait to southwestern Eurasian Basin caused an open ice cover and a relatively high flux of biogenic and lithic material. Polynyas probably occurred at the Barents Sea continental margin. From about 85° N and further into the interior Arctic, it is proposed that the sea-ice cover was permanently thick, resting upon cold, low-salinity halocline waters. This may explain the extreme low interior Arctic flux values. Red stars indicate locations of cores PS1230-1 and PS2837-5.

Abb. 11: Schematische Darstellung der Meereisverbreitung und Charakteristika des Oberflächenwassers im Bereich Framstraße/Arktischer Ozean während des Letzten Glazialen Maximums (ergänzt aus NØRGAARD-PEDERSEN et al. 2003). Auf dem Schnitt von Spitzbergen bis 90° N sind Proxydaten wie Sedimentations- und Akkumulationsraten, δ^{18}O-Werte planktischer Foraminiferen sowie der mittleren Temperaturen des Oberflächenwassers für drei unterschiedliche Gebiete angezeigt.

of planktic foraminifers (only a few hundred foraminifers g^{-1} sediment and <0.2 x 10^3 specimens cm^{-2} ky^{-1}, respectively), and very low IRD (>500 μm) values <1 % (Fig. 11, NØRGAARD-PEDERSEN et al. 2003). These data suggest the existence of an extensive and thick sea-ice cover with low seasonal variation, limiting planktic productivity ("low productivity zone") and minor IRD release in the eastern central Arctic during the LGM. Due to low temporal resolution, however, it has to be considered, that the data from the central Arctic Ocean are tentative and probably characterize average Marine Isotope Stage (MIS) 2 conditions rather than a specific LGM time slice (NØRGAARD-PEDERSEN et al. 2003).

MIS 2 (including the LGM) was already identified as a period of very limited bioproduction and extremely low sedimentation rates due to a massive sea-ice cover with limited seasonal variation from earlier studies of sediment cores from the eastern and western central Arctic Ocean (DARBY et al. 1997, NØRGAARD-PEDERSEN et al. 1998, POORE et al. 1999). Cores from the Northwind Ridge and the Chukchi Plateau (Amerasian Basin) are barren of foraminifers in the glacial interval (DARBY et al. 1997, PHILLIPS & GRANTZ 1997), suggesting an even thicker and more coherent sea-ice cover in the western central Arctic Ocean, which had a sufficient thickness to reduce solar irradiance to levels that precluded photosynthesis.

Grain-size distribution and IRD composition from this time period provides more detailed information on ice-sheet variability, ice export, and sea-ice versus iceberg transport. While there are very few icebergs calving into the Arctic Ocean, crossing the central basins, and exiting Fram Strait today (SUDGEN 1982), large quantities of glacial ice drifted across the central Arctic Ocean and finally through Fram Strait during the late Pleistocene. These pulses in IRD input during MIS 2 are mainly related to sudden, massive iceberg calving events in the North American Arctic ice sheets, as reconstructed by DARBY et al. (2002) from sedimentary records from the western central Arctic Ocean to Fram Strait (Fig. 12). In these cores, IRD composition >250 μm and Fe oxides were used to trace the IRD in the glacial marine sediments back to its sources (see DARBY 2003 for background). A key core in their reconstruction is the AMS^{14}C-dated core PS1230-1 located in 1235 m water depth at 78.9° N, 4.8° W, in the central Fram Strait (Fig. 12) where most of the Arctic sea ice is exported today (90 % of the modern sea-ice drifts through Fram Strait between 0 and 10° W, VINJE et al. 1998).

The record of core PS1230-1 representing the last 34 Cal. kyrs. BP (upper MIS 3 to MIS 1), shows significant, rapid fluctuations in the percentages of Fe oxide grains from different sources (Fig. 12, DARBY et al. 2002). Fe oxide maxima in the pre-Holocene probably represent primarily iceberg transport on the basis of the abundance of coarse IRD in the Pleistocene section and on the similarity of the IRD grain-size distribution to glacial tills (DARBY et al. 2002).

During the late Pleistocene (MIS 3 / MIS 2), a major source of IRD was the northwestern Laurentide Ice Sheet that calved into the Arctic Ocean. This source is identified by detrital Fe oxide grains in PS1230-1 that precisely match those in the tills of Banks Island and Victoria Island (source area 8 in Fig. 12). A northwestern Laurentide source is also supported by the presence of light-coloured detrital carbonate, which is rela-
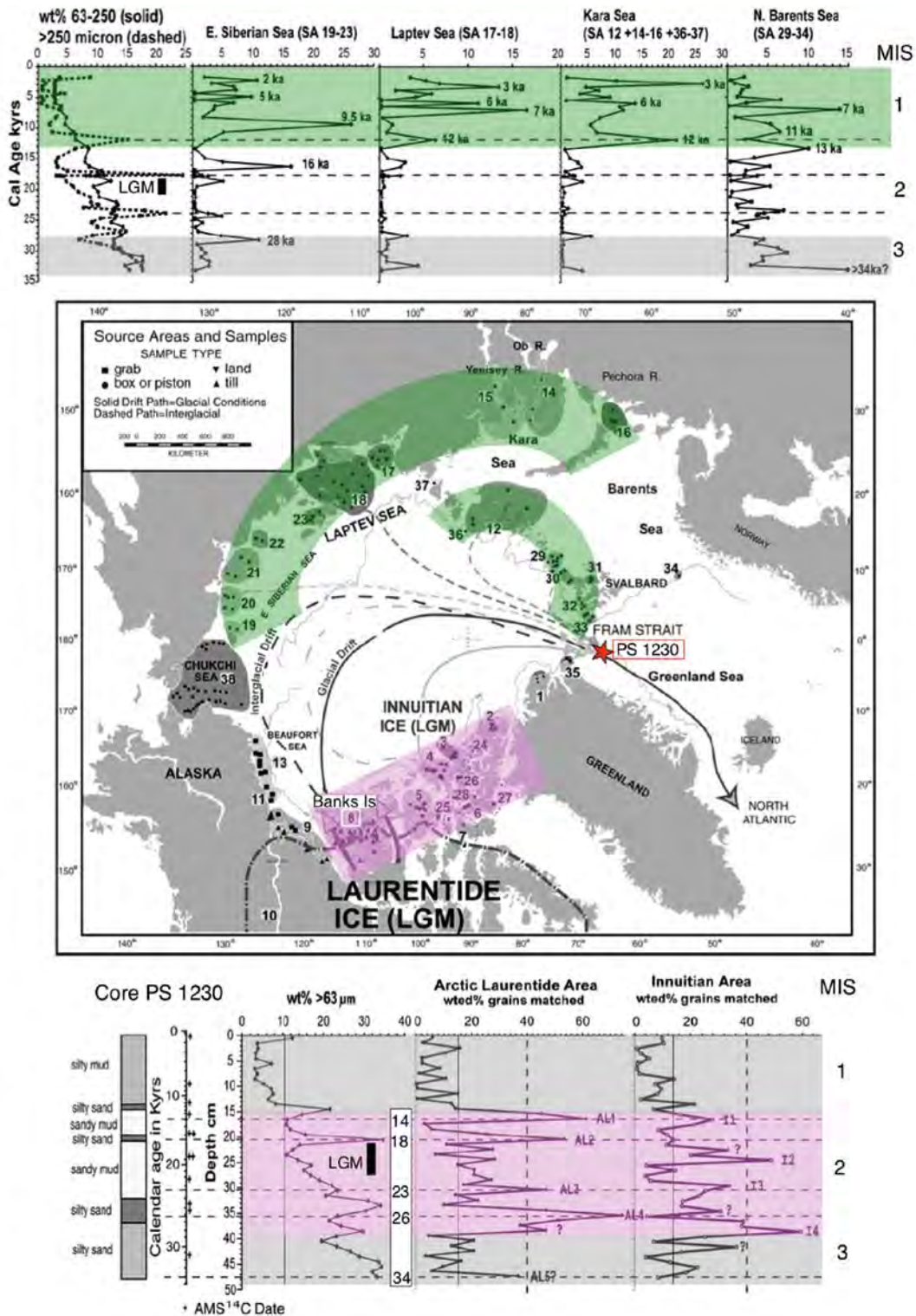
Fig. 12: Circum-Arctic source areas (samples 1-38) as defined by unique source compositions based on Fe oxide composition of sand-sized grains (DARBY 2003), drift paths of icebergs from Arctic Laurentide Ice Sheet and Innuitian Ice Sheet to Fram Strait (solid drift paths), and the location of core PS1230 (from DARBY et al. 2002, supplemented). Dashed drift paths of sea-ice in the Arctic show the influence of the Beaufort Gyre during warmer intervals like the Holocene by displacing North American ice drift paths westward. In green and pink, Eurasian and Canadian source areas, respectively, are highlighted. Graphs above and below the map show the amounts of terrigenous coarse fractions and Fe oxide grains from different circum-Arctic source areas determined in Fram Strait core PS1230 (from DARBY et al. 2002, supplemented). Bottom graphs: Arctic Laurentide (AL) and Innuitian (I) IRD events based on detrital Fe oxide mineral grain compositions matched to source area 8 (Banks Island) and source areas 2-7 plus 24-28, respectively, plotted *versus* core depth. Calendar years (kyrs. BP) and location of AMS[14]C datings (crosses) as well as major lithologies are indicated. Numbers 14 to 34 indicate ages of the main AL1 to AL 5 IRD events in Cal. kyrs. BP; bold black bar indicates the Last Glacial Maximum (LGM). Top graphs: IRD events originating from Siberian shelves, plotted *versus* age.

Abb. 12: Karte mit 38 unterschiedlichen, anhand von Fe-Oxiden in der Sandfraktion definierten, zirkum-arktischen Liefergebieten und Driftwegen von Eisbergen und Meereis. Die Kurven oberhalb und unterhalb der Karte zeigen Gehalte der terrigenen Grobfraktion und Fe-Oxide aus unterschiedlichen Liefergebieten im Kern PS1230. Abbildung ergänzt aus DARBY et al. (2002).

tively abundant in tills and derived from the extensive Paleozoic carbonates exposed on Victoria Island (e.g., BISCHOF et al. 1996). This is indicated by the coincidence of Fe oxide peaks in PS1230-1 with elevated detrital, light-coloured carbonate peaks of 4 to >8 % (Fig. 12). Another important but secondary source of Fe oxide grains in core PS1230-1 is the Innuitian ice sheet in the northern Canadian Islands (source areas 2 to 7 and 24 to 28 in Fig. 12; BISCHOF & DARBY 1999, DARBY et al. 2002).

The rapid onset and relatively short duration of the Fe oxide grain peaks suggest massive and fast deglaciation events in parts of the Laurentide and Innuitian ice sheets during MIS 2 (Fig. 12, at about 26, 23, 18 and 14 Cal. kyrs. BP), producing large armadas of icebergs, i.e., events probably similar to those recorded during Heinrich events in the North Atlantic. Indeed, the number of Arctic IRD events and their occurrence intervals over the last 34 ky are remarkably similar to those of Heinrich events, i.e., the events 1 to 4 seem to correspond to H0 to H3 (DARBY et al. 2002). The most prominent event seems to be the AL 2 event near 18 Cal. kyrs. BP, which coincides with a distinct IRD maximum, probably representing the decay of the LGM ice sheet (Fig. 12). Fe oxide peaks related to IRD input from the northwestern Laurentide Ice Sheet, occur at about the same time in cores from the Lomonosov,

Mendeleev, and Northwind ridges (DARBY et al. 2002). These major collapses of the Laurentide Ice Sheet and iceberg discharge events through Fram Strait caused major pulses of fresh-water export into the Greenland-Iceland-Norwegian (GIN) seas (North Atlantic) where it may have been effective in arresting the deep-water formation and the global THC (cf., PELTIER 2007 and references therein).

During MIS 1, the weight percentages of the terrigenous sediment fraction >63 μm in Core PS1230-1 decreased significantly, reaching <4 % during the last 10 Cal. kyrs. BP (Fig. 12). The predominance of the silt and clay fractions suggests transport by sea ice rather than iceberg rafting (PFIRMAN et al. 1989, REIMNITZ et al. 1998, NÜRNBERG et al. 1994). The contemporaneous increase in Fe oxide grains from unglaciated Eurasian shelves such as the Kara, Laptev, and East Siberian seas (Fig. 12) supports sea-ice rafting as a most important transport process during the Holocene (DARBY et al. 2002, DARBY 2003).

Elevated IRD values during the LGM, decreasing during the deglaciation to minimum Holocene values were also recorded at near-by core PS2837-5 (Fig. 13, BIRGEL & HASS 2004, for locations of cores PS1230-1 and PS2837-5 see Fig. 11).
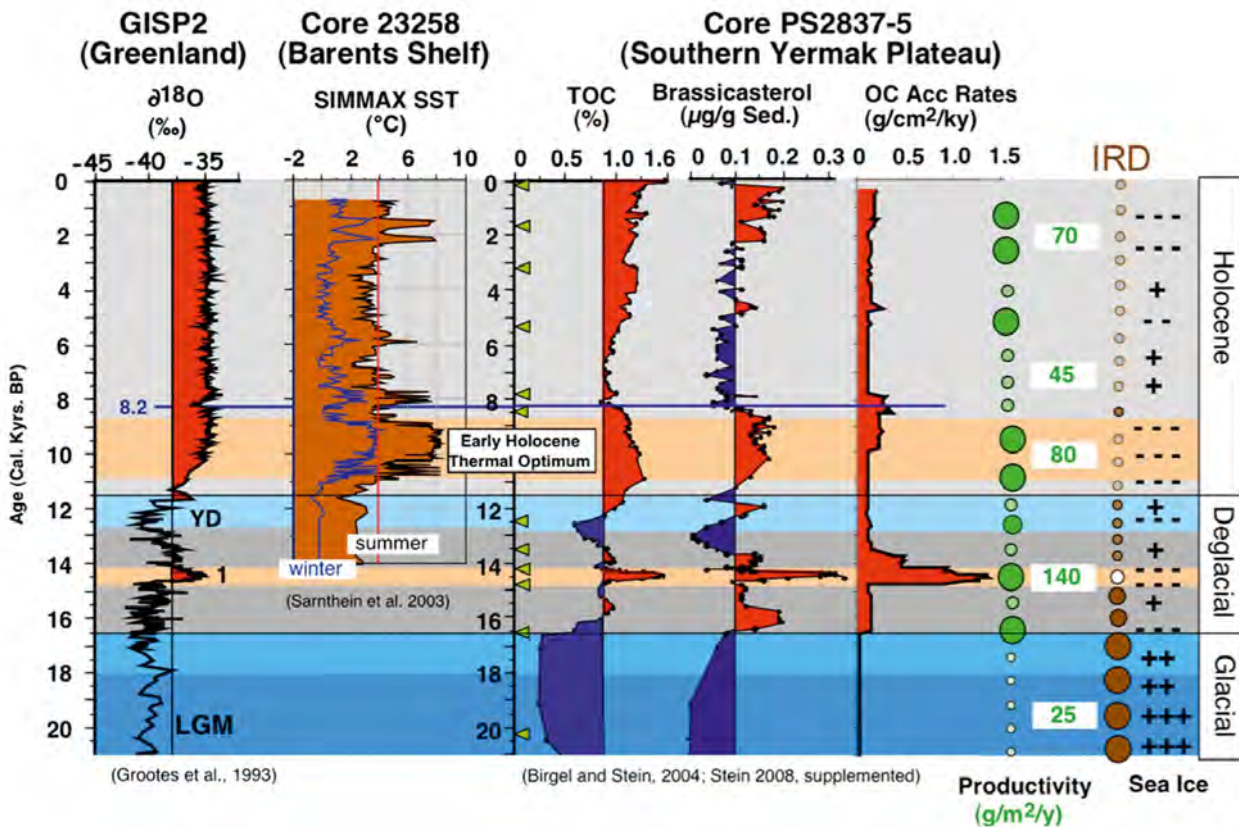

Fig. 13: Total organic carbon (%), brassicasterol (μg g^{-1}sed.) indicative for diatom productivity, and organic carbon accumulation rates (g C cm^{-2} ky^{-1}) of the last 20 ka at core PS2837-5; age scale in calendar years. Occurrence of ice-rafted debris (IRD; large/small brown circles = high/low amounts of IRD, white circle = absence of IRD (BIRGEL & HASS 2004). Primary productivity: large/small green circles = high/low productivity; calculation from organic carbon data following the approach of STEIN (1986), and general interpretation of data in terms of sea-ice cover (from +++ = very extended to --- = very reduced) are indicated. Records are related to the GISP2 ice core record and a sea-surface temperature record (based on foraminifera data) of core 23258 from the Barents Sea shelf. YD = Younger Dryas, 1 = Bølling interval. For location of cores see Figure 18.

Abb. 13: Organischer Kohlenstoffgehalt (TOC in %), Brassicasterol (μg g^{-1}Sed.) und Akkumulationsraten von organischem Kohlenstoff (g C cm^{-2} ky^{-1}) im Kernabschnitt der letzten 20.000 Jahre von Kern PS2837-5 sowie δ^{18}O-Kurve vom GISP2-Eiskern und aus Foraminiferendaten berechnete Oberflächenwassertemperatur in Kern M23258 vom Barentssee-Kontinentalrand. Weiterhin sind Vorkommen von IRD (BIRGEL & HASS 2004) und berechnete Paläoproduktivitäten (nach STEIN 1986) und deren Interpretation in Hinblick auf die Ausdehnung von Meereis dargestellt. Zur Lokation der Kerne siehe Abbildung 18.

Organic-carbon data determined at the same core provide additional qualitative information on the sea-ice cover in the Fram Strait at that time. Minimum total organic carbon (TOC) values and the near absence of the phytoplankton biomarker brassicasterol (indicative for very low diatom productivity) are interpreted to reflect a more or less closed sea-ice cover during the LGM (Fig. 13, BIRGEL & STEIN 2004, STEIN 2008). During the deglaciation, TOC and brassicasterol values as well as organic-carbon accumulation (flux) rates significantly increased, indicating a reduced sea-ice cover and increased primary productivity. An absolute maximum in productivity probably related to a minimum sea-ice cover occurred during the Bølling warm phase (Fig. 13). At that time, primary productivity may have reached 140 g C m^{-2} y^{-1} (following the approach by STEIN 1986), i.e., a value significantly higher than that recorded in this area today (about 50–100 g C m^{-2} y^{-1}, JIN et al. 2012). A second maximum in TOC and brassicasterol was found between about 11 and 9 Cal. kyrs. BP, coinciding with the Early Holocene Thermal Optimum and maximum summer sea-surface temperatures of about 8 °C in core 23258 (Fig. 13, SARNTHEIN et al. 2003, BIRGEL & STEIN 2004, for location of core see Fig. 18). These data point again towards a reduced sea-ice cover. In order to get a more detailed and (semi-) quantitative record of sea-ice cover and its variability during glacial to Holocene times, a novel biomarker approach was used in the study of core PS2837-5 (MÜLLER et al. 2009, see below).

A NOVEL BIOMARKER APPROACH FOR SEA-ICE RECONSTRUCTIONS

Our ability to quantitatively reconstruct past sea-ice distributions is now greatly improved by a novel biomarker approach, which is based on the determination of a highly-branched isoprenoid (HBI) with 25 carbon atoms (C$_{25}$ HBI monoene = "IP$_{25}$"), and developed by BELT et al. (2007). This biomarker is only biosynthesized by diatoms living in the Arctic ice, i.e., it seems to be an Arctic sea-ice diatom-specific biomarker and, as shown by these authors in their original study, seems to be a sensitive and stable proxy for sea-ice in sediments over at least the Holocene. The isotopically very heavy δ^{13}C signature of IP$_{25}$ determined in sea ice, sediment trap material and sediments further supports the use of IP$_{25}$ as sea-ice proxy (BELT et al., 2008). In sea-ice and sediment samples collected from various locations around Antarctica, on the other hand, no IP$_{25}$ was found. Instead, a HBI diene could be determined which co-occur in Arctic Ocean sediments together with IP$_{25}$ (MASSÉ et al. 2011). These authors propose that the presence of this also isotopically ^{13}C enriched HBI diene in Antarctic sediments might be a useful proxy indicator for organic matter derived from sea-ice diatoms. The analytical approach to identify and quantify the IP$_{25}$ biomarker (as well as the other relevant biomarkers) and currently used in our laboratory at the Alfred Wegener Institute, is summarized in Fig. 14 (cf., MÜLLER et al. 2011, FAHL & STEIN 2012).
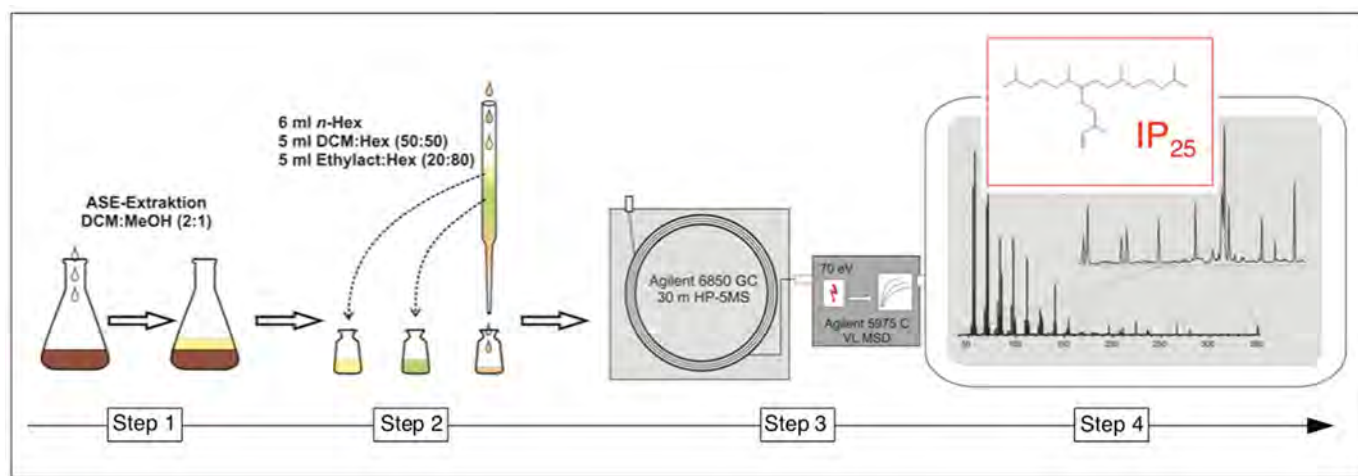
Fig. 14: Scheme summarizing the AWI analytical procedure for identification and quantification of IP$_{25}$ as well as sterols, developed by K. Fahl and J. Müller at the AWI (cf. MÜLLER et al. 2011; for more details see FAHL & STEIN 2012).
(1) For lipid biomarker analyses, the freeze-dried and homogenised sediments were extracted with an Accelerated Solvent Extractor (DIONEX, ASE 200; 100 °C, 5 min, 1000 psi) using a dichloromethane/methanol mixture (2:1 v/v). Prior to this step, 7-hexylnonadecane, squalane, and cholesterol-d$_6$ (cholest-5-en-3b-ol-d$_6$) were added as internal standards.
(2) Hydrocarbons and sterols were separated via open column chromatography (SiO$_2$) using n-hexane and methyl-acetate/n-hexane (20:80 v/v), respectively. Sterols were silylated with 500 μl BSTFA (60 °C, 2 h) (FAHL & STEIN 1999).
(3) Gas chromatography-mass spectrometry (GC-MS) compound analyses of both fractions were performed using an Agilent 6850 GC (30 m HP-5 ms column, 0.25 mm inner diameter, 0.25 μm film thickness) coupled to an Agilent 5975 C VL mass selective detector. The GC oven was heated from 60 °C to 150 °C at 15 °C min^{-1}, and then at 10 °C min^{-1} to 320 °C (held 15 min) for the analysis of hydrocarbons (IP$_{25}$, C$_{25}$-HBI-diene, and n-alkanes) and at 3 °C min^{-1} to 320 °C (held 20 min) for sterols, respectively. Helium was used as carrier gas.
(4) Individual compound identification was based on comparisons of their retention times with that of reference compounds (applies to brassicasterol and n-alkanes) and on comparisons of their mass spectra with published data (for sterols see BOON et al. (1979) and VOLKMAN (1986), for IP$_{25}$ see BELT et al. (2007), and for C$_{25}$-HBI diene see JOHNS et al. 1999). The Kovats Index calculated for IP$_{25}$ is 2085. Biomarker concentrations were calculated on the basis of their individual GC-MS ion responses compared with those of respective internal standards.
(5) IP$_{25}$ and C$_{25}$-HBI diene were quantified using their molecular ion m/z 350 and m/z 348 in relation to the abundant fragment ion m/z 266 of 7-hexylnonadecane and by means of an external calibration curve (R^2 = 0.9989) to balance the different responses of the used ions (for further details see FAHL & STEIN, 2012). Brassicasterol (24-methylcholesta-5,22E-dien-3ß-ol) and dinosterol (4a,23,24-trimethyl-5a-cholest-22E-en-3ß-ol) were quantified as trimethylsilyl ethers using the molecular ions m/z 470 and m/z 500, respectively, and m/z 464 for cholesterol-d$_6$. Fragment ion m/z 57 was used to quantify the short-chain n-alkanes (n-C$_{15}$, n-C$_{17}$, n-C$_{19}$) via squalane. Finally, biomarker concentrations were corrected to the amount of extracted sediment.

Abb. 14: Zusammenstellung der am AWI benutzten und von K. Fahl und J. Müller aufgebauten GC- und GC/MS-Analytik zur Identifizierung und Quantifizierung von IP$_{25}$, Dien und Sterolen (FAHL & STEIN 1999, 2012, MÜLLER et al. 2011).

In follow-up studies, the identification of this new sea-ice proxy IP$_{25}$ in marine surface sediments and sediment cores from the Canadian Arctic Archipelago (BELT et al. 2008, 2010, VARE et al. 2009), the shelf north off Iceland (MASSÉ et al. 2008), the Barents Sea (VARE et al. 2010), northern Fram Strait and off East Greenland (MÜLLER et al. 2009, 2011, 2012), the Kara and Laptev seas (XIAO et al. 2012) the Lomonosov Ridge (central Arctic Ocean, FAHL & STEIN 2012) as well as from the Bering Sea (MÉHEUST et al. 2012) allowed reconstructions of the ancient sea-ice variability in these regions during the last 30 Cal. kyrs. BP (see maps of Figs. 1, 3 and 15). Within this paper (see below), we demonstrate for the first time that IP$_{25}$ is also preserved in Arctic Ocean sediments as old as 130 to 150 ka (MIS 6). For older (pre-MIS6) sediments, no IP$_{25}$ determinations have been carried out so far (at least according to our knowledge), except for some test measurements in Eocene samples from the IODP-ACEX record (see discussion above and Fig. 1 for location) in which, however, no IP$_{25}$ was found (Stein unpubl. data 2010), and a pilot study of samples from ODP site 912 (Fram Strait; see Fig. 15 for location), in which IP$_{25}$ was even found in two million years old sediments (STEIN & FAHL 2012).

A one-year IP$_{25}$ record is available from a sediment trap deployed in August 2004 at 200 m water depth in Franklin Bay, Arctic Canada (BELT et al. 2008, see Fig. 15, location ARC-6). This one-year proxy record with a prominent IP$_{25}$ maximum in May/June 2005 represents the seasonal sea-ice variability with maximum sea-ice algae growth during spring. For the first time, such an IP$_{25}$ data set was obtained from an array of two sediment traps deployed at the southern Lomonosov Ridge in the central Arctic Ocean at water depth of 150 m and 1550 m ("LOMO-2") and recording the seasonal variability of sea-ice cover in 1994/1995 (FAHL & STEIN 2012, for location see Figs. 1 and 15). The IP$_{25}$ data, together with other biomarker proxies and abundances of different diatom species (FAHL & NÖTHIG 2007, FAHL & STEIN 2012), indicate a predominantly permanent sea-ice cover at the trap location between November 1995 und June 1996 (IP$_{25}$ absent or insignificant), an ice-edge situation with maximum phytoplankton productivity and sea-ice algae input in July/August 1996 (maximum in IP$_{25}$), and the start of new-ice formation in late September (drop in IP$_{25}$) (Fig. 16). From these data it seems to be that the maximum August 1996 IP$_{25}$ concentration decreased from about 12 ng m^{-2} d^{-1} to about 2 ng m^{-2} d^{-1} during its fall through the water column from 150 to 1550

Sediment traps
  LOMO-2 (FAHL & STEIN 2012)
  Fram Strait; Laptev Sea, Kara Sea (continuing research FAHL et al.
  ARC-6 (BELT et al. 2008)

Surface sediments
  Box 1 (MÜLLER et al. 2011)
  Box 2, 3, 4 (continuing PhD research, XIAO et al.
  Box 5 (BELT et al. 2007, 2010)

Deglacial-Holocene sediments
  PS2837, MSM5/5-712, -723, PS2641
  (MÜLLER et al. 2009, 2012, unpublished)
  PS2458 (FAHL & STEIN 2012)
  PS72/350 (Stein et al. unpublished)
  BASICC-1, -8, -43 (VARE et al. 2010)
  ARC-3, -4, -5, -6 (BELT et al. 2008, 2010)
  MD99-2275 (MASSÉ et al. 2008)

MIS 3 to MIS 1
  PS2185, PS2170, PS2163 (continuing PhD research, Xiao et al.)
  PS2767 (Stein et al. unpublished)
  Bering Sea (continuing PhD research; MÉHEUST et al.)
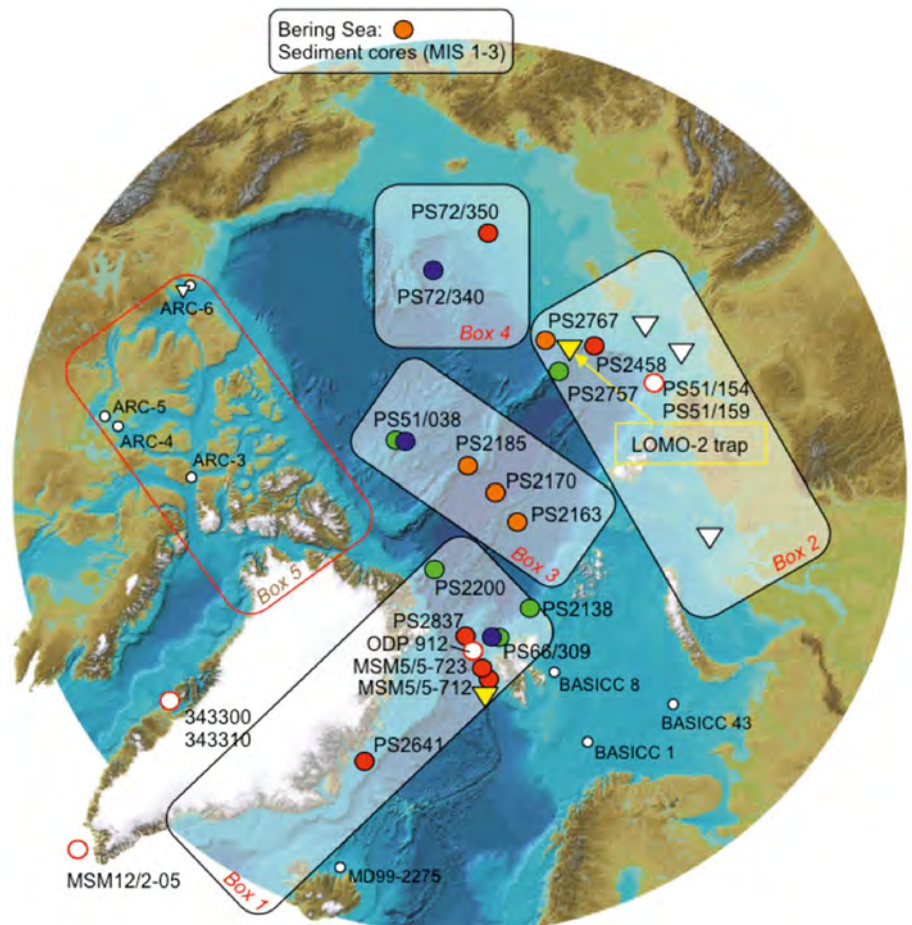
MIS 6 to MIS 5 (Saalian/Eemian transition)
  PS2138, PS2200, PS2757, PS51/038, PS66/309
  (Stein et al. unpublished)

MIS 6 to MIS 1
  PS72/340, PS51/038, PS66/309
 (continuing PhD research, XIAO et al.)

**ODP Site 912 (0-2 Ma)**
  (STEIN & FAHL 2012)

Fig. 15: Map showing locations/areas with published Arctic Ocean IP$_{25}$ data /records and on-going IP$_{25}$ studies at the AWI. In addition, cores selected for future IP$_{25}$ studies in the Baffin Bay (343300 and 343310), south of Greenland (MSM12/2-05), the Laptev Sea (PS51/154 and PS51/159) and ODP Site 912 are shown.

Abb. 15: Übersichtskarte mit Lokationen von Arbeitsgebieten und Kernstationen, an denen Untersuchungen von IP$_{25}$-Messungen am AWI durchgeführt wurden oder zurzeit laufen bzw. geplant sind. Zusätzlich sind Gebiete mit publizierten IP$_{25}$-Daten anderer Arbeitsgruppen dargestellt. Zitate mit weiteren Details sind angegeben.
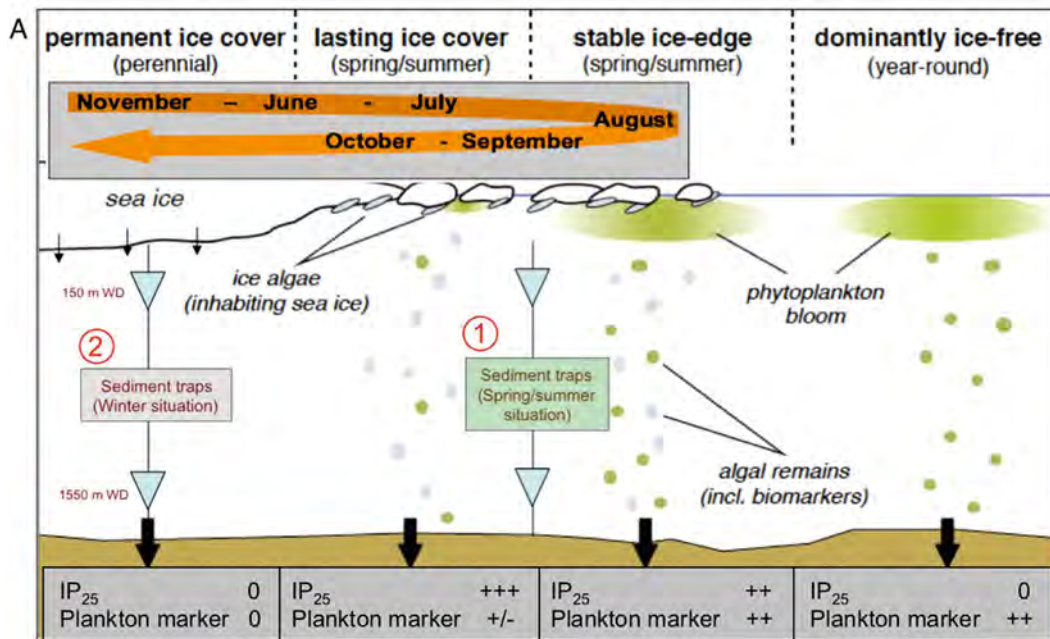
Fig. 16: (A) Generalized scheme of sea surface conditions and respective productivities of ice algae and phytoplankton, and sedimentary content of IP_{25} and phytoplankton-derived biomarkers for each setting (MÜLLER et al. 2011, supplemented). This scheme indicates the seasonal variability of sea-ice cover in 1995/96 as well as summer/spring (1) and winter (2) situations at the sediment trap location on Lomonosov Ridge.
(B) Seasonal variability of IP_{25} fluxes in 1995/1996 as determined at the shallow (150 m) and deep (1550 m) sediment traps (FAHL & STEIN 2012). For location of trap see Figures 1 and 3.

Abb. 16: (A) Oberflächenwasser- Charakteristika und Schema der Eisalgen- und Phytoplankton-Produktion sowie der IP_{25}- und Phytoplankton-Sedimentdaten (MÜLLER et al. 2011). Skizziert wird die saisonale Meereis-Variabilität mit Sommer-/Frühjahrs-Situation (1) und Wintersituation (2) an der Sedimentfallenposition LOMO-2. B = Saisonale Variabilität von IP_{25} in den Sedimentfallen aus 150 m bzw. 1550 m Wassertiefe (verändert nach FAHL & STEIN 2012). Zur Lokation der Sedimentfalle vgl. Abbildungen 1 oder 3.
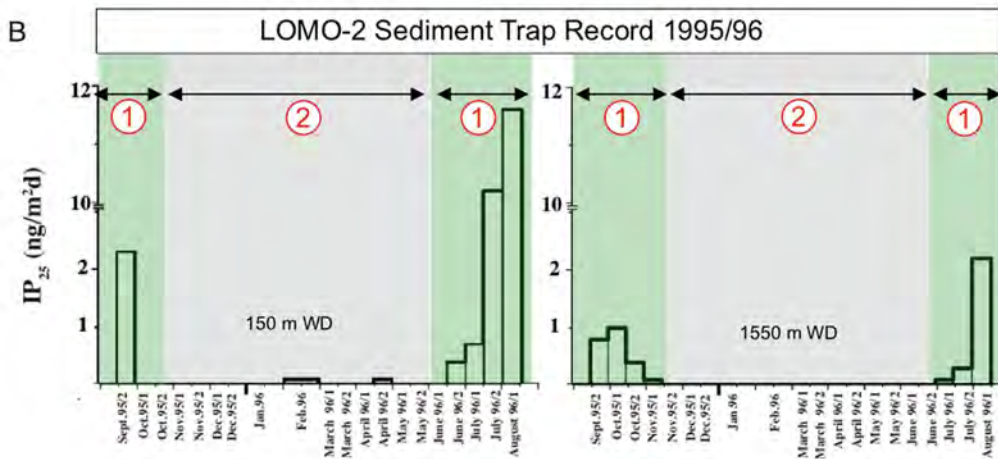
m water depth, i.e., decreased by a factor of about six. This decrease in concentration during transfer through the water column may be related to decomposition and decay of the organic compounds (FAHL & STEIN 2012), a decomposition, which certainly will continue down-core with increasing core depth and age. One should have in mind this process when comparing and interpreting absolute IP_{25} concentrations in sedimentary records of cores from different environments as well as samples from different core depth and age.

The one-year IP_{25} record obtained from the LOMO-2 sediment traps also clearly show one known ambiguity in the interpretation of IP_{25} data (cf., BELT et al. 2007, MÜLLER et al. 2009). IP_{25} is absent under a permanent ice cover limiting light penetration and, thus, sea-ice algal growth, i.e., $IP_{25} = 0$ as it also would be under totally ice-free conditions (Fig. 16). In other words, both extreme climatic situations, i.e., ice-free versus permanent sea-ice cover, would result in the same IP_{25} value of about zero. Here, MÜLLER et al. (2009, 2011) recently succeeded in overcoming this difficulty of interpretating IP_{25} data. These authors demonstrated that in surface sediments from the subpolar North Atlantic (cf., Fig. 17) and sediment cores from Fram Strait, the

ambiguity of the IP_{25} signal can be circumvented by additional use of phytoplankton-derived, open-water biomarkers such as brassicasterol or dinosterol (e.g., VOLKMAN 2006). Under a thick sea-ice cover, both IP_{25} and the phytoplankton-derived biomarker concentrations are about zero, under open-water conditions IP_{25} is zero whereas the phytoplankton biomarker concentrations may reach maximum values, and under an ice-edge situation, both IP_{25} and phytoplankton biomarker concentrations may reach very high values (Fig. 16).

In a next step, MÜLLER et al. (2011) have combined the environmental (sea surface) information carried by IP_{25} and phytoplankton biomarkers in a phytoplankton-IP_{25} index, the so-called "PIP_{25} Index". Since there is a significant concentration difference between IP_{25} and phytoplankton-derived biomarkers (e.g., brassicasterol or dinosterol), MÜLLER et al. (2011) recommend using a concentration balance factor c (based on mean concentrations of IP_{25} and the phytoplankton biomarker in a specific data set) for the calculation of the PIP_{25} index:

$$PIP_{25} = IP_{25} / (IP_{25} + (\text{phytoplankton marker} \cdot c))$$

with c = mean IP$_{25}$ concentration / mean phytoplankton biomarker concentration

The "PIP$_{25}$ approach" was used successfully to reconstruct (spring) sea-ice coverage in the subpolar North Atlantic (Fig. 17, MÜLLER et al. 2011). The PIP$_{25}$ ratios shown together with satellite-based sea-ice distribution in Figure 17A, were calculated using brassicasterol as phytoplankton biomarker ("P$_B$IP$_{25}$"). Using dinosterol concentrations (instead of brassicasterol) for the calculation of respective PIP$_{25}$ indices ("P$_D$IP$_{25}$") yields basically similar results for the study area, as pointed out by MÜLLER et al. (2011). For a more quantitative comparison of the biomarker and satellite data, IP$_{25}$ and PIP$_{25}$ values were plotted versus the sea-ice concentrations as they are displayed for the individual sediment sampling sites (Fig. 17B, MÜLLER et al. 2011). As expected, IP$_{25}$ concentrations correlate positively with ice coverage (R^2 = 0.67). This correlation, however, also highlights the fundamental ambiguity of the sea-ice proxy as relatively low IP$_{25}$ contents are observed not only for minimum but also maximum ice coverage. Thus, the sedimentary IP$_{25}$ content on its own should not be used as a direct measure for sea-ice

concentrations. This and also the slightly higher correlation of PIP$_{25}$ values with sea-ice concentrations (Fig. 17B, R^2 = 0.74) strengthen the argument that the coupling of IP$_{25}$ with a phytoplankton marker (e.g. brassicasterol) seems to be a valuable and more reliable approach for realistic sea-ice reconstructions (at least in the study area of the polar/subpolar North Atlantic). Furthermore, a comparison of this biomarker-based assessment of the sea-ice distribution in the study area with (1) modern remote-sensing data and (2) numerical-modelling results reveal a good agreement between organic geochemical, satellite and modelling observations (MÜLLER et al. 2011). The good correlation between modelled sea-ice parameters and the biomarker-based estimate of sea ice coverage substantiates that linking proxy and model data occurs to be a promising concept in terms of a cross-evaluation. This integrative data-model approach by MÜLLER et al. (2011) may provide a first step towards more quantitative sea-ice reconstructions by means of IP$_{25}$.

When using the PIP$_{25}$ index to distinguish between different sea-ice conditions, one should have in mind that coevally high amounts of both biomarkers (suggesting ice-edge conditions)
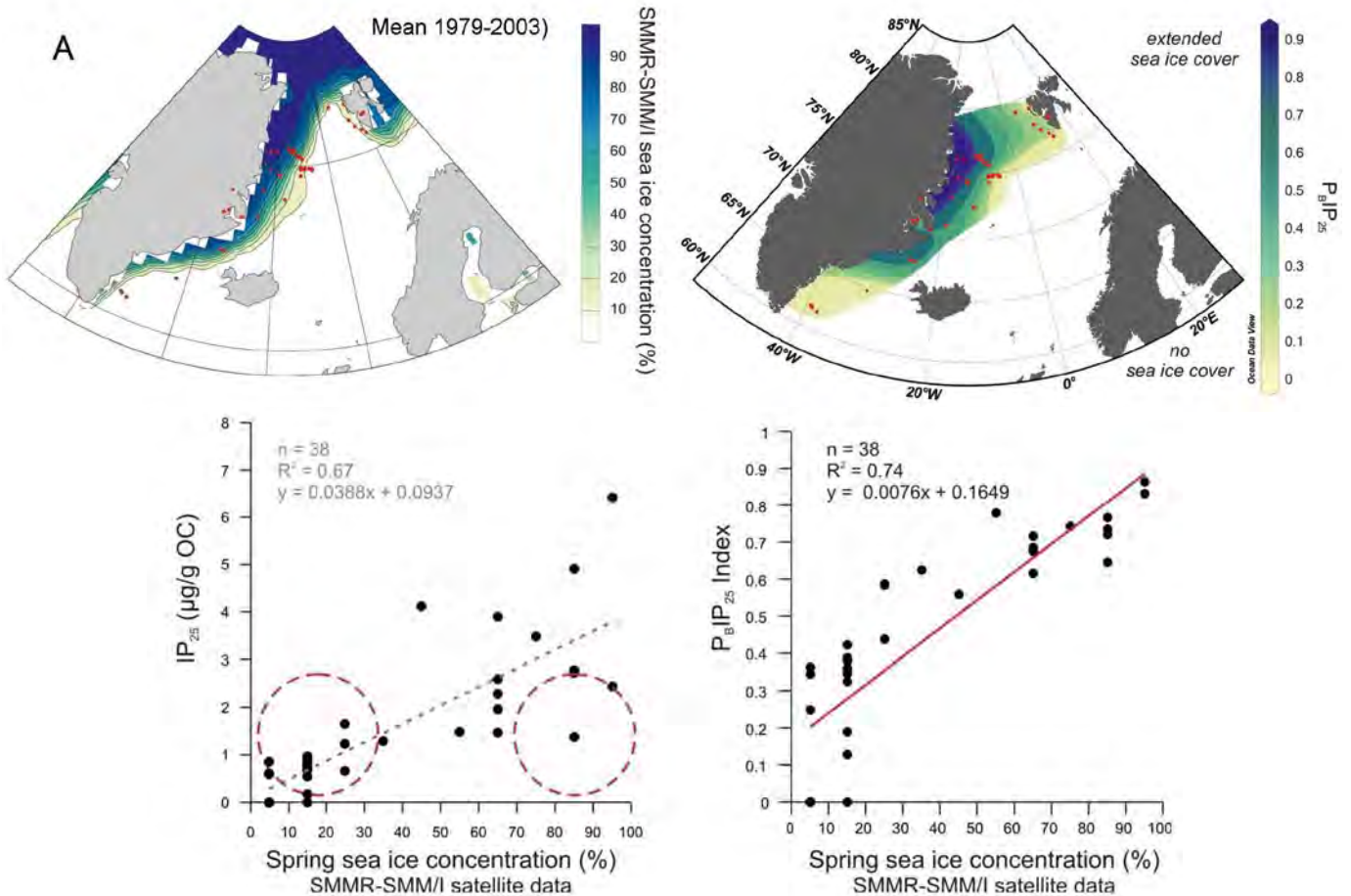
Fig. 17: Top: Comparison of the biomarker-based estimate of sea-ice coverage using the PIP$_{25}$ index (combination of IP$_{25}$ and brassicasterol data: P$_B$IP$_{25}$) with SMMR-SSM/I satellite derived mean spring (March-April-May) sea-ice concentrations. Red dots indicate location of studied surface sediment samples. Bottom: Correlation of spring (March-April-May) sea-ice concentrations (± 5 %) derived from satellite data (SMMR and SSM/I; averaged over the period of 1979-2003) with IP$_{25}$ contents and PIP$_{25}$ values (combination of IP$_{25}$ and brassicasterol data: P$_B$IP$_{25}$). Coefficients of determination (R^2) are given for the respective regression lines. Red dashed circles highlight low IP$_{25}$ concentrations, which misleadingly may be interpreted as indicative of low sea-ice concentrations though they result from severe sea-ice coverage limiting ice algae growth; (from MÜLLER et al. (2011).

Abb. 17: Vergleich der mittels IP$_{25}$ und PIP$_{25}$ rekonstruierten Meereisverbreitung mit der auf SMMR-SSMI-Satelliten-Daten basierenden gemessenen Meereisverbreitung (Frühjahr = März-April-Mai) im nördlichen Nordatlantik. Rote Punkte sind Lokationen der untersuchten Oberflächensedimentproben; (aus MÜLLER et al. 2001).

as well as coevally low contents (suggesting permanent-like ice conditions) would give a similar or even the same PIP_{25} value. Especially, for the latter situation of permanent sea-ice conditions both biomarker concentrations may approach values around zero and the calculation PIP_{25} index may become indeterminable (or misleading). That means, for a correct interpretation of the PIP_{25} data it requires essential awareness of the individual IP_{25} and phytoplankton biomarker concentrations to avoid misleading interpretations (MÜLLER et al. 2011). Although the "PIP_{25} approach" still has its limitations and needs further development and verification using additional data from other Arctic areas, the main idea of pairing IP_{25} with a productivity measure to distinguish between multiple ice and ice-free conditions, both characterized by zero IP_{25} (as introduced by MÜLLER et al. 2009, 2011), remains an important further development of the original IP_{25} approach.

RECONSTRUCTIONS OF LATE QUATERNARY ARCTIC SEA-ICE VARIABILITY BASED ON IP_{25}

The high potential of the novel biomarker proxies for a more detailed reconstruction of paleo-sea-ice cover and its variability through time is demonstrated in three examples:
- Sea-ice variability in the Fram Strait over the last 30 Cal. kyrs. BP.
- Deglacial to Holocene variability of central Arctic sea-ice cover and the Younger Dryas Event.
- Comparison of historical sea ice and IP_{25} proxy records: The last millennium.

In addition first data from an IP_{25} pilot study of MIS 6 sediments from the northern Barents Sea continental margin, are shortly presented.

*Sea-ice variability in the Fram Strait
over the last 30 Cal. kyrs. BP*

MÜLLER et al. (2009) determined the sedimentary abundance of the novel IP_{25} sea-ice proxy in core PS2837-5, recovered on the Yermak Plateau (81°13.99' N, 02°22.85' E, water depth of 1042 m) during "Polarstern" Expedition ARK-XIII/2 and located close to the modern summer sea-ice margin (Fig. 18, STEIN & FAHL 1997). The 8.76 m thick sedimentary sequence of the core represents the last Glacial to Holocene time interval (NØRGAARD-PEDERSEN et al. 2003). The main aim of the MÜLLER et al. (2009) study was to generate a record of sea-ice conditions in the northernmost Atlantic Ocean for the past 30,000 years, a study which was the first application of the novel sea-ice biomarker IP_{25} in determining Arctic sea-ice records prior to the Holocene.

At 29.6 Cal. kyrs. BP, during a short-lived event, and between 27 and 24 Cal. kyrs. BP, increased IP_{25} and brassicasterol concentrations and fluxes indicate favourable conditions for both sea-ice diatom and phytoplankton growth (Fig. 19). Since primary production is enhanced at the ice edge (SMITH et al. 1987), resulting in higher sedimentary concentrations of marine-derived biomarkers (BIRGEL et al. 2004), these elevated concentrations and fluxes of IP_{25} and brassicasterol probably reveal the occurrence of a fairly stationary ice margin (ca. 81° N, 2° E) during this otherwise perennially ice-covered interval (Fig. 19, situation (a)). An ice-edge
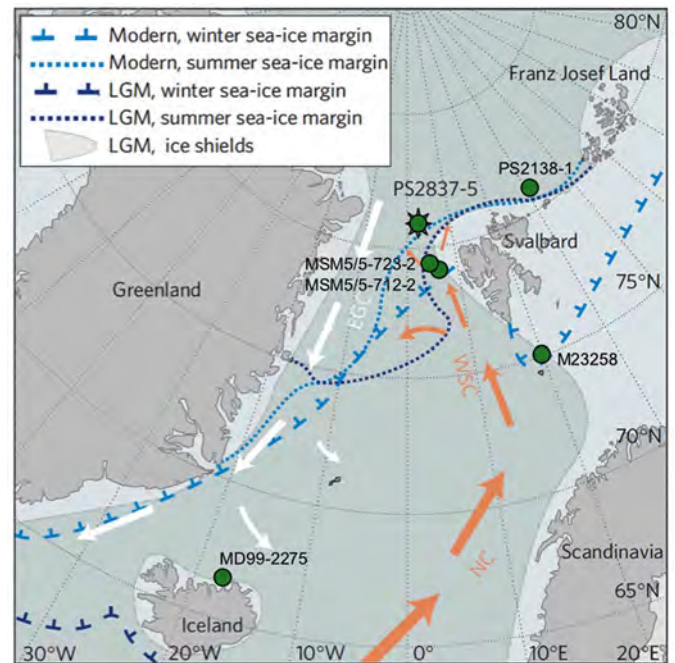

Fig. 18: Map showing the PS2837-5 core site in the northern Fram Strait, major ocean currents and sea-ice margins (from MÜLLER et al. 2009, supplemented). Light-shaded areas indicate the extent of the Greenland, Iceland and Scandinavian Ice Shields during the Last Glacial Maximum (LGM). Orange arrows refer to warm Atlantic Water inflow through the Norwegian (NC) and West Spitsbergen (WSC) currents; white arrows indicate cold polar water transported by the East Greenland Current (EGC). In addition, site locations of other cores discussed in the text, are indicated.

Abb. 18: Karte des Nordatlantiks mit Oberflächenströmungen, Meereisgrenze, und Ausdehnung der Eisschilde im Letzten Glazialen Maximum (LGM). Lokationen von Kern PS2837-5 sowie weiteren im Text genannten Sedimentkernen sind eingezeichnet (MÜLLER et al. 2009, ergänzt).

situation is also supported by PIP_{25} values around 0.5–0.6 (Fig. 19, cf., MÜLLER et al. 2011). For most of the interval between 30 and 17 Cal. kyrs. BP (Late Weichselian to early deglaciation), however, IP_{25} and brassicasterol concentrations (and fluxes) are almost zero, especially during the Last Glacial Maximum (LGM) and the early deglaciation (23.5–17 Cal. kyrs. BP) (Fig. 19). MÜLLER et al. (2009) interpreted the absence of both IP_{25} and brassicasterol as a period of permanently closed sea-ice cover, possibly resulting from an extension of the Svalbard-Barents Sea-Ice Sheet (SBIS) to the shelf edge during this time (ANDERSEN et al. 1996) and a distinct weakening of warm Atlantic water inflow into northern Fram Strait (Fig. 19, situation (b)). Under such conditions, sea-ice diatom and phytoplankton growth is limited since the presence of thick pack ice inhibits light penetration and enhanced stratification reduces nutrient availability. These observations suggest that the summer sea-ice margin during the LGM must have been located south of approx. 81° N.

Coincident with intensified Atlantic Water advection and the onset of the SBIS disintegration at about 17 Cal. kyrs. BP (ANDERSEN et al. 1996, KNIES et al. 1999), higher fluxes of IP_{25} occurred, likely as a result of reduced ice thickness and thus better light penetration and nutrient availability suitable for sea-ice diatom growth. An increase in brassicasterol concentrations lagged those observed for IP_{25} by about 400 yr (Fig. 19), consistent with a progressive retreat of the ice sheet
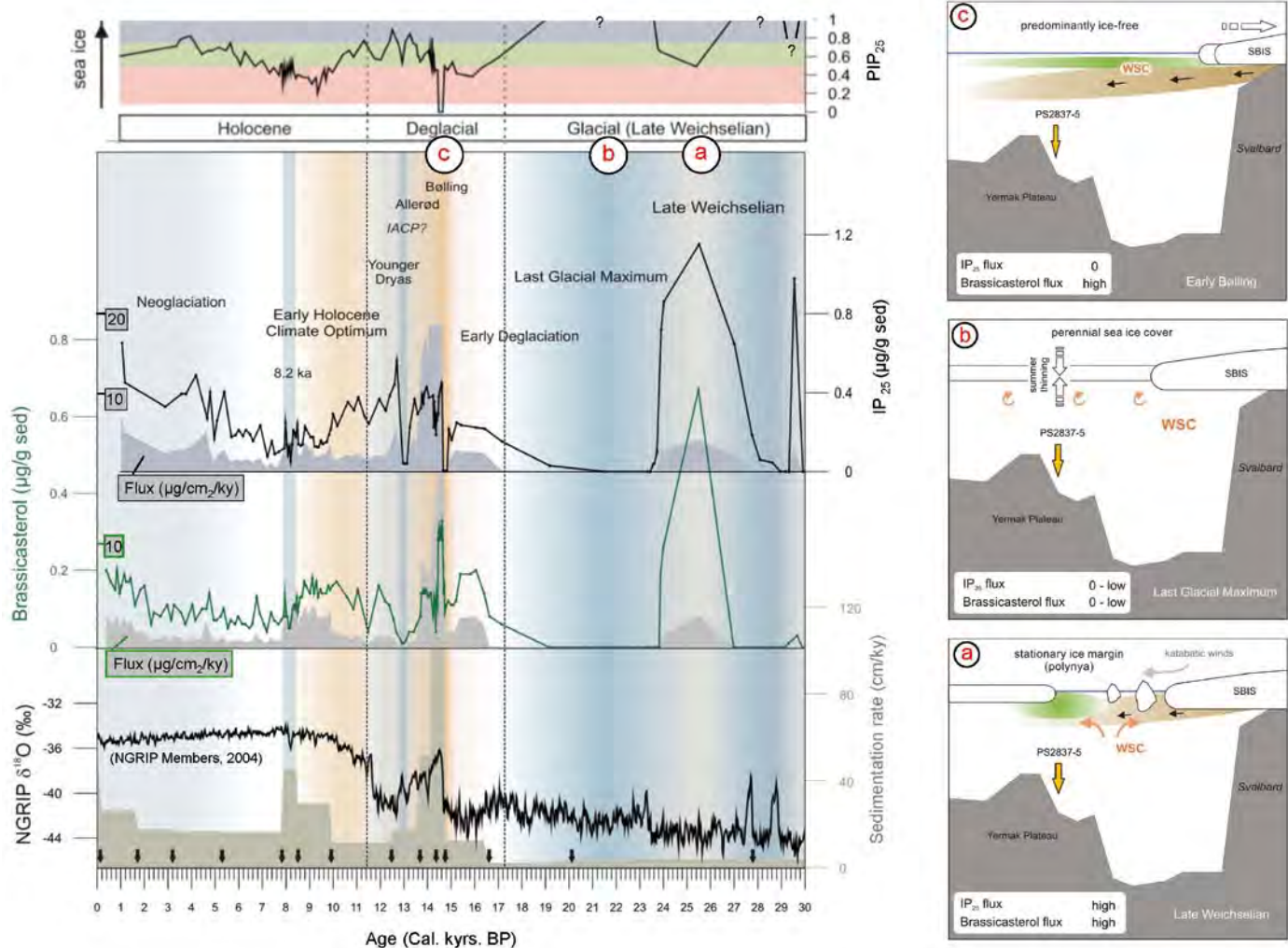
Fig. 19: Concentrations (μg g^{-1} sediment) and accumulation (flux) rates (μg cm^{-2} ky^{-1}) of brassicasterol and IP$_{25}$, PIP$_{25}$ ratios and sedimentation rates (cm ky^{-1}) of the last 30 Cal. kyrs. BP at core PS2837-5 ((BIRGEL & HASS 2004, MÜLLER et al. 2009) and δ^{18}O values from the NGRIP ice core (NGRIP MEMBERS 2004). Black arrows indicate depth of AMS^{14}C datings. Colour code in the PIP$_{25}$ record highlights periods with reduced sea-ice cover (red = PIP$_{25}$ <0.5) marginal ice zone (green = PIP$_{25}$ between 0.5 and 0.8) and extended ice-cover (grey, PIP$_{25}$ >0.8) (classification according to Müller et al., 2011). Different paleoenvironmental situations for three specific time intervals are presented in schematic models: (a) late Weichselian, (b) Last Glacial Maximum, and (c) the Bølling warm interval. Supplemented figure based on MÜLLER et al. (2009).

Abb. 19: Biomarkerdaten – IP$_{25}$, brassicasterol, und PIP$_{25}$ – in Kern PS2837-5 (BIRGEL & HASS 2004, MÜLLER et al. 2009, 2011) sowie δ^{18}O-Kurve vom NG-RIP-Eiskern. Drei Situationen mit unterschiedlichen Meereisausdehnungen sind dargestellt: (a) spätes Weichsel, (b) Letztes Glaziales Maximum (LGM) und (c) Bølling-Warminterval (nach MÜLLER et al. 2009).

and more frequent summer ice melt and open water conditions. Close to the onset of the Bølling warm phase shortly after about 15 Cal. kyrs. BP, exceptionally high sedimentation rates resulting from huge deglacial meltwater plumes carrying high amounts of fine-grained terrigenous (Svalbard) material, led to extremely high flux and preservation of brassicasterol (Fig. 19, BIRGEL & HASS 2004, MÜLLER et al. 2009). Coeval with this rapid warming, a sudden drop in IP$_{25}$ fluxes occurred for ca. 200 yr (14.8-14.6 Cal. kyrs. BP), reflecting a significantly reduced sea-ice cover. That means, open water phytoplankton has probably benefited dramatically from such essentially ice-free conditions (Fig. 19, situation (c)).

The Early Bølling was followed by an interval of variable sea-ice cover, probably close to the sea-ice edge (ca. 14.6-13 Cal. kyrs. BP), as reflected by the relatively high IP$_{25}$ and brassicasterol values as well as PIP$_{25}$ ratios between 0.5 and 0.8 (Fig. 19). With the onset of the Younger Dryas (YD) cooling

shortly after 13 Cal. kyrs. BP, IP$_{25}$ and brassicasterol values drop drastically to almost zero, suggesting a distinct increase in sea-ice coverage. An almost identical evolution resulting in maximum sea-ice coverage at the beginning of the YD was recorded at Arctic Ocean core PS2458 (FAHL & STEIN 2012, see further discussion below). During the subsequent Mid-Late YD interval, sea-ice diatom and phytoplankton activity improved due to less severe sea-ice conditions (probably a sea-ice edge situation), as indicated by increased IP$_{25}$ and brassicasterol concentrations and fluxes (Fig. 19). Such conditions probably resulted from a weak but constant inflow of warm water from the Atlantic via the West Spitsbergen Current, generating climate conditions also suitable for primary productivity (MÜLLER et al. 2009).

With the beginning of the Holocene, IP$_{25}$ values decrease whereas at the same time brassicasterol values increase, suggesting diminishing sea-ice conditions. Minimum sea-ice

coverage probably occurs between about 10 and 6.5 Cal. kyrs. BP, i.e., during the Early Holocene Climate Optimum, as indicated by reduced IP_{25} values and a minimum in PIP_{25} ratios of <0.4 (Figs. 19 and 20). This is in agreement with multi-proxy compilations based on calcareous microfossils, drift wood, bowhead whale and IP_{25} data from other Arctic sites (Fig. 21) as well as climate models indicating that early Holocene temperatures were higher than today and that the Arctic contained less ice, consistent with a high intensity of orbitally-controlled spring and summer insolation that peaked about 10-11 Cal. kyrs. BP and gradually decreased thereafter (Fig. 21, e.g., CRUCIFIX et al. 2002, LASKAR et al. 2004, GOOSSE et al., 2007, JAKOBSSON et al. 2010a, POLYAK et al. 2010).

At about 8.2 Cal. kyrs. BP, i.e., contemporaneously with the prominent "8.2 ka cooling event" (e.g., ALLEY et al. 1997,
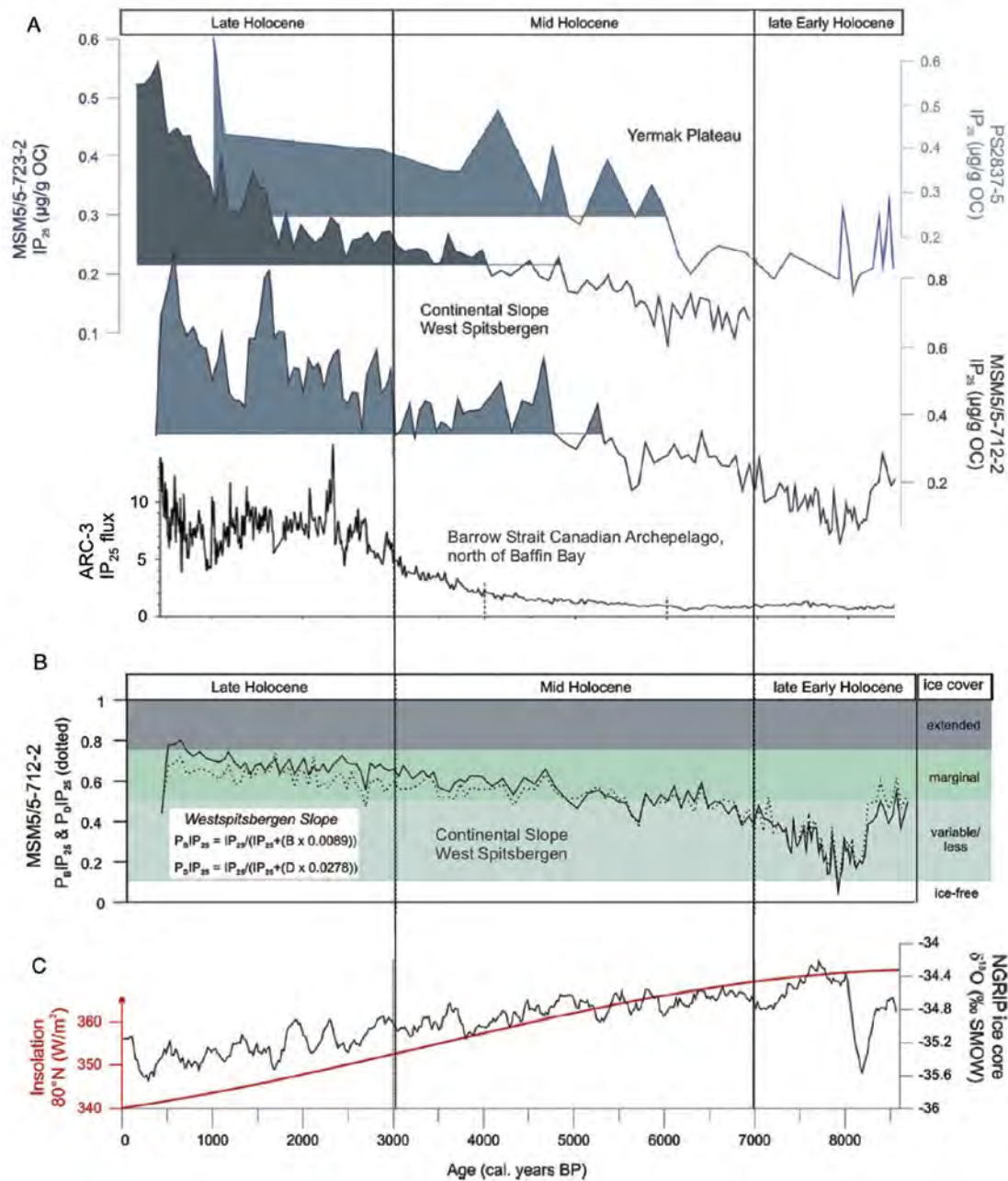
Fig. 20: A = Comparison of IP_{25} concentrations (standardized to gram organic carbon) of sediment cores from the Yermak Plateau (core PS2837-5) and the eastern Fram Strait (MSM5/5-712-2 and MSM5/5-723-2) (MÜLLER et al. 2012), and IP_{25} flux rates in core ARC-3 recovered in the Canadian Archipelago area (VARE et al. 2009). B = PIP_{25} indices calculated for core MSM5/5-712-2, using IP_{25} and brassicasterol (P_BIP_{25}; solid line) as well as IP_{25} and dinosterol accumulation rates (P_DIP_{25}; dotted line) and respective balance factors following MÜLLER et al. (2011). Estimates of sea ice conditions ($PIP_{25} > 0.1$ variable, $PIP_{25} > 0.5$ marginal, $PIP_{25} > 0.75$ extended ice cover are highlighted) (after MÜLLER et al. (2012). C = Summer insolation for 80° N (red curve, LASKAR et al. 2004) and $\delta^{18}O$ values from the NGRIP ice core (NGRIP MEMBERS 2004) strengthen a Holocene cooling. For core locations see figures 1 and 18.

Abb. 20: A = Konzentration von IP_{25} in Sedimentkernen vom Yermak-Plateau und der Fram-Straße (PS2837-5, MSM5/5-712-2 und MSM5/5-723-2, MÜLLER et al. 2009, 2012) sowie IP_{25}-Fluxraten aus der kanadischen Arktis (ARC-3, VARE et al. 2009). B = PIP_{25}-Verhältnisse von Kern MSM5/5-712-2 (MÜLLER et al. 2012). C = Sommer-Insolationswerte für 80° N (LASKAR et al. 2004) und $\delta^{18}O$-Werte im NGRIP-Eiskern (NGRIP MEMBERS 2004). Für Kern-Lokationen vgl. Abbildungen 1 und 18.

CLARKE et al. 2004, KLEIVEN et al. 2008), a short-term, rapid decrease is observed in the brassicasterol and IP_{25} records (Fig. 19). Values are low and similar to those determined for the Early YD and the LGM when near-permanent sea-ice coverage reduced not only the growth of phytoplankton but also that of ice algae. Similarly, MÜLLER et al. (2009) interpreted minimum fluxes of IP_{25} and brassicasterol as indicative for a near-perennial sea-ice cover at the western Yermak Plateau (northern Fram Strait) at about 8.2 Cal. kyrs. BP.

Coinciding with a mid-late Holocene cooling trend observed in the subpolar North Atlantic domain (e.g., ANDERSEN et al., 2004, HALD et al. 2007, MILLER et al. 2010) and a long-term decrease in summer insolation, IP_{25} values increased in Fram Strait cores PS2837-5 and, more clearly due to higher resolution record, MSM5/5-712-2 and MSM5/5-723-2 (see Fig. 18 for location), indicating an extension of sea-ice cover (Fig. 20, MÜLLER et al. 2009, 2012). Sustained oceanic surface cooling that stimulated the sea-ice formation during winter and retarded its retreat/melt during the late spring and early summer months is also supported by RASMUSSEN et al. (2007) and JENNINGS et al. (2002) who reconstruct increasingly cooler

conditions along the West Spitsbergen shelf and an increased sea-ice export through Fram Strait by means of benthic and planktic foraminifera and IRD records.

During the last 3-2 Cal. kyrs. BP, the increase in sea-ice coverage as well as amplitude of variability becomes even more pronounced (Fig. 20). Maximum IRD release and a sustained increase in the accumulation of IP_{25} during the past 3,000 years – a period that is widely acknowledged as Neoglacial cooling phase (for recent review see MILLER et al. 2010) – point to an extended sea-ice cover at the West Spitsbergen continental margin (MÜLLER et al. 2012). Further reconstructions of gradually cooled sea surface temperatures, lowered productivity, and a higher polar water ouflow to the Nordic Seas during the past 3,000 years BP support this general increase in sea-ice coverage (KOC et al. 1993, ANDREWS et al. 2001, JENNINGS et al. 2002, ANDERSEN et al. 2004). A very similar and more or less contemporaneous increase in sea-ice cover was also recorded in Barrow Strait, Canadian Archipelago north of Baffin Bay (Fig. 20, VARE et al. 2009, see Figs. 1 and 15 for location), as well as in the Bering Sea (MÉHEUST et al. 2012). The general increase in sea-ice cover and cooling
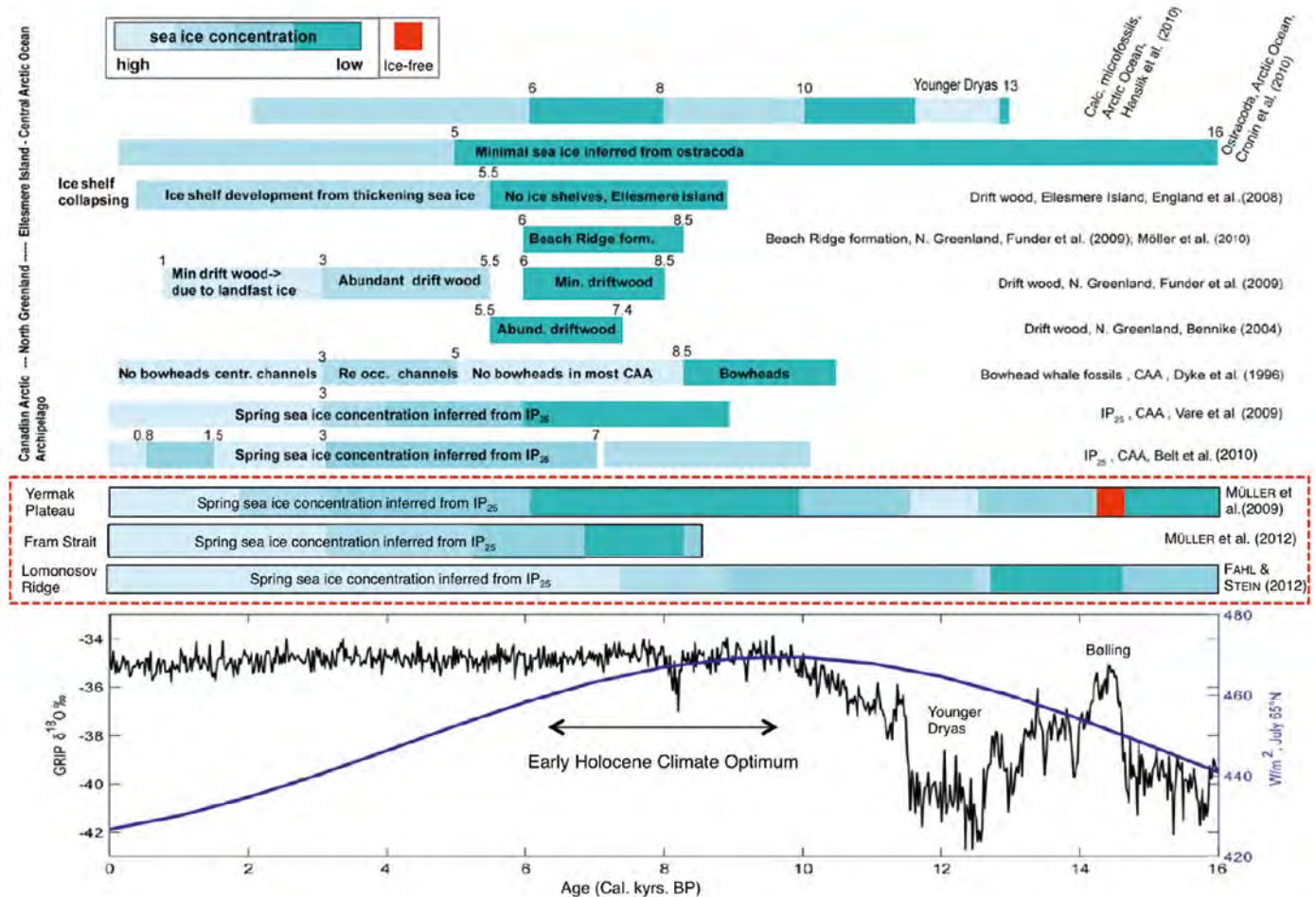
Fig. 21: Summary of results on the Arctic Ocean sea-ice variations throughout the last 15 Cal. kyrs. BP based on different proxy reconstructions (from JAKOBSSON et al. 2010a, supplemented). The inferred scale of sea-ice concentration is a highly qualitative scale in order to compare the results from the different studies. Recent own studies using the novel IP_{25} biomarker approach are added and highlighted. References are listed at the right margin. The GRIP $\delta^{18}O$ record is from JOHNSEN et al. (2001) and the solar insolation from BERGER & LOUTRE (1991).

Abb. 21: Übersichtsdarstellung zur Meereisverbreitung im Arktischen Ozean nach verschiedenen Proxydaten während der letzten 15.000 Jahre vor Heute (JAKOBSSON et al. 2010a, ergänzt durch weitere eigene IP_{25}-Datensätze). GRIP $\delta^{18}O$-Kurve von JOHNSEN et al. (2001), Insolationskurve nach BERGER & LOUTRE (1991).

of surface waters in the northpolar region during this Neoglacial cooling phase occur more or less contemporanously with an advance of glaciers in western Norway (NESJE et al. 2001), a decrease in temperature and precipitation in Siberia (ANDREEV & KLIMONOV 2000), and a decrease in Siberian river discharge into the Arctic Ocean (STEIN et al. 2004). This variability may reflect natural cyclic climate variations to be seen in context with the interannual and interdecadal environmental changes recorded in the High Northern Latitudes over the last decades, such as the North Atlantic Oscillation/Arctic Oscillation (NAO/AO) pattern (e.g., DICKSON et al. 2000). That means, for example, the reduced Siberian river discharge during the past 2-3 Cal. kyrs. BP and vegetation changes in northeast European Russia, indicating the development of a colder and dryer climate in the Eurasian Arctic, may be related to negative NAO-like conditions (STEIN et al. 2004, SALONEN et al. 2011, see MÜLLER et al. 2012 for more detailed discussion).

Deglacial/Holocene variability of central Arctic sea-ice cover and the Younger Dryas Event

In order to study the deglacial/Holocene variability of central Arctic sea-ice cover, core PS2458-4 has been studied in detail for its biomarker composition, focussing on IP_{25} and brassicasterol data (FAHL & STEIN 2012). The core was recovered from the upper eastern Laptev Sea continental slope (78°09.95' N, 133°23.86' E, water depth 983 m, see Fig. 15 for location) during "Polarstern" Cruise ARK-IX/4 and consists of a 8 m long sedimentary sequence of dominantly very dark olive-gray silty clay of mainly terrigenous origin (FÜTTERER 1994). Based on several AMS-^{14}C datings carried out on bivalves, a very reliable chronology is available for the sediment section between about 250 and 650 cm core depth (Figs. 22 and 23), representing a time interval between about 14.7 and 9.3 Cal. kyrs. BP (SPIELHAGEN et al. 2005). That means, very prominent cold and warm phases such as the Bølling/Allerød warm period and the Younger Dryas (YD) Cooling Event are represented within the studied sediment section. The base of the core has an extrapolated age of about 16.5 ka, i.e., Heinrich Event 1 (HE 1) was probably recovered in the lowermost part of the core (Fig. 22, FAHL & STEIN 2012).

Looking at the long-term trend of the IP_{25} record of Core PS2458-4, an increase in IP_{25} from the Bølling-Allerød warm period towards the Modern is obvious, interpreted as long-term increase in sea-ice cover near the core location (FAHL & STEIN 2012). With the long-term increase in sea ice during deglacial-Holocene times, the HBI diene ($C_{25:2}$) decreases. This decrease is even more pronounced if the diene/IP_{25} ratio is used

(Fig. 22). A very similar trend was described by VARE et al. (2009) in a sediment core from the Canadian Arctic Archipelago (see Fig. 15 for location). Following ROWLAND et al. (2001) who found that the more unsaturated HBI isomers (i.e., the diene in comparison to the monoene) are formed at higher diatom growth temperatures, we as well as VARE et al. (2009) postulate warmer climatic conditions during periods characterized by higher relative concentrations of the diene over the IP_{25}, i.e., higher diene/IP_{25} ratios. That means, the diene/IP_{25} ratio might be indicative for higher sea-surface temperatures (SSTs). Our interpretation is also supported by the generally positive correlation between diene/IP_{25} ratios determined in surface sediments from the Kara and Laptev seas and mean summer SST from the same area extracted from the World Ocean Atlas (XIAO et al., 2012).

In Figure 23, the biomarker records of the well-dated core section between 250 and 650 cm core depth are plotted versus age to have a closer look at the short-term variability. Within the Bølling-Allerød warm interval, minimum IP_{25} and PIP_{25} values were found. In detail, PIP_{25} values display three minimum values at 14.6, 13.5, and 13.1 Cal. kyrs. BP (Fig. 23), indicating a minimum sea-ice cover during these events. Further support for warmer, more ice-free climate conditions during that period also comes from the elevated HBI diene concentrations determined in the core PS2458-4 section (FAHL & STEIN 2012). Whereas in the Holocene interval the diene/IP_{25} ratio is around 3 and shows a low variability, the diene/IP_{25} ratios are distinctly higher in the Bølling-Allerød period
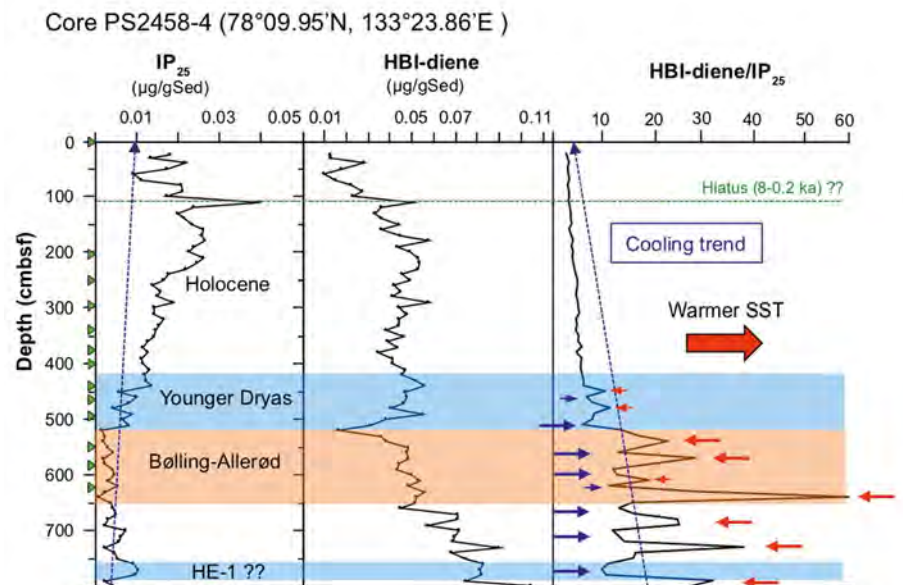
Fig. 22: Concentrations of IP_{25} and HBI-diene (μg g⁻¹ sed.) and diene/IP_{25} ratios determined in sediments from ore PS2458-4, plotted *versus* core depth (data from FAHL & STEIN 2012). Bølling-Allerød, Younger Dryas and Holocene intervals are indicated. Green triangles mark depth of AMS-^{14}C datings, stippled horizontal green line marks a possible hiatus at about 100 cm core depth (for age modell see SPIELHAGEN et al. 2005). Heinrich Event 1 (HE 1) is probably represented in the lowermost part of the section if using the extrapolated age of 16.4 Cal. kyrs. BP. Small blue arrows highlight colder intervals, small red arrows highlight warmer intervals. Stippled blue arrows indicate long-term increase in sea ice and cooling trend, respectively. Based on these biomarker records, sea ice and SST display a high-amplitude, centennial-scale variability during deglacial times, whereas towards the Holocene climate became more stable.

Abb. 22: Konzentrationen von IP_{25} und HBI-Dien (in μg g⁻¹ Sed.) sowie Dien/IP_{25}-Verhältnisse im Kern PS2458-4 (FAHL & STEIN 2012). Die Zeitabschnitte Heinrich-Event 1 (HE-1, extrapoliertes Alter), Bølling-Allerød, Jüngere Dryas und Holozän sind angezeigt. Kleine blaue (rote) Pfeile markieren kalte (warme) Zeitabschnitte.
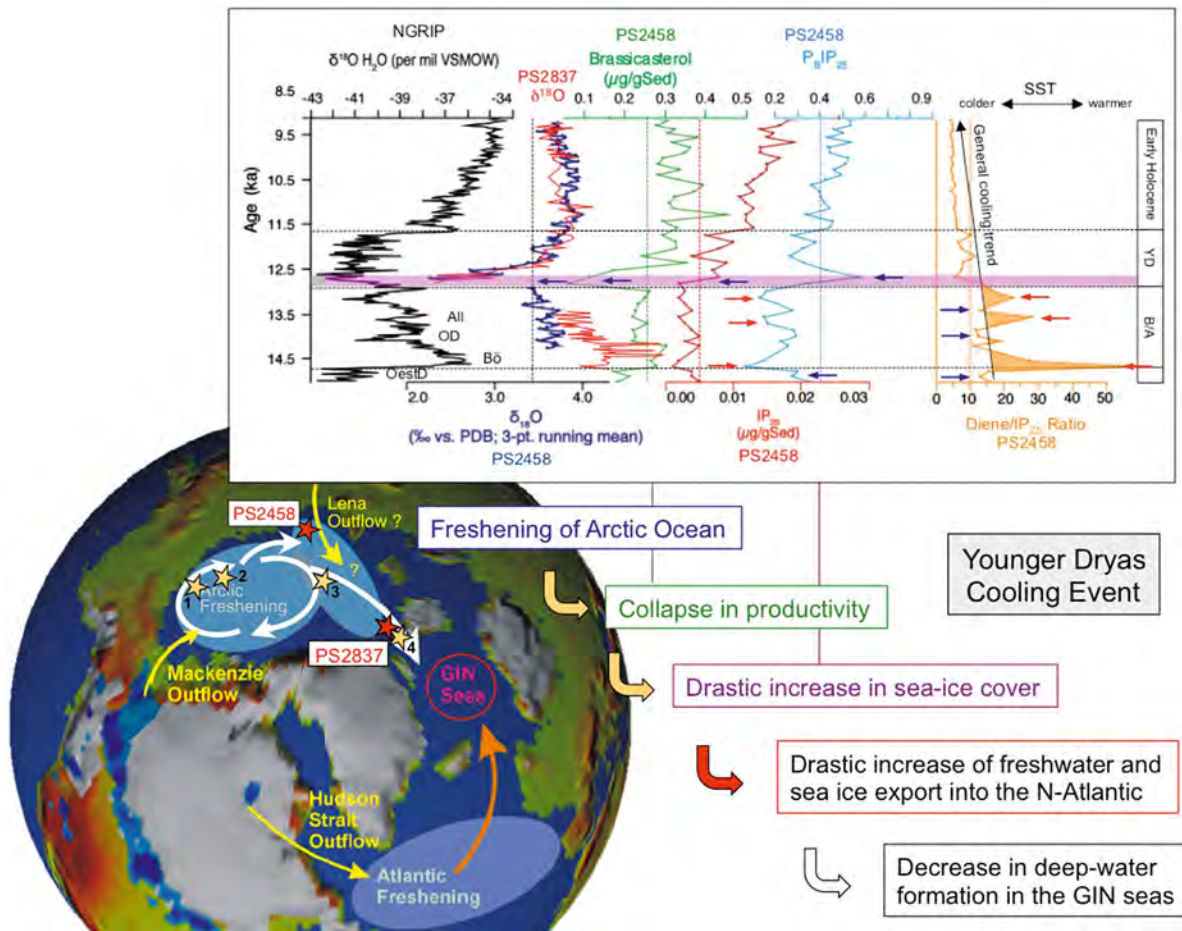
Fig. 23: Oxygen isotopes of planktic foraminifer *Neogloboquadrina pachyderma* sin. (SPIELHAGEN et al. 2005), concentrations of brassicasterol and IP$_{25}$, diene/IP$_{25}$ ratio, and PIP$_{25}$ index (combination of IP$_{25}$ and brassicasterol data: P$_B$IP$_{25}$) determined in the AMS-^{14}C dated interval 14.7 to 9.3 Cal. kyrs. BP of core PS2458-4, and paleoenvironmental interpretation. In addition, the NGRIP δ^{18}O record (NGRIP MEMBERS, 2004) as well as a δ^{18}O record of planktic foraminifer *N. pachyderma* sin. determined at core PS2837-5 (red curve, NØRGAARD-PEDERSEN et al. 2003), are shown. Small blue arrows highlight colder intervals, small red arrows highlight warmer intervals. The long black arrow indicates long-term cooling trend. All = Allerød; OD = Older Dyras; Bø = Bølling; OestD = Oldest Dyras; YD = Younger Dryas; B/A = Bølling/Allerød. (from Fahl & Stein 2012, supplemented).

In the map of the Northern Hemisphere, areas in which intense freshwater forcing likely occurred, and distribution of land ice (light grey) and pro-glacial lakes (blue) at the beginning of the Younger Dryas (12.9 Cal. kyrs. BP) are shown (PELTIER et al. 2006, supplemented). As possible additional (more local) source for freshwater supply into the Arctic Ocean, Lena discharge into the Laptev Sea was added (according to SPIELHAGEN et al. 2005). Locations of cores showing distinct deglacial meltwater events in δ^{18}O and δ^{13}C records of planktic foraminifers near the Younger Dryas Event, are indicated: 1 = Chukchi margin (POLYAK et al. 2007); 2 = Mendeleev Ridge (POORE et al. 1999); 3 = Eurasian Basin (STEIN et al. 1994a, 1994b, NØRGAARD-PEDERSEN et al. 1998, 2003); 4 = Fram Strait (BAUCH et al. 2001a) as well as Yermak Plateau core PS2837-5 (NØRGAARD-PEDERSEN et al. 2003).

Abb. 23: δ^{18}O-Kurve von planktischen Foraminiferen (SPIELHAGEN et al. 2005), Konzentrationen von Brassicasterol und IP$_{25}$, Dien/IP$_{25}$ und PIP$_{25}$-Verhältnisse (FAHL & STEIN 2012) im Kern PS2458-4 und δ^{18}O-Kurve von planktischen Foraminiferen im Kern PS2837-5 (NØRGAARD-PEDERSEN et al. 2003) für den Zeitabschnitt 14.7 bis 9.3 ka sowie Interpretation der Proxydaten in Hinblick auf Süßwassereintrag, Meereisbildung, Meereisexport und Tiefenwasserbildung im Nordatlantik (ergänzt nach FAHL & STEIN 2012). Die Karte zeigt Gebiete mit verstärktem Süßwassereintrag zum Beginn der Jüngeren Dryas (ergänzt nach PELTIER et al. 2006). Lokationen von Sedimentkernen mit starkem Süß-/Schmelzwassersignal zum Beginn der Jüngeren Dryas sind eingetragen (Ziffern 1 bis 4)

and vary between about 10 and 60 (Fig. 23), i.e., the more unsaturated HBIs become more predominent in comparison to IP$_{25}$, suggesting significantly warmer but also more variable climate conditions during this time interval. The absolute maximum in the diene/IP$_{25}$ ratio of 60, coinciding with the absolute PIP$_{25}$ minimum of 0.05, supports minimum sea-ice (probably almost ice-free) conditions during the peak Bølling warm interval (Fig. 23, FAHL & STEIN 2012). Such extreme ice-free conditions during the Bølling peak warm interval were also described in core PS2837-5 from Fram Strait, contemporaneously with a distinct maximum in phytoplankton productivity (Figs. 19 and 21, MÜLLER et al. 2009).

At the end of the Bølling-Allerød interval, i.e., towards the transition to the YD cold interval, major changes in fresh-

water discharge, primary productivity, and sea-ice cover were recorded in the sedimentary section of core PS2458-4. With the onset of the YD, a strong freshwater signal was determined by a very prominent minimum in δ^{18}O of planktic foraminifers (Fig. 23, SPIELHAGEN et al. 2005). The exact onset of the rapid outburst of freshwater is somewhat critical as directly below the δ^{18}O minimum at 12.7 Cal. kyrs. BP foraminifers are absent in the sediments, interpreted as a drop in salinity below critical limit for foraminifer growth. That means that probably at this time (about 13 Cal. kyrs. BP) the maximum freshwater discharge occurred (SPIELHAGEN et al. 2005). Parallel to the distinct freshwater event, phytoplankton productivity seems to be drastically decreased, followed by a sudden increase in sea-ice cover, as reflected in the abrupt drop in brassicasterol concentrations and the very prominent PIP$_{25}$ increase,

respectively (Fig. 22, FAHL & STEIN 2012). These data may indicate that enhanced freshwater flux related to a local Lena river input (SPIELHAGEN et al. 2005) and/or contributions from other (Canadian?) freshwater sources (FAHL & STEIN 2012) may have increased sea-ice formation in the southern Lomonosov Ridge area close to the Laptev Sea continental margin at the beginning of the YD (for further discussion see FAHL & STEIN 2012).

Some evidence for a distinct freshwater event near the beginning of the YD was also found in sediment cores from other Arctic Ocean areas. For example, during the last deglaciation, strong meltwater signals are recorded in sharp depletions in $\delta^{18}O$ as well as $\delta^{13}C$ values determined in planktic foraminafers in sediment cores from the Mendeleev Ridge and Makarov Basin through the Lomonosov Ridge and Amundsen Basin to the eastern Gakkel Ridge/Nansen Basin region (STEIN et al. 1994a, 1994b, NØRGAARD-PEDERSEN et al., 1998, 2003, POORE et al. 1999, ANDERSSON et al. 2003, POLYAK et al. 2007). Very low sedimentation rates, however, make it difficult to clearly identify the YD Event in these cores. "Marine" evidence for a major Mackenzie drainage event in the Canadian Arctic related to the decay of the Laurentide Ice Sheet, and increased sea-ice formation at the onset of the YD was proposed from elevated IRD with a mineralogical (dolomite) signature indicative for a Canadian origin, found in a sediment core from Lomonosov Ridge close to the North Pole (NOT & HILLAIRE-MARCEL 2012). Finally, a strong contemporaneous meltwater input from the Arctic Ocean into the North Atlantic was also deduced due to the distinct decrease in planktic $\delta^{18}O$ identified in the Fram Strait core PS1230-1 (BAUCH et al. 2001a; see Fig. 11 for location) as well as in the Yermak Plateau core PS2837 (Fig. 23, NØRGAARD-PEDERSEN et al. 2003) at the beginning of the YD interval. Thus, the described deglacial freshwater and sea-ice event (probably) coinciding

with the YD Cooling Event, seems to be a basin-wide event having influenced the entire Arctic Ocean.

The importance and consequences of such a major Arctic Ocean freshwater and sea-ice event has to be seen in context with the ongoing discussion of trigger mechanisms for the onset of the YD cooling event, e.g., an extraterrestrial impact hypothesis (ISRADE-ALCÁNTARA et al. 2011 and references therein) and a paleoceanography-driven hypothesis (e.g., BROECKER et al. 1989, MCMANUS et al. 2004, BROECKER 2006). Most recently BROECKER et al. (2010) concluded that, based on the study of Terminations IV to I in Antarctic ice-core records, there is perhaps even no need for a one-time catastrophic event to explain the YD and similar YD-like events accompanied previous deglacial periods as well. In the paleoceanography community, there is still broad support for the hypothesis that the YD cooling event was probably a response to a slowdown in Atlantic Meridional Overturning Circulation (AMOC) due to a huge meltwater input into the North Atlantic, related to the deglacial decay of the Laurentide Ice Sheet (e.g., BROECKER et al. 1989, MCMANUS et al. 2004, BROECKER 2006). Here, almost contemporaneously with the onset of the YD, a huge outflow event of 9.5 10^3 km³ freshwater (or a flux of 0.30 Sv if assuming a release within one year) from the North American glacial Lake Agassiz into the North Atlantic has been proposed (e.g., TELLER et al. 2002), which may have weakened the deep-water formation in the Greenland, Islandic, Norwegian seas and, thus, the global THC during this interval (BROECKER et al. 1989, CLARK et al. 2002, TELLER et al. 2002, MCMANUS et al. 2004). There is, however, an ongoing debate about the origin and pathways of freshwater (Fig. 23, e.g., BROECKER 2006, BROECKER et al. 2010), i.e., whether the freshwater/meltwater was directly supplied (via Hudson Bay) into the Atlantic Ocean (BROECKER et al. 1989) or whether the drainage of Lake Agassiz was towards the
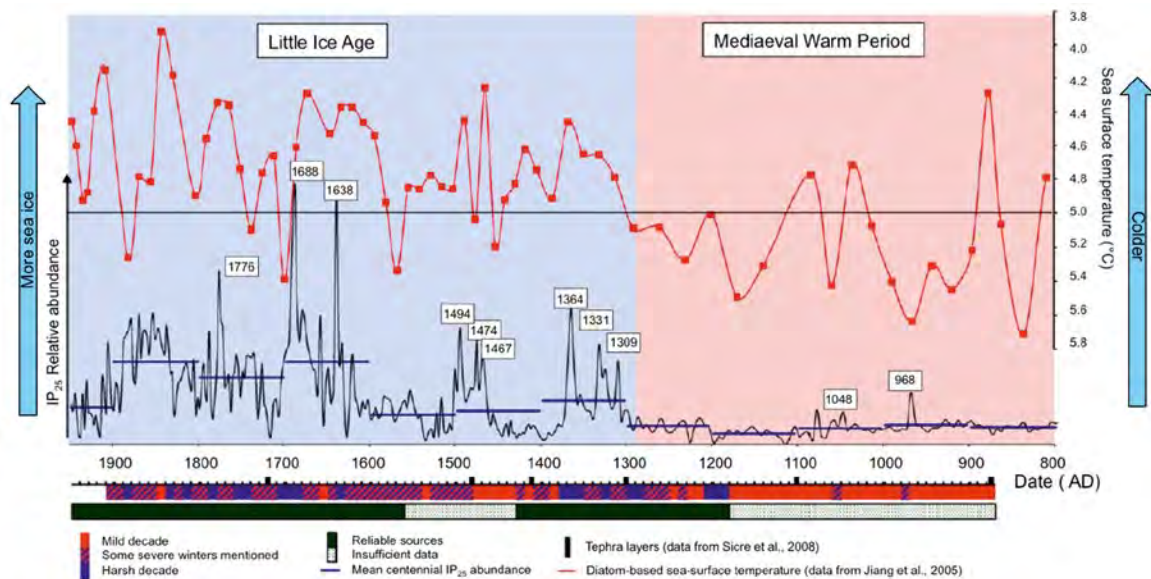
Fig. 24: Relative abundances of IP$_{25}$ determined in core MD99-2275 for the period 800-1950 AD in comparison to historical records of Icelandic sea ice (according to OGILVIE 1992 and OGILVIE & JÓNSSON 2001) and diatom-based sea surface temperature. Note the reversed scale of the sea surface temperature. Six tephra layers were used to constrain the (AMS^{14}C-dated) age model (SICRE et al. 2008). Figure from MASSÉ et al. (2008), supplemented.

Abb. 24: Relative Konzentrationen von IP$_{25}$ in Kern MD99-2275 für den Zeitabschnitt 800-1950 (MASSÉ et al. 2008) im Vergleich zu historischen Aufzeichnungen der Meereisverbreitung um Island (OGILVIE 1992 und OGILVIE & JÓNSSON 2001) und rekonstruierten Oberflächenwassertemperaturen nach Diatomeenverteilungen. Abbildung ergänzt aus MASSÉ et al. (2008).

Arctic Ocean with a subsequent export of freshwater through Fram Strait into the Atlantic (TARASOV & PELTIER 2005, PELTIER et al. 2006). PELTIER et al. (2006), for example, could show that such freshening of the surface of the Arctic Ocean would have been as efficient for shutting down the Atlantic THC as would direct Atlantic freshening. A third option, of course, could be that both hypotheses are right.

As stated by BROECKER (2006), a clear proof of the path taken by the flood was still missing. MURTON et al. (2010) could identify such a missing flood path, evident from gravels and a regional erosion surface, running through the Mackenzie River system in the Canadian Arctic Coastal Plain. From optically stimulated luminescence (OSL) dating, these authors have determined the approximate age of this Mackenzie River flood into the Arctic Ocean to be shortly after 13 Cal. kyrs. BP, supporting the hypothesis that a trigger of the YD Event may have been along the Arctic route. Our new data from core PS2458 certainly cannot prove or disprove this hypothesis. However, these data (Fig. 23), especially in combination with the other $\delta^{18}O$ records of planktic foraminifers from the central Arctic Ocean towards the Fram Strait (see above), point at least to increased, wide-spread freshening and sea-ice formation in the Arctic and related freshwater and sea-ice export through Fram Strait near the beginning of the YD. That means, these observations are in line with the hypothesis that freshwater (and ice) export from the Arctic into the North Atlantic may have played an important trigger role during the onset of the YD cold reversal, as proposed by TARASOV & PELTIER (2005).

Comparison of historical sea ice and IP$_{25}$ proxy records: The last millennium

MASSÉ et al. (2008) have measured the sea-ice proxy IP$_{25}$ to obtain a complete and continuous, high resolution (ca. 2–5 yr!) record of sea-ice distribution for the last millennium, using a well-dated sediment core recovered from the area directly north of Iceland and characterized by very high sedimentation rates (core MD99-2275: 66° 33.06‘ N, 17° 41, 59‘ W, 410 m water depth, for location see Fig. 18). This unique high-resolution proxy record was compared with historical data documenting past sea ice over the last about one thousand years (i.e., going back to the early days of Icelandic colonization, OGILVIE 1992 and OGILVIE & JÓNSSON 2001) and with diatom-based sea surface temperature reconstructions, indicating a strong correlation between these data sets on both longer and shorter time scales (JIANG et al. 2005) (Fig. 24). That means, during the Warm Mediaeval Period (MWP) between 800 and 1300 AD the Icelandic climate was relatively mild and sea ice extension was reduced. During the time interval between 1300 and 1900 AD, a period corresponding to the Little Ice Age (LIA), on the other hand, the climatic conditions around northern Iceland detriorated, i.e., this period is characterized by a significant cooling of surface water and and an increase in sea ice. Even on shorter-time scales, partly excellent correlations between historical observations and IP$_{25}$ values are obvious, indicating abrupt climate changes around Iceland. For example, the IP$_{25}$ record displays strong peaks in sediments dated to 1776, 1688, 1638, 1364, 1331 and 1309, corresponding to decades where large amounts of sea ice have been described around Iceland (OGILVIE & JÓNSSON 2001) and colder diatom-based sea

surface temperatures have been determined (JIANG et al. 2005) (Fig. 24, MASSÉ et al. 2008). With this high-resolution study, MASSÉ et al. (2008) could demonstrate very well that IP$_{25}$ is a reliable proxy for historical sea ice reconstructions.

Pilot study of core PS2138-1: IP$_{25}$ found in MIS 6 sediments

So far, IP$_{25}$ could be detected in sediments no older than 30 Cal. kyrs. BP (MÜLLER et al. 2009). However, in order to test whether IP$_{25}$ can also be found in sediments older than 30 ka (MÜLLER et al., 2009), we carried out a pilot study, using a set of samples taken from core PS2138-1 representing the last 150 Cal. kyrs. BP (i.e., MIS 6 to MIS 1, for core location see Fig. 18). In previous studies of this well-dated sediment core, detailed sedimentological, organic geochemical and micropaleontological investigations were performed for reconstruction of the late Quaternary history of the Svalbard-Barents Sea Ice Sheet and related paleoceanographic circulation patterns in the Arctic Ocean along the Barents Sea continental margin (KNIES et al. 1999, 2000, MATTHIESSEN & KNIES 2001, WOLLENBURG et al. 2001, 2004).

Using a transfer function approach to estimate paleoproductivity from relative abundance data of benthic foraminiferal species, WOLLENBURG et al. (2001, 2004) determined the paleoproductivity and its change during the last about 150 Cal. kyrs. BP in core PS2138-1 (Fig. 25). From this record it is obvious that calculated paleoproductivity values generally correlate with the growth and decay of the Svalbard Ice Sheet (ELVERHØI et al. 1995, KNIES et al. 1998, MANGERUD et al. 1998). The highest paleoproductivity occurred in interglacial period MIS 5.5 and at the termination of interstadials to stadials within MIS substages 6.3(?), 5.3, 5.1, 3.2, and Termination Ia. These productivity maxima are related to distinct ice retreat and partly coincide with the increased inflow of temperate and saline Atlantic Water into the Arctic Ocean (WOLLENBURG et al. 2001). During glacial periods, on the other hand, productivity was significantly reduced, suggesting increased sea-ice cover. During the latter intervals, also significant concentrations of the sea-ice proxy IP$_{25}$ were found, in accordance with the interpretation by Wollenburg et al. (2001) (Fig. 25).

Although only a limited number of samples have been studied for IP$_{25}$ here and also large gaps exit in the record of core PS2138-1, these preliminary results are very promising. Our qualitative IP$_{25}$ data indicate that IP$_{25}$ may also occur in sediments as old as MIS 6, i.e., the IP$_{25}$ approach can also be used for the reconstruction of sea-ice cover during glacials significantly older than MIS 2. A more detailed IP$_{25}$ study of MIS 5 and MIS 6 sedimentary sections from several Arctic Ocean cores is underway (see Fig. 15, STEIN et al. unpublished).

CONLUSIONS AND OUTLOOK

Arctic Ocean sea-ice cover and its change through Cenozoic times

The Cenozoic history of Arctic Ocean sea-ice cover can be reconstructed by different sedimentological, mineralogical, micropaleontological, and organic-geochemical proxies, as
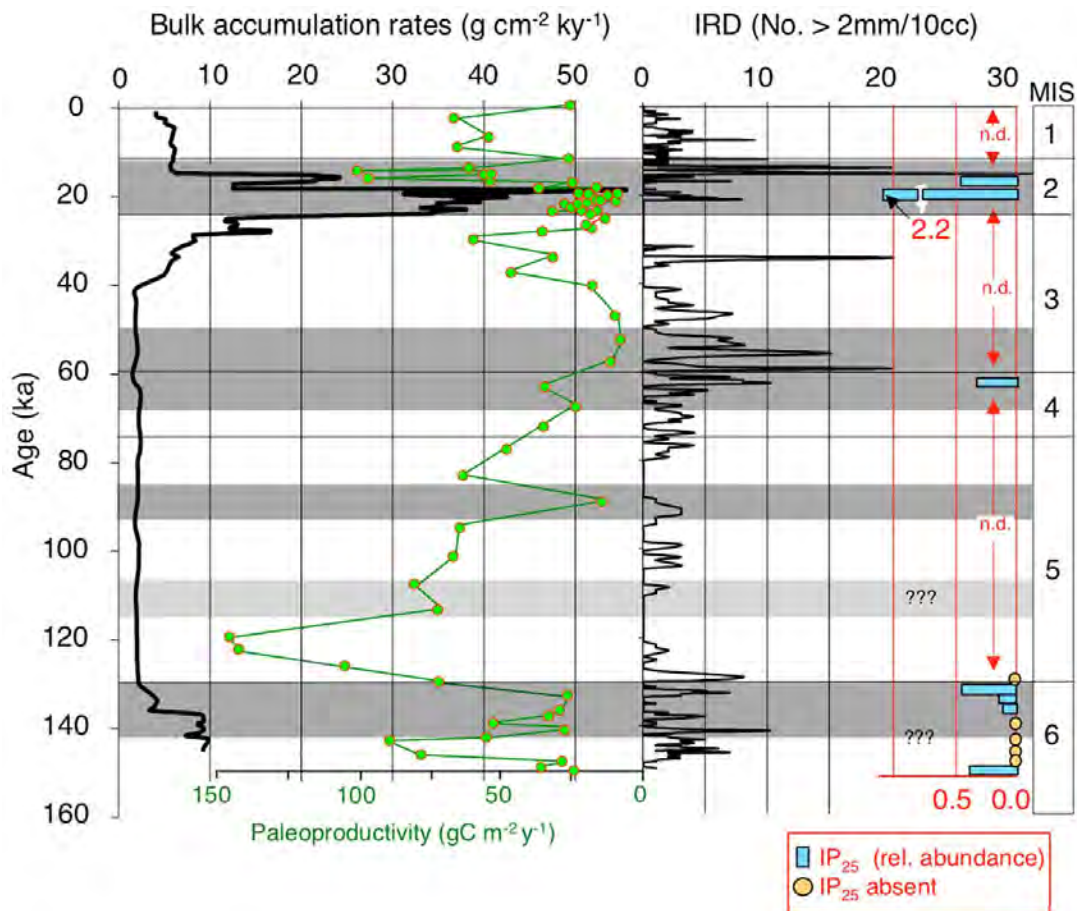
Fig. 25: Relative abundance of IP_{25} (this study), bulk accumulation rates and IRD variability (KNIES et al. 2000) and a paleoproductivity record based on benthic foraminifers (WOLLENBURG et al. 2001) determined for core PS2138-1 (for location see Fig. 18) and plotted *versus* age. Within our pilot study the first IP_{25} measurements were carried-out in a selected set of samples, proving that IP_{25} is even preserved in sediments as old as about 150 ka (MIS 6); n.d. = no data so far. Grey bars indicate time intervals of an extended ice sheet on Svalbard (MANGERUD et al. 1998). According to WINKELMANN et al. (2008), the extension of the ice sheet was much smaller around 110 ka (MIS 5.4) than originally proposed by MANGERUD et al. (1998) (light grey bar).

Abb. 25: Relative Konzentration von IP_{25} (diese Arbeit), Gesamtakkumulationsraten und IRD-Verteilungen (KNIES et al. 2000) und aus benthischen Foraminiferenvergesellschaftungen berechnete Paläoproduktivitäten (WOLLENBURG et al. 2001) im Kern PS2138-1 für den Zeitabschnitt der letzten 150 ka (MIS 6 bis MIS 1). Graue Balken zeigen Zeitabschnitte mit ausgedehnter Vereisung auf Svalbard (MANGERUD et al. 1998).

presented and discussed for a selected set of examples in this review paper.

- Records of ice-rafted debris (IRD), specific sea-ice related needle-shaped diatoms, and mineralogical composition of the terrigenous sediment fraction determined in the ACEX drill core recovered on Lomonosov Ridge during IODP Expedition 302, give information about the first onset of Arctic Ocean seasonal sea-ice cover at about 47 Ma, the development of first perennial (?) sea-ice cover near 14 Ma, and the variability of sea-ice cover through Neogene-Pleistocene times (e.g., DARBY 2008, KRYLOV et al. 2008, ST. JOHN 2008, STICKLEY et al. 2009, O'REGAN et al. 2010).

- Records of IRD and its mineralogy, in combination with abundances of planktic foraminifers, allowed reconstruction of glacial and interglacial variability of sea-ice cover and ice-sheet fluctuations during late Quaternary times, i.e., MIS 6 to MIS 1 (e.g., SPIELHAGEN et al. 1997, 2004, STEIN 2008). These data, however, also raise new interesting questions about pre-MIS 6 variations that need to be studied more carefully (e.g., POLYAK et al. 2009, 2010, O'REGAN et al. 2010).

- Fluxes of planktonic foraminifers and $\delta^{18}O$ records determined in well-dated sediment cores from the Eurasian sector of the Arctic Ocean constrained sea-ice distribution during the Last Glacial Maximum (LGM) (e.g., NØRGAARD-PEDERSEN et al. 2003).

- Abundances of specific Fe oxides determined in a sediment core from the central Fram Strait were used to identify the circum-Arctic source areas of the terrigenous sediment fraction (IRD), providing insights into the LGM, deglacial to Holocene Arctic Ocean sea-ice cover and ice-sheet decay (DARBY et al. 2002).

- The "IP_{25}" sea-ice proxy in combination with phytoplankton biomarkers (BELT et al. 2007, MÜLLER et al. 2009, 2011) determined in sediment cores from the Fram Strait and from the southern Lomonosov Ridge close to the Laptev Sea continental margin, allowed reconstructions of the Arctic Ocean sea-ice cover and its variability over the last 30 ka, suggesting extended sea-ice cover during the LGM, minimum sea-ice cover (to ice-free conditions) during the Bølling as well as the Early Holocene Climate Optimum, and significantly increased sea-ice cover at the onset of the Younger Dryas (YD) Cooling Event and during the late

Holocene "Neoglacial" period (MÜLLER et al. 2009, 2012, FAHL & STEIN 2012).

- The freshening of the Arctic Ocean, coinciding with a prominent increase in sea-ice cover at the onset of the YD may support the hypothesis that Arctic Ocean freshwater and sea-ice export might have been an important mechanism for shutting down the North Atlantic Deep Water (NADW) formation, triggering the YD cooling event (BROECKER 2006, NOT & HILLAIRE-MARCEL 2012, FAHL & STEIN 2012).
- The diene/IP_{25} ratio – possibly a new proxy for SST reconstruction – reached maximum values during the Bølling-Allerød warm period and decreased during the Holocene cooling trend (FAHL & STEIN 2012).
- Observations of historical sea ice records off northern Iceland during the last millennium demonstrates a strong correlation between documented sea ice occurrences and the IP_{25} proxy record (MASSÉ et al. 2008).
- For the first time, IP_{25} could be identified in Arctic Ocean sediments older than 30 ka, i.e., IP_{25} was found 150 ka old (MIS 6) in sediments from core PS2138-1 recovered at the Barents Sea continental margin.

IP$_{25}$, PIP$_{25}$, and diene/IP$_{25}$: challenges for future paleoenvironmental reconstructions

The novel IP_{25} approach (BELT et al. 2007) is certainly a very promising proxy approach that may allow more detailed reconstructions of past Arctic Ocean sea-ice cover. The combination of IP_{25} with a phytoplankton marker (in terms of a phytoplankton marker-IP_{25} index "PIP_{25}", MÜLLER et al. 2011) proves highly valuable to properly interpret the sea-ice proxy signal as an under- or over-estimation of sea-ice coverage can be circumvented and more quantitative estimates of paleo-sea-ice coverage seem to be possible. Although the "PIP_{25} approach" still has its limitations and needs further development and verification by additional data from other Arctic areas, the fundamental idea of pairing IP_{25} with a phytoplankton productivity measure to distinguish between multiple ice conditions characterized by zero IP_{25} (as introduced by MÜLLER et al. 2009, 2011), remains an important development of the original IP_{25} approach. Based on the new biomarker data from core PS2458-4 (FAHL & STEIN 2012, and this paper) as well as surface sediments from the Kara-Laptev seas (XIAO et al. 2012), we propose that the diene/IP_{25} ratios might have a potential for becoming a new temperature proxy for low-SST environments (cf. ROWLAND et. al. 2001, SACHS et.al. 2008). To prove this hypothesis, however, certainly more ground-truth data are needed.

In order to establish the IP_{25} approach as key proxy for the reconstruction of past Arctic Ocean sea-ice conditions, however, more basic data from sea ice and sediment traps (i.e., algae abundances, IP_{25}, phytoplankton biomarkers, IRD) as well as surface sediments and sediment cores (IP_{25}, phytoplankton biomarkers, IRD) with large spatial coverage from different environments of the entire Arctic Ocean (i.e., permanently ice-covered central Arctic Ocean, marginal seas with seasonally open-water conditions, polynyas, etc.) are still needed. Concerning the temporal applicability of IP_{25} as paleo-sea-ice proxy, it has to be tested how old the sediment could be for using this approach. In our pilot study we could show that

IP_{25} may occur in Arctic Ocean sediment as old as MIS 6, and STEIN & FAHL (2012) even found IP_{25} in two million years old sediments from the Fram Strait area. The IP_{25} approach can also be used for the reconstruction of sea-ice cover during glacials significantly older than MIS 2. However, what about Pleistocene, Neogene or even older sediments? In a few test measurements we carried-out on ACEX sediments of Eocene age, no IP_{25} was found.

When interpreting IP_{25} and PIP_{25} records and comparing absolute numbers, determined in different studies and/or in material from different areas and with different sample storage times and temperature (i.e., old versus fresh material and deep-frozen versus storage under plus temperatures), possible differences in biomarker decomposition/degradation within the water column, at the seafloor and within the sediments as well as IP_{25} losses during sample storage, have to be considered. Here, improved knowledge of production, degradation and preservation/burial of the IP_{25} signal is urgently needed.

A correct identification of IP_{25} in extracts by GC-MS and a correct quantification of IP_{25}, which requires some understanding of instrumental response factors between IP_{25} and the internal standard, are essential in this approach (see BROWN 2011, MÜLLER et al. 2011, BELT et al. 2012a, 2012b, FAHL & STEIN 2012). In this context, an analytical standard protocol should be developed in order to allow a direct comparison of IP_{25} data obtained in different laboratories.

The challenge of future scientific drilling

Considering the importance of the Arctic Ocean for the global ocean circulation and the climate system, more high-resolution paleoceanographic data sets from key areas are needed to reconstruct the climatically important parameters such as sea-ice cover – the major focus of this paper – but also sea-surface temperature, salinity, inflow of Atlantic Water, and river discharge. This kind of data sets going back beyond the time scale of direct measurements can be used to determine the natural variability of these parameters as a background for an assessment of anthropogenically influenced changes in the last 100 to 150 years. For studying the (sub-)millennial climate variability on longer time scales, i.e., under different boundary conditions during pre-Quaternary times, as well as for studying the long-term climate change from Greenhouse to Icehouse conditions during Mesozoic-Cenozoic times, however, new drill cores from the Arctic Ocean are needed (Fig. 26). That means, undisturbed and complete sedimentary sequences have to be drilled on depth transects across the major ocean ridge systems, i.e., the Lomonosov Ridge, the Alpha-Mendeleev Ridge, and the Chukchi Plateau and Northwind Ridge. High-resolution records allowing to study climate variability on Milankovich and millennial to sub-millennial time scales can be drilled along the continental margins characterized by high sedimentation rates. Here, key areas are the Arctic Ocean marginal seas characterized by variable sea-ice cover and strong river discharge. Key location for studying the history of exchange of the Arctic Ocean with the world's oceans are the Fram Strait, Yermak Plateau and Chukchi Plateau areas. Part of these drilling campaigns will hopefully become reality within the new phase of the International Ocean Discovery Program (IODP) post 2013 (COAKLEY & STEIN 2010, STEIN
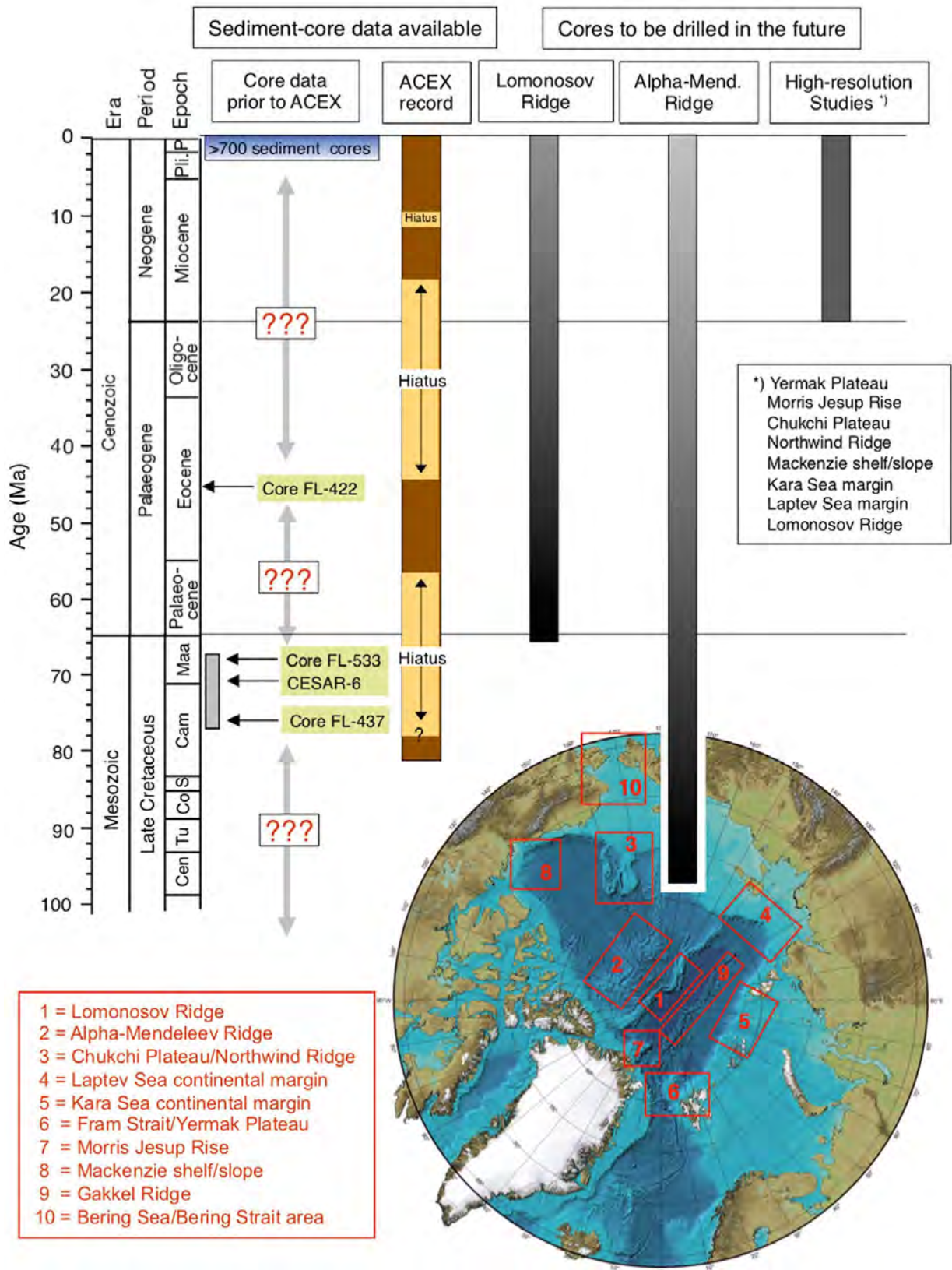
Fig. 26: Stratigraphic coverage of existing sediment cores in the central Arctic Ocean prior to IODP-ACEX (based on THIEDE et al. 1990) and the section recovered during the ACEX drilling expedition (BACKMAN et al. 2006, BACKMAN et al. 2008), and stratigraphic coverage and key areas for future scientific drilling campaigns in the Arctic Ocean. The middle Eocene sediments recovered at core FL-422 are arbitrarily placed at 45 Ma, the three Late Cretaceous (Maastrichtian/Campanian) cores are arbitrarily placed on the time axis as well. Each of these four cores (all recovered on Alpha Mendeleev Ridge) documents a time period of at the most a few hundred kyrs (BACKMAN et al. 2008). Figure from Stein (2011) and further references therein.

Abb. 26: Stratigraphie der bislang verfügbaren Sedimentkerne im Arktischen Ozean (ergänzt nach THIEDE et al. 1990) und Stratigraphie der ACEX-Bohrung (BACKMAN et al. 2008) sowie Stratigraphie und Lokationen möglicher zukünftiger wissenschaftlicher Bohrungen im Arktischen Ozean (aus STEIN 2011).

2011 and further references therein; for details see also New IODP Science Plan (BICKLE et al. 2012; also online available at http://www.iodp.org/science-plan-for-2013-2023).

ACKNOWLEDGMENTS

References

ACIA (2004): Impacts of a Warming Arctic: Arctic Climate Impact Assessment.- Cambridge University Press, Cambridge, 1-139, http://www.acia.uaf.edu

ACIA (2005): Arctic Climate Impact Assessment.- Cambridge University Press, 1-1042.

Alley, R.B., Mayewski, P.A., Sowers, T., Stuiver, M., Taylor, K.C., Clark, P.U. (1997): Holocene climatic instability: a prominent, widespread event 8200 yr ago.- Geology 25: 483-486

Andersen, E.S., Dokken, T.M., Elverhøi, A., Solheim, A., Fossen, I. (1996): Late Quaternary sedimentation and glacial history of the western Svalbard margin.- Mar. Geol. 133: 123-156.

Andersen, C., Koç, N., Jennings, A. & Andrews, J.T. (2004): Nonuniform response of the major surface currents in the Nordic Seas to insolation forcing: implications for the Holocene climate variability.- Paleoceanography 19: PA 2003.

Andersson, C., Risebrobakken, B., Jansen, E. & Dahl, S.O. (2003): Late Holocene surface ocean conditions of the Norwegian Sea (Vøring Plateau).- Paleoceanography 18(2): 1044.

Andreev, A.A. & Klimanov, V.A. (2000): Quantitative Holocene climatic reconstruction from Arctic Russia.- J. Paleolimnol. 24: 81-91.

Andrews, J.T., Helgadottir, G., Geirsdottir, A. & Jennings, A.E. (2001): Multi-century-scale records of carbonate (hydrographic?) variability on the northern Iceland margin over the last 5000 years.- Quat. Res. 56: 199-206.

Backman, J., Jakobsson, M., Frank, M., Sangiorgi, F., Brinkhuis, H., Stickley, C., O'Regan, M., Løvlie, R., Pälike, H., Spofforth, D., Gattacecca, J., Moran, K., King, J. & Heil, C. (2008): Age model and core-seismic integration for the Cenozoic Arctic Coring expedition sediments from the Lomonosov Ridge.- Paleoceanography 23: PA1S03.

Backman, J. & Moran, K. (2008): Introduction to special section on Cenozoic paleoceanography of the central Arctic Ocean.- Paleoceanography 23: PA1S01, doi: 10.1029/2007PA001516.

Backman, J., Moran, K., McInroy, D.B., Mayer, L.A., and the Expedition 302 Scientists (2006): Proceedings IODP, 302.- College Station, Texas (Integrated Ocean Drilling Program Management International, Inc.). doi:10.2204/iodp.proc.302.104.2006.

Barry, R.G. (1996): The parameterization of surface albedo for sea ice and its snow cover.- Prog. Phys. Geogr. 20: 63-79.

Bauch, H.A., Erlenkeuser, H., Spielhagen, R.F., Struck, U., Matthiessen, J., Thiede, J. & Heinemeier, J. (2001a): A multiproxy reconstruction of the evolution of deep and surface waters in the subarctic Nordic seas over the last 30,000 yr.- Quat. Sci. Rev. 20: 659-678.

Behrends, M. (1999): Reconstruction of sea-ice drift and terrigenous sediment supply in the Late Quaternary: heavy-mineral associations in sediments of the Laptev-Sea continental margin and the central Arctic Ocean.- Reports Polar Res. 310: 1-167.

Behrends, M., Hoops, E. & Peregovich, B. (1999): Distribution patterns of heavy minerals in Siberian rivers, the Laptev Sea and the eastern Arctic Ocean: an approach to identify sources, transport and pathways of terrigenous matter.- In: H. KASSENS, H. BAUCH, I. DMITRENKO, H. EICKEN, H.W. HUBBERTEN, M. MELLES, J. THIEDE & L. TIMOKHOV (eds), Land-Ocean Systems in the Siberian: Dynamics and History. Springer-Verlag, Heidelberg, 265-286.

Belt, S.T., Massé, G., Rowland, S.J., Poulin, M., Michel, C., LeBlanc, B. (2007): A novel chemical fossil of palaeo sea ice: IP25.- Org. Geochem. 38: 16-27.

Belt, S.T., Massé, G., Vare, L.L., Rowland, S.J., Poulin, M., Sicre, M.-A., Sampei, M. & Fortier, L. (2008): Distinctive ^{13}C isotopic signature distinguishes a novel sea ice biomarker in Arctic sediments and sediment traps.- Mar. Chemistry 112(3-4): 158-167.

Belt, S.T., Vare, L.L., Massé, G., Manners, H.R., Price, J.C., MacLachlan, S.E., Andrews, J.T. & Schmidt, S. (2010): Striking similarities in temporal changes to spring sea ice occurrence across the central Canadian Arctic Archipelago over the last 7000 years.- Quat. Sci. Rev. 29 (25-26): 3489-3504.

Belt, B.T., Brown, T.A., Cabedo Sanz, P. & Navarro Rodriguez, A. (2012): Structural confirmation of the sea ice biomarker IP25 found in Arctic marine sediments.- Environmental Chemistry Letters DOI: 10.1007/s10311-011-0344-0.

Belt, B.T., Brown, T.A., Navarro Rodriguez, A., Cabedo Sanz, P., Tonkin, A. & Ingle, R. (2012b): A reproducible method for the extraction, identification and quantification of the Arctic sea ice proxy IP25 from marine sediments.- Analytical Methods, DOI: 10.1039/c2ay05728j.

Bennike, O. (2004): Holocene sea-ice variations in Greenland: onshore evidence.- The Holocene 14: 607-613.

Berger, A. & Loutre, M.F. (1991): Insolation values for the climate of the last 10 million years.- Quat. Sci. Rev. 10: 297-317.

Bickle, M. et al. (eds) (2012): Illuminating Earth's Past, Present, and Future.- The International Ocean Discovery Program – Exploring the Earth under the Sea. Science Plan for 2013-2023: 1-84.

Birgel, D. & Hass, C. (2004): Oceanic and atmospheric variations during the last deglaciation in the Fram Strait (Arctic Ocean): a coupled high-resolution organic-geochemical and sedimentological study.- Quat. Sci. Rev. 23: 29-47.

Birgel, D. & Stein, R. (2004): Northern Fram Strait und Yermak Plateau: distribution, variability and burial of organic carbon and paleoenvironmental implications.- In: R. STEIN & R.W. MACDONALD (eds), The Organic Carbon Cycle in the Arctic Ocean. Springer Verlag, Heidelberg, 279-295.

Birgel, D., Stein, R. & Hefter, J. (2004): Aliphatic lipids in recent sediments of the Fram Strait/Yermak Plateau (Arctic Ocean): composition, sources and transport processes.- Mar. Chemistry 88: 127-160.

Bischof, J.F., Clark, D.L. & Vincent, J.S. (1996): Pleistocene paleoceanography of the central Arctic Ocean: the sources of ice rafted debris and the compressed sedimentary record.- Paleoceanography 11: 743-756.

Bischof, J.F. & Darby, D.A. (1999): Quaternary ice transport in the Canadian Arctic and extent of late Wisconsinan glaciation in the Queen Elizabeth Islands.- Can. J. Earth Sci. 36: 2007-2022.

Boon, J.J., Rijpstra, W.I.C., de Lange, F., de Leeuw, J.W., Yoshioka, M. & Shimizu, Y. (1979): The Black Sea sterols - A molecular fossil for dinoflagellate blooms.- Nature 277: 125-127.

Broecker, W.S. (1997): Thermohaline circulation, the Achilles heel of our climate system: will man-made CO_2 upset the current balance?- Science 278,:1582-1588.

Broecker, W.S. (2006): Was the Younger Dryas triggered by a flood?- Science 312: 1146-1148.

Broecker, W.S., Denton, G.H., Edwards, R.L., Cheng, H., Alley, R.B. & Putnam, A.E. (2010): Putting the Younger Dryas cold event into context.- Quat. Sci. Rev. 29: 1078-1081.

Broecker, W.S., Kennett, J.T., Flower, B.P., Teller, J.T., Trumbore, S., Bonani, G. & Wolfli, W. (1989): Routing of meltwater from the Laurentide Ice Sheet during the Younger Dryas cold episode.- Nature 341: 318-320.

Brown, T.A. (2011): Production and preservation of the Arctic sea ice diatom biomarker IP25.- Petroleum and Environmental Geochemistry Group, School of Geography, Earth and Environmental Sciences. Plymouth, University of Plymouth, 1-291; http://hdl.handle.net/10026.1/314.

Carstens, J. & Wefer, G. (1992): Recent distribution of planktonic foraminafera in the Nansen Basin, Arctic Ocean.- Deep-Sea Res. 30: 507-524.

Clark, D.L. & Hanson, A. (1983): Central Arctic Ocean sediment texture: A key to ice transport mechanism.- In: B.F. MOLNIA (ed), Glacial-marine sedimentation. Plenum Press, New York, 301-330.

Clarke, G.K.C., Leverington, D.W., Teller, J.T. & Dyke, A.S. (2004): Paleohydraulics of the last outburst flood from glacial Lake Agassiz and the 8200 BP cold event.- Quat. Sci. Rev. 23(3-4): 389-407.

Clark, P.U., Pisias, N.G., Stocker, T.F. & Weaver, A.J. (2002): The role of the thermohaline circulation in abrupt climate change.- Nature 415: 863-869.

Coakley, B. & Stein, R. (2010): Arctic Ocean Scientific Drilling: the next frontier.- Sci. Drilling 9: 45-49; doi:10.2204/iodp.sd.9.09.2010.

Colony, R. & Thorndike, A.S. (1985): Sea ice motion as a drunkard's walk.- J. Geophys. Res. 90: 965-974.

Coxall, H.K., Wilson, P.A., Pälike, H., Lear, C.H. & Backman, J. (2005): Rapid stepwise onset of Antarctic glaciation and deeper calcite compensation in the Pacific Ocean.- Nature 433: 53-57.

Cronin, T.M., Gemery, L., Briggs Jr., W.M., Jakobsson, M., Polyak, L. & Brouwers, E.M. (2010): Quaternary Sea-ice history in the Arctic Ocean based on a new Ostracode sea-ice proxy.- Quat. Sci. Rev. doi:10.1016/j.quascirev.2010.05.024.

Cronin, T.M., Smith, S.A., Eynaud, F., O'Regan, M. & King, J. (2008): Quaternary paleoceanography of the central Arctic based on Integrated Ocean Drilling Program Arctic Coring Expedition 302 foraminiferal assemblages.- Paleoceanography 23: PA1S18. doi: 10.1029/2007PA001484.

Crucifix, M., Loutre, M.-F., Tulkens, P., Fichefet, T. & Berger, A. (2002): Climate evolution during the Holocene: a study with an Earth system model of intermediate complexity.- Climate Dyn. 19: 43-60.

Darby, D.A. (2003): Sources of sediment found in sea ice from the western Arctic Ocean, new insights into processes of entrainment and drift patterns.- J. Geophy. Res. 108, C8, 3257, doi:10.1029/2002JC001350.

Darby, D.A. (2008): The Arctic perennial ice cover over the last 14 million years.- Paleoceanography, doi:10.1029/2007PA001479.

Darby, D.A., Bischof, J.F. & Jones, G.A. (1997): Radiocarbon chronology of depositional regimes in the western Arctic Ocean.- Deep-Sea Res. II 44(8): 1745-1757.

Darby, D.A., Bischof, J.F., Spielhagen, R.F., Marshall, S.A. & Herman, S.W. (2002): Arctic ice export events and their potential impact on global climate during the late Pleistocene.- Paleoceanography 17, doi: 10.1029/2001PA000639.

De Angeles, H. & Kleman J. (2005): Palaeo-ice streams in the northern Keewatin sector of the Laurentide Ice Sheet.- Annals Glaciol. 42: 135-144.

Dethleff, D. (2005): Entrainment and export of Laptev Sea ice sediments, Siberian Arctic.- J. Geophys. Res. 110(C07009). doi:10.1029/2004JC002740.

Dethleff, D., Rachold, V., Tintelnot, T. & Antonow, M. (2000): Sea-ice transport of riverine particles from the Laptev Sea to Fram Strait based on clay mineral studies.- Internat. J. Earth Sci. 89: 496-502.

Dickson, R.R., Osborn, T.J., Hurrell, J.W., Meincke, J., Blindheim, J., Adlandsvik, B., Vinje, T., Alekseev, G. & Maslowski, W. (2000): The Arctic Ocean response to the North Atlantic Oscillation.- J. Clim. 13(15): 2671-2696.

Dokken, T.M. & Hald, M. (1996): Rapid climatic shifts during isotope stages 2-4 in the Polar North Atlantic.- Geology 24: 599-602.

Dyke, A.S., Andrews, J.T., Clark, P.U., England, J.H., Miller, G.H., Shaw, J. & Veillette, J.J. (2002): The Laurentide and Innuitian ice sheets during the Last Glacial Maximum.- Quat. Sci. Rev. 21: 9-31.

Dyke, A.S., England, J., Reimnitz, E. & Jetté, H. (1997): Changes in driftwood delivery to the Canadian Arctic archipelago: the hypothesis of postglacial oscillations of the Transpolar Drift.- Arctic 50: 1-16.

Dyke, A.S., Hooper, J. & Savelle, J.M. (1996): A history of sea ice in the Canadian Arctic Archipelago based on postglacial remains of the bowhead whale (*Balaena mysticetus*).- Arctic 49: 235-255.

Eicken, H., Gradinger, R., Graves, A., Mahoney, A. & Rigor, I. (2005): Sediment transport by sea ice in the Chukchi and Beaufort Seas: Increasing importance due to changing ice conditions?- Deep-Sea Res. (II) 52: 3281-3302.

Eicken, H., Reimnitz, E., Alexandrov, V., Martin, T., Kassens, H. & Viehoff, T. (1997): Sea-ice processes in the Laptev Sea and their importance for sediment export.- Cont. Shelf Res. 17: 205-233.

Eldrett, J.S., Harding, I.C., Wilson, P.A., Butler, E. & Roberts, A.P. (2007): Continental ice in Greenland during the Eocene and Oligocene.- Nature, doi:10.1038/nature05591.

Elverhøi, A., Svensen, J.I., Solheim, A., Andersen, E.S., Milliman, J., Mangerud, J. & Hooke, R.L. (1995b): Late Quaternary sediment yield from the High Arctic Svalbard Area.- J. Geol. 103: 1-17.

England, J.H., Lakeman, T.R., Lemmen, D.S., Bednarski, J.M., Stewart, T.G. & Evans, D.J.A. (2008): A millennial-scale record of Arctic Ocean sea ice variability and the demise of the Ellesmere Island ice shelves.- Geophys. Res. Lett. 35: xx-xx.

Fahl, K. & Nöthig, E.-M. (2007): Lithogenic and biogenic particle fluxes on the Lomonosov Ridge (central Arctic Ocean) and their relevance for sediment accumulation: vertical vs. lateral transport.- Deep-Sea Res. I, 54(8): 1256-1272.

Fahl, K. & Stein, R. (2012): Modern seasonal variability and deglacial / Holocene change of central Arctic Ocean sea-ice cover: new insights from biomarker proxy records.- Earth Planet. Sci. Lett., doi: 10.1016/j.epsl.2012.07.009.

Fahl, K. & Stein, R. (1999): Biomarkers as organic-carbon-source and environmental indicators in the Late Quaternary Arctic Ocean: "problems and perspectives".- Mar. Chem. 63: 293-309.

Flower, B. & Kennett, J. (1995): Middle Miocene deepwater paleoceanography in the Southwest Pacific; relations with East Antarctic ice sheet development.- Paleoceanography 10: 1095-1112.

Francis, J.A., Hunter, E., Key, J.R. & Wang, X. (2005): Clues to variability in Arctic minimum sea ice extent.- Geophys. Res. Lett. 32, L21501, doi:10.1029/2005GL024376.

Frank M., Backman, J., Jakobsson, M., Moran, K., O'Regan, M., King, J., Haley, B., Kubik, P. & Garbe-Schönberg, D. (2008): Beryllium isotopes in central Arctic Ocean sediments over the past 12.3 million years: stratigraphic and paleoclimatic implications.- Paleoceanography 23: PA1So1, doi:10.1029/2007PA001478.

Fronval, T. & Jansen, E. (1996): Late Neogene paleoclimates and paleoceanography in the Iceland Norwegian Sea: evidence from the Iceland and Vøring Plateaus.- In: J. THIEDE, A.M. MYHRE, J.V. FIRTH, G.L. JOHNSON, W.F. RUDDIMAN (eds), Proc. ODP, Sci. Results, 151, College Station, Texas (Ocean Drilling Program), 455-468.

Funder, S., Kjær, K.H., Linderson, H., Lyså, A. & Olsen, J. (2009): Driftwood and Ice - a sketchy history of Holocene multiyear sea ice in the Arctic Ocean.- Third Conf. Arctic Paleoclimate and its Extremes. APEX, Copenhagen, Denmark, p. 27.

Fütterer, D.K. (ed) (1994): The Expedition ARCTIC'93 Leg ARK IX/4 of RV "Polarstern" 1993.- Reports Polar Res. 149: 1-244.

Gloersen, P.W. Campbell, J., Cavalieri, D.J., Comiso, J.C., Parkinson, C.L., Zwally, H.J. (1992): Arctic and Antarctic sea ice, 1978-1987: Satellite passive-microwave observations and analysis.- NASA SP-511, 1-290.

Goosse, H., Driesschaert, E., Fichefet, T. & Loutre, M.-F. (2007): Information on the early Holocene climate constrains the summer sea ice projections for the 21st century.- Climate of the Past Discussions 2: 999-1020

Grootes, P.M., Stuiver, M., White, J.W.C., Johnsen, S. & Jouzel, J. (1993): Comparison of oxygen isotope records from the GISP2 and GRIP Greenland ice cores.- Nature 366: 552-554.

Hald, M., Andersson, C., Ebbesen, H., Jansen, E., Klitgaard-Kristensen, D., Risebrobakken, B.R., Salomonsen, G.R., Sarnthein, M., Sejrup, H.P. & Telford, R.J. (2007): Variations in temperature and extent of Atlantic Water in the northern North Atlantic during the Holocene.- Quat. Sci. Rev. 26: 3423-3440.

Hanslik, D., Jakobsson, M., Backman, J., Björck, S., Sellén, E., O'Regan, M., Fornaciari, E. & Skog, G. (2010): Quaternary Arctic Ocean sea ice variations and radiocarbon reservoir age corrections.- Quat. Sci. Rev. 29: 3430-*3441*.

Hass, H.C. (2002): A method to reduce the influence of ice-rafted debris on a grain-size record from the northern Fram Strait, Arctic Ocean.- Polar Res. 21: 299-306.

Hebbeln, D., Dokken, T., Andersen, E.S., Hald, M. & Elverhøi, A., (1994): Moisture supply for northern ice-sheet growth during the Last Glacial Maximum.- Nature 370: 357-360.

Hebbeln, D. & Wefer, G. (1991): Effects of ice coverage and ice-rafted material on sedimentation in the Fram Strait.- Nature 350: 409-411.

Hovland, M. (ed), 2001. The High-Arctic Drilling Challenge.- Final Report Arctic's Role in Global Change Program Planning Group (APPG), Ocean Drilling Program, 1-38.

Israde-Alcántara, I., James L. Bischoff, J.L., Domínguez-Vázquez, G., Lid, H.-C., DeCarli, P.S., Bunch, T.E., Wittke, J.H., Weaver, J.C., Firestone, R.B., West, A., Kennett, J.P., Mercer, C., Xie, S., Richman, E.K., Kinzie, C.R., Wendy S. & Wolbach, W.S. (2011): Evidence from central Mexico supporting the Younger Dryas extraterrestrial impact hypothesis.- PNAS, doi:10.1073/pnas.1110614109.

Jakobsson, M., Løvlie, R., Al-Hanbali, H., Arnold, E., Backman, J. & Mörth, M. (2000): Manganese color cycles in Arctic Ocean sediments constrain Pleistocene chronology.- Geology 28: 23-26.

Jakobsson, M., Løvlie, R., Arnold, E., Backman, J., Polyak, L., Knudsen, J. & Musatov, E. (2001) Pleistocene stratigraphy and paleoenvironmental variation from Lomonosov Ridge sediments, central Arctic Ocean.- Global Planet. Change 31: 1-22.

Jakobsson, M., Macnab, R., Mayer, L., Anderson, R., Edwards, M., Hatzky, J., Schenke, H.-W. & Johnson, P. (2008): An improved bathymetric portrayal of the Arctic Ocean: Implications for ocean modeling and geological, geophysical and oceanographic analyses.- Geophys. Res. Lett. 35, L07602, doi:10.1029/2008GL033520.

Jakobsson, M., Long, A., Ingolfsson, O., Kjær, K.H. & Spielhagen, R.F. (2010a): New insights on Arctic Quaternary climate variability from palaeo-records and numerical modelling.- Quat. Sci. Rev. 29: 3349-3358.

Jakobsson, M., Nilsson, J., O'Regan, M., Backman, J., Löwemark, L., Dowdeswell, J.A., Mayer, L., Polyak, L., Colleoni, F., Anderson, L.G.,

Björk, G., Darby, D., Eriksson, B., Hanslik, D., Hell, B., Marcussen, C., Sellén, E. & Wallin, A. (2010b): An Arctic Ocean ice shelf during MIS 6 constrained by new geophysical and geological data.- Quat. Sci. Rev. 29: 3505-3517.

Jennings, A.E., Knudsen, K.L., Hald, M., Hansen, C.V. & Andrews, J.T. (2002): A mid-Holocene shift in Arctic sea-ice variability on the East Greenland Shelf.- The Holocene 12: 49-58.

Jin, M., Deal, C., Lee, S.H., Elliott, S., Hunke, E., Maltrud, M. & Jeffery, N. (2012): Investigation of Arctic sea ice and ocean primary production for the period 1992–2007 using a 3-D global ice–ocean ecosystem model.- Deep-Sea Res. in press, doi: 1016/j.dsr2.2011.06.003.

Jiang, H., Eiriksson, J., Schultz, M., Knudsen, K.L. & Seidenkrantz, M.S. (2005): Evidence for solar forcing of sea surface temperature on the North Icelandic Shelf during the late Holocene.- Geology 33: 73-76.

Johannessen, O.M. Bengtsson, L., Miles, M.W., Kuzmina, S.I., Semenov, V.A., Alekseev, G.V., Nagurnyi, A.P., Zakharov, V.F., Bobylev, L.P., Pettersson, L.H., Hasselmann, K. & Cattle, H.P. (2004): Arctic climate change, observed and modelled temperature and sea-ice variability.- Tellus 56A: 328-341.

Johannessen, O.M., Shalina, E.V. & Miles, M.W. (1999): Satellite evidence for an Arctic sea ice cover in transformation.- Science 286: 1937-1939.

Johns, L., Wraige, E.J., Belt, S.T., Lewis, C.A., Masse, G., Robert, J.M. & Rowland, S.J. (1999): Identification of a C-25 highly branched isoprenoid (HBI) diene in Antarctic sediments, Antarctic sea-ice diatoms and cultured diatoms.- Org. Geochem. 30: 1471-1475.

Johnsen, S.J., Dahl-Jensen, D., Gundestrup, N., Steffensen, J.P., Clausen, H.B., Miller, H., Masson-Delmotte, V., Sveinbjörnsdottir, A.E. & White, J. (2001): Oxygen isotope and palaeotemperature records from six Greenland ice core stations: Camp Century, Dye-3, GRIP, GISP2, Renland and NorthGRIP.- J. Quat. Sci. 16: 299-307.

Kerr, R.A. (2007): Is battered Arctic sea ice down for the count?- Science 318: 33-34.

Kleiven, H.F., Kissel, C., Laj, C., Ninnemann, U.S., Richter, T.O. & Cortijo, E. (2008): Reduced North Atlantic Deep Water coeval with the glacial Lake Agassiz freshwater outburst.- Science 319: 60-64.

Kleman, J. & Glasser, N.F. (2007): The subglacial thermal organisation (STO) of ice sheets.- Quat. Sci. Rev. 26: 585-597.

Knies, J. & Gaina, C. (2008): Middle Miocene ice sheet expansion in the Arctic: views from the Barents Sea.- Geochem. Geophys. Geosyst 9: Q02015, doi:10.1029/2007GC001824.

Knies, J., Müller, C., Nowaczyk, N., Vogt, C. & Stein, R. (2000): A multiproxy approach to reconstruct the environmental changes along the Eurasian continental margin over the last 150 kyr.- Mar. Geol. 163: 317-344.

Knies, J. & Stein, R. (1998): New aspects of organic carbon deposition and its paleoceanographic implications along the northern Barents Sea margin during the last 30,000 years.- Paleoceanography 13: 384-394.

Knies, J., Vogt, C. & Stein, R. (1999): Late Quaternary growth and decay of the Svalbard-Barents-Sea Ice Sheet and paleoceanographic evolution in the adjacent Arctic Ocean.- GeoMar. Lett. 18: 195-202.

Knies, J., Kleiber, H.P., Matthiessen, J., Müller, C. & Nowaczyk, N. (2001): Marine ice-rafted debris records constrain maximum extent of Saalian and Weichselian ice-sheets along the northern Eurasian margin.- Global Planet. Change 31: 45-64.

Koç, N., Jansen, E. & Haflidason, H. (1993): Paleoceanographic reconstructions of surface ocean conditions in the Greenland, Iceland and Norwegian seas through the last 14 ka based on diatoms.- Quat. Sci. Rev. 12: 115-140.

Krause, G. (1969): Ein Beitrag zum Problem der Erneuerung des Tiefenwassers im Arkona-Becken.- Kieler Meeresforsch. 25: 268-271.

Krylov, A.A., Andreeva, I.A., Vogt, C., Backman, J., Krupskaya, V.V., Grikurov, G.E., Moran, K. & Shoji, H. (2008): A Shift in heavy and glay mineral provenance indicates a Middle Miocene onset of a perennial sea-ice cover in the Arctic Ocean.- Paleoceanography 23: PA1S06, doi: 10.1029/2007PA001497.

Kruglikova, S.B., Björklund, K.R., Hammer, Ø. & Anderson, O.R. (2009): Endemism and speciation in the polycystine radiolarian genus Actinomma in the Arctic Ocean: description of two new species Actinomma georgii n. sp. and A. turidae n. sp..- Mar. Micropal. 72: 26-48.

Kwok, R. & Rothrock, D.A. (2009): Decline in Arctic sea ice thickness from submarine and ICESat records: 1958-2008.- Geophys. Res. Lett. 36: L15501, doi:10.1029/2009GL039035.

Laskar, J., Robutel, P., Joutel, F., Gastineau, M., Correia, A.C.M. & Levrard, B. (2004): A long-term numerical solution for the insolation quantities of the Earth.- Astronomy Astrophys. 428: 261-285.

Levi, B.G. (2000): The decreasing Arctic ice cover.- Physics Today Jan. 2000: 19-20.

Lowenstein, T.K. & Demicco, R.V. (2006): Elevated Eocene atmospheric CO_2 and its subsequent decline.- Science 313: 1928.

Macdonald, R.W., Sakshaug, E. & Stein, R. (2004): The Arctic Ocean: modern status and recent climate change.- In: R. STEIN & R.W. MACDONALD

(eds), The Organic Carbon Cycle in the Arctic Ocean, Springer-Verlag, Berlin, 6-21.

Mangerud, J., Dokken, T., Hebbeln, D., Heggen, B., Ingolfsson, O., Landvik, J.Y., Meydahl, V., Svendsen, J.I. & Vorren, T.O. (1998): Fluctuations of the Svalbard-Barents Sea ice sheet during the last 150.000 years.- Quat. Sci. Rev. 17: 11-42.

Manighetti, B. & McCave, I.N. (1995): Late glacial and Holocene palaeocurrents through South Rockall Gap, NE Atlantic Ocean.- Paleoceanography 10: 611-626.

Maslanik, J.A., Serreze, M.C. & Barry, R.G. (1996): Recent decreases in Arctic summer ice cover and linkages to atmospheric circulation anomalies.- Geophys. Res. Lett. 23: 1677-1680.

Massé, G., Belt, S.T., Crosta, X., Schmidt, S., Snape, I., Thomas, D.N. & Rowland, S.J. (2011): Highly branched isoprenoids as proxies for variable sea ice conditions in the Southern Ocean. Antarctic Science 23, 487-498.

Massé, G., Rowland, S.J., Sicre, M.-A., Jacob, J., Jansen, E. & Belt, S.T. (2008): Abrupt climate changes for Iceland during the last millennium: Evidence from high resolution sea ice reconstructions. Earth Planet. Sci. Lett. 269: 565-569.

Matthiessen, J., Brinkhuis, H., Poulsen, N. & Smelror, M. (2009): Decahedrella martinheadii Manum 1997 – a stratigraphically and paleoenvironmentally useful Miocene acritarch of the mhigh northern latitudes.- Micropaleontology 55: 171-186.

Matthiessen, J. & Knies, J. (2001): Dinoflagellate cyst evidence for warm interglacial conditions at the northern Barents Sea margin during marine oxygen isotope stage 5.- J. Quat. Sci. 16: 727-738.

Matthiessen, J., Knies, J., Nowaczyk, N.R. & Stein, R. (2001): Late Quaternary dinoflagellate cyst stratigraphy at the Eurasian continental margin, Arctic Ocean: indications for Atlantic water inflow in the past 150,000 years.- Global Planet. Change 31: 65-86.

Maurer, J. (2007): Atlas of the cryosphere.- Boulder, Colorado USA, Nation. Snow Ice Data Center, digital media; http://nsidc.org/data/atlas/.

McManus, J.F., Francois, R., Gherardi, J.-M., Keigwin, L.D. & Brown-Lager, S. (2004): Collapse and rapid resumption of Atlantic meridional circulation linked to deglacial climate changes.- Nature 428: 834-837.

Méheust, M., Stein, R. & Fahl, K. (2012): Deglacial-Holocene variability of sea ice and surface water temperature in the Bering Sea: reconstruction based on IP_{25} and alkenone data.- Geophys. Res. Abstracts 14: EGU2012-3319-3, EGU General Assembly

Miller, K.G., Mountain, G.S., Browning, J.V., Kominz, M., Sugarman, P.J., Christie-Blick, N., Katz, M.E. & Wright, J.D. (1998): Cenozoic global sea-level, sequences, and the New Jersey transect: results from coastal plain and slope drilling.- Rev. Geophys. 36: 569-601.

Miller, G.H., Brigham-Grette, J., Alley, R.B., Anderson, L., Bauch, H.A., Douglas, M.S.V., Edwards, M.E., Elias, S.A., Finney, B.P., Fitzpatrick, J.J., Funder, S.V., Herbert, T.D., Hinzman, L.D., Kaufman, D.S., MacDonald, G.M., Polyak, L., Robock, A., Serreze, M.C., Smol, J.P., Spielhagen, R., White, J.W.C., Wolfe, A.P. & Wolff, E.W. (2010): Temperature and precipitation history of the Arctic.- Quat. Sci. Rev. 29: 1679-1715.

Möller, P., Larsen, N.K., Kjær, K.H., Funder, S., Schomacker, A., Linge, H. & Fabel, D. (2010): Early to middle Holocene valley glaciations on northernmost Greenland.- Quat. Sci. Rev. doi:10.1016/j.quascirev.2010.06.044.

Moran, K., Backman, J., Brinkhuis, H., Clemens, S.C., Cronin, T., Dickens, G.R., Eynaud, F., Gattacceca, J., Jakobsson, M., Jordan, R.W., Kaminski, M., King, J., Koc, N., Krylov, A., Martinez, N., Matthiessen, J., McInroy, D., Moore, T.C., Onodera, J., O'Regan, A.M., Pälike, H., Rea, B., Rio, D., Sakamoto, T., Smith, D.C., Stein, R., St. John, K., Suto, I., Suzuki, N., Takahashi, K., Watanabe, M., Yamamoto, M., Frank, M., Jokat, W. & Kristoffersen, Y. (2006): The Cenozoic palaeoenvironment of the Arctic Ocean.- Nature 441: 601-605.

Müller, J., Massé, G., Stein, R. & Belt, S. (2009): Extreme variations in sea ice cover for Fram Strait during the past 30 ka.- Nature Geoscience, DOI: 10.1038/NGEO665.

Müller, J., Wagner, A., Fahl, K., Stein, R., Prange, M. & Lohmann, G. (2011): Towards quantitative sea ice reconstructions in the northern North Atlantic: a combined biomarker and numerical modelling approach.- Earth Planet. Sci. Lett. 306: 137-148.

Müller, J., Werner, K., Stein, R., Fahl, K., Moros, M. & Jansen, E. (2012): Holocene cooling culminates in sea ice oscillations in Fram Strait.- Quat. Sci. Rev. 47: 1-14, doi:10.1016/j.quascirev.2012.04.024.

Murton, J.B., Bateman, M.D., Dallimore, S.R., Teller, J.T. & Yang, Z. (2010): Identification of Younger Dryas outburst flood path from Lake Agassiz to the Arctic Ocean.- Nature 464: 740-743.

Nesje, A., Matthews, J.A., Dahl, S.O., Berrisford, M.S. & Andersson, C. (2001): Holocene glacier fluctuations of Flatebreen and winter-precipitation changes in the Jostedalsbreen region, western Norway, based on glaciolacustrine sediment records.- The Holocene 11: 267-280.

Nghiem, S.V., Rigor, I.G., Perovich, D.K., Clemente-Colón, P., Weatherly, J.W. & Neumann, G. (2007): Rapid reduction of Arctic perennial sea ice.- Geophys. Res. Lett. 34, L19504, doi:10.1029/2007GL031138.

NGRIP Members (2004): High-resolution record of Northern Hemisphere climate extending into the last interglacial period.- Nature 431: 147-151.

Nørgaard-Pedersen, N., Mikkelsen, N., Lassen, S.J., Kristoffersen, Y. & Sheldon, E. (2007): Reduced sea ice concentrations in the Arctic Ocean during the last interglacial period revealed by sediment cores off northern Greenland.- Paleoceanography 22: PA1218,

Nørgaard-Pedersen, N., Spielhagen, R.F., Erlenkeuser, H., Grootes, P.M., Heinemeier, J. & Knies, J. (2003): The Arctic Ocean during the Last Glacial Maximum: atlantic and polar domains of surface water mass distribution and ice cover.- Paleoceanography 18: 1-19.

Nørgaard-Pedersen, N., Spielhagen, R.F., Thiede, J. & Kassens, H. (1998): Central Arctic surface ocean environment during the past 80.000 years.- Paleoceanography 13: 193-204. doi:10.1029/2006PA001283.

Not, C. & Hillaire-Marcel, C. (2012): Enhanced sea-ice export from the Arctic during the Younger Dryas.- Nature Communications 3:647. Doi:10.1038/ncomms1658.

Nürnberg, D., Wollenburg, I., Dethleff, D., Eicken, H., Kassens, H., Letzig, T., Reimnitz, E. & Thiede, J. (1994): Sediments in Arctic sea ice: implications for entrainment, transport and release.- In: J. THIEDE, T. VORREN & R.F. SPIELHAGEN (eds), Mar. Geol. 119: 185-214.

Ogilvie, A.E.J. (1992): Documentary evidence for changes in the climate of Iceland AD 1500 to 1800.- In: R.S. BRADLEY & P.D. JONES (eds), Climate since AD 1500, London New York, 92-117.

Ogilvie, A.E.J. & Jónsson, T. (2001): "Little ice Age" research: a perspective from Iceland.- Clim. Change 48: 9-52.

O'Regan, M. (2011): Late Cenozoic paleoceanography of the central Arctic Ocean.- IOP Conf. Series, Earth and Environmental Sci. 14, doi:10.1088/1755-1315/14/1/012002.

O'Regan, M., King, J., Backman, J., Jakobsson, M., Pälike, H., Moran, K., Heil, C., Sakamoto, T., Cronin, T. Jordan, R. (2008): Constraints on the Pleistocene chronology of sediments from the Lomonosov Ridge.- Paleoceanography 23: PA1S19.

O'Regan, M., St. John, K., Moran, K., Backman, K., King, J., Haley, B.A., Jakobsson, M., Frank, M. & Röhl, U. (2010): Plio-Pleistocene trends in ice rafted debris on the Lomonosov Ridge.- Quat. Internat. 219: 168-176, doi:101016/jquaint200908010.

Pagani, M., Pedentchouk, N., Huber, M., Sluijs, A., Schouten, S., Brinkhuis, H., Sinninghe Damsté, J.S., Dickens, G.R. & the IODP Expedition 302 Scientists (2006): The Arctic's hydrologic response to global warming during the Palaeocene-Eocene thermal maximum.- Nature 442: 671-675.

Parkinson, C.L., Cavalieri, D.J., Gloersen, P., Zwally, J.H., Comiso, J.C. (1999): Arctic sea ice extents, areas, and trends, 1978-1996.- J. Geophys. Res. 104: 20837-20856.

Peltier, W.R. (2007): Rapid climate change and Arctic Ocean freshening.- Geology 35: 1147-1148.

Pearson, P.N. & Palmer, M.R. (2000): Atmospheric carbon dioxide concentrations over the past 60 million years.- Nature 406: 695-699.

Peltier, W.R., Vettoretti, G. & Stastna, M. (2006): Atlantic meridional overturning and climate response to Arctic Ocean freshening.- Geophys. Res. Lett. 33, doi:10.1029/2005GL025251.

Pfirman, S.L., Colony, R., Nürnberg, D., Eicken, H. & Rigor, I. (1997): Reconstructing the origin and trajectory of drifting Arctic sea ice.- J. Geophys. Res. 102(C6): 12575-12586.

Pfirman, S., Gascard, J.-C., Wollengurg, I., Mudie, P. & Abelmann, A. (1989): Particle-laden Eurasian Arctic sea ice: observations from July and August 1987.- Polar Res. 7: 59-66.

Pflaumann, U., Sarnthein, M., Chapman, A.L., Funnell, B., Huels, M., Kiefer, T., Maslin, M., Schulz, H., Swallow, J., van, K.S., Vautravers, M., Vogelsang, E. & Weinelt, M. (2003): Glacial North Atlantic sea-surface conditions reconstructed by GLAMAP 2000.- Paleoceanography 18: 1065, doi:10.1029/2002PA000774.

Phillips, R.L. & Grantz, A. (1997): Quaternary history of sea ice and paleoclimate in the Amerasia Basin, Arctic Ocean, as recorded in the cyclical strata or Northwind Ridge.- Geol. Soc. Amer. Bull. 109: 1101-1115.

Phillips, R.L. & Grantz, A. (2001): Regional variations in provenance and abundance of ice-rafted clasts in Arctic Ocean sediments: Implications for the configuration of Late Quaternary oceanic and atmospheric circulation in the Arctic. Mar. Geol. 172, 91–115.

Poirier, A. & Hillaire-Marcel, C. (2011): Improved Os-isotope stratigraphy of the Arctic Ocean.- Geophys. Res. Lett. 38, doi: 10.1029/2011GL047953.

Polyak, L., Alley, R.B., Andrews, J.T., Brigham-Grette, J., Cronin, T.M., Darby, D.A., Dyke, A.S., Fitzpatrick, J.J., Funder, S., Holland, M., Jennings, A.E., Miller, G.H., O'Regan, M., Savelle, J., Serreze, M., St. John, K., White, J.W.C. & Wolff, E. (2010): History of sea ice in the Arctic. Quat. Sci. Rev. 29: 1757-1778.

Polyak, L., Bischof, J., Ortiz, J., Darby, D., Channell, J., Xuan, C., Kaufman, D., Lovlie, R., Schneider, D. & Adler, R. (2009): Late Quaternary stratigraphy and sedimentation patterns in the western Arctic Ocean.- Global Planet. Change 68: 5-17.

Polyak, L.V., Curry, W.B., Darby, D.A., Bischof, J. & Cronin, T.M. (2004): Contrasting glacial/interglacial regimes in the western Arctic Ocean as exemplified by a sedimentary record from the Mendeleev Ridge.- Palaeogeogr. Palaeoclim. Palaeoecol. 203: 73-93.

Polyak, L.V., Darby, D.A., Bischoff, J.F. & Jakobsson, M. (2007): Stratigraphic constraints on late Pleistocene glacial erosion and deglaciation of the Chukchi margin, Arctic Ocean.- Quat. Res. 67: 234-245.

Polyakov, I.V., Johnson, M.A., Colony, R.L., Bhatt, U. & Alekseev, G.V. (2002): Observationally based assessment of polar amplification of global warming.- Geophys. Res. Lett. 29: 1878 (doi:1029/2002GL011111).

Polyakov, I.V. & Johnson, M.A. (2000): Arctic decadal and interdecadal variability.- Geophys. Res. Lett. 27: 4097-4100.

Poore, R.Z., Osterman, L., Curry, W.B. & Phillips, R.L. (1999): Late Pleistocene and Holocene meltwater events in the western Arctic Ocean.- Geology 27: 759-762.

Rasmussen, T.L., Thomsen, E., Slubowska, M.A., Jessen, S., Solheim, A. & Koç, N. (2007): Paleoceanographic evolution of the SW Svalbard margin (76° N) since 20,000 ^{14}C yr BP.- Quat. Res. 67: 100-114.

Reimnitz, E., McCormick, M., McDougall, K. & Brouwers, E. (1993): Sediment export by ice rafting from a coastal polynya, Arctic Alaska, U.S.A.- Arct. Alpine Res. 25: 83-98.

Reimnitz, E., McCormick, M., Bischof, J. & Darby, D. (1998): Comparing sea-ice sediment load with Beaufort Sea shelf deposits: is entrainment selective?- J. Sed. Res. 68: 777-787.

Rigor, I.G., Wallace, J.M. & Colony, R. (2002): Response of sea ice to the Arctic Oscillation.- J. Clim. 15: 2648-2663.

Rothrock, D.A., Yu, Y. & Maykut, G.A. (1999): Thinning of the Arctic sea-ice cover.- Geophys. Res. Lett. 26: 3469-3472.

Rowland, S.J., Belt, S.T., Wraige, E.J., Massé, G., Roussakis, C. & Robert, J.-M. (2001): Effects of temperature on polyunsaturation in cytostatic lipids of *Haslea ostrearia*.- Phytochemistry 56: 597-602.

Sachs, J.P., Pahnke, K., Smittenberg, P. & Zhang, Z. (2008): In: S. ELIAS (ed), Encyclopedia of Quaternary Science, Elsevier, Amsterdam,QUAT 00313.

Sakshaug, E. (2004): Primary and secondary production in the Arctic Seas.- In: R. STEIN, R.W. MACDONALD (eds), The organic carbon cycle in the Arctic Ocean. Springer Verlag, Heidelberg, 57-82.

Salonen, J.S., Seppö, M., Väliranta, M., Jones, V.J., Self, A., Heikkilä, M., Kultti, S. & Yang, H. (2011): The Holocene thermal maximum and late-Holocene cooling in the tundra of NE European Russia Quat. Res. 75: 501-511.

Sarnthein, M., Pflaumann, U. & Weinelt, M. (2003a): Past extent of sea ice in the northern North Atlantic inferred from foraminiferal paleotemperature estimates.- Paleoceanography 18: 25-1 - 25-8.

Sarnthein, M., van Kreveld, S., Erlenkeuser, H., Grootes, P.M., Kucera, M., Pflaumann, U., Schulz, M. (2003c): Centennial-to-millennial-scale periodicities of Holocene climate and sediment injections off the Barents shelf, 75 °N.- Boreas 32: 447-461.

Schlüter, M., Sauter, E.J., Schäfer, A. & Ritzrau, W. (2000): Spatial budget of organic carbon flux to the seafloor of the northern North Atlantic (60° N - 80° N).- Global Biogeochem. Cycles 14: 329-340.

Serreze, M.C., Holland, M.M. & Stroeve, J. (2007): Perspectives on the Arctic's shrinking sea-ice cover.- Science 315: 1533-1536.

Sicre, M.-A., Jacob, J., Ezat, U., Rousse, S., Kissel, K., Eiriksson, J., Knudsen, K.-L., Jansen, E., & Turon, J.L. (2008): Decadal variability of sea surface temperatures off North Iceland over the last 200 yrs.- Earth Planet. Sci. Lett. 268: 137-142.

Smith, D. (1998): Recent increase in the length of the melt season of perennial Arctic sea ice.- Geophys. Res. Lett. 25: 655-658.

Smith, W.O.Jr, Baumann, M.E.M., Wilson, D.L. & Aletsee, L. (1987): Phytoplankton biomass and productivity in the marginal ice zone of the Fram Strait during summer 1984. -J. Geophys. Res. 92: 6777-6786.

Spielhagen, R.F., Baumann, K.-H., Erlenkeuser, H., Nowaczyk, N.R., Nørgaard-Pedersen, N., Vogt, C. & Weiel, D. (2004): Arctic Ocean deepsea record of Northern Eurasian ice sheet history.- Quat. Sci. Rev. 23: 1455-1483.

Spielhagen, R.F., Bonani, G., Eisenhauer, A., Frank, M., Frederichs, T., Kassens, H., Kubik, P.W., Mangini, A., Nörgaard-Pedersen, N., Nowaczyk, N.R., Schäper, S., Stein, R., Thiede, J., Tiedemann, R., Wahsner, M. (1997): Arctic Ocean evidence for Late Quaternary initiation of northern Eurasian ice sheets.- Geology 25: 783-786.

Spielhagen, R.F., Erlenkeuser, H. & Siegert, C. (2005): History of freshwater runoff across the Laptev Sea (Arctic) during the last deglaciation.- Global Planet Change 48: 187-207.

St. John, K. (2008): Cenozoic ice-rafting history of the central Arctic Ocean: terrigenous sands on the Lomonosov Ridge.- Paleoceanography 23, doi:10.1029/2007PA001483.

St. John. K. & Krissek, L.A. (2002): The late Miocene to Pleistocene icerafting history of southeast Greenland.- Boreas 31: 28-35.

Stabeno, P. & Overland, J.E. (2001): Bering Sea shifts toward an earlier spring transition.- EOS Transactions AGU 82: 317, 32.

Stein, R. (1986): Surface-water paleo-productivity as inferred from sediments

deposited in oxic and anoxic deep-water environments of the Mesozoic Atlantic Ocean.- In: E.T. DEGENS et al. (eds), Biochemistry of Black Shales, Mitteil. Geol. Paläont. Inst. Univ. Hamburg 60: 55-70.

Stein, R. (1991): Organic carbon accumulation in Baffin Bay and paleoenvironment in High-Northern Latitudes during the past 20 m.y..- Geology 19: 356-359.

Stein, R. (2008): Arctic Ocean sediments: processes, proxies, and palaeoenvironment.- Developments in Marine Geology, Vol. 2, Elsevier, Amsterdam, 1-587.

Stein, R. (2011): The great challenges in Arctic Ocean paleoceanography. IOP Conf. Series Earth Environ. Sci. 14, doi: 10.1088/1755-1315/14/1/012001.

Stein, R. & Fahl, K. (1997): Scientific cruise report of the Arctic Expedition ARK-XIII/2 of RV "Polarstern" in 1997-. Reports Polar Res. 255: 1-235.

Stein, R. & Fahl, K. (2012): Biomarker proxy IP25 shows potential for studying entire Quaternary Arctic sea-ice history.- Org. Geochem. doi: 10.1016/j.Orggeochem.2012.11.005.

Stein, R., Nam, S.-I., Schubert, C., Vogt, C., Fütterer, D. & Heinemeier, J. (1994a): The last deglaciation event in the eastern central Arctic Ocean. Science 264: 692-696.

Stein, R., Schubert, C.J., Vogt, C. & Fütterer, D. (1994b): Stable isotope stratigraphy, sedimentation rates, and salinity changes in the Latest Pleistocene to Holocene eastern central Arctic Ocean.- Mar. Geol. 119: 333-355.

Stein, R., Dittmers, K., Fahl, K., Kraus, M., Matthiessen, J., Niessen, F., Pirrung, M., Polyakova, Ye., Schoster, F., Steinke, T. & Fütterer, D.K. (2004): Arctic (Palaeo) river discharge and environmental change: evidence from Holocene Kara Sea sedimentary records.- Quat. Sci. Rev. 23: 1485-1511.

Stein, R., Boucsein, B. & Meyer, H. (2006): Anoxia and high primary production in the Paleogene central Arctic Ocean: first detailed records from Lomonosov Ridge.- Geophys. Res. Lett. 33, L18606, doi: 10.1029/2006GL026776.

Stein, R., Matthiessen, J. & Niessen, F. (2010a): Re-Coring at Ice Island T3 Site of Key Core FL-224 (Nautilus Basin, Amerasian Arctic): Sediment characteristics and stratigraphic framework.- Polarforschung 79: 81-96.

Stein, R., Matthiessen, J., Niessen, F., Krylov, R., Nam, S. & Bazhenova, E. (2010b): Towards a better (litho-) stratigraphy and reconstruction of Quaternary paleoenvironment in the Amerasian Basin (Arctic Ocean).- Polarforschung 79: 97-121.

Steinsund, P.I. & Hald, M. (1994): Recent calcium carbonate dissolution in the Barents Sea: Paleoceanographic applications.- Mar. Geol. 117: 303-316.

Stickley, C.E., John, K.S., Koc, N., Jordan, R.W., Passchier, S., Pearce, R.B. & Kearns, L.E. (2009): Evidence for middle Eocene Arctic sea ice from diatoms and ice-rafted debris.- Nature 460: 376-380.

Stroeve, J., Holland, M.M., Meier, W., Scambos, T. & Serreze, M. (2007): Arctic sea ice decline: faster than forecast.- Geophys. Res. Lett. 34, L09501, doi:10.1029/2007GL029703.

Sudgen, D. (1982): Arctic and Antarctic - A modern geographical synthesis. Blackwell Publ., Oxford, 1-472.

Svendsen, J.I., Alexanderson, H., Astakhov, V.I., Demidov, I., Dowdeswell, J.A., Funder, S., Gataullin, V., Henriksen, M., Hjort, C., Houmark-Nielsen, M., Hubberten, H.-W., Ingólfsson, O., Jakobsson, M., Kjær, K.H., Larsen, E., Lokrantz, H., Lunkka, J.P., Lyså, A., Mangerud, J., Matioushkov, A., Murray, A., Möller, P., Niessen, F., Nikolskaya, O., Polyak, L., Saarnisto, M., Siegert, C., Siegert, M.J., Spielhagen, R.F. & Stein, R. (2004): Late Quaternary ice sheet history of Northern Eurasia.- Quat. Sci. Rev. 23: 1229-1272.

Tarasov, L. & Peltier, W.R. (2005): Arctic freshwater forcing of the Younger Dryas cold reversal.- Nature 435: 662-665.

Teller, J.T., Leverington, D.W. & Mann, J.D. (2002): Freshwater outbursts to the oceans from glacial Lake Agassiz and their role in climate change during the last deglaciation.- Quat. Sci. Rev. 21: 879-887.

Thiede, J., Clark, D.L. & Hermann, Y. (1990): Late Mesozoic and Cenozoic paleoceanography of the northern polar oceans.- In: The Geology of North America, Vol. L, The Arctic Ocean Region, 427-458.

Thiede, J., Jenssen, C., Knutz, P., Kuijpers, A., Mikkelsen, N., Nørgaard-Pedersen, N. & Spielhagen, R.F. (2011): Millions of years of Greenland ice sheet history recorded in ocean sediments.- Polarforschung 80: 141-159.

Thiede, J., Winkler, A., Wolf-Welling, T., Eldholm, O., Myhre, A., Baumann, K.-H., Henrich, R. & Stein, R. (1998): Late Cenozoic history of the polar North Atlantic: results from ocean drilling.- In: A. ELVERHØI, J. DOWDESWELL, S. FUNDER, J. MANGERUD & R. STEIN (eds), Glacial and Oceanic History of the Polar North Atlantic Margins. Quat. Sci. Rev. 17: 185-208.

Thomas, E. (2008): Descent into the Icehouse.- Geology 36: 191-192.

Thorndike, A.S. (1986): Kinematics of sea ice.- In: N. UNTERSTEINER (ed), The Geophysics of Sea Ice, Nato ASI Ser. B Physics 146: 489-549.

Tripati, A., Backman, J., Elderfield, H. & Ferretti, P. (2005): Eocene bipolar glaciation associated with global carbon cycle changes.- Nature 436: 341-346.

Tripati, A.K., Eagle, R.A., Morton, A., Dowdeswell, J.A., Atkinson, K.L., Bahé, Y., Dawber, C.F., Khadun, E., Shaw, R.M.H., Shorttle, O. & Thanabalasundaram, L. (2008): Evidence for glaciation in the Northern Hemisphere back to 44 Ma from ice-rafted debris in the Greenland Sea.- Earth Planet. Sci. Lett. 265: 112-122.

Vare, L.L., Massé, G. & Belt, S.T. (2010): A biomarker-based reconstruction of sea ice conditions for the Barents Sea in recent centuries.- The Holocene, doi:10.1177/0959683609355179.

Vare, L.L., Massé, G., Gregory, T.R., Smart, C.W. & Belt, S.T. (2009): Sea ice variations in the central Canadian Arctic Archipelago during the Holocene. Quat. Sci. Rev. 28: 1354-1366.

Vinje, T., Nordlund, N. & Kvambekk, A. (1998): Monitoring ice thickness in Fram Strait.- J. Geophys. Res. C 103:10437-10449.

Vinnikov, K.Ya., Robock, A., Stouffer, R.J., Walsh, J.E., Parkinson, C.L., Cavalieri, D.J., Mitchell, J.F.B., Garrett, D. & Zakharov, V.F. (1999): Global warming and Northern Hemisphere sea ice extent.- Science 286: 1934-1936.

Vogt, C. (1997): Regional and temporal variations of mineral assemblages in Arctic Ocean sediments as climatic indicator during glacial/interglacial changes.- Report. Polar Res. 251: 1-309.

Vogt, C. (2004): Mineralogy of sediment core PS2185-6.- PANGAEA, doi:10.1594/PANGAEA.138270

Volkman, J.K. (1986): A review of sterol markers for marine and terrigenous organic matter.- Org. Geochem. 9: 83-99.

Volkman, J.K. (2006): Lipid markers for marine organic matter.- In: J.K. VOLKMAN (ed), Handbook of Environmental Chemistry. Springer-Verlag, Berlin, Heidelberg, 27-70.

Wahsner, M., Müller, C., Stein, R., Ivanov, G., Levitan, M., Shelekova, E. & Tarasov, G. (1999): Clay mineral distributions in surface sediments from the central Arctic Ocean and the Eurasian continental margin as indicator for source areas and transport pathways: a synthesis.- Boreas 28: 215-233.

Wassmann, P., Bauerfeind, E., Fortier, M., Fukuchi, M., Hargrave, B., Moran, B., Noji, T., Nöthig, E.M., Olli, K., Peinert, R., Sasaki, H. & Shevchenko, V.P. (2004): Particulate organic carbon fluy to the Arctic Ocean seafloor.- In: R. STEIN & R.W. MACDONALD (eds), The Organic Carbon Cycle in the Arctic Ocean, Springer Verlag, Heidelberg, 101-138.

Wassmann, P. (2011): Arctic marine ecosystems in an era of rapid climate change.- Progress Oceanogr. 90: 1-17.

Weller, P. & Stein, R. (2008): Paleogene biomarker records from the central Arctic Ocean (IODP Expedition 302): organic-carbon sources, anoxia, and sea-surface temperature.- Paleoceanography 23, PA1S17, doi:10.1029/2007PA001472.

Wheeler, P.A., Gosselin, M., Sherr, E., Thiebault, D., Benner, R. & Whitledge, T.E. (1996): Active cycling of organic carbon in the central Arctic Ocean.- Nature 380: 697-699.

Winkelmann, D., Schäfer, C., Stein, R. & Mackensen, A. (2008): Terrigenous events and climate history of the Sophia Basin, Arctic Ocean.- Geochem. Geophys. Geosyst. 9, doi:10.1029/2008GC002038.

Wolf, T.C.W. & Thiede, J. (1991): History of terrigenous sedimentation during the past 10 m.y. in the North Atlantic (ODP Legs 104, 105, and DSDP 81).- Mar. Geol. 101: 83-102.

Wolf-Welling, T.C.W., Cremer, M., O'Connell, S., Winkler, A. & Thiede, J. (1996): Cenozoic Arctic gateway paleoclimate variability: indicatiosn from changes in coarse-fraction compositions (ODP Leg 151).- In: J. THIEDE, A.M. MYHRE, J. FIRTH et al., Proceedings ODP, Sci. Results 151, College Station, Texas (Ocean Drilling Program) 515-525.

Wollenburg, J.E., Knies, J. & Mackensen, A. (2004): High-resolution paleoproductivity fluctuations during the past 24 kyr as indicated by benthic foraminifera in the marginal Arctic Ocean.- Palaeogeogr. Palaeoclimatol. Palaeoecol. 204: 209-238.

Wollenburg, J.E., Kuhnt, W. & Mackensen, A. (2001): Changes in Arctic Ocean palaeoproductivity and hydrography during the last 145 kyr: the benthic foraminiferal record.- Paleoceanography 16: 65-77.

Wright, J.D., Miller, K.G. & Fairbanks, R.G. (1992): Early and middle Miocene stable isotopes: implications for deep water circulation and climate.- Paleoceanography 7: 357-389.

Wüst, G. & Brögmus, W. (1955): Ozeanographische Ergebnisse einer Untersuchungsfahrt mit Forschungskutter "Südfall" durch die Ostsee Juni/Juli 1954 (anlässlich der totalen Sonnenfinsternis auf Öland).- Kieler Meeresforsch. 11: 3-21.

Xiao, X., Fahl, K. & Stein, R. (2012): Modern spatial (seasonal) variability in sea ice cover of the Kara and Laptev seas: reconstruction from new biomarker data determined in surface sediments. Quat. Sci. Rev., submitted.

Zachos, J., Pagani, M., Sloan, L., Thomas, E. & Billups, K. (2001): Trends, rhythms, and aberrations in global climate 65 Ma to Present.- Science 292: 868-693.

Zachos, J.C., Dickens, G.R. & Zeebe, R.E. (2008): An early Cenozoic perspective on greenhouse warming and carbon-cycle dynamics.- Nature 451: 281-283.

Scientific Deep Drilling in the Arctic Ocean: Status of the Seismic Site Survey Data Base[*]

by Wilfried Jokat

Abstract: In the last decades, several geophysical research expeditions have led to a significant growth of the seismic database in the central Arctic Ocean. In particular, the combination of seismic data with results of scientific deep drilling in 2004 have dramatically changed the view on the Arctic climate evolution. Since then, several proposals have been submitted to the Integrated Ocean Drilling Program (IODP) to solve certain scientific problems through deep drilling. Seismic data are crucial to foster any progress regarding these proposals in the Arctic, in order to justify the selection of the drill sites. This contribution reviews the current distribution of seismic reflection data, especially in the High Arctic. This study will focus on various areas of the High Arctic and briefly address the scientific questions for these specific regions.

Zusammenfassung: In den letzten zwei Dekaden führten mehrere wissenschaftliche Expeditionen in die Hocharktis dazu, dass die geowissenschaftliche Datenbasis kontinuierlich wuchs. Insbesondere die Kombination einer wissenschaftlichen Tiefbohrung aus dem Jahr 2004 mit seismischen Daten veränderte die Sicht auf die Klimaentwicklung der Arktis dramatisch. Als Folge dieser ersten erfolgreichen Tiefbohrung im zentralen arktischen Ozean wurden mehrere Bohrvorschläge beim "Integrated Ocean Drilling Program" (IODP) eingereicht, um auch andere Fragestellungen mit entsprechenden Tiefbohrungen zu beantworten. Kritisch für jeglichen Fortschritt zur Verwirklichung dieser Bohrvorschläge sind seismische Daten mit denen die Auswahl der Bohrpositionen gerechtfertigt werden kann. In diesem Beitrag soll die momentane Verfügbarkeit der seismischen Daten insbesondere im zentralen arktischen Ozean zusammengefasst und vorgestellt werden. Die Beschreibung wird sich auf einige Regionen konzentrieren und die speziellen Fragestellungen kurz anreißen.
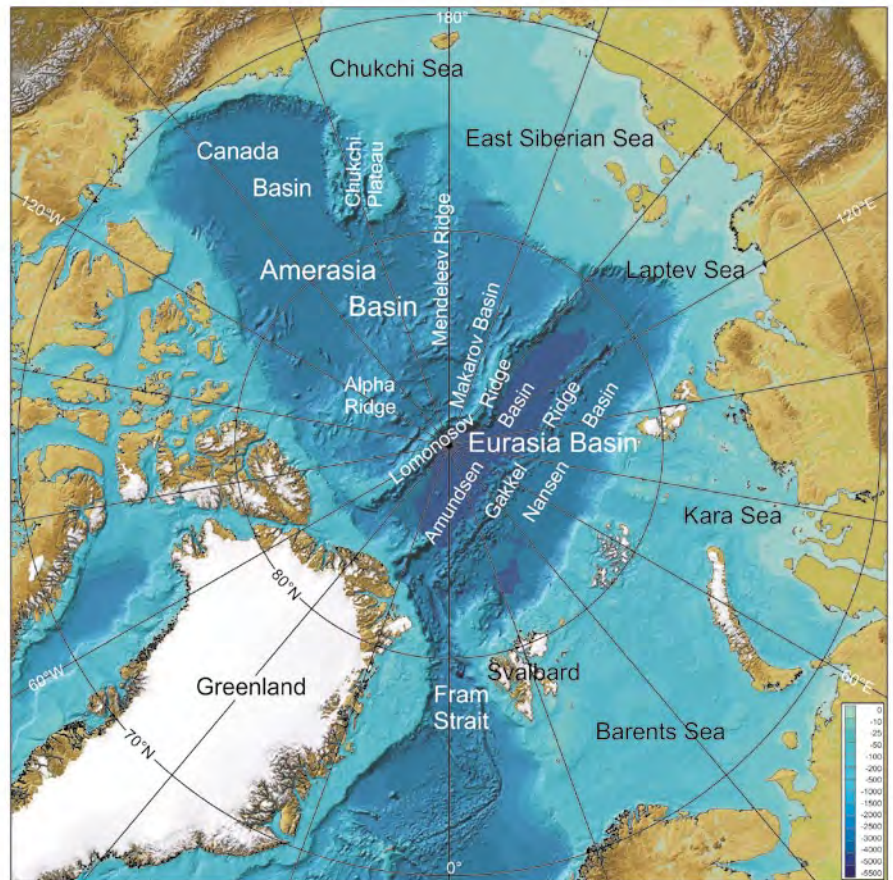
Fig.1: Physiography of the Arctic Ocean showing major structural tectonic units discussed in this study.

Abb.1: Physiographie des arktischen Ozean mit den wichtigsten tektonischen Strukturelementen, die in diesem Beitrag diskutiert werden.

INTRODUCTION

Compared to most of the global oceans the Arctic underwent quite a complex tectonic history, which created several ridges and basins (Fig. 1). These structures were created during a two-phase tectonic evolution of the central Arctic Ocean: the Eurasia Basin formed during the Cenozoic, and the Amerasia Basin during the Mesozoic. The seafloor spreading in the Eurasia Basin along the ultraslow spreading Gakkel Ridge is still going on, and well documented by Cenozoic magnetic seafloor spreading anomalies (KARASIK 1968, VOGT et al.

1979). Interestingly, the Gakkel Ridge terminates in the East towards the Siberian shelf, namely the Laptev Sea. In contrast to other continental rift systems, the stretching of the continental crust in the Laptev Sea and southwards, is not accompanied by massive volcanism. The Eurasia Basin is bounded to the south by the Siberian and Svalbard shelves, while in the north the Lomonosov Ridge, almost 1800 km long, forms the boundary to the Mesozoic part of the Arctic Ocean. Around 56 Myr ago the Lomonosov Ridge was part of the Siberian shelves and rifted apart when the formation of the Eurasia Basin started (JOKAT et al. 1992). Thus, it is in general agreed that the Lomonosov Ridge is a continental sliver.

Explaining the tectonic history is more difficult, since no extinct spreading centre is to be identified, which helps to constrain the tectonic history of the Amerasia Basin (VOGT et al. 1982). A few weak magnetic stripes are to be observed in

the Canada Basin. However, they cannot be dated, because the basement is covered by several kilometres of sediments. The most intriguing structure in the Amerasia Basin is the Alpha-Mendeleev Ridge striking almost parallel to the Lomonosov Ridge (Fig. 1). All existing geophysical data point towards a volcanic origin of this ridge complex (HUNKINS 1961, VOGT et al. 1982, FORSYTH et al. 1986, JACKSON et al. 1986). The magnetic field shows highly irregular anomalies with no evidences for any magnetic seafloor spreading anomalies. The Russian deep seismic experiment revealed crustal thickness below the ridge of 32 km (LEBEDEVA-IVANOVA et al. 2006) with a velocity-depth distribution similar to those of submarine Large Igneous Provinces (LIP) elsewhere. However, problematic for any conclusive understanding of this complex are samples from the basement, which can be analysed and dated.

For constraining the long-term climate history of the Arctic Ocean, the Lomonosov and Alpha Mendeleev ridges are important to investigate. Since the water depths of both ridges are well above the adjacent basins, they are less influenced by mass wasting events from the surrounding margins. Therefore, the sediments on top of both structures should hold a more or less complete, but undisturbed sediment package for the Cenozoic (Lomonosov Ridge; JOKAT et al. 1992, JOKAT 2005) and the Mesozoic/Cenozoic (Alpha – Mendeleev Ridge; JOKAT 2003, DOVE et al. 2010) respectively. Though, for all relevant geological structures of the global oceans the general bathymetry is fairly well known, still most of the central Arctic Ocean has never been visited by any scientific expedition. The sea-ice cover is the most important limiting factor. It allows ship-based expeditions only in August/September, and because of the highly variable sea-ice cover, there is no guarantee that the proposed research area can be reached.

For seismic investigations in the central Arctic Ocean a second icebreaking ship is essential to allow the acquisition of any high quality data, which can be used e.g. for any site selection to retrieve long sediment cores (JOKAT et al. 1995). The selection of sites for scientific drilling requires an even greater effort. Normally, several expeditions are necessary to find appropriate locations and to fulfil the safety requirements for the later drilling campaign. Since only few icebreakers are available for such an effort it simply takes time to coordinate the scientific icebreakers from different countries, and to convince funding agencies to support such efforts.
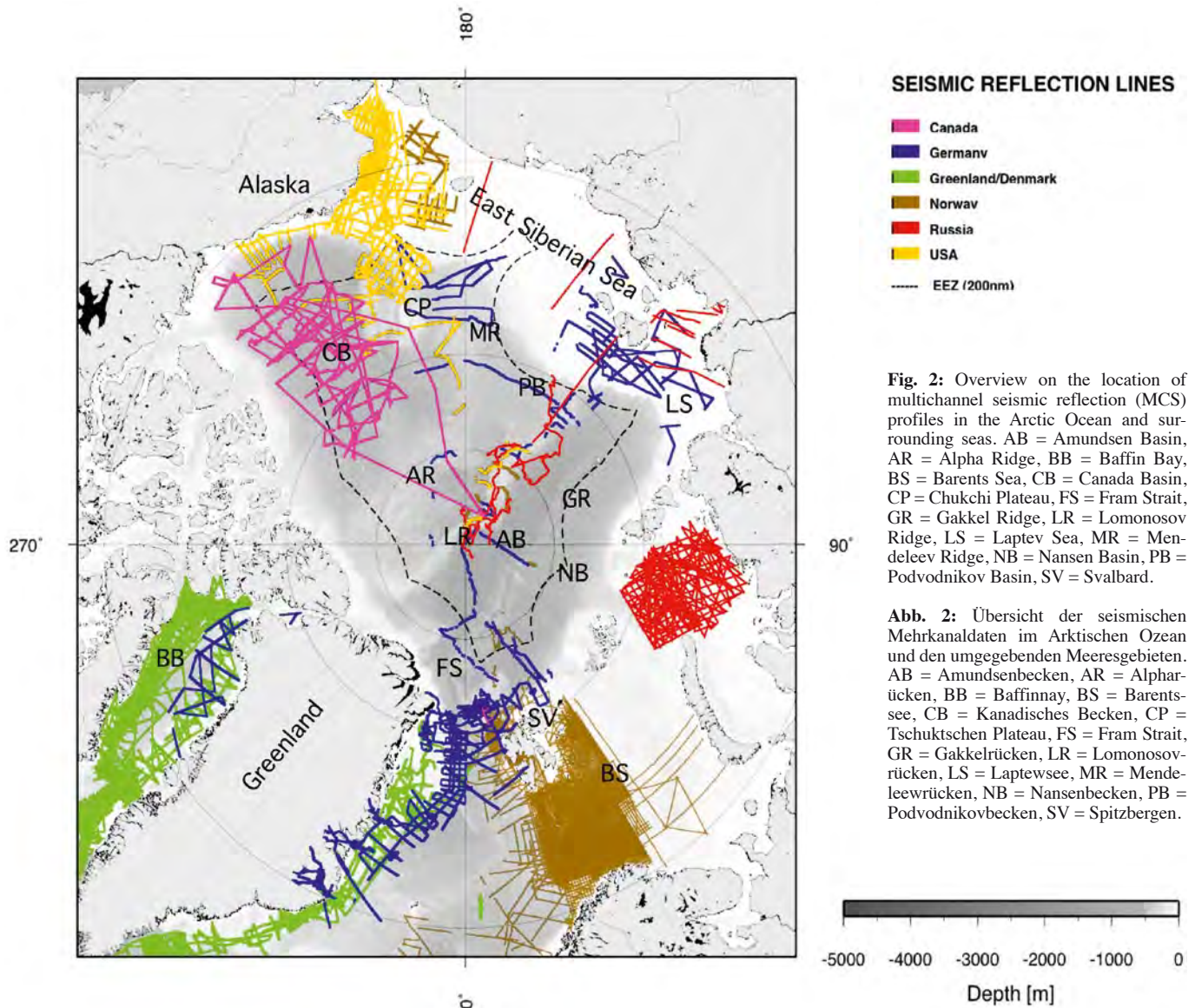
An important issue in the last century was to develop a technology setup to conduct geophysical surveys in ice covered areas. The first natural approach was to use the ice floes themselves as carrier. Russian, American, Canadian institutions equipped large and thick ice floes with ice camps, which were regularly supplied by aircrafts. The natural drift of the ice floes allowed the acquisition of seismic data but also of geological samples. Such drift camps allowed to investigate areas, which could not be reached by any conventional research vessel in the 1950's and 1960's of the last century. In any case these ice islands were the first break through for geoscience in the Arctic by gathering first order information on bathymetry, sediment thickness and geology (shallow cores, dredges; HALL 1973, HUNKINS 1961). The

critical factor of these ice-island geophysical experiments was the limited energy for the seismic sources. It simply constrained the vertical penetration of the sound energy into the sediments. Thus, a mix of weak seismic sources (sparker, small airguns) and strong dynamite blasts were used to investigate the sedimentary and crustal structure of various Arctic ridges and basins (HUNKINS 1961, HALL 1973, JACKSON et al. 1990). Another constraint was that the drift direction of the ice floe could not be predicted. It was a drift into the "unkown", which was to some extend successful since some ice islands carried an ice camp for several years (T3 1967-1970; HALL 1973).

The situation changed in 1980's, when icebreaking research vessels such as RV "Polarstern" became available for research also in the central Arctic Ocean. The use of the icebreakers should allow within the summer season to approach any specific location in the Arctic Ocean. A first and successful attempt to gather seismic data from a single icebreaker operation was made by North American scientists on the Chukchi Plateau and Canada Basin (GRANTZ et al. 2004). However, several meter thick ice floes made seismic profiling during ice breaking extremely difficult.

In 1991, a different approach was initiated. During the joint multi-disciplinary Arctic Ocean expedition – the ARCTIC'91 – of the ice-breaking research vessels "Oden" and "Polarstern" it was planned to work in a tandem. Norwegian and German geophysicists used this tandem setup trying to obtain multichannel seismic data. The plan was that "Oden" as leading vessel did the icebreaking, while the seismic gear – airguns and streamer – was towed in a more or less standard configuration behind "Polarstern's" stern in a passage through the ice more or less open (JOKAT et al. 1995). This approach proved to be the next break-through for seismic data acquisition in the ice-covered areas of the central Arctic Ocean. For the first time long seismic profiles were acquired within a few days showing the deeper sedimentary structure of the Amundsen Basin and the Lomonosov Ridge (JOKAT et al. 1992, JOKAT et al. 1995a, 1995b). The quality of the records after some data processing was comparable to open water data quality. This international Arctic expedition in 1991 with the overwhelming amount of new high quality seismic data from the central Arctic Ocean demonstrated the efficient setup of two icebreakers working in tandem for geophysics.

Since then numerous High Arctic expeditions were conducted with ice breaking vessels from several countries to retrieve seismic information. In most cases the setup of "Oden" and "Polarstern" was adapted to ensure and optimize the data acquisition. The tremendous amount of new seismic data of >10,000 km gathered in the Canada Basin, a formerly almost un-surveyed area, was investigated by a combined effort of Canadian and US icebreakers. Even industry has adapted and modified this setup for gathering seismic data along the ice rim of East Greenland but with streamer lengths up to 8000 m. Again, the leading icebreaking vessel to some extend guarantees an efficient and predictable seismic data acquisition by the following seismic vessel. Finally, though this tandem set-up was extremely successful in the Arctic, it turned out that the major difficulty for geophysics, at least, in the past was to organize two ice breaking research vessels for a joint scientific expedition.

Fig. 2: Overview on the location of multichannel seismic reflection (MCS) profiles in the Arctic Ocean and surrounding seas. AB = Amundsen Basin, AR = Alpha Ridge, BB = Baffin Bay, BS = Barents Sea, CB = Canada Basin, CP = Chukchi Plateau, FS = Fram Strait, GR = Gakkel Ridge, LR = Lomonosov Ridge, LS = Laptev Sea, MR = Mendeleev Ridge, NB = Nansen Basin, PB = Podvodnikov Basin, SV = Svalbard.

Abb. 2: Übersicht der seismischen Mehrkanaldaten im Arktischen Ozean und den umgegebenden Meeresgebieten. AB = Amundsenbecken, AR = Alpharücken, BB = Baffinnay, BS = Barentssee, CB = Kanadisches Becken, CP = Tschuktschen Plateau, FS = Fram Strait, GR = Gakkelrücken, LR = Lomonosovrücken, LS = Laptewsee, MR = Mendeleewrücken, NB = Nansenbecken, PB = Podvodnikovbecken, SV = Spitzbergen.

SCIENCE AND DRILLING IN THE ARCTIC OCEAN

Advances towards a better understanding of the Arctic long-term tectonic history as well as short- and long-term climate changes are highly dependent on the availability of deep scientific drill holes in the central Arctic Ocean and its marginal seas. Though, there is, in general, a strong support from the scientific community to close the knowledge gaps in the Arctic, several issues have to be solved. One general problem in promoting scientific drilling in such remote areas is obvious: while drilling proposals in many other regions can rely on existing "old" data or industry information to justify their scientific objectives, Arctic Ocean drilling is, compared to the rest of the world's oceans, in an adverse stage. Beside numerous short piston and gravity cores, only one scientific deep drill site exists in the central Arctic Ocean (BACKMAN et al. 2006, MORAN et al. 2006). This 450 m long core from the Lomonosov Ridge was drilled during the Arctic Coring Expedition (ACEX) in 2004 with the assistance of three icebreakers. Here, the main scientific results can be summarized as follows:

- During the Paleocene-Eocene Thermal Maximum (PETM) event, surface water temperatures reached values as high as 25 °C (SLUIJS et al. 2006, 2008)

- An anoxic deep-water environment, indicated by a high total organic carbon content (TOC) and specific biomarker composition, occurred from at least 56 to 44 Ma (STEIN et al. 2006).
- Evidences for a freshwater fern Azolla were found in sediments dated around 49 Ma (BRINKHUIS et al. 2006).
- First evidence of sea ice based on diatoms was already found at 47 Ma (STICKLEY et al. 2009). Evidence of ice rafted material (IRD) was found in sediments as old as 46.3 Ma, suggesting that the Earth's transition from a Greenhouse to an Icehouse world was bipolar (MORAN et al. 2006, ST. JOHN 2008).
- During the middle Eocene (49 to 45 Ma), surface-water temperatures decreased from 25 to 10 °C; between 46.3 and Ma, with the onset of sea ice, an environment similar to the present-day Baltic Sea – warm ice-free water in the summer and sea ice in the winter – has been proposed (WELLER & STEIN 2008).
- Since approximately 14 Ma, perennial sea-ice cover may have possibly occurred (DARBY 2008, KRYLOV et al. 2008).

Unfortunately, the ACEX sequence is incomplete as a hiatus lasting from 44.4 to 18.4 Ma occurred at about 198 mbsf. Up-to-date, there is a lot of speculation on the processes

causing this hiatus. Currently, there are conflicting findings and hypotheses to explain such a pronounced hiatus on Lomonosov Ridge (LR):

- More or less strong currents at this part of the LR prevented the deposition of large amounts of sediment. Such strong currents may have played an important role as is visible also in the seismic section crossing the drill location (JOKAT et al. 1992). Here, the flanks of the lowermost sediment package are eroded and overlain by a conformable Miocene drape.
- A more complex subsidence history of the LR, which consequently caused a much longer sub-aerial or shallow water exposure of the LR crest than previously assumed (JOKAT et al. 1995). This model involves an uplift of LR during Oligocene times (O'REAGAN et al. 2008, MINAKOV & PODLADCHIKOV 2012).
- Sub-aerial or shallow water position of LR caused by a sea level decline during Cenozoic times, and a subsequent erosion and/or non-deposition of ridge sediments (POIRIER

& HILLAIRE-MARCEL 2011). Currently, there is no evidence for such a strong decline in sea level.

These hypotheses can only be addressed with a new deep drilling campaign. Though the ACEX drilling funded by IODP proved to be one of the most successful scientific expeditions in providing surprising results on the Arctic environment, it probably will not be repeated in the near future. Currently, the major problem is to provide seismic data on LR, which convincingly show that the hiatus is not present at selected drill sites in order to retrieve a more complete Cenozoic sediment section. This is especially important when justifying the expenses of a two- or three-ship drilling expedition.

Because of the strong global competition within IODP, it is of outmost importance to propose a set of sites in the Arctic and its marginal seas, which are suitable to answer the following questions:
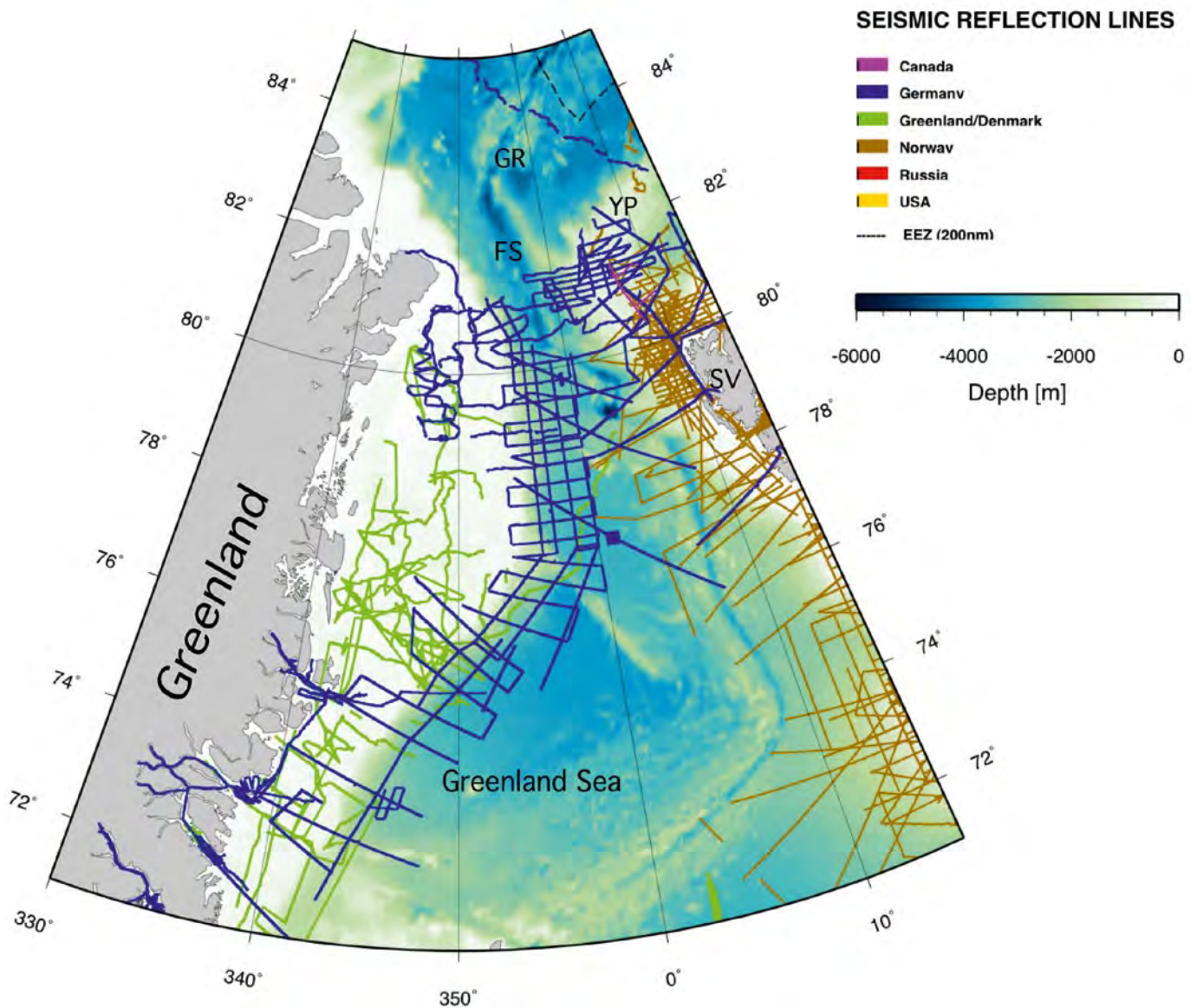
Fig. 3: Multichannel seismic reflection (MCS) profiles off East Greenland and in the Fram Strait. YP = Yermak Plateau, GR = Gakkel Ridge, FS = Fram Strait, SV = Svalbard.

Abb. 3: Seismische Mehrkanalprofile vor Ostgrönland und in der Framstraße. GR = Gakkelrücken, YP = Yermakplateau, FS = Stramstraße, SC = Spitzbergen.

- How long lasted the Arctic Ocean anoxic state; both in Mesozoic and Cenozoic times?
- Did the Arctic Ocean face strong sea level declines, which would explain the large hiatus on LR? If so, deeper sites have to be selected, which were not affected by these events.
- When did the sea-ice cover start to evolve and how did it fluctuate during Cenozoic times? How does this compare to Antarctica?
- What were the paleo-oceanographic consequences of a shallow and/or deep-water gateway in the Fram Strait?

In the central Arctic Ocean, the more or less continuous sedimentation on ridge systems has a greater potential to provide a complete sedimentary record than the in parts heavily eroded circum-Arctic shelf areas.

In summary, this contribution aims to describe the seismic database (Fig. 2), which is currently available from scientific institutions or commercial companies to support scientific drilling in the Arctic. The description focuses on the central Arctic Ocean and areas off East Greenland, Northern Svalbard and the East Siberian Sea, where at least IODP pre-proposals exist, and where seismic data acquisition has been quite a challenge because of the sea-ice cover. The seismic network on the shelves might be incomplete because of on-going industrial data acquisition or confidentiality of such information. Thus, industry navigation information on existing lines has been incorporated wherever available.

EAST GREENLAND

Today, the Greenland ice sheet is the last remnant of the vast Northern Hemisphere glaciations (NHG) of the past. It still has an ice thickness of up to 3000 m, and the question arises why the Greenland ice sheet has survived the global warming since the last glacial maximum. Based on current knowledge, there is clear evidence that glaciations have intensified since some 3 Ma (e.g. KLEIVEN et al. 2002). However, it is quite unlikely that ice sheets did not exist in polar regions before then. For example, TRIPATI et al. (2008) propose that already some 44–30 Ma, East Greenlandic glaciers or/and ice caps existed based on IRD found in an ODP drill hole off East Greenland. Before this finding, models proposed a stepwise intensification of the NHG after the Middle Miocene Climate Optimum (about 15-17 Ma) based on IRD records in the high northern latitudes (NANSEN ARCTIC DRILLING PROGRAM NAD SCIENCE COMMITTEE 1992, THIEDE et al. 2011). Also, dispute continues as to whether both polar regions have always been simultaneously glaciated or not. Furthermore, ice sheets located around the Arctic Ocean probably showed a different temporal and spatial behaviour.

In this context, more than 10,000 km of multichannel seismic data (MCS), (Fig. 3) (BERGER & JOKAT 2008, 2009), were acquired in the last decade north of the Jan Mayen Fracture Zone along the NE-Greenland margin. Again, partial heavy sea ice prevented the use of longer streamers (>1000 m active length) and large airgun arrays. However, the seismic network allows selecting several promising scientific drilling locations in the Greenland Basin in order to provide constraints for hypotheses on the history of Greenland's glaciations. Finally, one of the major problems in convincing IODP to accept a proposal for drilling off East Greenland is the limited sediment-age information from scientific drill holes, which are either non-existent or rather incomplete in their recovery.

FRAM STRAIT

When discussing the climate evolution of the Arctic Ocean, the kinematic history of the Fram Strait plays an outstanding role. Since the opening of this gateway, the Arctic Ocean environment most likely changed radically with the continuous widening of the Fram Strait. At some point, large volumes of water from the North Atlantic must have entered the Arctic Ocean and most likely have caused a complete ventilation of the Arctic Basin (JAKOBSSON et al. 2007), possibly no later than around 17.5 Ma. Here, it should be noted that the initial strike slip movements between North Greenland and Svalbard, which finally led to the formation of the Fram Strait, already started some 55 Ma ago. Thus, details on the widening/ deepening of the Fram Strait, or the existence of even older shallow water seaways through a "proto" Fram Strait are of great interest. Furthermore, the variability of the sea-ice cover and the current systems in the Fram Strait as a response to glacial and inter-glacial periods is also of interest when comparing the present-day situation.

To provide answers to these questions, the margins of the Fram Strait and the thick drift sediments along the Yermak Plateau are important target areas (GEISSLER et al. 2011). In the past decade, a large number of new MCS (Fig. 3) have been acquired, mainly in difficult ice conditions, along the northern part of the Yermak Plateau and the continental margin of NE Greenland. Along the Svalbard/Yermak margin, the objectives are twofold: i) mapping of the thick drift deposits as far north as sea ice conditions would allow, and ii) finding suitable drill locations more distant to the Svalbard mainland to recover sediments which are less influenced by local mountain glaciers.

LOMONOSOV RIDGE

While the previously discussed sites are located at the rim of the Arctic Ocean, the next target areas are located in the central Arctic Ocean. Most of the multi channel seismic data across the Lomonosov Ridge (LR) were acquired with a short streamer (300 m) and the support of a leading icebreaker (JOKAT 2005). Furthermore, LR was the location of a spectacular drilling campaign in 2004 (IODP Exp. 302, BACKMAN et al. 2006, MORAN et al. 2006). The Arctic Coring Expedition (ACEX) aimed to recover sediments dating back to early Cenozoic times to unravel the climate and environmental history of the Arctic Ocean. Two powerful ice breakers – the Russian "Sovetskiy Soyuz" and the Swedish "Oden" – and an ice strengthened drill ship ("Vidar Viking") managed to drill several scientific holes up to 450 m deep in heavy pack ice. The unexpected results completely changed the view on the evolution of the Arctic Ocean (see above).

Beside the tremendous success of the drilling campaign, several problems remain since a large hiatus between 44 and 18.2 Myr did not allow to obtain a complete and/or high resolution record on the climate history for the Cenozoic Arctic

Ocean. Currently, there are several hypotheses on the causes of this hiatus (see above). Although the seismic data across the LR are substantially more incomplete than off Svalbard / East Greenland, there are several portions of LR located closer to the East Siberian shelf at 81–80° N (Fig. 4) displaying no structural evidence in the seismic data that such a significant hiatus is present. Here, a reasonable seismic network exists to support this interpretation, but higher sedimentation rates require deeper drill holes to reach the same sediment ages as for the ACEX cores. Fortunately, these sites are located closer to the present-day ice edge, and might allow easier access for a drilling ship. Because of the current sea-ice retreat, an extensive ice management with two icebreakers might no longer be needed. Here, the site survey information is rather complete to launch a renewed effort for scientific drilling.

ALPHA-MENDELEEV RIDGE

The Alpha-Mendeleev Ridge (AMR) is a 1800 km long magmatic ridge system located in the part of the Arctic Ocean, which started to form already in the Mesozoic. The basement consists most likely of basalts and is covered by sediments with variable thickness. In the central part of the AMR, sediment thicknesses of 500 m and more than 1000 m close to the East Siberian Shelf are observed. These sediments have the potential to broaden our knowledge on the climate history of the Arctic Ocean back to 90 Ma. Shallow cores gathered from ice islands in the 1960's show that Maastrichtian black shales are present close the sea floor. Systematic probing will extend the time series of the ACEX drilling, terminating at around 56 Ma.

In the last decade, seismic data acquisition was almost impossible even with the help of two powerful icebreakers. Level sea ice of more than 5 m prevented any regular survey. However, the sea-ice retreat in the last years has radically changed the situation. Since 2007, e.g. RV "Polarstern" was able to reach the Alpha Ridge twice without any major problems, unfortunately without seismic gear on board to collect seismic data. While the junction of the AMR with the East Siberian shelf is reasonable well surveyed, this is absolutely not the case for the central part of this giant ridge system. Here, additional seismic surveys (Fig. 2) are needed to provide a sound network for a convincing selection of drill sites.
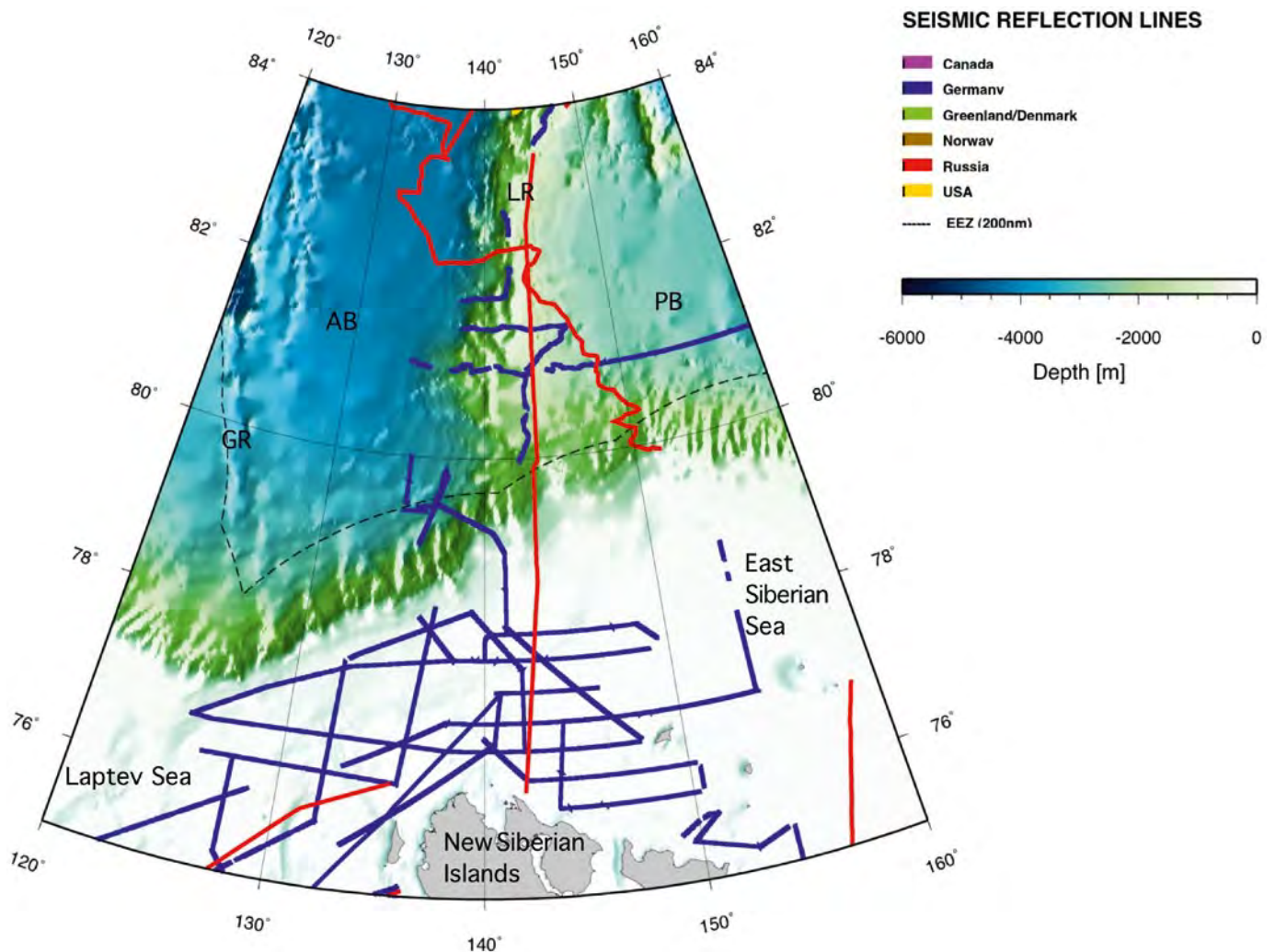
Fig. 4: Multichannel seismic reflection (MCS) profiles at the junction of the Lomonosov Ridge (LR) with the East Siberian Sea. GR = Gakkel Ridge, AB = Amundsen Basin, PB = Podvodnikov Basin.

Abb. 4: Seismische Mehrkanalprofile an der Schnittstelle zwischen dem Lomonosov Rücken (LR) und der Ostsibirischen See. GR = Gakkelrücken, AB = Amundsenbecken, PB = Podvodnikov Basin.
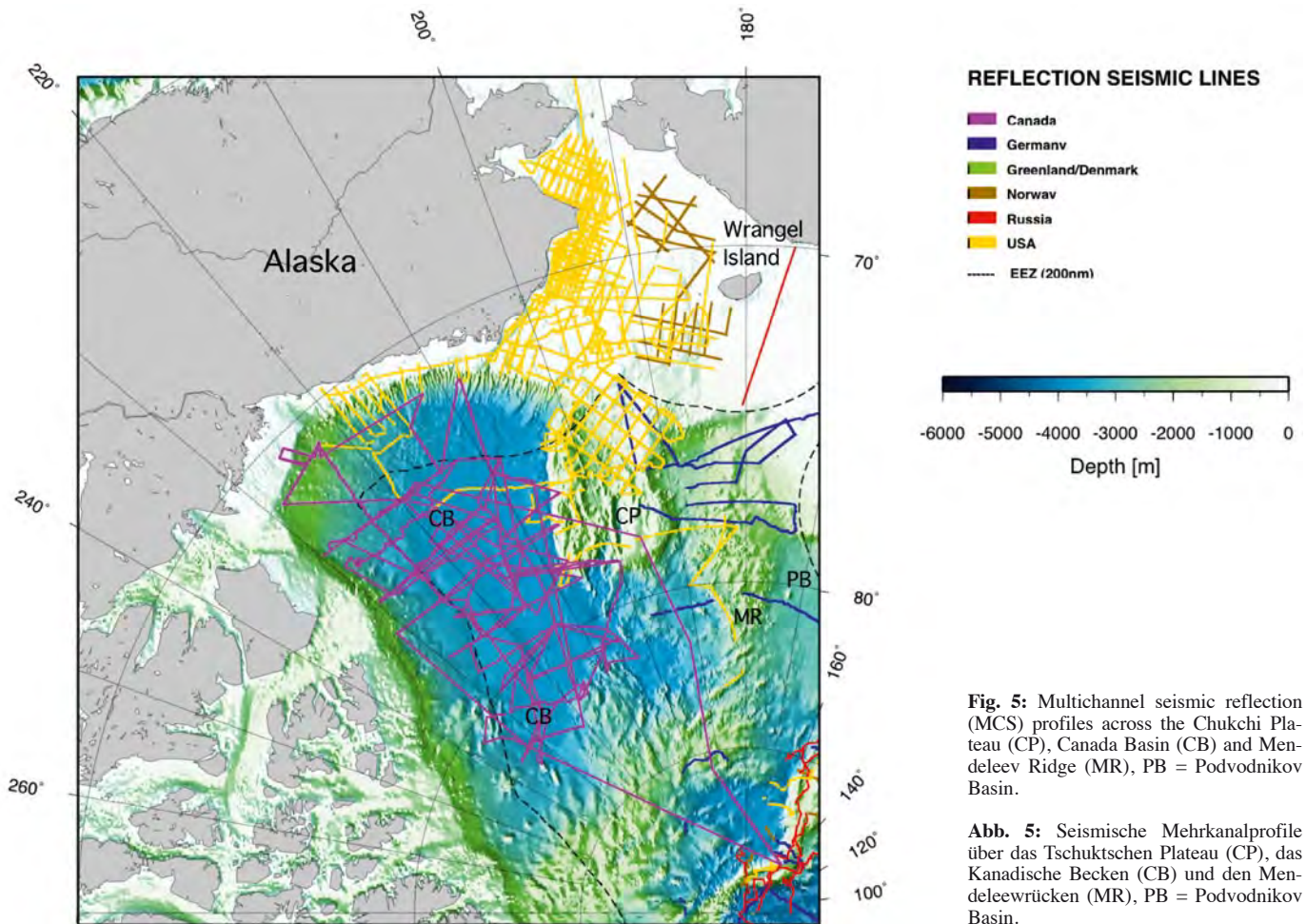
Fig. 5: Multichannel seismic reflection (MCS) profiles across the Chukchi Plateau (CP), Canada Basin (CB) and Mendeleev Ridge (MR), PB = Podvodnikov Basin.

Abb. 5: Seismische Mehrkanalprofile über das Tschuktschen Plateau (CP), das Kanadische Becken (CB) und den Mendeleewrücken (MR), PB = Podvodnikov Basin.

CHUKCHI PLATEAU / EAST SIBERIAN SEA

Glaciations have been considered to be the major short term driving process for sea level variations since the Middle Miocene. The advances and retreats of glaciers, ice sheets and ice streams are well documented in sedimentary sequences along many polar continental margins. Typical prograding sequences of unsorted material as well as eroded top sets are the direct evidences for a glacial overprint of such margins. However, these sequences are difficult to date because of the massive horizontal glacial transport. Furthermore, the sedimentary record is most likely incomplete because of unknown glacial erosion of older sequences during glacial times. Thus, we need data on parts of the Arctic margins not having experienced strong and repeated glacial erosion, and therefore possessing the capability of capturing sea level variations in sedimentary low/high stand system tracts. A comparison with global sea level curves as well as drilling results off Svalbard and Greenland and scientific drill holes especially from low latitudes will provide important insights into the impact of northern latitude glaciations on global sea level declines and rises during the Cenozoic.

Seismic profiles just south of the Chukchi Plateau (Fig. 5) indicate that this area might be the best region to provide a sound answer to this problem. The seismic data imaged a thick stack of prograding sequences, which were only affected in the upper part by glacial erosion. These two profiles were supplemented in 2011 by an US survey (Univ. Fairbanks)

also covering the southern Chukchi Plateau. Furthermore, this network could be linked to several commercial drill holes, which allow a first order age classification of the sedimentary sequence. Thus, after the final processing and interpretation of these data sets, there should be an excellent seismic database available for a sound selection of scientific drill sites.

CONCLUSIONS

This short contribution indicates that today the seismic database available for the selection of locations for scientific drill sites has significantly grown compared to the early 90's of the last century. These changes are partially due to the regular use of scientific icebreakers for conducting scientific programs in the High Arctic as well as being a consequence of the retreat of sea-ice cover in the last five years. Areas previously not accessible for such experiments at the rim of the Arctic Ocean, like the Chukchi Plateau, can nowadays be seismically investigated with standard seismic vessels. However, the situation in the central Arctic Ocean has only slightly improved. Here, the major problem is still to organize two-ship experiments, which in combination allow some sort of standard seismic data acquisition in sea ice several metres thick.

However, even the growing seismic data base does not solve the major problem of being successful in the IODP proposal system: for most of the drilling proposals submitted up to 2011, there were no well constrained age models. Considering

the global competition within the IODP programme, this fact remains to be one of the major issues to overcome now. Since the IODP programme is also facing strong budget cuts, there are tendencies to support proposals only where a sufficient level of knowledge already exists, rather than promoting drilling into "the unknown". This problem can only be tackled by: (i) an icebreaker with shallow or deep drilling capabilities, and (ii) making new funding available, which directly supports scientific drilling campaigns in the Arctic Ocean and the adjacent seas.

ACKNOWLEDGMENTS

References

Backman, J., Moran, K., McInroy, D.B., Mayer, L.A. & Expedition 302 Scientists (2006): Arctic Coring Expedition (ACEX).- Proceedings IODP, 302. doi:10.2204/iodp.proc.302.

Berger, D. & Jokat, W. (2008): A seismic study along the East Greenland margin from 72° N to 77° N.- Geophys. J. Internat. 174(2): 733-748, doi:10.1111/j.1365-246X.2008.03794.x

Berger, D. & Jokat, W. (2009): Sediment deposition in the northern basins of the North Atlantic and characteristic variations in shelf sedimentation along the East Greenland Margin.- Mar. Petrol. Geol. doi: 10.1016/j.marpetgeo.2009.04.005

Brinkhuis, H., Schouten, S., Collinson, M.E., Sluijs, A., Damste, J.S.S., Dickens, G.R., Huber, M., Cronin, T.M., Onodera, J., Takahashi, K., Bujak, J.P., Stein, R., van der Burgh, J., Eldrett, J.S., Harding, I.C., Lotter, A.F., Sangiorgi, F., Cittert, H.V.V., de Leeuw, J.W., Matthiessen, J., Backman, J. & Moran, K. (2006): Episodic fresh surface waters in the Eocene Arctic Ocean.- Nature 441: 606-609.

Darby, D.A. (2008): Arctic perennial ice cover over the last 14 million years.- Paleoceanography 23: PA1S07, doi:10.1029/2007PA001479.

Dove, D., Coakley, B., Hopper, J., Kristoffersen, Y. & HLY0503 Team (2010): Bathymetry, controlled source seismic and gravity observations of the Mendeleev ridge: implications for ridge structure, origin, and regional tectonics.- Geophys. J. Internat. 183: 481–502, doi: 10.1111/j.1365-246X.2010.04746.x

Forsyth, D.A., Asudeh, I., Green, A.G. & Jackson, H.R. (1986): Crustal structure of the northern Alpha Ridge beneath the Arctic Ocean.- Nature 322: 349-352.

Geissler, W.H., Jokat, W. & Brekke, H. (2011): The Yermak Plateau in the Arctic Ocean in the light of reflection, seismic data - implication for its tectonic and sedimentary evolution.- Geophys. J. Internat. 187(3): 1334-1362, doi: 10.1111/j.1365-246X.2011.05197.x

Grantz, A., Hart, P.E. & May, S.D. (2004): Seismic reflection and refraction data acquired in Canada Basin, Northwind Ridge and Northwind Basin, Arctic Ocean in 1988, 1992 and 1993, U.S. Geological Survey Open-File Report, 2004-1243, pp. 33.

Hall, J.K. (1973): Geophysical evidence for ancient seafloor spreading from Alpha Cordillera and Mendeleyev Ridge.- In: M.G. PITCHER (ed), Arctic Geology 19: 542-561, Amer. Assoc. Petrol. Geol. Memoir.

Hunkins, K.L. (1961): Seismic studies of the Arctic Ocean floor.- Geol. Arctic 1: 645-665.

Jackson, H.R., Forsyth, D.A. & Johnson, G.L. (1986): Oceanic affinities of the Alpha Ridge, Arctic Ocean.- Marine Geol. 73: 237-261.

Jackson, H.R., Forsyth, D.A., Hall, J.K. & Overton, A. (1990): Seismic reflection and refraction.- In: A. GRANTZ, G.L. JOHNSON & W.J. SWEENEY (eds), Geol. Soc. Amer., The Geology of North America, The Arctic Region, Vol. L: 153-170.

Jakobsson, M., Backman, J., Rudels, B., Nycander, J., Mayer, L., Sangiorgi, F., Brinkhuis, H., O'Regan, M., Jokat, W., Frank, M., King, J. & Morane, K. (2007): The early Miocene onset of a ventilated circulation regime in the Arctic Ocean.- Nature 447: 987-990, doi: 10.1038/nature05924.

Jokat, W. (2003): Seismic investigations along the western sector of Alpha Ridge, Central Arctic Ocean.- Geophys. J. Internat. 152: 185-201. doi: 10.1046/j.1365-246X.2003.01839.x

Jokat, W. (2005): The sedimentary structure of the Lomonosov Ridge between 88° N and 80° N: consequences for tectonic and glacial processes.- Geophys. J. Internat. 163: 698-726, doi: 10.1111/j.1365-246X.2005.02786.x

Jokat, W., Buravtsev, V. & Miller, H. (1995): Marine seismic profiling in sea ice covered regions.- Polarforschung 64: 9-17.

Jokat, W., Uenzelmann-Neben, G., Kristoffersen, Y. & Rasmussen, T. (1992): ARCTIC'91: Lomonosov Ridge - a double sided continental margin.- Geology 20: 887-890.

Jokat, W., Weigelt, E., Kristoffersen, Y., Rasmussen, T. & Schöne, T. (1995a): Geophysical and bathymetric results from the Morris Jesup Rise, Yermak Plateau and Gakkel Ridge.- Geophys. J. Internat. 123: 601-610, doi: 10.1111/j.1365-246X.1995.tb06874.x

Jokat, W., Weigelt, E., Kristoffersen, Y., Rasmussen, T. & Schöne, T. (1995b): New insights into evolution of the Lomonosov Ridge and the Eurasian Basin.- Geophys. J. Internat. 122: 378-392.

Karasik, A.M. (1968): Magnetic Anomalies of the Gakkel Ridge and the origin of the Eurasia Subbasin of the Arctic Ocean.- Geofizicheskie metody razvedki i Arktike 5: 8-19 (in Russian).

Kleiven, H.F., Jansen, E, Fronval, T. & Smith, T.M. (2002): Intensifcation of Northern Hemisphere glaciations in the circum Atlantic region (3.5-2.4 Ma) - ice-rafted detritus evidence.- Palaeogeogr. Palaeoclimat. Palaeoecol. 184 (2002) 213-223

Krylov, A.A., Andreeva, I.A., Vogt, C., Backman, J., Krupskaya, V.V. Grikurov, G.E., Moran,K. & Shoji, H. (2008): A shift in heavy and clay-mineral provenance indicates a middle Miocene onset of a perennial sea ice cover in the Arctic Ocean.- Paleoceanography 23: PA1S06, doi: 10.1029/2007PA001497.

Lebedeva-Ivanova, N.N., Zamansky, Y.Y., Langinen, A.E. & Sorokin, M.Y. (2006): Seismic profiling across the Mendeleev Ridge at 82° N: evidence of continental crust.- Geophys. J. Internat. 165: 527-544, doi: 10.1111/j.1365-246X.2006.02859.x

Minakov, A.N. & Podladchikov, Y.Y. (2012): Tectonic subsidence of the Lomonosov Ridge.- Geology 40: 99-102; doi:10.1130/G32445.1.

Moran, K., Backman, J., Brinkhuis, H., Clemens, S.C., Cronin, T., Dickens, G.R., Eynaud, F., Gattacceca, J., Jakobsson, M., Jordan, R.W., Kaminski, M., King, J., Koc, N., Krylov, A., Martinez, N., Matthiessen, J., McInroy, D., Moore, T.C., Onodera, J., O'Regan, M., Pälike, H., Rea, B., Rio, D., Sakamoto, T., Smith, D.C., Stein, R., St. John, K., Suto, I., Suzuki, N., Takahashi, K., Watanabe, M., Yamamoto, M., Farrell, J., Frank, M., Kubik, P., Jokat, W. & Kristoffersen, Y. (2006): The Cenozoic palaeoenvironment of the Artic Ocean.- Nature 441: 601-605.

Nansen Arctic Drilling Program NAD Science Committee (1992): The Arctic Ocean record: Key to Global Change (Initial Science Plan).- Polarforschung 61: 1-102.

O'Regan, M. Moran, K., Backman, J., Jakobsson, M., Sangiorgi, F., Brinkhuis, H., Pockalny, R., Skelton, A., Stickley, C., Koc, N., Brumsack, H.J. & Willard, D. (2008): Mid-Cenozoic tectonic and paleoenvironmental setting of the central Arctic Ocean.- Paleoceanography 23: PA1S20, doi: 10.1029/2007PA001559

Poirier, A. & Hillaire-Marcel, C. (2011): Improved Os-isotope stratigraphy of the Arctic Ocean.- Geophys. Res. Lett. 38: L14607, doi: 10.1029/2011GL047953

Sluijs, A., Schouten, S., Pagani, M., Woltering, M., Brinkhuis, H., Damste, J.S.S., Dickens, G.R., Huber, M., Reichart, G.J., Stein, R., Matthiessen, J., Lourens, L.J., Pedentchouk, N., Backman, J. & Moran, K. (2006): Subtropical Arctic Ocean temperatures during the Palaeocene/Eocene thermal maximum.- Nature 441: 610-613.

Sluijs, A., Röhl, U., Schouten, S., Brumsack, H.-J., Sangiorgi, F., Sinninghe Damste, J.S. & H. Brinkhuis (2008): Arctic late Paleocene - early Eocene paleoenvironments with special emphasis on the Paleocene-Eocene thermal maximum (Lomonosov Ridge Integrated Ocean Drilling Program Expedition 302), Paleoceanography 23: PA1S11, doi: 10.1029/2007PA001495.

St. John, K. (2008): Cenozoic ice-rafting history of the central Arctic Ocean: terrigenous sands on the Lomonosov Ridge.- Paleoceanography 23: PA1S05. doi: 10.1029/2007PA001483.

Stein, R., Boucsein, B. & Meyer, H. (2006): Anoxia and high primary production in the Paleogene central Arctic Ocean: first detailed records from the CLR.- Geophys. Res. Lett. 33: L18606. doi: 10.1029/2006GL026776.

Stickley, C.E., St. John, K., Koc, N., Jordan, R.W., Passchier, S., Pearce, R.B., Kearns, L.E. (2009): Evidence for middle Eocene Arctic sea ice from diatoms and ice-rafted debris.- Nature 460: 376-380, doi: 10.1038/nature 08163.

Thiede, J., Jessen, C., Knutz, P., Kuijpers, A., Mikkelsen, N., Nørgaard-Pedersen, N. & Spielhagen, R.F. (2011): Million of years of Greenland ice sheet history recorded in ocean sediments.- Polarforschung 80 (3): 141-159.

Tripati, A.K., Robert A., Eagle, R.A., Morton A., Dowdeswell, J.A., Atkinson, K.L., Bahé Y, Dawber C.F., Khadun E. Shaw R.M.H., Shorttle, O. & Thanabalasundaram, L. (2008): Evidence for glaciation in the northern hemisphere back to 44 Ma from ice-rafted debris in the Greenland Sea.- Earth Planet. Sci. Lett. 265: 112-122.

Vogt, P.R., Taylor, P.T., Kovacs, L.C. & Johnson, G.L. (1979): Detailed aeromagnetic investigations of the Arctic Basin.- J. Geophys. Res. 84: 1071-1089.

Vogt, P.R., Taylor, P.T., Kovacs, L.C. & Johnson, G.L. (1982): The Canada Basin: aeromagnetic constraints on structure and evolution.- Tectonophysics 89: 295-336.

Weller, P. & R. Stein (2008): Paleogene biomarker records from the central Arctic Ocean (Integrated Ocean Drilling Program Expedition 302): Organic carbon sources, anoxia, and sea surface temperature.- Paleoceanography 23: PA1S17, doi:10.1029/2007PA001472.

A first southern Lomonosov Ridge (Arctic Ocean) 60 ka IP$_{25}$ sea-ice record

by Ruediger Stein[1] and Kirsten Fahl[1]

Abstract: Here, we present a low-resolution biomarker sea-ice record from the High Arctic (southern Lomonosov Ridge), going back in time to about 60 ka (MIS 3 to MIS 1). Variable concentrations of the sea-ice diatom-specific highly branched isoprenoid (HBI) with 25 carbon atoms ("IP$_{25}$"), in combination with the phytoplankton biomarker brassicasterol, suggest variable seasonal sea-ice coverage and open-water productivity during MIS 3. During most of MIS 2, the spring to summer sea-ice margin significantly extended towards the south, resulting in a drastic decrease in phytoplankton productivity. During the Early Holocene Climate Optimum, brassicasterol reached its maximum, interpreted as signal for elevated phytoplankton productivity due to a significantly reduced sea-ice cover. During the mid-late Holocene, IP$_{25}$ increased and brassicasterol decreased, indicating extended sea-ice cover and reduced phytoplankton productivity, respectively. The HBI diene/IP$_{25}$ ratios probably reached maximum values during the Bølling-Allerød warm period and decreased during the Holocene, suggesting a correlation with sea-surface temperature.

Zusammenfassung: Mit dieser Pilotstudie wurde erstmals der neue Biomarker für Meereis (IP$_{25}$) in bis zu 60,000 Jahre alten Sedimenten vom südlichen Lomonosov-Rücken nahe des ostsibirischen Kontinentalrandes nachgewiesen. Obwohl weder die zeitliche Auflösung der Datenpunkte noch das Altersmodell dieser Studie hochaufgelöste Klimarekonstruktionen erlauben, ist es möglich, wichtige erste generelle Aussagen über die Veränderung der Meereisbedeckung in der hohen Arktis im Verlauf der Marinen Isotopenstadien (MIS) 3 bis 1 zu machen. Im MIS 3 weisen Minima und Maxima der untersuchten Biomarker auf eine kurzfristige Variabilität der Meereisbedeckung und Primärproduktition hin, die auf kurzfristige Klimaschwankungen zurückzuführen sein könnten. Im letzten Glazial führte eine ausgedehnte Meereisbedeckung wahrscheinlich zu einer deutlichen Abnahme der Primärproduktion. Während der Bølling-Allerød-Warm-Periode deuten dagegen minimale IP$_{25}$-Werte und maximale Werte für Phytoplankton-Biomarker auf eine drastisch reduzierte Eisbedeckung und erhöhte Primärproduktion hin. Im weiteren Verlauf des Holozäns nimmt dann die Meereisbedeckung wieder zu. Parallel dazu weist der Phytoplankton-Biomarker auf eine Abnahme der Primärproduktion. Das Verhältnis C$_{25}$-HBI dien/IP$_{25}$ erreicht maximale Werte in der Bølling-Allerød-Warmperiode und nimmt dann – parallel mit der holozänen Klimaabkühlung – ab, was auf eine Korrelation zwischen diesem Verhältnis und der Oberflächenwassertemperatur hinweisen mag.

INTRODUCTION

A most prominent characteristic of the modern Arctic Ocean is the sea-ice cover with its strong seasonal variability in the marginal (shelf) seas (Fig. 1; e.g., JOHANNESSEN et al. 2004), STROEVE et al. 2007, STEIN 2008 for review). Furthermore, sea ice is a critical component in the climate system, contributing to changes in Earth's albedo, biological processes and deep-water formation, a driving mechanism of the global thermohaline circulation. Despite the importance of sea ice, however, detailed information about the extent and variability of sea ice in the geological past is still very sparse. In this context, a novel biomarker approach which is based on the determination of sea-ice diatom specific highly branched

isoprenoids (HBI) with 25 carbon atoms (C$_{25}$ HBIs - "IP$_{25}$"; BELT et al. 2007; for background information see also STEIN et al. this vol.), seems to be a major step forward in getting more qualitative and – especially in combination with other open-water phytoplankton biomarkers such as brassicasterol and/or dinosterol (MÜLLER et al. 2009, 2011) – even more quantitative data on paleo-sea-ice distributions.

In following-up studies, the identification of this new sea-ice proxy IP$_{25}$ in marine sediment cores from the Canadian Arctic Archipelago (BELT et al. 2010, VARE et al. 2009, GREGORY et al. 2010), the shelf north of Iceland (MASSÉ et al. 2008), the Barents Sea (VARE et al. 2010), northern Fram Strait and off East Greenland (MÜLLER et al. 2009, 2011, 2012), and the Lomonosov Ridge in the central Arctic Ocean (FAHL & STEIN 2012) allowed reconstructions of the ancient sea-ice variability in these regions during the last 30 Cal. kyrs. BP (ka).

As result of this first study, we present a first IP$_{25}$ record from the High Arctic, going back in time to about 60 ka.

METHODS AND MATERIAL

Core PS2767-4 (79°44.6' N, 144°00.4' E) was recovered at the interception of the southern Lomonosov Ridge and the East Siberian Sea continental margin at a water depth of 584 m during RV "Polarstern" Expedition ARK-XI/1 in 1995 (RACHOR 1997), located close to the modern September ice edge (Fig. 1). This core – together with several other cores from the Laptev Sea continental margin – has already been studied in order to identify organic-carbon sources (i.e., primary productivity *versus* terrigenous input) and their variations related to climate change, using organic geochemical bulk parameters and selected biomarkers (*n*-alkanes) (STEIN et al. 2001). For the Holocene to postglacial time interval, the age model of the sediment cores was primarily based on AMS[14]C datings and magnetic susceptibility records (STEIN et al. 2001). In most of the cores, the base of the Holocene is characterized by a prominent decrease in magnetic susceptibility that can be used to correlate all the cores from the Laptev Sea continental margin (e.g., STEIN & FAHL 2000). For the sediment cores representing older, pre-Holocene intervals, the stratigraphy is based on oxygen isotope stratigraphy, magnetostratigraphy, biostratigraphy (especially dinoflagellates), lithostratigraphy, and magnetic susceptibility records (STEIN et al. 2001 and further references therein). As the number of AMS[14]C datings is very limited and no further new chronological data have been produced so far, the existing age model is still tentative. Based on this age model, core PS2767-4 probably represents the last about 60 ka.
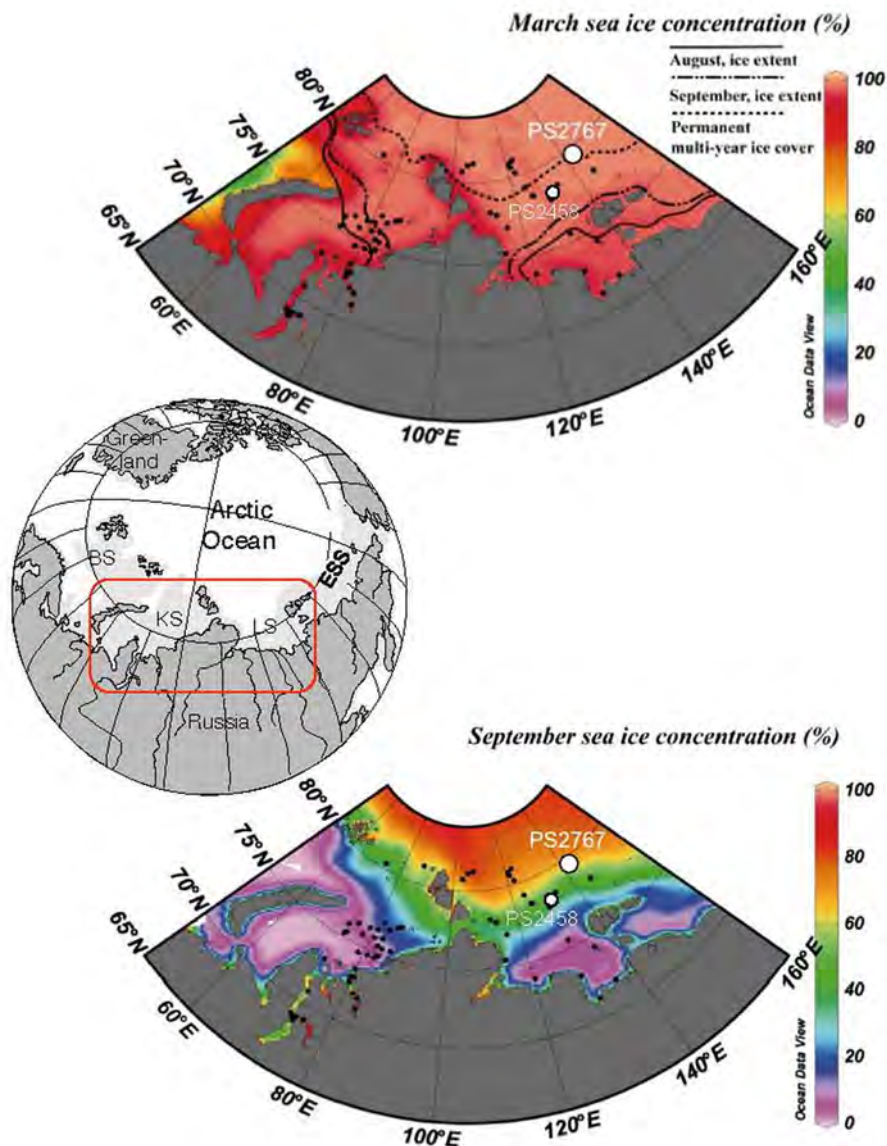
For biomarker analyses we follow the procedure published by MÜLLER et al. (2011) and FAHL & STEIN (2012). Briefly summarized, the extraction of the freeze-dried sediments was carried out by an Accelerated Solvent Extractor. For quantification the internal standards 7-hexylnonadecane, squalane and cholesterol-d_6 (cholest-5-en-3β-ol-D_6) were added prior to analytical treatment. Separation of the hydrocarbons and sterol fractions was carried out via open-column chromatography (for further details and instrumental conditions see FAHL & STEIN 2012 and further references therein). Individual compound identification was based on comparisons of their retention times with that of reference compounds and published mass spectra. The details about the quantification of the C_{25}-HBI alkenes (i.e., IP_{25} and HBI diene) and brassicasterol (24-methylcholesta-5,22E-dien-3β-ol) are described in FAHL & STEIN (2012) and FAHL & STEIN (1999), respectively.

RESULTS AND DISCUSSION

With the biomarker records determined in the sediments from core PS2767-4 we yield some direct information about the development and variability of the sea-ice conditions in the High Arctic at the interception of the Lomonosov Ridge and the East Siberian Sea continental margin during the last about 60 ka. Although the data set produced within this study neither represents a high-resolution record nor has a precise age model needed for paleoenvironmental reconstruction with centennial-to millennial-scale resolution, it allows some statements related to general trends in sea ice and climate conditions from MIS 3 to MIS 1.

Fig. 1: Averaged sea-ice concentration in (A) March and (B) September from 1978-2007 (http://nsidc.org). Dashed line indicates southern boundary of permanent sea-ice cover (>60 % through the year). August and September boundaries of sea-ice cover represent the 30 % isoline for the specific months. Locations of core PS2767-4 and core PS2458-4 are indicated.

Abb. 1: Durchschnittliche Meereiskonzentration für März (A) und September (B) für das Zeitintervall 1978-2007 (http://nsidc.org). Die gestrichelte Linie zeigt die südliche Grenze der permanenten Meereisbedeckung (>60 % Eisbedeckung das ganze Jahr über). Zusätzlich sind für die Monate August und September die südlichen Grenzen für eine Meereisbedeckung von >30 % eingetragen. Die Lokationen der Kerne PS2767-4 und PS2458-4 sind angezeigt.

Based on the biomarker data (Fig. 2), the records can be divided into three sections, coinciding approximately with MIS 3, MIS 2, and MIS 1. During MIS 3, i.e., between about 60 and 30 ka, variable concentrations of the phytoplankton biomarker brassicasterol and the sea-ice proxy IP_{25} were determined, suggesting variable seasonal sea-ice coverage and open-water periods typical for ice-edge situations (cf. MÜLLER et al. 2011, FAHL & STEIN 2012). These minimum and maximum values may reflect short-term climate changes (Fig. 2) although, of course, our low-resolution record does not allow to resolve such high-frequency climate variability.

For most of the interval between 30 and 15 ka (Late Weichselian glacial phase to early deglaciation), both brassicasterol and IP_{25} concentrations reached minimum values around zero

(Fig. 2). Following MÜLLER et al. (2009), the absence of both IP_{25} and brassicasterol is interpreted as a period of permanently closed sea-ice cover. Under such conditions, sea-ice diatom and phytoplankton growth is limited since the presence of thick pack ice inhibits light penetration and enhanced stratification reduces nutrient availability. These observations suggest that the spring to summer sea-ice margin significantly extended towards the south during most of MIS 2, coinciding with a minimum in summer insolation (Fig. 2). This situation is very similar to that described for the Fram Strait area based on the same set of biomarkers (MÜLLER et al. 2009).

At the end of the glacial, both brassicasterol and IP_{25} concentrations increased which may suggest conditions favourable
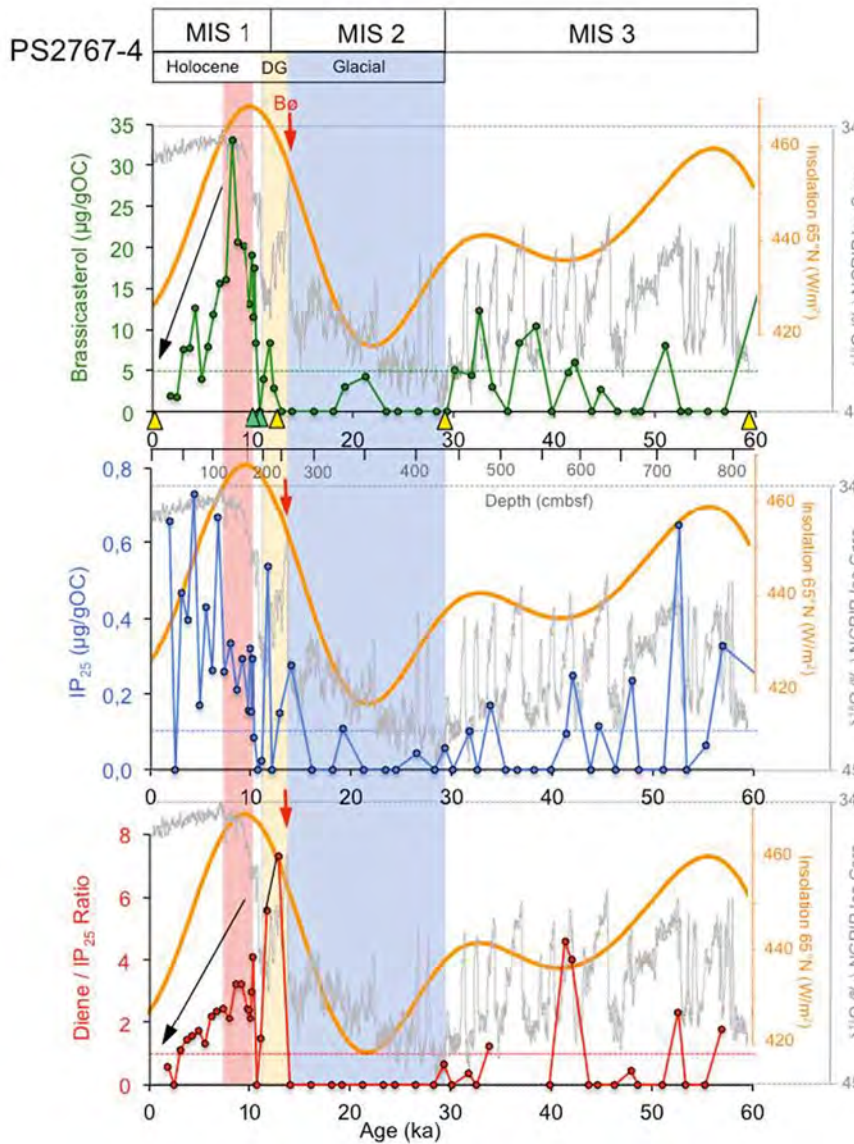
Fig. 2: Concentrations of brassicasterol (green curve) and IP$_{25}$ (blue curve) (in μg/g OC) as well as HBI$_{25}$ diene/IP$_{25}$ ratios (red curve) determined in Core PS2767-4 and plotted versus age. Marine Isotope Stages (MIS) and age model according to STEIN et al. (2001); green triangles indicate depth of AMS[14]C datings, yellow triangles top and base of MIS 1 to MIS 3. Glacial phase (blue bar), deglacial phase – DG (yellow bar) and Holocene with Holocene Climate Optimum (red bar) are highlighted. Red arrow indicates Bølling peak warm interval (Bø). As background information for the climatic evolution during the last 60 ka, the insolation record (orange curve; BERGER & LOUTRE 1999)) and the oxygene isotope record of the NGRIP Ice Core (light gray curve NGRIP MEMBERS 2004) are shown.

Abb. 2: Konzentrationen des Phytoplankton-Biomarkers Brassicasterol (grüne Kurve) und des Meereis-Biomarkers IP$_{25}$ (blaue Kurve) und das Verhältnis der Biomarker HBI$_{25}$-Dien/IP$_{25}$ (rote Kurve), ein möglicher Biomarker-Proxy für die Oberflächenwassertemperatur (cf. ROWLAND et al. 2001), geplottet gegen das Alter. Marine Isotopenstadien (MIS) und Altermodell nach STEIN et al. (2001): Grüne Dreiecke markieren Tiefen von AMS[14]C-Altern, gelbe Dreiecke Top und Basis von MIS 1 bis 3. Glazialphase (blauer Balken), Abschmelzphase (gelber Balken) und das Holozän mit dem Holozänen Klimaoptimum (roter Balken) sind farblich hervorgehoben. Als Hintergrundinformation sind zusätzlich die Insolationskurve für 65° N (orange Kurve; BERGER & LOUTRE 1999) und die Sauerstoffisotopenkurve des NGRIP-Eiskerns (hellgraue Kurve; NGRIP MEMBERS 2004) dargestellt.

less coincided with the Early Holocene Climate Optimum (cf., KAUFMAN et al. 2004, CRONIN et al. 2010), interpreted as signal for increased phytoplankton productivity due to a reduced sea-ice cover. During the Holocene, sea-ice cover increased and phytoplankton productivity decreased, as reflected in the opposing trends of the two biomarker records (Fig. 2). This interpretation is in agreement with multi-proxy compilations based on calcareous microfossils, drift wood, bowhead whale and IP$_{25}$ data from other Arctic sites as well as climate models indicating that early Holocene temperatures were higher than today and that the Arctic contained less ice, consistent with a high intensity of orbitally-controlled spring and summer insolation that peaked around 10–11 ka and gradually decreased thereafter (Fig. 2; e.g., CRUCIFIX et al. 2002, GOOSSE et al. 2007, JAKOBSSON et al. 2010 and further references therein).

In addition to IP$_{25}$, the C$_{25}$-HBI diene was determined in the sediment samples from core PS2767-4 as well. Both isomers, IP$_{25}$ and the HBI diene, display a quite similar, mostly parallel variability in the available Arctic sedimentary records (VARE et al. 2009, FAHL & STEIN 2012). In addition to its use as sea-ice proxy, however, the combination of IP$_{25}$ and the HBI diene might give additional information about the sea-surface temperature. This assumption is based on the study by ROWLAND et al. (2001) who found that the grade of unsaturation increases with diatom growth temperature (for further background information see also STEIN et al. 2012, this vol.). Such a relationship seems to be reflected in the HBI diene/IP$_{25}$ ratio determined in close-by core PS2458-4 (see Fig. 1 for location), reaching maximum values during the Bølling-Allerød warm interval and decreasing parallel to the Holocene climate cooling trend (FAHL & STEIN 2012). The HBI diene/IP$_{25}$ ratio determined in the sedimentary record of core PS2767-4 shows a very similar deglacial to Holocene trend as core PS2458-4 and seems to support the interpretation by FAHL & STEIN (2012). During the glacial cold interval, the HBI diene is totally absent whereas during the deglacial phase an absolute maximum of the HBI diene/IP$_{25}$ ratio was determined, probably coinciding with the Bølling peak warm interval (Fig. 2). During the Holocene, the HBI diene/IP$_{25}$ ratio decreases, parallel to the Holocene cooling trend. Unfortunately, the age model as well as the time-resolution of the core PS2767-4 record are not good enough to prove the hypothesis that the HBI diene/IP$_{25}$ ratio might have the potential for becoming a new temperature proxy for low-SST environments. Here, certainly more data and ground-truth studies are needed.

for production of phytoplankton and sea-ice algae as typical for an ice-edge situation (cf., MÜLLER et al. 2009, 2011, FAHL & STEIN 2012). During the Early Holocene, between about 10 and 7 ka, brassicasterol values reached a prominent maximum, followed by a steady decrease during the late Holocene. The IP$_{25}$ values, on the other hand, display a high-amplitude variability with an opposite trend towards higher IP$_{25}$ values during the Holocene. The brassicasterol maximum more or

CONCLUSIONS

Within this pilot study, the novel sea-ice proxy IP_{25} developed by Belt et al. (2007) was determined in a low-resolution record going back in time to about 60 ka. Concentrations of IP_{25}, in combination with the phytoplankton biomarker brassicasterol, give first information about changes in the sea-ice cover in the East Siberian Sea continental margin area during MIS 3 to MIS 1. The HBI diene/IP_{25} ratios seem to follow the deglacial to Holocene warming and cooling trends, suggesting a correlation with sea-surface temperature.

ACKNOWLEDGMENT

References

Berger, A. & Loutre, M. F. (1999): Parameters of the Earths orbit for the last 5 Million years in 1 kyr resolution.- doi:10.1594/PANGAEA.56040.

Belt, S.T., Massé, G., Rowland, S.J., Poulin, M., Michel, C. & LeBlanc, B. (2007): A novel chemical fossil of palaeo sea ice: IP_{25}.- Org. Geochem. 38: 16-27.

Belt, S.T., Vare, L.L., Massé, G., Manners, H.R., Price, J.C., MacLachlan, S.E., Andrews, J.T. & Schmidt, S. (2010): Striking similarities in temporal changes to spring sea ice occurrence across the central Canadian Arctic Archipelago over the last 7000 years.- Quat. Sci. Rev. 29(25-26): 3489-3504.

Cronin, T.M., Gemery, L., Briggs, W.M., Jakobsson, M., Polyak, L. & Brouwers, E.M. (2010): Quaternary Sea-ice history in the Arctic Ocean based on a new ostracode sea-ice proxy.- Quat. Sci. Rev. 29: 3415-3429.

Crucifix, M., Loutre, M.F., Tulkens, P., Fichefet, T. & Berger, A. (2002): Climate evolution during the Holocene: a study with an Earth system model of intermediate complexity.- Climate Dyn. 19: 43-60.

Fahl, K. & Stein, R. (1999): Biomarkers as organic-carbon-source and environmental indicators in the Late Quaternary Arctic Ocean: Problems and perspectives.- Mar. Chem. 63: 293-309.

Fahl, K. & Stein, R. (2012): Modern seasonal variability and deglacial/Holocene change of central Arctic Ocean sea-ice cover: new insights from biomarker proxy records.- Earth Planet. Sci. Lett. 351-352:123-133; doi:10.1016/j.epsl.2012.07.009.

Goosse, H., Driesschaert, E., Fichefet, T. & Loutre, M.-F. (2007): Information on the early Holocene climate constrains the summer sea ice projections for the 21st century.- Climate of the Past Discuss. 2: 999-1020.

Gregory, T.R., Smart, C.W., Hart, M.B., Massé, G., Vare, L.L. & Belt, S.T. (2010): Holocene palaeoceanographic changes in Barrow Strait, Canadian Arctic: foraminiferal evidence.- J. Quat. Sci. 25: 903-910.

Jakobsson, M., Long, A., Ingolfsson, O., Kjær, K.H. & Spielhagen, R.F. (2010): New insights on Arctic Quaternary climate variability from palaeo-records and numerical modelling.- Quat. Sci. Rev. 29: 3349-3358.

Johannessen, O.M., Bengtsson, L., Miles, M.W., Kuzmina, S.I., Semenov, V.A., Alekseev, G.V., Nagurnyi, A.P., Zakharov, V.F., Bobylev, L.P., Pettersson, L.H., Hasselmann, K. & Cattle, H.P. (2004): Arctic climate change: observed and modelled temperature and sea-ice variability.- Tellus A 56: 328-341.

Kaufman, D.S., Ager, T.A., Anderson, N.J., Anderson, P.M., Andrews, J.T., Bartlein, P.J., Brubaker, L.B., Coats, L.L., Cwynar, L.C., Duvall, M.L., Dyke, A.S., Edwards, M.E., Eisner, W.R., Gajewski, K., Geirsdottir, A., Hu, F.S., Jennings, A.E., Kaplan, M.R., Kerwin, M.W., Lozhkin, A.V., MacDonald, G.M., Miller, G.H., Mock, C.J., Oswald, W.W., Otto-Bliesner, B.L., Porinchu, D.F., Rühland, K., Smol, J.P., Steig, E.J. & Wolfe, B.B. (2004): Holocene thermal maximum in the western Arctic (0–180° W).- Quat. Sci. Rev. 23: 529-560.

Massé, G., Rowland, S.J., Sicre, M.-A., Jacob, J., Jansen, E. & Belt, S.T. (2008): Abrupt climate changes for Iceland during the last millennium: Evidence from high resolution sea ice reconstructions.- Earth Planet. Sci. Lett. 269: 565-569.

Müller, J., Massé, G., Stein, R. & Belt, S.T. (2009): Variability of sea-ice conditions in the Fram Strait over the past 30,000 years.- Nat. Geosci. 2(11): 772-776.

Müller, J., Wagner, A., Fahl, K., Stein, R., Prange, M. & Lohmann, G. (2011): Towards quantitative sea ice reconstructions in the northern North Atlantic: a combined biomarker and numerical modelling approach.- Earth Planet. Sci. Lett. 306: 137-148.

Müller, J., Werner, K., Stein, R., Fahl, K., Moros, M. & Jansen, E. (2012): Holocene cooling culminates in sea ice oscillations in Fram Strait.- Quat. Sci. Rev. 47: 1-14, doi:10.1016/j.quascirev.2012.04.024.

Rachor, E. (1997): Scientific Cruise Report of the Arctic Expedition ARK-XI/1 of RV „Polarstern" in 1995.- Rep. Polar Res. 226: 1-157.

Rowland, S.J., Belt, S.T., Wraige, E.J., Massé, G., Roussakis, C. & Robert, J.M. (2001): Effects of temperature on polyunsaturation in cytostatic lipids of Haslea ostrearia.- Phytochemistry 56: 597-602.

Stein, R. (2008): Arctic Ocean Sediments: Processes, Proxies, and Paleoenvironment.- Developments in Marine Geology 2. Elsevier, Amsterdam, 1-592.

Stein, R. & Fahl, K. (2000): Holocene accumulation of organic carbon at the Laptev Sea continental margin (Arctic Ocean): sources, pathways, and sinks.- GeoMar. Lett. 20: 27-36.

Stein, R., Boucsein, B., Fahl, K., Garcia de Oteyza, T., Knies, J. & Niessen, F. (2001): Accumulation of particulate organic carbon at the Eurasian continental margin during late Quaternary times: controlling mechanisms and paleoenvironmental significance.- Glob. Planet. Change 31: 87-104.

Stein, R., Fahl, K. & Müller, J. (2012): Proxy reconstruction of Arctic Ocean sea ice history – From IRD to IP_{25}.- Polarforschung 82: xx-xx.

Stroeve, J., M., Holland, M., Meier, W., Scambos, T. & Serreze, M. (2007): Arctic sea ice decline: faster than forecast.- Geophys. Res. Lett. 34(L09501), 1-5.

Vare, L.L., Massé, G. & Belt, S.T. ((2010): A biomarker-based reconstruction of sea ice conditions for the Barents Sea in recent centuries.- The Holocene, doi: 10.1177/0959683609355179.

Vare, L.L., Massé, G., Gregory, T.R., Smart, C.W. & Belt, S.T. (2009): Sea ice variations in the central Canadian Arctic Archipelago during the Holocene.- Quat. Sci. Rev. 28: 1354-1366.

Mitteilungen

Wie fossile Moleküle helfen können, Klimamodelle zu verbessern*

von Juliane Müller[1]

VON MEEREIS, WETTER UND KLIMA

Das markanteste Merkmal des Arktischen Ozeans ist seine Eisbedeckung – noch. Seit 1979, dem Start der Meereisbeobachtung durch Satelliten, wurde eine Verringerung der Ausdehnung des Sommermeereises um 12 Prozent pro Jahrzehnt gemessen (NSIDC 2011). Das entspricht einem Verlust von insgesamt etwa drei Millionen Quadratkilometern – zum Vergleich: Der indische Subkontinent nimmt eine Fläche von 3,3 Millionen Quadratkilometern ein. Schließlich wurde der fortschreitende Eisrückzug von einer deutlichen Zunahme des wissenschaftlichen und auch des öffentlichen Interesses an der arktischen Meereisbedeckung begleitet. Und so gewann neben den Diskussionen über die Zukunft indigener Bevölkerungsgruppen (zum Beispiel der Inuit), dem Schicksal von Eisbären oder Fischpopulationen oder der neuen Verfügbarkeit von Bodenschätzen, Energierohstoffen und Schifffahrtsrouten in den hohen Breiten auch die Bedeutung des Meereises selbst an Aufmerksamkeit (SOLOMON et al. 2007).

Denn das arktische Meereis ist nicht nur anfällig für Klimaschwankungen. Durch seine Wechselwirkungen mit der Atmosphäre und dem Ozean und auch durch seine Funktion als Puffer zwischen diesen beiden Elementen beeinflusst das Eis den globalen Wärmehaushalt. Wie eine effektive Dämmschicht reduziert das Meereis den Austausch von Wärme und Feuchtigkeit zwischen dem Ozean und der Atmosphäre. Dies wiederum beeinflusst die Intensität und Ausrichtung von atmosphärischen Zirkulationsmustern, ist also maßgebend für überregionale Wetterlagen. Des Weiteren kontrolliert das Eis das Wärmebudget der Ozeane durch sein Vermögen, die Sonneneinstrahlung zu reflektieren (Albedo), wodurch die Erwärmung der oberen Wasserschichten vermindert wird. Schließlich stellt das Eis ein enormes Süßwasserreservoir dar, das auf den Salzgehalt und die Dichtestruktur des Meerwassers und somit auf globale Meeresströmungen einwirkt. Während der „Großen Salzanomalie" in den 1970er-Jahren führte beispielsweise ein ungewöhnlich hoher Export von Meereis aus dem Arktischen Ozean in den Nordatlantik zur Bildung einer Süßwasserlinse von geringerer Dichte, was eine Abschwächung des Golfstroms und somit eine Abküh-

lung des Nordatlantiks und Europas bewirkte (DICKSON et al. 1988). Die unterschiedlichen Temperatur- und Salzgehalte der Wassermassen, die im europäischen Nordmeer zwischen Grönland, Island und Skandinavien aufeinandertreffen, stellen also einen der wichtigsten Antriebsmechanismen für die europäische Wärmepumpe, den Golfstrom, dar. Hier, im nördlichsten Bereich des Atlantiks, spielt die Framstraße, die einzige Tiefwasserverbindung zwischen dem Arktischen Ozean und den restlichen Weltmeeren, eine besondere Rolle im Klimageschehen. Bereits der norwegische Polarforscher Fridtjof Nansen bewies mit seiner Fram-Expedition (1893–1896), dass der Großteil des arktischen Meereises (ca. 3000 $km^3 y^{-1}$) durch diese schmale Passage nach Süden in den Nordatlantik transportiert wird. Gleichzeitig beherrscht ein Ausläufer des Golfstroms den östlichen Bereich der Framstraße vor Spitzbergen und befördert warmes Atlantikwasser nach Norden bis in den Arktischen Ozean hinein. Dieses Wechselspiel von Warmwasserimport und Kaltwasser- bzw. Meereisexport hält das globale Förderband von kalten und warmen Meeresströmungen in Schwung, indem es die thermohaline Konvektion im Nordatlantik antreibt – in diesem Zusammenhang spricht man auch von der atlantischen meridionalen Zirkulation: Das warme Atlantikwasser kühlt auf seinem Weg nach Norden entlang der skandinavischen Küste bis nach Spitzbergen, wo es auf kaltes Wasser und Meereis trifft, kontinuierlich ab. Durch diese Abkühlung und die Erhöhung des Salzgehalts während der Eisbildung nimmt die Dichte des Oberflächenwassers zu, und es sinkt in tiefere Bereiche des Ozeans hinab, wo es schließlich als Nordatlanti-

Abb. 1: Bundestagspräsident Dr. Norbert Lammert überreicht die Urkunde für einen 2. Preis beim Deutschen Studienpreis 2012 der Körber-Stiftung an Dr. Juliane Müller. Der Festakt fand am 6. November 2012 im Kaisersaal der Deutschen Parlamentarischen Gesellschaft in Berlin statt. Foto: Körber-Stiftung/David Ausserhofer.

---

[1] Alfred Wegener Institute for Polar and Marine Research, Am Alten Hafen 26, D-27568 Bremerhaven, Germany; <juliane.mueller@awi.de>

sches Tiefenwasser zurück nach Süden in Richtung Antarktis strömt. Diese enorme Umwälzung von Wassermassen im europäischen Nordmeer wirkt wie ein riesiger Pumpmechanismus, der den Golfstrom in Gang hält.

SCHWINDENDES ARKTISCHES MEEREIS UND EUROPAS WÄRMEPUMPE

Inwieweit die Stärke des Golfstroms, der Nordeuropa ein für diese Breiten ungewöhnlich mildes Klima beschert, von Veränderungen in diesem Konvektionsprozess beeinträchtigt wird, ist bereits Thema vieler Klimastudien. Momentan wird ein durch die zunehmende Erwärmung beschleunigtes Aussüßen des Arktischen Ozeans durch höhere Niederschläge, eine höhere Zufuhr von Süßwasser aus den Flüssen der Anrainerstaaten und insbesondere durch den sich selbst verstärkenden Prozess des Schmelzens von Meereis beobachtet. Dieses Aussüßen wird das empfindliche Gleichgewicht der unterschiedlichen Wassermassen im Nordatlantik stören. Eine damit verbundene Verminderung der thermohalinen Konvektion beziehungsweise des Pumpmechanismus hätte eine Abschwächung des Golfstroms zur Folge (PELTIER et al. 2006). Darüber hinaus resultiert eine Abnahme der Eisbedeckung nachweislich in einer Destabilisierung der Luftdruckverhältnisse in der Arktis, was zu häufigeren und stärkeren Stürmen im arktischen und atlantischen Sektor führt (JAISER et al. 2012).

Das Verhalten des arktischen Meereises spielt demnach eine bisher eher vernachlässigte, allerdings überaus wichtige Rolle für die Abschätzung der Folgen des Klimawandels. Bedauerlicherweise unterschätzen Computermodelle die Geschwindigkeit des Eisrückgangs im Arktischen Ozean um mehrere Jahrzehnte (STROEVE et al. 2007). Mithilfe eben jener Computermodelle sollen jedoch Klimaszenarien simuliert werden, die wertvolle Informationen über künftige atmosphärische und ozeanische Zirkulationsmuster liefern könnten; Informationen über Veränderungen der Temperatur- und Niederschlagswerte, Sturmintensitäten und -häufigkeiten. Wo genau wird es zu ausgedehnten Dürreperioden oder wo wird es wiederholt zu Überschwemmungen kommen? Die begrenzte Fähigkeit dieser Modelle, die genaue Meereisentwicklung und das resultierende Verhalten von Ozeanströmungen und Luftmassenbewegungen vorherzusagen, stellt demnach ein gravierendes Defizit in der Klima(folgen)forschung dar.

Um nun die Vorhersagefähigkeit von Klimamodellen zu verbessern, hilft der Blick in die Vergangenheit. Können die Modelle die Meereisbedeckung früherer Zeiträume zuverlässig reproduzieren, verbessert dies auch die Prognosen über kommende Meereisschwankungen? Eine Kontrolle solcher Paläomodellierungen erfolgt durch Klima- oder Proxydaten, wie sie zum Beispiel aus Sedimentkernen gewonnen werden. Unter einem Proxy (englisch: Stellvertreter) wird in der Klimaforschung ein Anzeiger verstanden, der Informationen über frühere Umweltbedingungen liefert. So können Pollen oder Baumringe Aufschluss über Niederschlags- und Temperaturverhältnisse an Land geben, während die Isotopenverteilungen in den fossilen Kalkschalen von marinen Einzellern die Temperatur und den Salzgehalt des Meerwassers reflektieren. Solche auf Proxydaten basierenden Studien über längst vergangene (präindustrielle) Umweltbedingungen in der

Arktis helfen also einerseits, die natürliche Variabilität des Klimas abzuschätzen; andererseits dienen sie als Datengrundlage für computergestützte Simulationen jener Prozesse, die solche natürlichen Schwankungen auslösen beziehungsweise begleiten.

Die gezielte Paläorekonstruktion über ein Vorhandensein oder Fehlen von Eis in einer bestimmten Meeresregion gestaltet sich aufgrund der Natur des Eises jedoch als äußerst schwierig. Während das Kommen und Gehen von Gletschern anhand eindeutiger Signaturen im Gestein (z.B. Gletscherschrammen) leicht erfasst werden kann, hinterlässt das Gefrieren oder Schmelzen von Meerwasser bzw. Meereis faktisch keine Spuren. Und so konnte die Frage, ob, wann, oder gar wie lange Teile der Arktis mit Meereis bedeckt waren, bisher nur indirekt beantwortet werden.

DER MOLEKULARE FINGERABDRUCK VON EISALGEN

Ein vielversprechender Ansatz, wie eine Paläoeisbedeckung eindeutig nachgewiesen werden kann, wurde im Jahr 2007 von der Arbeitsgruppe um Simon T. Belt und Guillaume Massé an der Universität Plymouth (England) vorgestellt (BELT et al. 2007). Ein neuer Proxy, ein hoch verzweigtes Isoprenoidmolekül, das ausschließlich von im Meereis lebenden Diatomeen (Kieselalgen) produziert wird, sollte als Eisanzeiger fungieren. Solche Moleküle, die spezifisch für den Organismus sind, der sie synthetisiert, werden auch Biomarker genannt. Dieser Biomarker für Meereisalgen war neu und wurde kurzerhand IP_{25} getauft (für „Ice Proxy" mit 25 Kohlenstoffatomen). Mittels organisch-geochemischer Analysen identifizierten Simon T. Belt und seine Kollegen den Eismarker IP_{25} in Meereisproben und in marinen Oberflächensedimenten des saisonal bis permanent mit Meereis bedeckten kanadisch-arktischen Archipels und schlussfolgerten, dass mit dem Nachweis dieses Biomarkers in marinen Sedimenten eine vorangegangene Meereisbedeckung belegt werden könne.

Nach der Blüte der Eisalgen im Frühling und mit der einsetzenden Eisschmelze im Sommer sinken die Überreste der Algen inklusive IP_{25} auf den Meeresboden, wo sie im Sediment abgelagert werden. Anders als das empfindliche Kieselgehäuse der Algen, das anfällig für Korrosion ist, sind die organischen Lipide, zu denen IP_{25} gehört, recht stabil und über Jahrtausende im Sediment konservierbar – man nennt Biomarker daher auch geochemische oder molekulare Fossilien. Während das Vorhandensein von IP_{25} in entsprechend alten Sedimenten eine Paläoeisbedeckung anzeigt, kann das Fehlen des Biomarkers jedoch unterschiedliche Gründe haben. Entweder fehlte das Meereis, oder aber die Eisdecke war ungewöhnlich dick und kompakt. Unter einer permanenten, auch im Sommer nicht schmelzenden und mehrere Meter dicken Eisschicht verschlechtern sich die Lebensbedingungen für die sonst gut angepassten Eisalgen extrem. Es kann nicht genügend Licht durch das Eis dringen, um das Wachstum der Einzeller anzuregen. So bleibt die Frühjahrsblüte der Eisalgen aus, und es gelangt kein IP_{25} in das darunterliegende Sediment. Diese Ambivalenz stellt einen grundlegenden Schwachpunkt in der Anwendung des neuen Eismarkers dar.

Im Rahmen einer Untersuchung der wechselnden Klima- und

Umweltbedingungen in der Framstraße während der letzten 30.000 Jahre (MÜLLER 2011) fand sich schließlich die Lösung des Problems: Statt sich nur auf den einen Biomarker IP$_{25}$ zu konzentrieren, hilft die Berücksichtigung anderer molekularer Hinterlassenschaften im Sediment. Marines Phytoplankton (hierzu gehören beispielsweise Braun- oder Grünalgen, Dinoflagellaten oder Diatomeen) gedeiht vorzugsweise im offenen, eisfreien Wasser. Während der Metabolismus der im Meereis lebenden Eisalgen (Eisdiatomeen) auf eine reduzierte Lichtverfügbarkeit eingestellt ist, reagiert das Phytoplankton äußerst empfindlich auf den Lichtmangel unterhalb des Meereises. Ähnlich dem für Eisalgen charakteristischen Molekül IP$_{25}$ gibt es auch spezielle Biomarker, die von den Organismen des Phytoplanktons synthetisiert werden. Hierzu gehören bestimmte Sterole (Brassicasterol, Dinosterol) oder einfache, kurzkettige n-Alkane, die ebenso wie IP$_{25}$ nach dem Absterben und der Zersetzung des organischen Materials im Meeresboden „gespeichert" werden. Die Verknüpfung dieser beiden Biomarkertypen, von denen der eine als Eisanzeiger (IP$_{25}$) und der andere als Anzeiger für eisfreie Bedingungen (Phytoplanktonbiomarker) fungiert, sollte demnach eine eindeutige Unterscheidung zwischen dem Fehlen von Meereis (kein IP$_{25}$, aber viele Phytoplanktonbiomarker im Sediment) und dem Vorhandensein einer permanenten, mehrere Meter dicken Eisschicht (weder IP$_{25}$ noch Phytoplanktonbiomarker im Sediment nachweisbar) ermöglichen. Um die Anwendbarkeit dieser Methode zu prüfen, folgte ein „Feldversuch".

EIN ABBILD DER MODERNEN VERBREITUNG VON MEEREIS IN DER FRAMSTRASSE

Es wurde eine Vielzahl von Oberflächensedimenten aus verschiedenen Gebieten der Framstraße hinsichtlich ihres Inventars an Biomarkern untersucht (MÜLLER et al. 2011). Im Bereich der marinen Geologie repräsentieren Oberflächensedimente – das sind die obersten Zentimeter des Meeresbodens – eine Momentaufnahme der jüngsten Umwelt- beziehungsweise Klimabedingungen eines Untersuchungsgebietes. Da die Meereisbedeckung in der Framstraße aufgrund der Zufuhr von warmem Atlantikwasser einerseits und dem Export polaren Wassers und Meereises andererseits höchst variabel ist, stellt dieses Gebiet ein ideales „Testgelände" für die Überprüfung des neuen Biomarkeransatzes dar. Wie Satellitenaufnahmen zeigen, ist das Vorkommen von Meereis im Osten der Framstraße auf die küstennahen Gebiete vor Spitzbergen begrenzt, während der breite kontinentale Schelf von Ostgrönland beinahe das ganze Jahr über mit Meereis bedeckt ist. Der Großteil des arktischen Packeises, das entlang der grönländischen Küste nach Süden in den Atlantik treibt, schmilzt jedoch, bevor es das Irminger Meer vor der Südostküste Grönlands erreicht, so dass dieses Gebiet bereits im Frühling eisfrei ist. Würde das Vorkommen von IP$_{25}$ und der Phytoplanktonbiomarker in den Sedimentproben der unterschiedlichen Gebiete diese Verbreitung des Meereises auch widerspiegeln?

In den Proben aus dem Irminger Meer und aus den Gebieten vor Spitzbergen, wo es kein oder nur wenig Meereis gibt, fehlt IP$_{25}$ oder ist in nur sehr geringen Konzentrationen vorhanden, während die Phytoplanktonbiomarker stark angereichert sind. Vor der Küste Grönlands, die bis in den Sommer hinein mit Eis bedeckt ist, verhält es sich genau andersherum: Viel IP$_{25}$

und nur wenige Phytoplanktonbiomarker sind im Sediment konserviert. Dieser Befund passte hervorragend in das Konzept und ließ vermuten, dass der Ansatz, die beiden verschiedenen Biomarker zu kombinieren, sehr gut funktioniert. Rätsel gaben jedoch die gleichzeitig hohen Konzentrationen von IP$_{25}$ und Phytoplanktonbiomarkern in den Proben der Dänemarkstraße zwischen Grönland und Island und entlang des äußeren kontinentalen Schelfs von Grönland auf. Wie können sowohl die Konzentrationen des Eismarkers als auch die der Phytoplanktonbiomarker gleichzeitig erhöht sein? Vergleiche mit den Satellitendaten zeigten, dass an genau diesen Stellen die Meereisbedeckung ihre maximale Frühjahrsausdehnung erreicht – diese Zonen werden auch als Eisrandlagen bezeichnet. Das Wachstum von Phytoplankton wird im Bereich von Eisrandlagen durch die kontinuierliche Freisetzung von Nährstoffen aus dem langsam schmelzenden Eis enorm stimuliert, so dass es regelmäßig zu Phytoplanktonblüten entlang des Eisrandes kommt (SMITH et al. 1987). Dieses Phänomen ist also verantwortlich für die hohen Konzentrationen von Phytoplanktonbiomarkern in den Sedimentproben, die auch reich an IP$_{25}$ sind. Für die Paläorekonstruktion von Meereis ist diese Beobachtung von großer Bedeutung, da sie erstmalig eine Möglichkeit bietet, die Position früherer Eisrandlagen zu bestimmen. Auch für die (Paläo-) Klimaforschung sind diese Informationen äußerst wichtig, da es sich hierbei um die Kontaktzone zwischen offenen, mit der Atmosphäre in Austausch stehenden, und eisbedeckten, von der Atmosphäre abgeschirmten Wasserflächen handelt.

Eine rechnerische Verknüpfung der beiden Biomarker zu einem neuen Index erlaubte schließlich auch einen direkten und vor allem quantitativen Vergleich der Meereisverbreitung, wie sie durch die Biomarkerdaten abgebildet wird, mit der wirklichen, von Satelliten erfassten Eisverbreitung im Untersuchungsgebiet. Dieser Index zeigt das Verhältnis von IP$_{25}$ zu einem Phytoplanktonbiomarker an; daher auch der frei gewählte Name PIP$_{25}$ (für Phytoplankton-IP$_{25}$-Index). Hohe PIP$_{25}$-Werte deuten auf eine hohe Eisbedeckung hin, niedrige Werte verweisen auf eine geringe Eisbedeckung (Abb. 2). Erfreulicherweise korrelieren die PIP$_{25}$-Werte aller Sedimentproben sehr gut mit den aus Satellitendaten berechneten Meereiskonzentrationen für die jeweiligen Positionen der Sedimentproben. Wie hoch die Eisbedeckung einer definierten Fläche ist (je nach Auflösungs-
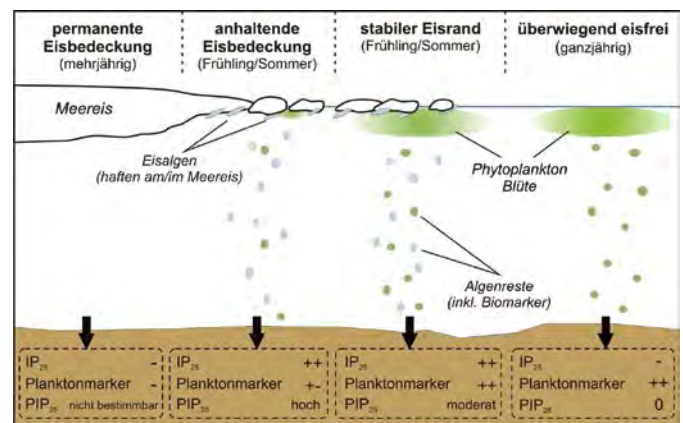

Abb. 2: Schematische Darstellung unterschiedlicher Meereisbedingungen mit entsprechender Produktivität von Phytoplankton und Eisalgen sowie den resultierenden Konzentrationen der Biomarker und PIP$_{25}$-Indizes im Sediment (MÜLLER et al. 2011).

vermögen des Satelliten kann das ein Areal von 6,25 bis zu 25 km² sein), wird standardgemäß in Konzentration angegeben: Bei einer Meereiskonzentration von 50 % ist demnach die Hälfte der Fläche eisbedeckt. Dieser direkte Vergleich einer auf Proxydaten basierenden Meereisrekonstruktion mit wirklichen Meereisdaten für die Frühjahrssaison ist der erste dieser Art, und die gute Korrelation belegt, dass der PIP_{25}-Index tatsächlich für quantitative Meereisrekonstruktionen genutzt werden kann. Zum Beispiel würde ein PIP_{25}-Index von 0,7 einer Meereiskonzentration von 70-80 % entsprechen. Idealerweise könnte man also anhand von PIP_{25}-Werten aus Sedimentbohrkernen direkte Aussagen über eine frühere Meereiskonzentration in einem Untersuchungsgebiet ableiten.

Insbesondere, weil die bislang recht vagen Aussagen über ein früheres Vorhandensein oder Fehlen von Meereis nicht in Klimamodelle integriert werden können, stellt dieser neue Ansatz eine grundlegende Innovation für die Klimaforschung dar. Wie stark oder wie schnell veränderte sich beispielsweise die arktische Meereiskonzentration während des letzten Interglazials vor etwa 125.000 Jahren, das in vielen Computersimulationen als Äquivalent zu den heutigen Bedingungen und zur Abschätzung des Ausmaßes des globalen Temperaturanstiegs herangezogen wird? Was waren die natürlichen Antriebsmechanismen hierfür? Wie veränderten sich die ozeanisch/atmosphärischen Zirkulationsmuster? Und schließlich: Wie reagierte das globale Klima?

Die Option, aus PIP_{25}-Werten abgeleitete Meereiskonzentrationen in Paläoklimamodelle einzulesen, um längst vergangene Klimaschwankungen und daran geknüpfte Ursache-Wirkungs-Prinzipien zu simulieren, würde die Zuverlässigkeit prognostischer Klimamodelle deutlich erhöhen.

DAMALS WIE HEUTE

Weitere Untersuchungen an langen Sedimentkernen, also an deutlich älterem Probenmaterial, sollten nun Aufschluss über die klimatische Entwicklung in der Framstraße während der letzten 30.000 Jahre geben. Hierbei konnte auch die Anwendbarkeit von IP_{25} – der neue Meereisproxy wurde bis zu diesem Zeitpunkt nur in maximal 10.000 Jahre alten Sedimenten nachgewiesen – in Kombination mit Phytoplanktonbiomarkern geprüft werden.

In den letzten 30.000 Jahren wandelte sich das globale Klima erheblich. Während des letzten Glazials, der letzten großen Kälteperiode, waren die Landmassen Nordamerikas und Nordeurasiens mit dicken Eisschilden bedeckt, die sich erst während des Deglazials vor circa 18.000 Jahren zurückzogen und schmolzen. Die Ausdehnung dieser Eisschilde ist anhand von geomorphologischen Strukturen (Moränenlandschaften, Findlinge) recht gut dokumentiert; für die Ausdehnung des Meereises gibt es jedoch nur wenige und oft sogar widersprüchliche Annahmen.

Mit der Untersuchung eines Sedimentkerns vom Yermak-Plateau, einer untermeerischen Hochfläche nordwestlich von Spitzbergen, konnte nun anhand von IP_{25} und der Phytoplanktonbiomarker eindeutig rekonstruiert werden, wie variabel die Meereisbedeckung während der letzten 30.000 Jahre war (MÜLLER et al. 2009). Dies erlaubte auch Rückschlüsse auf

die Veränderlichkeit der thermohalinen Zirkulation, also das Verhalten des Golfstroms. Im Zeitraum des „Letzten Glazialen Maximums" am Ende der Weichselkaltzeit vor 20.000 Jahren zeigt das Fehlen von IP_{25} und der Phytoplanktonbiomarker beispielsweise an, dass der nördliche Bereich der Framstraße über 6000 Jahre lang mit einer permanenten und sehr dicken Eisdecke überzogen gewesen sein muss; der nördliche Ausläufer des Golfstroms war deutlich geschwächt. Dies steht im krassen Kontrast zu einem abrupten Klimawechsel vor circa 15.000 Jahren, als die Meerenge zu Beginn des Bølling-Interstadials innerhalb weniger Jahrzehnte eisfrei wurde und es auch für mindestens 200 Jahre lang blieb. Der ungewöhnlich schnelle Rückzug des Meereises in der Framstraße wurde von einem rapiden Anstieg der Wassertemperaturen im Nordatlantik begleitet und zeigt, wie eng das Verhalten der Meereisbedeckung mit abrupten Klimaschwankungen verknüpft ist. Dies drückt sich auch in einem weiteren Ereignis vor 13.000 Jahren aus, als eine plötzliche Kaltphase mit einem erneuten Vorstoß des Meereises nach Süden und einer Verringerung der thermohalinen Zirkulation einherging. Für einige Jahrhunderte blieb die nördliche Framstraße, wie bereits während des „Letzten Glazialen Maximums", von dickem Eis bedeckt.

Was löste diese ständigen Wechsel von Kalt-und Warmphasen aus? Zu den natürlichen Ursachen für die häufigen und oftmals sehr schnell aufeinanderfolgenden Klimaschwankungen gehören Veränderungen in der Intensität der Sonneneinstrahlung, Schwankungen der atmosphärischen Kohlendioxid- und Methankonzentration oder durch den Zerfall großer Eisschilde ausgelöste Süßwasserereignisse, die die ozeanische (und auch atmosphärische) Zirkulation veränderten. Im warmen Holozän, das die letzten 11.000 Jahre umfasst, veränderte sich die Ausdehnung des Meereises in der Framstraße weniger dramatisch als am Ende der letzten Kaltzeit. Mithilfe der IP_{25}- und Phytoplanktonbiomarker-Daten eines Sedimentkerns aus der östlichen Framstraße konnte gezeigt werden, dass die Meereisbedeckung in diesem Gebiet über 8000 Jahre hinweg kontinuierlich zugenommen hat. Diese Entwicklung steht im Zusammenhang mit einer stetigen Abnahme der Sonneneinstrahlung auf der Nordhalbkugel und einem verringerten Wärmetransport durch den nordatlantischen Ausläufer des Golfstroms. Interessanterweise korrelieren kurzzeitige Fluktuationen in der Ausdehnung des Meereises vor Spitzbergen mit plötzlichen Gletscherbewegungen auf dem Archipel. Hier wird deutlich, wie schnell sich die Wechselwirkungen zwischen Ozean und Atmosphäre auf die Umwelt auswirken. In den Phasen des Rückzugs von Meereis konnte mehr Feuchtigkeit von der eisfreien Meeresoberfläche an die Atmosphäre abgegeben werden, wodurch die Niederschlagsrate über Spitzbergen erhöht wurde. Der Niederschlag, in Form von Schnee, beschleunigte somit das Wachstum der Gletscher. In den Phasen einer Meereiszunahme wiederum stagnierte das Gletscherwachstum oder nahm sogar ab, weil der für ein Wachstum benötigte Niederschlag fehlte. Zu dieser Zeit blockierte eine ausgedehnte Meereisdecke vor der Küste Spitzbergens den Wärme- und Feuchtigkeitsaustausch zwischen Ozean und Atmosphäre.

Dem langfristigen Abkühlungstrend im Holozän steht der momentan beobachtete, schnell voranschreitende Eisrückgang gegenüber. Die Position, an der der untersuchte Sedimentkern gezogen wurde, ist inzwischen nur noch sehr selten von Meereis bedeckt. Nun gilt das Holozän – das Zeit-

alter der Menschen – in Bezug auf Klimaschwankungen als vergleichsweise stabil, und so stellt sich die Frage, inwieweit die momentane Klimaentwicklung noch im Rahmen natürlicher Schwankungen liegt und wie die ozeanischen und atmosphärischen Rückkopplungsmechanismen aussehen werden.

Um diese Fragen zu beantworten, müssen Computermodelle die klimarelevanten Prozesse sowohl für die Vergangenheit als auch für die Zukunft zuverlässig abbilden können.

KLIMA IM WANDEL

Viele Paläoklimastudien, die sich nicht nur mit der Entwicklung in der Arktis, sondern auch in anderen Regionen befassen, zeigen, dass der momentan beobachtete Klimawandel kein Einzelfall, kein neues Phänomen ist. Neu ist hingegen, dass der Mensch (unter anderem) durch die Emission von Treibhausgasen zum Klimawandel beiträgt. Noch viel wichtiger aber ist, dass die Welt, anders als vor Jahrtausenden, mittlerweile von sieben Milliarden Menschen bewohnt wird. Der Rückgang des arktischen Meereises mag keine unmittelbare Auswirkung auf Regionen haben, die nicht zu den Anrainerstaaten des Arktischen Ozeans gehören. Die mit dem Eisrückgang verbundenen ozeanischen und atmosphärischen Veränderungen tragen jedoch auch zum überregionalen Klimawandel bei und beeinflussen somit die Ökologie, die Ökonomie und schließlich auch das Migrationsverhalten ganzer Nationen.

Der Schwerpunkt der meisten Klimastudien liegt auf der Simulation der kurz- und auch langfristigen Entwicklung regionaler und globaler Umweltbedingungen (Erwärmungstrends, Niederschläge etc.), um Prognosen abzugeben, die den politischen Entscheidungsträgern als Richtlinien für Handlungsstrategien dienen sollen. Viele Modelle scheitern jedoch schon an der Simulation der heutigen Klimabedingungen – sie können beispielsweise die Entwicklung der arktischen Meereisbedeckung während der letzten 30 Jahre nicht korrekt wiedergeben (STROEVE et al. 2007). Die Notwendigkeit, solche Modelle zu verbessern, liegt auf der Hand. Die richtige Simulation des Verhaltens von Meereis und der physikalischen Wechselwirkungen im Ozean-Atmosphäre-System stellt eine grundlegende Voraussetzung für die Berechnung vertrauenswürdiger Zukunftsprojektionen dar. Der neue PIP_{25}-Index bietet erstmals die Möglichkeit, eine Paläoeisbedeckung nicht nur qualitativ, sondern auch quantitativ abzubilden. Computermodelle können mithilfe dieser Daten kalibriert werden, sodass sie „lernen", nicht nur die komplexen Steuerungsmechanismen der Vergangenheit richtig wiederzugeben, sondern auch die zukünftigen Klimabedingungen realistisch vorherzusagen.

Zuverlässige Prognosen über den Wandel der Eisbedeckung im Arktischen Ozean und die damit einhergehenden Veränderungen der Albedo, der Wassertemperatur und -dichte, der ozeanischen Strömungsmuster, der Verteilung von Hoch- und Tiefdruckgebieten oder der Stabilität des submarinen Permafrosts werden die Planung von Maßnahmen des Klimafolgenschutzes deutlich erleichtern. Dass sich das Klima verändert, wird kaum zu ändern sein. Umso wichtiger ist es, abschätzen zu können, wie es sich verändern wird und wie diesem Wandel begegnet werden kann.

Literatur

Belt, S.T., Massé, G., Rowland, S.J., Poulin, M., Michel, C. & LeBlanc, B. (2007): A novel chemical fossil of palaeo sea ice: IP25.- Org. Geochem. 38: 16-27.

Dickson, R.R., Meincke, J., Malmberg, S.-A. & Lee, A.J. (1988): The "great salinity anomaly" in the Northern North Atlantic 1968-1982.- Progress Oceanogr. 20(2): 103-151.

Jaiser, R., Dethloff, K., Handorf, D., Rinke, A., Cohen, J. (2012): Impact of sea ice cover changes on the Northern Hemisphere atmospheric winter circulation.- Tellus A 64: 11595.

Müller, J. (2011): Last Glacial to Holocene variability in the sea ice distribution in Fram Strait/Arctic Gateway: A novel biomarker approach.- PhD thesis, University of Bremen.

Müller, J., Massé, G., Stein, R. & Belt, S.T. (2009): Variability of sea-ice conditions in the Fram Strait over the past 30,000 years.- Nature Geoscience2(11): 772-776.

Müller, J., Wagner, A., Fahl, K., Stein, R., Prange, M. & Lohmann, G. (2011): Towards quantitative sea ice reconstructions in the northern North Atlantic: A combined biomarker and numerical modelling approach.- Earth Planet. Sci. Lett. 306 (3-4): 137-148.

NSIDC (2011): National Snow and Ice Data Center, Boulder, USA. http://nsidc.org/news/press/ 20111004_MinimumPR.html.

Peltier, W.R., Vettoretti, G. & Stastna, M. (2006): Atlantic meridional overturning and climate response to Arctic Ocean freshening.- Geophys. Res. Lett. 33: L06713.

Smith, W.O., Jr., Baumann, M.E.M., Wilson, D.L. & Aletsee, L. (1987): Phytoplankton biomass and productivity in the marginal ice zone of the Fram Strait during summer 1984.. J. Geophys. Res. 92: 6777-6786.

Solomon, S., Qin, D., Manning, M., Chen, Z., Marquis, M., Averyt, K.B., Tignor, M. & Miller, H.L. (eds.) (2007): Contribution of Working Group I to the Fourth Assessment Report of the Intergovernmental Panel on Climate Change, Cambridge and New York.

Stroeve, J., Holland, M.M., Meier, W., Scambos, T. & Serreze, M. (2007): Arctic sea ice decline: Faster than forecast.- Geophys. Res. Lett: 34: L09501.

POLARFORSCHUNG

Mitteilungen für die Autoren: Die Zeitschrift POLARFORSCHUNG, herausgegeben von der DEUTSCHEN GESELLSCHAFT FÜR POLARFORSCHUNG E.V. (DGP) und dem ALFRED-WEGENER-INSTITUT FÜR POLAR- UND MEERESFORSCHUNG (AWI) dient der Publikation von Originalbeiträgen aus allen Bereichen der Polar- und Gletscherforschung in Arktis und Antarktis wie in alpinen Regionen mit polarem Klima. Manuskripte können in englischer (bevorzugt) und deutscher Sprache eingereicht werden und sind zu richten an: Deutsche Gesellschaft für Polarforschung, Schriftleitung Polarforschung, c/o Alfred-Wegener-Institut für Polar- und Meeresforschung, Postfach 12 01 61, D-27515 Bremerhaven, E-mail: <Dieter.Fuetterer@awi.de>. Eingesandt Manuskripte werden Fachvertretern zur Begutachtung vorgelegt und gelten erst nach ausdrücklicher Bestätigung durch die Schriftleitung als zur Veröffentlichung angenommen. Für detaillierte Angaben zur Manuskripterstellung siehe die Web-Seite der DGP: <http://www.dgp-ev.de>

Erscheinungsweise: POLARFORSCHUNG erscheint ab Jahrgang 2011, Band 81 mit jährlich zwei Heften
Open access: Alle Artikel sind in elektronischer Form im Internet verfügbar <http://www.polarforschung.de.>. POLARFORSCHUNG ist im Directory of Open Access Journals (DOAJ <http://www.doaj.org> geführt.
Bezugsbedingungen: Für Mitglieder der Deutschen Gesellschaft für Polarforschung e.V. (DGP) ist der Bezugspreis für die Zeitschrift im Mitgliedsbeitrag enthalten. Für Nichtmitglieder beträgt der Bezugspreis eines Heftes € 20,00; Bezug über den Buchhandel oder über die Geschäftsstelle.

Information for contributors: POLARFORSCHUNG – published by the DEUTSCHE GESELLSCHAFT FÜR POLARFORSCHUNG (DGP) and the ALFRED-WEGENER-INSTITUT FÜR POLAR- UND MEERESFORSCHUNG (AWI) – is a peer-reviewed, multidisciplinary research journal that publishes the results of scientific research related to the Arctic and Antarctic realm, as well as to mountain regions associated with polar climate. The POLARFORSCHUNG editors welcome original papers and scientific review articles from all disciplines of natural as well as from social and historical sciences dealing with polar and subpolar regions. Manuscripts may be submitted in English (preferred) or German. In addition POLARFORSCHUNG publishes Notes (mostly in German), which include book reviews, general commentaries, reports as well as communications broadly associated with DGP issues. Manuscripts and all related correspondence should be sent to: Deutsche Gesellschaft für Polarforschung e.V., Editorial Office POLARFORSCHUNG, c/o Alfred-Wegener-Institut für Polar- und Meresforschung, PO Box 12 01 61, D-27515 Bremerhaven, e-mail <Dieter.Fuetterer@awi.de>. Manuscripts can be considered as definitely accepted only after written confirmation from the Editor. – For a detailed guidance of authors please visit the DGP web page at: <http://www.dgp-ev.de>

Publication: POLARFORSCHUNG will be published efective of volume 81, 2011 two times a year.
Open access: PDF versions of all POLARFORSCHUNG articles are freely available from <http://www.polarforschung.de>. POLARFORSCHUNG is listed in the Directory of Open Access Journals (DOAJ) <http://www.doaj.org>
Subscription rates: For members of the German Society for Polar Research (DGP), subscription to POLARFORSCHUNG is included in the membership dues. For non-Members the price for a single issue is € 20,00.

Deutsche Gesellschaft für Polarforschung

25. Internationale Polartagung

17. - 22. März 2013 in Hamburg

German Society of Polar Research

25th International Polar Symposium

March 17 – 22, 2013 in Hamburg, Germany

Information: http://www.DGP-EV.de

E-Mail: polartagung@uni-hamburg.de